# The Enzyme Mediated Autodeposition of Casein: From Deposition of Defined Films to Nanostructuring with Single Particles

Dissertation zur Erlangung des akademischen Grades
Doctor rerum naturalium

vorgelegt
der Fakultät für Naturwissenschaften
der Universität Paderborn

von

Arne Alexander Rüdiger

Paderborn, der 03.04.2017

Die vorliegende Arbeit wurde unter Anleitung von Prof. Dr. Wolfgang Bremser im Department Chemie der Universität Paderborn vom 01.08.2013 bis 30.09.2016 angefertigt.

Vorsitzender der Prüfungskommission: Prof. Dr. Hans-Joachim Warnecke

Hauptgutachter: Prof. Dr. Wolfgang Bremser

Gutachter: Prof. Dr. Mats Johansson

Drittprüfer: Priv.-Doz. Dr. Hans Egold

**List of publications from this thesis:**


[1] O. I. Strube, A. A. Ruediger, W. Bremser, “Enzymatically controlled material design with casein — From defined films to localized deposition of particles.” *J. Biotechnol.* **2015**, *201*, 69-74.

[2] O. I. Strube, A. A. Ruediger, W. Bremser, “Buildup of biobased adhesive layers by enzymatically controlled deposition on the example of casein.” *Int. J. Adhes. Adhes.* **2015**, *63*, 9-13.

[3] A. A. Ruediger, E. Terborg, W. Bremser, O. I. Strube, “Influences on the film thickness in the enzymatic autodeposition process of casein.” *Prog. Org. Coat.* **2016**, *94*, 56-61.

[4] A. A. Ruediger, W. Bremser, O. I. Strube, “Nanoscaled biocoatings via enzyme mediated autodeposition of casein.” *Macromol. Mater. Eng.* **2016**, *301*, 1181-1190.

[5] A. A. Ruediger, W. Bremser, O. I. Strube, “The enzymatic autodeposition of casein: Effect of enzyme immobilization on deposition of protein structures.” *J. Coat. Technol. Res.* **2016**, *13*, 597-611.

[6] A. A. Ruediger, K. Brassat, J. Buerger, J. K. N. Lindner, W. Bremser, O. I. Strube, “Highly accessible nanostructures via enzyme mediated autodeposition.” *Langmuir* **2016**, submitted.

[7] O. I. Strube, W. Bremser, A. A. Ruediger, “Method for coating surfaces by enzymatic reaction of a biopolymer.” Patent WO 2015/150368A1, **2015**.

[8] A. A. Ruediger, O. I. Strube, W. Bremser, “Enzyme-catalyzed deposition of casein biocoatings.” *Coatings Science International (COSI)* **2014**, oral presentation.

[9] A. A. Ruediger, W. Bremser, O. I. Strube, “Nanostructuring via enzyme mediated autodeposition.” *Materials Science and Engineering* **2016**, oral presentation.

[10] A. A. Ruediger, W. Bremser, O. I. Strube, “Enzyme-mediated *in-situ* formation of casein biocoatings.” *Macromolecular Colloquium* **2015**, poster presentation.

[11] A. A. Ruediger, O. I. Strube, W. Bremser, “Nano structuring of casein micelles via an enzymatic process.” *Coatings Science International (COSI)* **2015**, poster presentation.

[12] K. Brassat, A. A. Ruediger, J. Buerger, W. Bremser, O. I. Strube, J. K. L. Lindner, “Site-selective protein immobilization on regular antidot patterns fabricated by nanosphere lithography.” *European Materials Research Society* **2016**, poster presentation.

**Eidesstattliche Erklärung**

Hiermit versichere ich, dass ich die Arbeit bis auf die offizielle Betreuung durch die Universität Paderborn selbständig angefertigt habe und keine anderen als die angegebenen und in Zitaten kenntlich gemachten Quellen und Hilfsmittel benutzt habe.

Paderborn, 01.04.2017

Arne Rüdiger

## Danksagung

Besonders hervorheben möchte ich, dass sowohl die Zeit des Studiums als auch die Zeit als wissenschaftlicher Mitarbeiter im Arbeitskreis „Coatings, Materials, and Polymers“ einen wunderschönen und lehrreichen Abschnitt meines Lebens ausgemacht haben. Ich danke Herrn Prof. Dr. Wolfgang Bremser und Herrn Dr. Oliver Strube für die Möglichkeit, diese Dissertation in ihrem Arbeitsbereich anfertigen zu können und möchte mich sehr herzlich für ihre großartige Betreuung und Unterstützung in den letzten Jahren bedanken.

Herrn Prof. Dr. Mats Johansson gilt ein ganz besonderer Dank ich für die Annahme des Amtes des Zweitgutachters.

Elke Terborg danke ich für die sehr gute Arbeit im Rahmen ihrer Bachelorarbeit „Quantitative Analyse des Schichtdickenwachstums in der enzymmoderierten Autophorese von Casein“ und Markus Lahme danke ich für seine Tätigkeiten als studentische Hilfskraft.

Bei Manuel Traut, Nadine Buitkamp und Daniel Briesenick möchte ich mich für die Unterstützung im Rahmen der REM-Messungen bedanken.

Ein herzlicher Dank geht an Andreas Wolk (Ulf) für die Freundschaft, die tolle Unterstützung und die Vielzahl an aufmunternden Diskussionen während der Zeit an der Universität Paderborn.

Katharina Brassat und dem Arbeitskreis Lindner des Departments Physik danke ich für die tolle Zusammenarbeit im Bereich der Nanostrukturierung.

Bei Christian Kunze und Ignacio Giner möchte ich mich für die Durchführung der XPS-Messungen sowie für die Hilfe bei der Interpretation der Spektren bedanken.

Ein spezieller Dank geht an meine Kollegen aus dem Arbeitskreis Bremser, die die dortige Zeit zu einer sehr schönen und lehrreichen Station meines Lebens gemacht haben. Ich danke Herrn Dr. Oliver Seewald und Herrn Dipl. Ing. Martin Samusch für die interessanten Gespräche und Denkanstöße. Meinen Laborpartnern und Freunden Andreas, Anna, Anne, Arthur, Daniel, David, Deniz und Simon danke ich für die tolle Zeit im Labor und das ganze Drumherum.

Besonders möchte ich mich auch bei meiner Familie und meinen Freunden für die wunderbare Motivation und Unterstützung in der gesamten Zeit bedanken.

**Abstract**

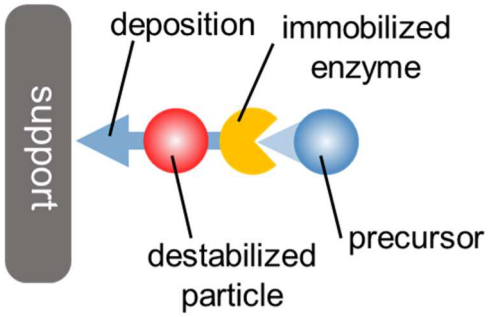


Formation of protein-based coatings and structures via Enzyme Mediated Autodeposition (EMA) is investigated on the example of casein as protein and chymosin as enzyme. Key factor of this method is the tethering of the enzyme onto the support. By this, destabilization and subsequent deposition of casein particles occur only in direct proximity to the support surface. Depositing particles cover immobilized enzyme, resulting in self-limitation of the process.

The type of enzyme immobilization is highly relevant, because it defines the achievable deposition structures. Investigated immobilization methods are physical adsorption, direct covalent binding, and covalent binding via polymeric spacers. Physical adsorption of enzyme enables the formation of continuous casein coatings with controllable film thickness by adjustment of reaction parameters, such as deposition time, p*H* value, and particle concentration. This method is also suitable for the *in situ* buildup of adhesive protein layers. Highest control and site-specificity of the process is provided by covalent attachment of enzyme. Direct covalent tethering results in defined formation of protein mono- or double layers, while the incorporation of spacer molecules enhances the mobility of enzyme. Consequently, the amount and radius of protein deposition is increased.

Combination of the EMA with the Nanosphere Lithography technique allows for tethering of enzyme only in designated areas. This enables the controlled deposition of single protein particles and allows for the nanostructuring of surfaces with biopolymers.

All enzyme immobilization and final protein deposition reactions are realized by easy-to-apply dip coating procedures and lack the necessity of harsh reaction conditions. Thus, an environmentally friendly character is preserved at all time. Deposited casein structures show improved mechanical and physico-chemical properties, such as enhanced flexibility and increased water resistance in comparison to conventionally processed casein films. Based on the attained results, the Enzyme Mediated Autodeposition provides new insights into biobased material design and might find applications in biosensors, micro- and nanoelectronics, and life-sciences.

**Kurzfassung**

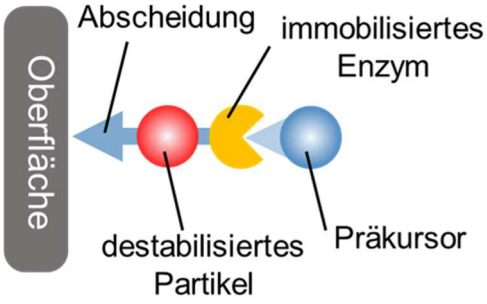


Ziel dieser Dissertation ist die Bildung und Charakterisierung proteinbasierter Beschichtungen und Strukturen durch die Enzymatische Autophorese (Englisch: Enzyme Mediated Autodeposition; EMA) anhand des Beispiels Casein und Chymosin. Casein stellt dabei die filmbildende Komponente und Chymosin das Enzym dar. Von zentraler Bedeutung ist die Immobilisierung des Enzyms auf der Materialoberfläche, die beschichtet respektive strukturiert wird. Somit wird eine Destabilisierung und anschließende Abscheidung der Caseinpartikel in direkter Nähe zur Materialoberfläche gewährleistet. Destabilisierte und abgeschiedene Partikel überlagern immobilisiertes Enzym. Dies verursacht eine prozessinhärente Selbstterminierung der Partikelabscheidung.

Die Art der Enzymimmobilisierung bestimmt die Morphologie der abgeschiedenen Strukturen. Relevante Enzymimmobilisierungen sind die physikalische Adsorption, die kovalente Anbindung und die kovalente Anbindung über Spacermoleküle. Die physikalische Adsorption des Enzyms auf einer Materialoberfläche ermöglicht die Abscheidung kontinuierlicher Proteinschichten. Die Anpassung der Reaktionsparameter, i.e. Abscheidungszeit, p*H*-Wert und Partikelkonzentration, gewährleistet eine Kontrolle über die resultierende Schichtdicke der Beschichtung. Zudem eignet sich die Enzymimmobilisierung durch physikalische Adsorption zur *in situ* Erzeugung proteinbasierter Klebstoffschichten. Das höchste Maß an Prozesskontrolle und Ortsspezifität wird durch eine kovalente Anbindung des Enzyms erreicht. Dies ermöglicht die Bildung von Mono- und Doppellagen aus Caseinpartikeln. Die Verwendung von Spacermolekülen in der kovalenten Enzymimmobilisierung erhöht die Mobilität des Enzyms. Dadurch lassen sich Menge und Radius der Proteinabscheidung gezielt beeinflussen.

Eine Enzymimmobilisierung ausschließlich in bestimmten Arealen auf einer Materialoberfläche lässt sich durch die Kombination der Enzymatischen Autophorese mit der Nanokugel-Lithographie (Englisch: Nanosphere Lithography; NSL) realisieren. Mit dieser Methodik lassen sich gezielt einzelne Caseinpartikel auf der Materialoberfläche abscheiden und eine Strukturierung des Materials im Nanometerbereich erzielen. Dies stellt beim aktuellen Stand

der Technik eine Nanostrukturierung von Oberflächen mit Biopolymeren unter höchster Präzision und einer konkurrenzlosen Wirtschaftlichkeit dar.

Alle Enzymimmobilisierungen sowie Proteinabscheidungen werden als einfache Tauchverfahren unter reaktionsfreundlichen Bedingungen realisiert, wodurch die Enzymatische Autophorese zu jedem Zeitpunkt einen umweltfreundlichen Charakter wahrt. Enzymatisch abgeschiedene Caseinstrukturen weisen im Vergleich zu konventionellen Caseinfilmen verbesserte mechanische und physikochemische Eigenschaften, wie erhöhte Flexibilität und Wasserstabilität, auf. Basierend auf den erzielten Ergebnissen dieser Dissertation zeigt die Enzymatische Autophorese ein großes Anwendungspotential im Bereich des biobasierten Materialdesigns, z.B. in der Biosensorik, der Mikro- und Nanoelektronik und den Lebenswissenschaften.

# List of contents

## Abbreviations and acronyms

| | |
|---|---|
| AFM | Atomic force microscope/microscopy |
| APTES | (3-aminopropyl)triethoxysilane |
| $CaCl_2$ | Calcium chloride |
| $c_C$ | Casein concentration |
| CCP | Colloidal calcium phosphate |
| CLEA | Crosslinked enzyme aggregate |
| d | Distance, if lengths or thicknesses are considered or diameter, if dimension of sphere-like particles is considered. |
| DLS | Dynamic light scattering |
| DMT | Derjaguin-Muller-Toporov |
| DNA | Deoxyribonucleic acid |
| EDX | Energy dispersive X-ray spectroscopy |
| EMA | Enzyme Mediated Autodeposition |
| EtOAc | Ethyl acetate |
| ETOH | Ethanol |
| GLYMO | (3-glycidoxypropyl)trimethoxysilane |
| HCl | Hydrochloric acid |
| $K_M$ | Michaelis constant |
| KOH | Potassium hydroxide |
| NaCl | Sodium chloride |
| NaOH | Sodium hydroxide |
| PS | Polystyrene |
| QNM | Quantitative NanoMechanics |
| RH | Relative humidity |
| RT | Room temperature |
| [S] | Substrate concentration |
| SEM | Scanning electron microscope/microscopy |
| STM | Scanning tunneling microscope/microscopy |
| $t_D$ | Time of deposition |
| $T_g$ | Glass transition temperature |

| | |
|---|---|
| THF | Tetrahydrofuran |
| U | Enzyme unit; amount of enzyme that catalyzes conversion of 1 µmol substrate per minute. |
| WPI | Whey protein isolate |

Abbreviations of amino acids:

| | |
|---|---|
| A: | Alanine (Ala) |
| C: | Cysteine (Cys) |
| D: | Aspartic acid (Asp) |
| E: | Glutamic acid (Glu) |
| F: | Phenylalanine (Phe) |
| G: | Glycine (Gly) |
| H: | Histidine (His) |
| I: | Isoleucine (Ile) |
| K: | Lysine (Lys) |
| L: | Leucine (Leu) |
| M: | Methionine (Met) |
| N: | Asparagine (Asn) |
| P: | Proline (Pro) |
| Q: | Glutamine (Gln) |
| R: | Arginine (Arg) |
| S: | Serine (Ser) |
| T: | Threonine (Thr) |
| V: | Valine (Val) |
| W: | Tryptophan (Trp) |
| Y: | Tyrosine (Tyr) |

## List of figures

## List of tables

# 1 Prologue

## 1.1 Introduction

Biopolymers are attaining a growing importance in modern sciences and technologies. Coatings and adhesives based on biopolymers are especially meaningful, because with respect to certain fields of application they often exhibit superior properties compared to their synthetic counterparts. Such properties comprise biocompatibility, sustainability, multi-functionality, e.g. medical and anti-fouling properties, biodegradability, and non-toxicity. With respect to many applications, biopolymers are the means of choice. Therefore, they are of interest for both, academic and industrial research and development.

Additional benefits, connected to research on biobased materials, arise from the growing awareness of people and governments about sustainability and an environmentally friendly attitude towards life. This facilitates and supports the evaluation of biopolymers due to a broad acceptance and funding opportunities. An important group of biopolymers, which exhibit versatile properties and functionalities, is represented by proteins. They are abundant in nature and constitute a sustainable resource of biopolymers. Recent investigations and developments consider the use of soy protein, gelatin, wheat gluten, and particularly casein.

Casein coatings have a long tradition in history of mankind and are commonly manufactured by conventional solution casting and spin coating processes. However, these processes suffer from limited control over particle deposition and film formation. On the other hand, methods, offering high precision, like gas phase deposition techniques, are generally not applicable for proteins. Incompatibility problems also exist with regard to frequently applied industrial dip coating techniques, such as electrodeposition and autodeposition processes. These techniques offer a good compromise between applicability and level of control. Nonetheless, they are limited to metallic supports as well as to a certain number of addressable particles, excluding most biobased materials. Thus, with respect to the growing demand for the incorporation of biopolymers in coating applications and their controlled addressment onto supports, there is an essential need for the development of a sophisticated and versatile deposition technique.

## 1.2 Aim of work

Purpose of this study is the investigation and evaluation of a revolutionary method for the generation of biological coatings and structures. This motivation is accompanied by the goal of realizing an overall high level of control and precision of the process. Moreover, an environmentally friendly and sustainable character is pursued at all time.

The investigated method is called Enzyme Mediated Autodeposition and will incorporate the unrivaled specificity of enzymes. The system is based on the enzyme chymosin and the major milk protein casein. Chymosin represents the initiating component for particle deposition and consequently, provides the control of the process. Casein is the film-forming component, which will be deposited in a highly precise manner, enabling the formation of well-designed coatings and structures. Deposition of casein takes places via cleavage reaction by chymosin. This leads to a polarity change of casein, which then becomes hydrophobic and starts to precipitate from aqueous colloidal dispersion. In order to obtain the envisaged high control over particle deposition and film formation, the enzyme will be immobilized on the support material. Consequently, initiation of casein deposition takes place in direct proximity to the support surface. Uncontrolled cleavage reactions and therefore precipitation of casein in the bulk phase is excluded. The role of the applied immobilization method for chymosin will be an essential object of the overall evaluation. It is assumed that different methods for enzyme coupling yield versatile results, allowing for a broad ensemble of achievable deposition structures.

In addition, special focus will be put on the feasibility of the investigated method in the structuring of surfaces with biomolecules. At the moment, this is a very important and challenging field for many sciences and technologies, e.g. life sciences, micro- and nanoelectronics, and biosensoring. Especially the medical sector exhibits a great demand for the controlled formation of biological and biocompatible coatings and structures, regarding fields like implantology, drug delivery, and wound healing.

Examination of the aforementioned system will be conducted with respect to deposition behavior, film formation, achievable structures, and applicability in modern fields of sciences. It is to be expected that evaluation and verification of a novel method for the controlled deposition of biopolymers will have revolutionary impacts on the conventionally applied methods and processes, used for the formation of biocoatings.

# 2 Status quo

## 2.1 Biopolymers

### 2.1.1 General remarks and classification of biopolymers

Polymers are quantitatively the most important products of the chemical industry. They are used in manifold applications in everyday life, e.g. in coatings, adhesives, packaging films, plastics, and cosmetics. Almost all current polymers are produced from fossil fuels. However, the manufacture of synthetic polymers is strongly connected to a massive consumption of material and energy resources, leading to severe problems in terms of sustainability. Due to their inherent non-biodegradability, synthetic polymers also exhibit a significant contribution to the increasing amount of solid waste. Especially, by taking into account that many of them are used only once in their application.

Indeed, polymeric waste can, at least to a certain percentage amount, be recycled or be used via combustion for energy generation, but this must be carefully considered from economical and ecological perspectives.[1] In recent decades, there has been a progressive interest in a sustainable chemistry. This development is especially supported and driven forward by governments, both in Europe and in the USA.[2] Thus, biopolymers will play an important role in future research, developments, and daily life.

Here, the term biopolymer is understood as designation for polymers, which are directly derived as a raw material from a natural and renewable resource, such as polysaccharides and proteins. Notable species with an important meaning for polymeric applications are chitin/chitosan, cellulose, hemicellulose, lignin, collagen, milk proteins, corn zein, and wheat gluten.

In the following, it will not be focused on biobased polymers that are derived via classical syntheses from renewable monomers, such as polylactic acid or polyethylene, obtained from bio-ethanol, or polymers modified with fatty acids from vegetable oils. Also biopolymers which are directly derived from genetically modified microorganisms, such as polyhydroxybutyrate, are not discussed here. Nevertheless, these biobased polymers have mentionable importance for the coatings technology and find versatile applications.[3–5]

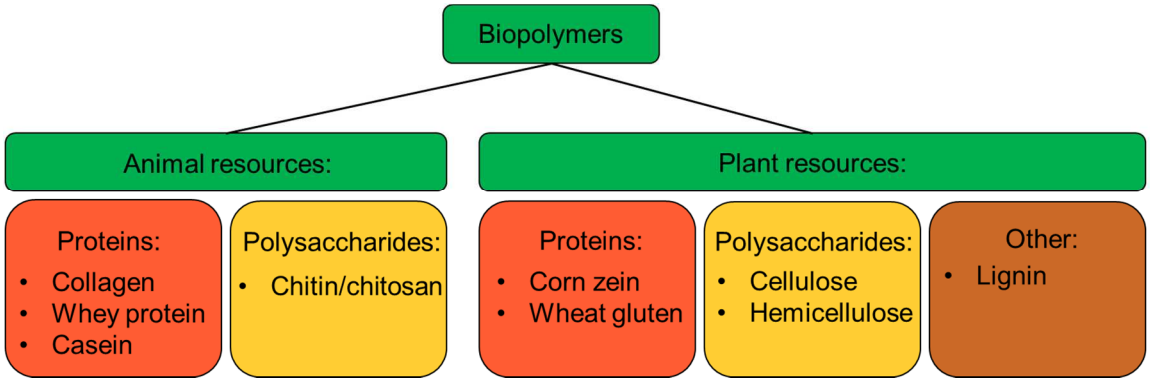


*Figure 1. Classification of biopolymers.*

Biopolymers can be classified by their natural origin, which can be either an animal or a plant resource. Furthermore, they can be divided into the two most abundant groups, i.e. polysaccharides and proteins. **Figure 1** shows an illustration of the classification of biopolymers, including important examples.

### 2.1.2 Properties, processing, and applications of biopolymers

Biopolymers are relatively inexpensive and offer advantageous features.[6] Based on their natural origin and their biological molecular structure, they are, in general, non-toxic, biodegradable, biocompatible, biofunctional, and sustainable.[3,7–9] Biopolymers are therefore suitable for applications, where these features are essentially important, e.g. in life sciences, biotechnology, medicine, and food technology as well as in conventional coating and adhesive systems (**Figure 2**).

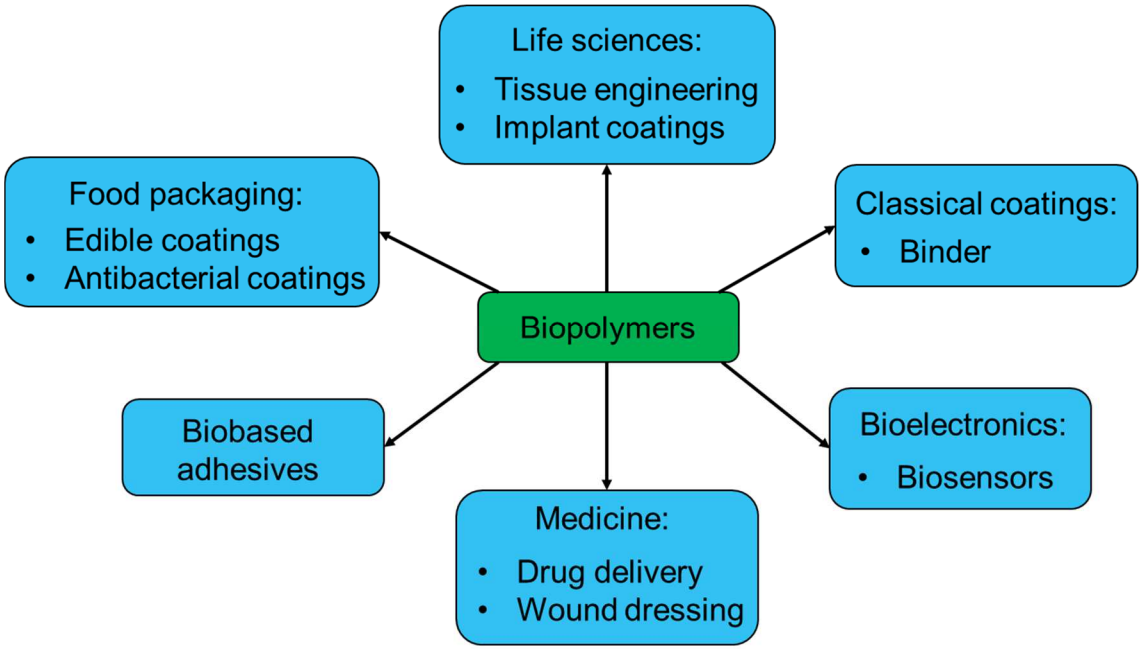


*Figure 2. Applications of biopolymers in modern technologies.*

Most biopolymers have a remarkably polar nature or at least exhibit regions with high polarity and show an excellent film-forming behavior. However, they tend to form brittle coatings and films. This is caused by their strong inter- and intramolecular interactions. These are based on van der Waals forces, hydrophobic and ionic interactions, and hydrogen bonding. Especially, the high density of formed hydrogen bonds leads to stiff polymer networks. Thus, often plasticizers, such as glycerol, ethylene glycol, sorbitol, or water are used to reduce the brittleness by interfering with hydrogen bonds between polymer chains.[10] This results, for instance, in an increase of elongation at break, but may also be accompanied by contrary effects, such as reduction of tensile strength.[11] Moreover, chemical modification or blending with other polymers, either synthetic or biobased ones, can significantly enhance mechanical properties of biopolymers.[12,13] Here, it is important to mention that in direct comparison protein-based films and coatings have better mechanical and functional properties, compared to their polysaccharide-based counterparts.[14]

An additional consequence of the polar nature of biopolymers is their poor moisture resistance. On the other hand, they have excellent barrier properties against non-polar gases, e.g. oxygen and carbon dioxide. To increase the moisture barrier properties, hydrophobic additives, like natural waxes or lipids, can be incorporated into biopolymer-based films and coatings.[15] Nonetheless, overall permeabilities are strongly connected to the amount of surrounding water and water molecules which are present inside the biopolymer network. Permeabilities increase with higher moisture contents, because the $T_g$ is lowered as a result of an increasing molecular mobility of the polymer chains. Here, also changes in viscosity, diffusivity, and flexibility occur.[16,17]

Processing of biopolymers is different from industrial processing of synthetic polymers. This is predominantly based on their heat sensitivity. Thus, processes including biopolymers are generally performed via solution casting.[18] To this, the polymers are dispersed in an aqueous solution, occasionally performed at slightly elevated temperatures and/or with the addition of organic solvents, e.g. ethanol. The resulting dispersion is then poured onto the targeted object or area and a continuous biopolymer layer is formed upon solvent evaporation and arrangement of polymer chains. In addition, other methods in connection with biopolymers are also commonly used, such as dip, spin, and spray coating processes.[19] Frequently applied industrial processes, which are based on plastification, e.g. extrusion, cannot be applied, because biopolymers have no

defined melting point and undergo fast denaturation or even decomposition upon heating.

Biopolymers have been extensively studied and are applied as coating material or represent the material itself for biomedical devices, like implants and scaffolds for tissue engineering.[20,21] Use of biopolymers for drug delivery systems and antibacterial coatings are also applications which are worth of mentioning.[22,23] Biopolymers are also successfully used as binders for conventional coating systems and have particular importance for biobased adhesives.[24,25] Some biopolymers exhibit naturally selective permeabilities for oxygen and carbon dioxide, when processed into films.[11] These selective properties are especially important for food packaging, because oxygen is a key factor for deterioration. It causes food oxidation and thereby, induces several undesired food changes, such as odor, color, and flavor. Biopolymer films should avoid high oxygen diffusion towards the food, to extend shelf life of the product.[26] On the other hand, carbon dioxide is produced by some foods due to deterioration and needs to be removed from the package.[27] Therefore, biopolymers with selective gas permeabilities are desired for applications in food technologies.

### 2.1.3 Important biopolymers for coating applications

**Chitin** is the second most abundant biopolymer and is found in the exoskeleton of crustaceans and in fungal cell walls (**Figure 3**).[28] It is poorly soluble in water and in common organic solvents. For technological applications it is often converted via de-acetylation into its more soluble derivative **chitosan**. Compared to chitin, chitosan is soluble in acidic, neutral, and alkaline solutions.[29] One of the most interesting properties of chitosan is its antimicrobial activity.[23] Therefore, it is of special importance for future applications in food, medical, and anti-fouling technologies. For instance, antibacterial chitosan films were successfully applied on fresh fruits and vegetables to increase their shelf life.[30] In medical applications, chitosan is used as antibacterial and cytocompatible coating for implants.[31] Moreover, it can also be processed into medical devices itself, such

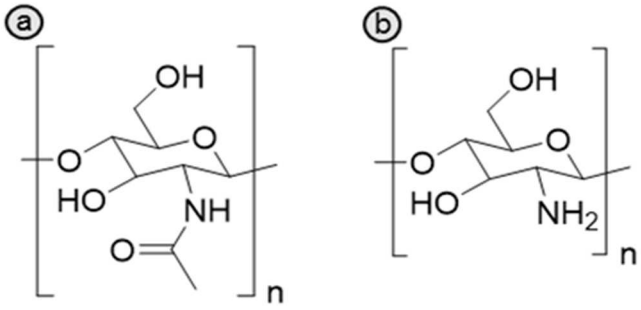


*Figure 3. Molecular structures of a) chitin and b) chitosan.*

as stents, via crosslinking with suitable agents, e.g. genipin.[32] Such chitosan-based stents exhibited superior mechanical and physiological properties compared to commercially available epoxide resin and metallic stents.

In general, chitosan films have good mechanical properties and exhibit a selective permeability to oxygen and carbon dioxide. On the other hand, they are highly permeable to water, which limits their use. Chemical and physical modifications, such as addition of crosslinking agents, irradiation, and ultrasonic treatments, are required to enhance mechanical and diffusion properties.[11] Chitosan can also be blended with other biopolymers to improve its properties. Moreira *et al.* combined the antimicrobial properties of chitosan with the excellent thermoplastic and film-forming properties of casein to prepare composite films.[33] These films were applied on several foods and successfully increased shelf life of the nutrients. Chitosan is, based on its good mechanical properties and antimicrobial activity, a biopolymer that will probably attract great attention in the future.

**Cellulose** is the most abundant occurring natural material (**Figure 4**). It has also a poor solubility in water and in common organic solvents.[6] This is based on its extremely high molecular weight, large density of hydrogen bonds, and partial crystallinity. With regard to coating processing cellulose needs to be chemically modified. First, its molecular weight is reduced via acidic hydrolysis of ether bridges between glucose units. Secondly, the number of hydrogen groups is decreased by esterification and etherification reactions with low molecular weight compounds. This yields flexible and transparent films, which are resistant to oil and fat migration and show moderate mechanical and barrier properties. Thus, cellulose ester- and ether-based films and coatings are meaningful for food packaging and medical applications, such as drug delivery.[34–36]

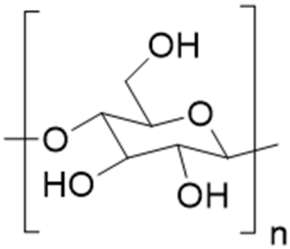

*Figure 4. Molecular structure of cellulose.*

Also waterborne systems for conventional coating applications are mentioned in literature.[37] Nevertheless, the attained moderate mechanical properties and the highly elaborate modification and processing of cellulose do not justify its use in conventional coating applications.

**Lignin** is a polydisperse and complexly branched amorphous biopolymer.[38] It is located in the cell wall of woody tree species and is mainly built upon the phenylpropane subunit accompanied by some substituent groups. It provides water-proofing of wood cell walls and is part of the water transport and regulation system.

Lignin has poor film-forming abilities, but has a lower tendency to sorb water compared to other biopolymers, e.g. cellulose. Its meaning for modern coating applications is low. Nevertheless, lignin may obtain a higher importance in the near future. At the moment, it appears as waste product of the pulp and paper industry and is mainly used as energy resource via combustion. Chemical modification of lignin presents an attractive option to overcome limitations.[39] Moreover, due to its high content of phenol, lignin can be used to replace up to 40 % of phenol in phenol-formaldehyde resins and can also be used for the synthesis of polyurethanes.[6]

**Hemicellulose** is a naturally branched and amorphous polysaccharide. It is bound to lignin and cellulose in cell walls and consists of hexose and pentose sugars, which are polymerized to a degree of about 500 units per molecule (degree of polymerization of cellulose is about 10.000).[40]

Coatings made of hemicellulose are very hygroscopic and even modification with hydrophobic agents or esterification and polymer grafting are insufficient in overcoming this drawback.[41] Therefore, only few coating applications of lignin are known, e.g. in food packaging or drug delivery systems.[8]

**Wheat gluten** is the proteinaceous fraction obtained as a byproduct of the isolation of starch from wheat flour.[42] The gluten proteins are derived from the storage proteins of the wheat grain.[43] Gluten has one of the lowest prices of all available plant proteins and consists of two classes of proteins with equal percentage amounts, i.e. gliadin and glutenin.[44] Wheat gluten has a high amount of non-polar amino acids, such as proline, leucine, and glutamine. In addition, it lacks mentionable amounts of ionizable residues. As a consequence, wheat gluten has a highly hydrophobic character and is insoluble in water.

Films made of wheat gluten can be prepared by solution casting, but high amounts of organic solvents are required. Another option for the incorporation into coating formulations is based on chemical modification. Water solubility of gluten can be provided by acylation, e.g. with anhydrides of succinic, maleic, and acetic acid.[44,45] Aqueous wheat gluten dispersions have excellent film-forming characteristics and exhibit a strong adhesion to various surfaces. Like

other proteins, gluten is very brittle and thus, incorporation of plasticizers is essential. Gas and water barrier properties of wheat gluten coatings are moderate, but can be enhanced by crosslinking of the peptide chains.[2]

Notable applications of wheat gluten in the coatings technology are the combination with conventional systems, such as UV-curable coatings, and the use as binder in papercoatings.[44,46,47]

**Collagen** is the most occurring fibrous protein in animals. Due to its importance for the structural framework of animals, it obtained the nickname “steel of biological materials”.[48] Since collagen is insoluble in water, it is usually pretreated before application in coatings by conversion into soluble **gelatin**.[49] Collagen is only used for some applications in coatings technology.[50,51]

On the other hand, gelatin, i.e. partially hydrolyzed collagen, is able to form flexible and strong films, when mixed with plasticizers, such as glycerol or sorbitol.[19] As gelatin is poorly water-resistant, it needs to be modified with other biomolecules or synthetic polymers to overcome its limitations. To this, gelatin is combined with lipids, soy protein isolate, chitosan, pectin, polyvinyl alcohol, or polyethylene.[49] Gelatin-based films are commonly used in food packaging.[52] Moreover, applications in bioengineering, e.g. tissue engineering, artificial skin, neuronal regeneration, and bone grafts, have been studied, due to the good antigenicity, biodegradability, and biocompatibility of gelatin.[53] Therefore, future applications of gelatin will predominantly focus on life sciences.

**Zein** is the main protein of corn and accounts for 45-50 % of the total protein amount.[54] It forms tough, glossy, and fat resistant films upon casting from aqueous alcohol solutions. Such films are predominantly used in direct food preservation, but also the use of zein as paper coating for magazine covers has been described.[55,56] Zein also presents a suitable encapsulation matrix for pesticides with agricultural purposes.[54] However, neither conventional coating applications nor use in life sciences are known.

**Milk proteins** are an important and interesting group of proteins. The proteinaceous amount in bovine milk accounts for about 3 wt%.[57] There are two main milk proteins, i.e. casein and whey proteins. Casein makes up approximately 78 wt% and whey proteins account for about 17 wt% of total milk proteins. Whey proteins represent a number of different proteins, whereby lactalbumin and lactoglobulin are the predominant ones.[58]

Today, milk proteins are probably the best well-studied and characterized food proteins. The first publication about milk proteins was published by Berzelius in 1814, followed by numerous studies and publications up to the present day.[59]

The whole amount of milk proteins can be used to form edible films and coatings, which can retard moisture loss, exhibit good gas barrier properties, show good tensile strength and moderate elongation, and have no flavor or taste.[14] This is usually achieved via solution casting methods, using water or ethanol (or a combination of both) as dispersing medium. Processing of films can be complicated due to presence of lactose, which tends to undergo crystallization, resulting in non-homogeneous films.[60] Thus, milk proteins are generally used in isolated forms for the application in films and coatings.

Whey protein isolate (WPI; 90 wt% protein content) forms aqueous protein dispersions, which are insoluble in water upon drying.[61] Due to this unique property, it seems especially suitable for coating applications. WPI forms edible and flexible films with good oxygen and carbon dioxide barrier properties. This makes it interesting for potential packaging applications. Nonetheless, compared to other biopolymers, whey protein films have the poorest oxygen barrier properties.[62] Main applications of whey protein coatings are as packaging material for the extension of food shelf life and quality.[63,64] Applications in other sectors, such as conventional coatings technology or life sciences, are rare, because whey protein-based films have not been extensively studied so far. This is probably based on their high separation and purification costs as well as their inferior physical properties.[14]

On the other hand, the main milk protein casein is able to easily form films from aqueous dispersions with excellent mechanical and chemical properties.[65] This is based on its random coil nature and its ability to form extensive intermolecular interactions.[66] Casein is a very interesting biopolymer for the coatings technology with versatile applications in manifold sectors. However, unmodified casein is susceptible to moisture and films are easily dissolved in water due to its hydrophilic nature.[67] This is the major drawback of casein.[68]

## 2.2 Casein

### 2.2.1 Bovine casein

Casein is the major protein occurring in the milk of female mammals. Its amount and composition differs from mammalian species to species. Bovine milk is the most commonly used resource for milk proteins in the Western world. There are four major casein components in bovine milk, which account for 24-29 g/L of the whole milk. These major components are $\alpha_{s1}$-casein (38 wt%), $\alpha_{s2}$-casein (10 wt%), β-casein (36 wt%), and κ-casein (13 wt%). In addition, also a minor component, called γ-casein (3 wt%), is present.[69] **Table 1** summarizes these data.

*Table 1. Contents of caseins in bovine milk.*

| Casein fraction: | Amount in g/L[a)] | Rel. amount in wt% |
|---|---|---|
| $\alpha_{s1}$-casein | 9.5 | 38 |
| $\alpha_{s2}$-casein | 2.5 | 10 |
| β-casein | 9.0 | 36 |
| κ-casein | 3.25 | 13 |
| γ-casein | 0.75 | 3 |

a) Based on a total casein amount of 25 g/L.

The cellular synthesis and secretion of bovine casein have been intensively studied and described in literature.[70–72] **Figure 5** illustrates the particular steps. The individual caseins are produced in the endoplasmic reticulum of mammalian cells as precaseins, exhibiting N-terminal signal peptides. This allows for the interaction of caseins with signal recognition particles and receptors in the cell membrane. Precaseins migrate into the Golgi apparatus, where excision of the signal peptides and phosphorylation and glycosylation (only κ-casein) of caseins take place. The resulting spherical first casein particles exhibit diameters of about 10 nm. In the next step, calcium phosphate is bound to the phosphorylated caseins, which are subsequently enclosed into small vesicles.[73] Here, aggregation of small casein particles leads to the formation of colloidal casein particles. In the end, the vesicles leave the Golgi apparatus and move to the apical membrane of the cell. Exocytosis occurs and the colloidal casein particles are passed into the alveolar lumen. The duration of the complete casein synthesis and secretion is about 30 min.

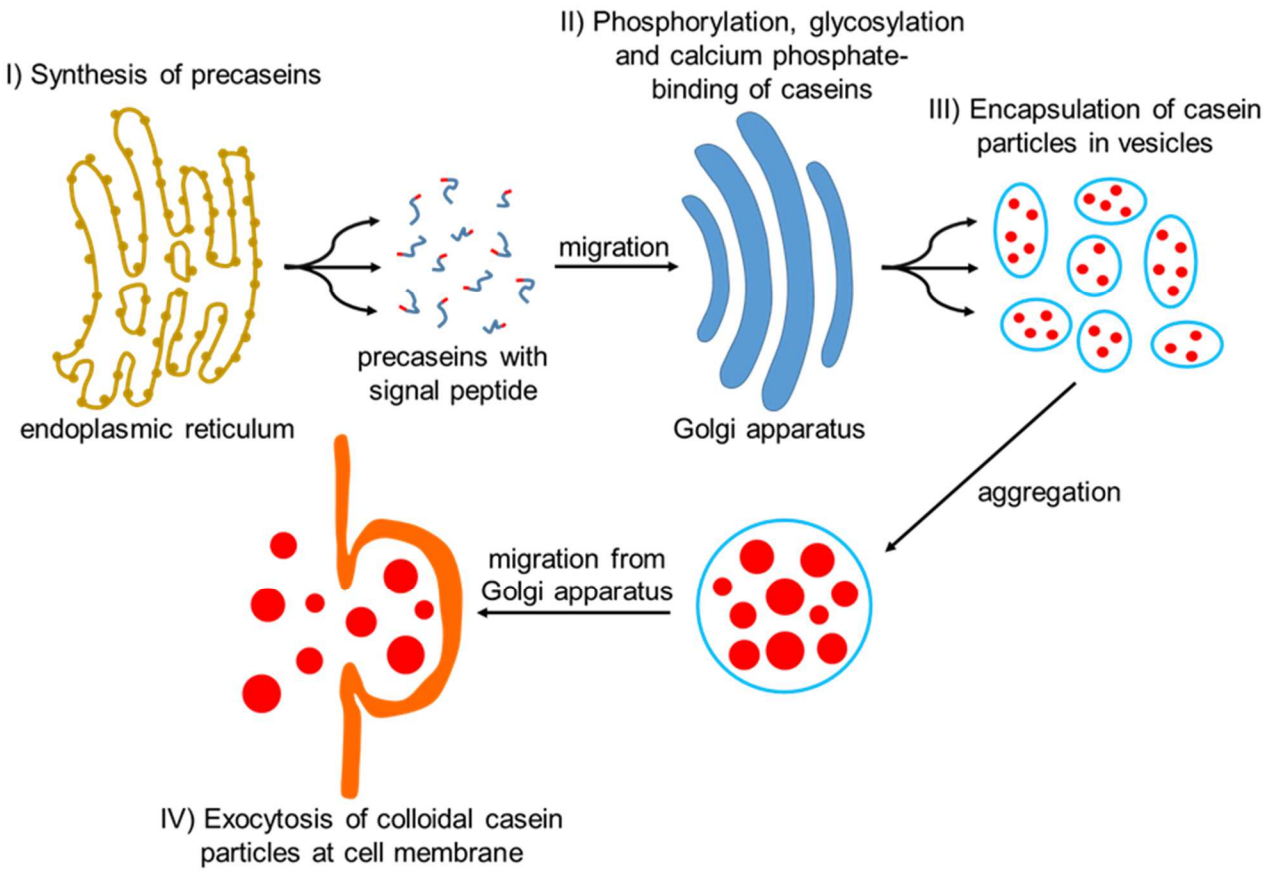


*Figure 5. Synthesis and secretion of colloidal casein particles. The illustrations refer to Farrell et al.*[71]

### 2.2.2 Chemical compositions and structures of caseins

Each casein fraction has its unique amino acid composition (primary structure) and molecular weight. This leads to individual properties of the respective caseins. In comparison to other proteins, all caseins exhibit only little secondary structure, such as α-helices or β-sheets. As a consequence, they are highly flexible proteins with random coil character.[74] Due to their lack of frequent secondary structures, caseins do not crystallize. Moreover, their tertiary structure is described in literature as “definite unordered”.[75] An explanation for the highly flexible nature of casein peptide chains is based on their ability to form the above mentioned colloidal protein particles.

All casein fractions have phosphorylated serine residues, but show different degrees of phosphorylation. This enables the interaction of caseins with calcium and calcium phosphate. Binding of calcium phosphate has two important aspects. Transport of these mineral salts in casein particles ensures an easy support of the mammalian newborns with sufficient calcium for their bone growth and prevents the mammary gland from calcification at the same time.[74] In contrast to the other caseins, κ-casein is the only casein which is glycosylated. Depending on the respective genetic variant, carbohydrates are bound to particular serine and threonine residues.[70] This glycosylation of κ-casein is responsible for the water dispersibility of total casein. A broad genetic variety of all four major caseins occurs in bovine milk. This is probably due to versatile genetic mutations of bovine species during evolution. Holt’s comprehensive study from 1992 describes the presence of the genetic variants and provides an excellent overview about predominant species and their primary structures.[70]

In Western breeds of cattle, at least five genetic variants of $\alpha_{s1}$-casein have been identified, whereas the B variant with eight phosphorylated serine residues ($\alpha_{s1}$-casein B-8P) is predominant. It consists of 199 amino acids and has a molecular weight of 23,600 g/mol.[74] The majority of its charge density is located on a hydrophilic part in the middle of the molecule between its hydrophobic N- and C-terminals. **Figure 6** displays a reduced sequence structure of $\alpha_{s1}$-casein B-8P as well as its primary structure.

Four genetic variants of $\alpha_{s2}$-casein have been identified so far with variant A as the predominant one. This variant has eleven phosphorylated serine residues per molecule ($\alpha_{s2}$-casein A-11P) and consists of 207 amino acid residues. Its molecular weight accounts for 25,200 g/mol. **Figure 7** shows the reduced sequence structure and the primary structure of $\alpha_{s2}$-casein A-11P.

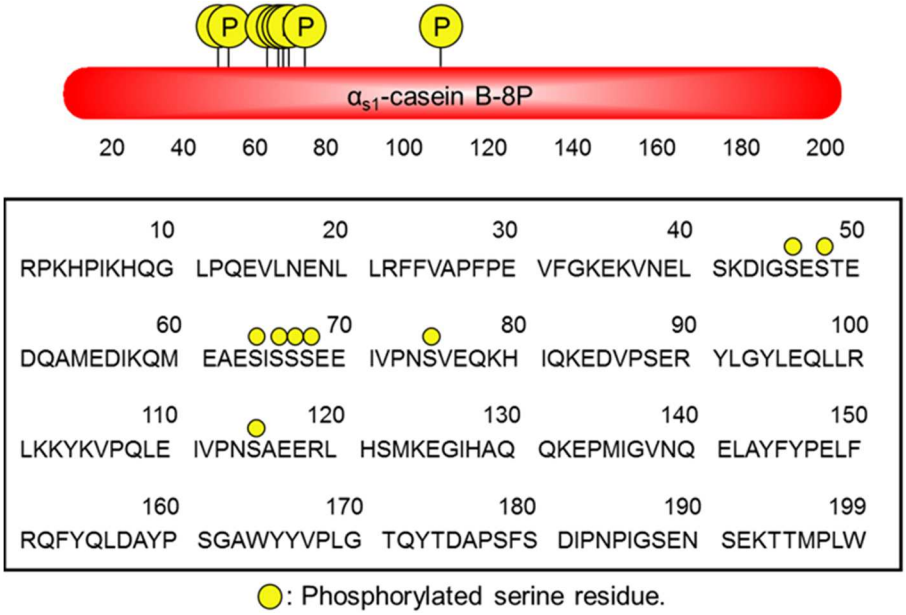


*Figure 6. Reduced sequence structure and primary structure of $\alpha_{s1}$-casein. Primary structure refers to Eigel et al. (1984) and Stewart et al. (1984).*[76,77]

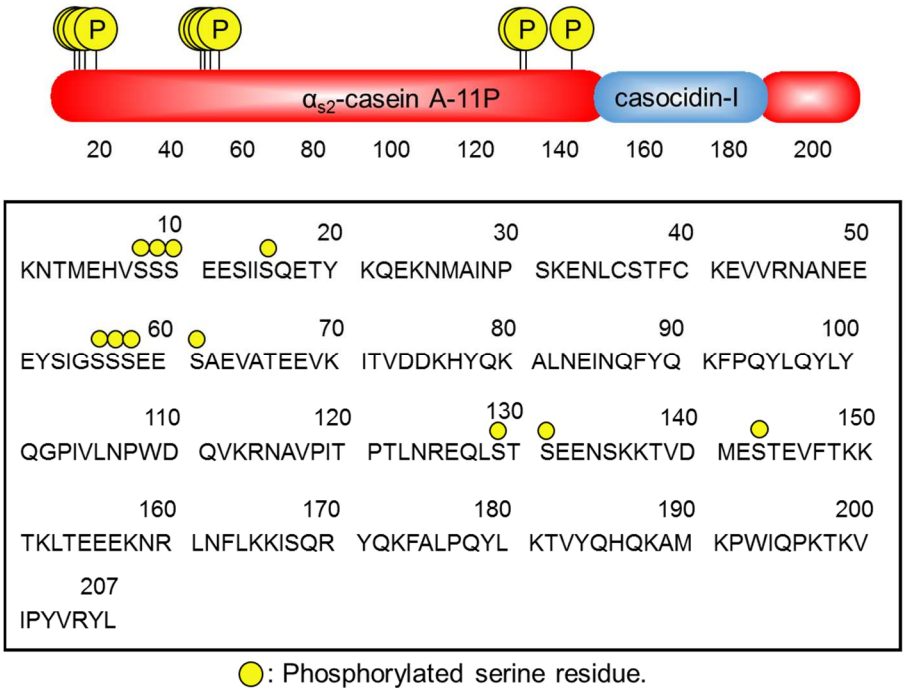


*Figure 7. Reduced sequence structure and primary structure of $\alpha_{s2}$-casein. Primary structure refers to Eigel et al. (1984) and Stewart et al. (1987).*[76,78]

Seven genetic variants of β-casein are known with three variants, i.e. $A^1$, $A^2$, and $A^3$, occurring in major amounts in Western breeds. The predominant variant $A^2$ has five phosphorylated serine residues and is called β-casein $A^2$-5P. This variant consists of 209 amino acid residues and has a molecular weight of 24,000 g/mol (**Figure 8**).

In case of κ-casein, only two genetic variants have been identified so far. The predominant one is Type A. This variant consists of 169 amino acid residues and has a molecular weight of 19,000 g/mol. Normally it has one phosphorylated serine residue at position 149 (κ-casein A-1P). However, variants are also known which exhibit up to three phosphorylated residues.[70] In addition, κ-casein has glycosylated amino acid residues. This glycosylation occurs through *O*-glycosidic linkages between *N*-acetyl-galactosamine residues and threonine or serine residues of the peptide chain. Glycosylation of κ-casein has been observed at $Thr^{121}$, $Thr^{131}$ (or $Ser^{132}$), $Thr^{133}$, $Thr^{136}$, $Thr^{142}$, $Ser^{149}$, and $Thr^{165}$.[79,80] Not all of these amino acid residues are glycosylated all the time, resulting in a varying degree of glycosylation, just as it has been observed for phosphorylation. **Figure 9** shows the reduced sequence structure of κ-casein A-1P with six glycosylated residues and its primary structure.

As a special annotation to κ-casein, the aspartic protease chymosin is able to specifically cleave the $Phe^{105}$-$Met^{106}$ peptide bond in κ-casein.[81] This results in the formation of a hydrophobic part, called para-κ-casein (Pos.: 1–105) and a hydrophilic part, called caseinomacropeptide (Pos.: 106–169; see Figure 9). The phosphorylated and glycosylated amino acid residues are all localized on the hydrophilic part and are responsible for its highly hydrophilic nature.

**Table 2** summarizes the structural characteristics of the four major caseins.

*Table 2. Structural characteristics of major caseins.*

| Casein fraction: | Major genetic variant | Number of amino acids | Molecular weight in g/mol | Degree of phosphorylation | Degree of glycosylation |
|---|---|---|---|---|---|
| $\alpha_{s1}$-casein | B-8P | 199 | 23,600 | 8 | / |
| $\alpha_{s2}$-casein | A-11P | 207 | 25,200 | 11 | / |
| β-casein | $A^2$-5P | 209 | 24,000 | 5 | / |
| κ-casein | A-1P | 169 | 19,000 | 1 | ≤ 7 |

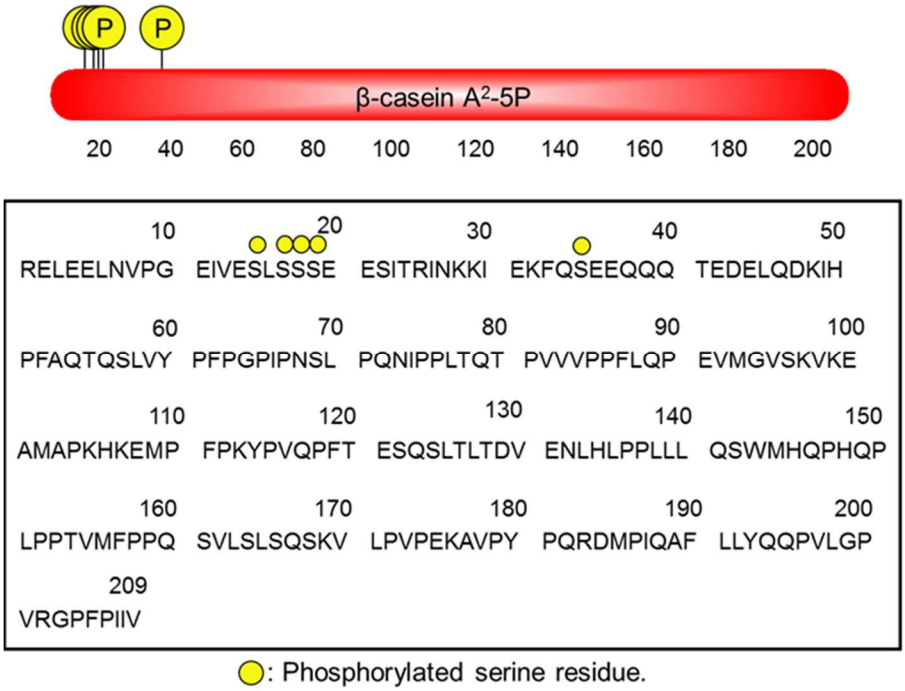


*Figure 8. Reduced sequence structure and primary structure of β-casein. Primary structure refers to Eigel et al. (1984) and Stewart et al. (1987).*[76,78]

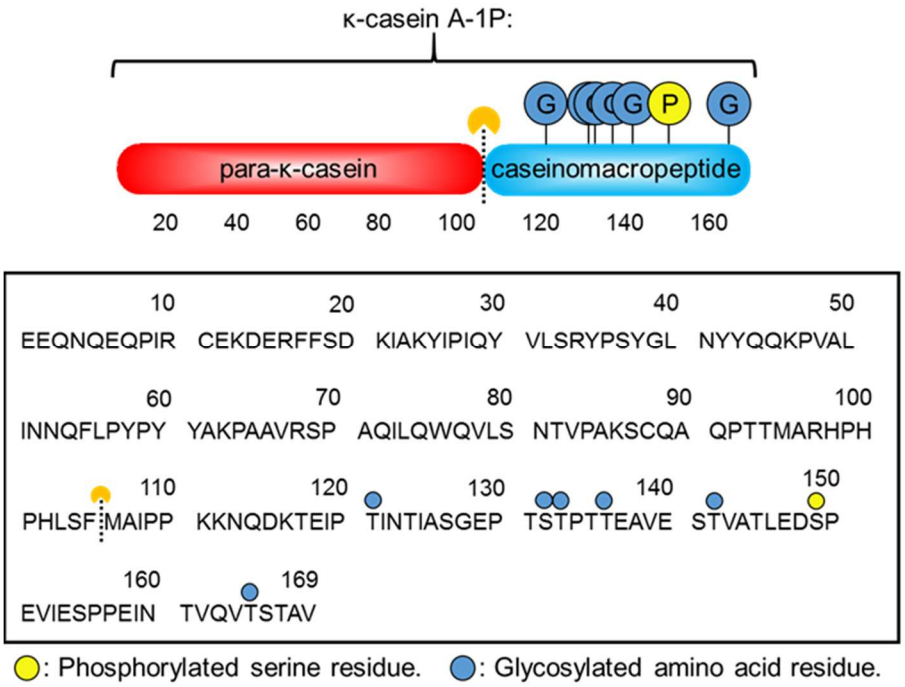


*Figure 9. Reduced sequence structure and primary structure of κ-casein. Primary structure refers to Eigel et al. (1984) and Thompson et al. (1985).*[76,82]

### 2.2.3 Physico-chemical properties of caseins

Based on their respective chemical structure, the particular caseins have very individual physico-chemical properties. In the following, the most important properties are considered.

$\alpha_{s1}$-casein is capable of binding $Ca^{2+}$ due to the availability of sufficient phosphorylated serine residues. Thus, it is calcium sensitive, which means that the protein will aggregate and precipitate in the presence of $Ca^{2+}$ ions. It is not able to participate in the formation of disulfide bonds, because it lacks any cysteine residue. The majority of its charge density is localized on the hydrophilic middle part, which is enclosed by its hydrophobic N- and C-terminal (Figure 6). The isoelectric point of $\alpha_{s1}$-casein is at 4.5.[74]

$\alpha_{s2}$-casein exhibits the highest amount of phosphorylated serine residues compared to the other caseins. It is highly calcium sensitive and the most hydrophilic casein. It has two regions with a high charge density and a hydrophilic N-terminal and a hydrophobic C-terminal (Figure 7). It has an isoelectric point of 5.0. Moreover, $\alpha_{s2}$-casein is able to form disulfide bonds due to the availability of cysteine residues. Interestingly, a distinct peptide segment of $\alpha_{s2}$-casein, which is called casocidin-I peptide (Pos.: 150–188), was verified to exhibit antibacterial activity. For example, it inhibits the growth of *Escherichia coli* and *Staphylococcus* bacteria.[83]

β-casein has an isoelectric point of 4.8 and belongs also to the calcium sensitive caseins. It has several phosphorylated serine residues. Like $\alpha_{s1}$-casein it has no cysteine residues and thus, lacks the opportunity for the formation of disulfide bridges. It consists of a polar N-terminal and a large hydrophobic C-terminal (Figure 8). This means that β-casein has an amphiphilic structure that is similar to conventional surfactants. It exhibits emulsifying properties.[84] Nevertheless, it is the most hydrophobic casein, because it contains more hydrophobic amino acid residues than any of the other caseins.[75]

The last major component, κ-casein, differs strongly from the other casein fractions. It exhibits an isoelectric point of 5.6 and is not calcium sensitive, because it lacks sufficient phosphorylated amino acid residues to interact with $Ca^{2+}$ ions.[85] It is capable of the formation of disulfide bonds due the presence of cysteine residues, providing intra- and intermolecular crosslinks. It is the only casein which has glycosylated amino acid residues. This glycosylation provides the highly amphiphilic character of κ-casein. All glycosylated residues are localized on the C-terminal and make this peptide segment highly hydrophilic.

As mentioned before, this peptide segment (caseinomacropeptide) can be split off by chymosin (Figure 9). The remaining C-terminal (para-κ-casein) has neither any phosphorylated nor any glycosylated amino acid residues and is highly hydrophobic.

**Figure 10** shows schematic molecular structures of the particular caseins which illustrate the presence of polar and non-polar terminals and segments. To conclude, caseins are very individual molecules with specific properties, but have all rather a hydrophobic than a hydrophilic character.

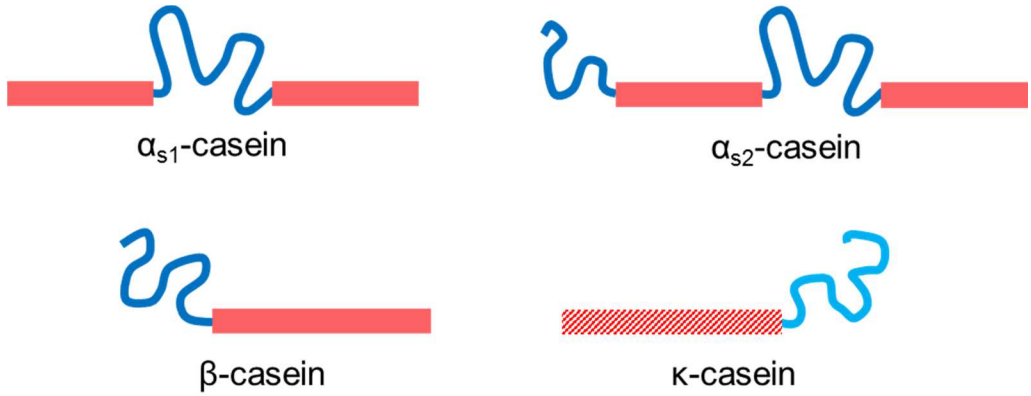


*Figure 10. Schematic molecular structures of caseins. Rectangular bars display hydrophobic segments. Blue lines represent hydrophilic segments (caseinomacropeptide part of k-casein is highlighted in light blue).*

### 2.2.4 The casein micelle

In aqueous environment, caseins self-organize and form very complex colloidal aggregates, i.e. the casein micelle.[71] The proteinaceous amount of the micelles accounts for 92 % and 8 % are low molecular mass substances, predominantly calcium phosphate.[86] The size distribution of these micelles is very polydisperse and their diameters vary between 50 nm and 500 nm, whereas the mean diameter is about 120 nm.[87] Since casein micelles serve as nutrition per se and provide the transport of calcium for nursing mammals, a distinct size of the micelles is naturally not essential. Aggregation of small pre-micelles to colloidal casein micelles during synthesis in the mammary gland happens randomly and yields micelles of different sizes (see section 2.2.1). Stability of the casein micelle is provided by κ-casein, which acts as a stabilizing agent due to its highly amphiphilic structure. The other main caseins, i.e. $\alpha_{s1}$-, $\alpha_{s2}$-, and β-casein, are present in the interior of the micelle. Only the hydrophilic part of κ-casein (caseinomacropeptide) protrudes into the aqueous environment and enables water dispersibility of the entire micelle.[88] Over the years, several models for the casein micelle structure have been developed. These models can be reduced to three main models which co-exist in present literature: The sub-micelle model, the nanocluster model, and the dual-binding model. Illustrations of the three models are shown in **Figure 11**.

The sub-micelle model was the first model and was introduced by Walstra in 1990 (**Figure 11a**). It suggests the existence of sub-micelles with diameters of about 15 nm which are linked together by colloidal calcium phosphate (CCP) bridges.[89] This assumption was based on neutron and X-ray diffraction analyses, which verified the presence of subunits. The model proposed the existence of two different types of sub-micelles. One type exhibits a high amount of κ-casein that is located on the surface of the subunit. The other type contains no or very little κ-casein. The latter ones form the inner core of the casein micelle, while the sub-micelles with κ-casein limit the size of the micelle by forming the interface to the surrounding aqueous medium.

As proposed by Walstra in 1990, stability of the casein micelle is provided by the CCP which crosslinks the sub-micelles. However, subsequent experiments showed this to be very unlikely. CCP can be removed from the casein micelle by acidification at low temperatures, whereas no disruption of the micelle occurs.[90] Moreover, treatment with urea disrupts the micelle, while no dissolution of CCP takes place.[91] Therefore, stability of the casein micelle

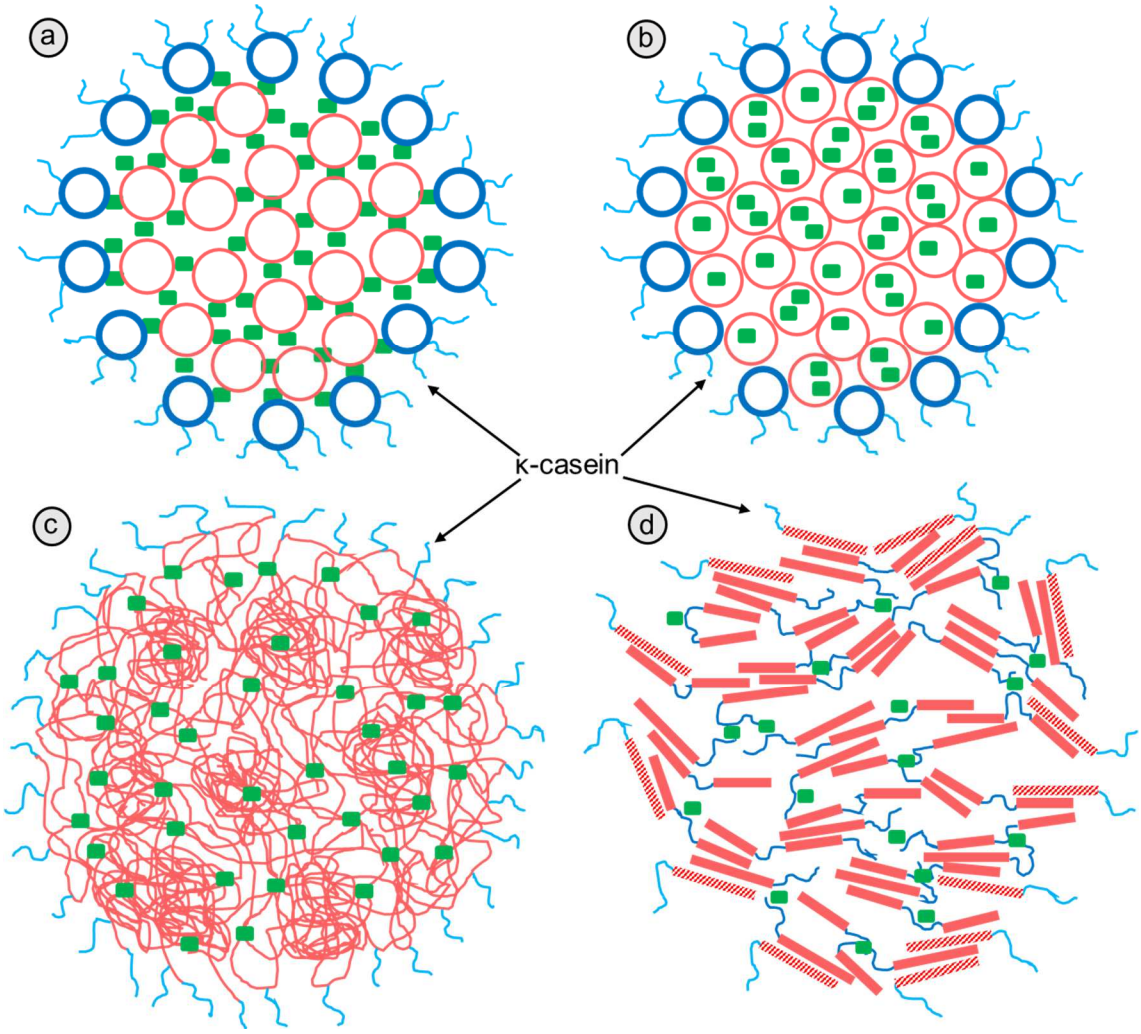


*Figure 11. Illustrations of casein micelle models. a) Sub-micelle model from 1990, b) revised sub-micelle model, c) nanocluster model, and d) dual-binding model. CCP is indicated by green squares (■).*

cannot solely be provided by CCP, but additional interactions, such as hydrophobic interactions and hydrogen bonding, must be involved. In 1999, Walstra proposed a revised version of his sub-micelle model (**Figure 11b**). Now, the CCP was incorporated as nano-sized particles into the sub-micelles and did no longer "cement" the subunits together.[92] This model finds broad acceptance in literature and explains well the properties of the casein micelle.

The second model, i.e. the nanocluster model, is endorsed by Holt and De Kruif.[70,93] This model describes the casein micelle as a continuously crosslinked protein gel (**Figure 11c**). Crosslinks between the particular caseins arise from hydrophobic interactions, hydrogen and ion bondings, and van der Waals interactions. The CCP is imbedded as nano-clusters with diameters of about 2 nm within the casein network. The calcium sensitive caseins bind via their phosphorylated serine residues to CCP particles and

thereby limit their size by forming a protein layer. The average distance between neighboring CCP nanoclusters is about 20 nm. The space between is filled with crosslinked casein molecules, whose density fluctuates.[93] This distance corresponds well to determined diameters of the by Walstra proposed sub-micelles and explains the existence of such subunits. The nanocluster model is not in severe conflict with the sub-micelle model as the macroscopic view of the micelle is similar, but rather helped to redesign the first sub-micelle model.

The latest model, the so-called dual-binding model, was introduced by Horne in 1998 and focusses in detail on the intermolecular interactions that provide the stability of the casein micelle.[90,94,95] It suggests a two-step mechanism. At first, crosslinks are formed mainly via hydrophobic interactions between particular casein molecules. This results in kind of a polymerization of the molecules to a small degree. Subsequently, small CCP crosslinking bridges are formed between the casein molecules. κ-casein acts as a chain terminator and limits the growth of the casein micelle (**Figure 11d**). The major drawback of this model is the assumption of CCP only as small CCP bridges (ångström-sized). This is inconsistent with conducted small-angle neutron and X-ray scattering experiments, since contribution of such small CCP bridges would not be detectable.[93] Therefore, larger CCP particles must be available in the casein micelle, e.g. as it was proposed in the revised sub-micelle model and by Holt and De Kruif. Summarizing, the dual-binding model should not be considered as a totally independent model, but it can be considered as a supplementary model. It provides detailed reasons for the molecular binding of casein molecules and CCP.

Until now, none of the developed casein micelle models have proved to be “the true model”. Discussion is still conducted intensively and from time to time also aggressively in literature. In general, all three models agree with the presence of a stabilizing κ-casein layer on the surface of the micelle, while the inner core consists of the hydrophobic caseins. κ-casein is unevenly distributed on the micelle surface, covering only about one third of the entire surface.[91] It forms islands which are surrounded by α- and β-casein molecules, resulting in hydrophobic patches. This also explains that other molecules, e.g. enzymes are able to penetrate the surface of the micelle. For instance, chymosin must pass the stabilizing layer of κ-casein to reach its specific cleavage site. In addition, diffusion of the other caseins away from the micelle has been observed. For example, β-casein is liberated from the micelle upon cooling.[91]

### 2.2.5 Stability and coagulation of casein micelles

Casein micelles are undoubtedly very stable particles compared to other protein structures. They are very resistant towards the effects of organic solvents, heat and cold, and they can be dried without affecting their properties.[96,97]

As mentioned before, stabilization of casein micelles is provided by a layer of κ-casein molecules or more precisely its hydrophilic macropeptide parts, which are present on the micelle surface. This layer leads to an electrosteric stabilization of the entire particle. The mechanism is based on the formation of a net charge on the surface, which is negative at the p*H* of native milk (i.e. p*H* 6.7), and a steric repulsion provided by the protruding hydrophilic parts of κ-casein.[98] In literature, this stabilizing κ-casein layer is prominently named as "hairy layer".[99,100] **Figure 12** illustrates on a molecular level the presence of the "hairy layer".

The thickness of the "hairy layer" accounts for about 10–12 nm.[91,101] Thus, steric hindrances caused by the protruding protein chains are more important for the stabilization of the micelle than resulting repulsive forces based on net charges. Entropic repulsion by the "hairy layer" becomes effective with respect to advancing micelles long before an effective distance for electrostatic repulsion is reached. Destabilization of casein micelles takes place via removal of the "hairy layer" or via collapse of the protruding κ-casein chains, e.g. as consequence of a net charge reduction or interactions with organic solvents.

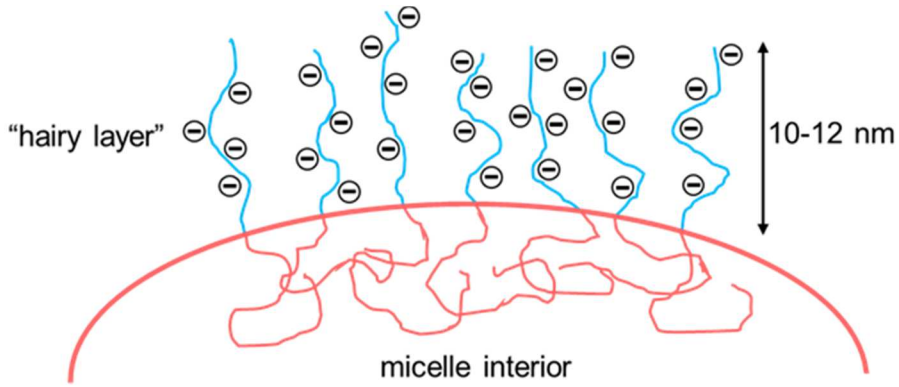


*Figure 12. Stabilization of casein micelle via "hairy layer" of κ-casein at pH of native milk. The hydrophilic parts of κ-casein (caseinomacropeptide) protrude into the aqueous environment, while the hydrophobic parts (para-κ-casein) are located inside the micelle.*

Casein micelles are very heat stable. Milk can be heated at p*H* 6.7 to 100 °C for 24 h without affecting the stability of the micelles and even withstands heating up to 140 °C for at least 20-25 min.[102] The excellent heat stability of caseins is not fully understood, but it is very likely that their lack of frequent secondary and tertiary structures plays an important role. For instance, the globular whey proteins of milk are more heat-sensible due to their noticeable presence of secondary and tertiary structures.[103]

Nonetheless, longer reaction times at temperatures of about 140 °C or more result in destabilization and coagulation of casein micelles. This occurs due to denaturation of particular casein molecules and/or the entire casein micelle. Three major effects of heat-induced destabilization are known:[104] I) Subjection to elevated temperatures leads to a partial dephosphorylation of the caseins, decreasing their interaction potential with CCP. II) Dissociation of carbohydrates, which provide the water solubility of caseinomacropeptide, may take place. Consequently, the decline in water solubility of κ-casein affects the dispersibility of the entire micelle. III) Precipitation of previously soluble calcium phosphate onto the casein micelle can occur. This interferes the formation of the “hairy layer” and leads to coagulation. **Figure 13** summarizes the possible reasons for the heat-induced destabilization and coagulation of casein micelles.

In industrial cheesemaking, the acid induced and the enzymatic coagulation of milk are the most frequently used techniques.[105] Also combinations of these two techniques are commonly applied at elevated temperatures and $CaCl_2$ is often added to facilitate coagulation of the calcium sensitive caseins. However, many different methods exist for cheesemaking, considering the large variety of cheeses and industrially used milk (additionally to cow’s milk).

Acid induced coagulation is performed via acidification to the isoelectric point of casein, i.e. at p*H* 4.6.[106] Above this p*H* value, the micelles are stabilized by a negative net charge, as this is the case for naturally occurring milk. To induce coagulation of milk, bacteria, such as *Lactobacillus delbrueckii* or *Streptococcus thermophiles*, are used.[107] Acidification occurs via fermentation of lactose into lactic acid, resulting in charge neutralization of the protruding κ-casein chains. Consequently, casein micelles lack sufficient stabilization and start to aggregate. Destabilization of dispersed casein micelles can be easily achieved by use of inorganic acids, such as sulfuric acid or hydrochloric acid. The coagulation mechanism of dispersed casein particles occurs in the same way as for casein in milk (**Figure 14a**).

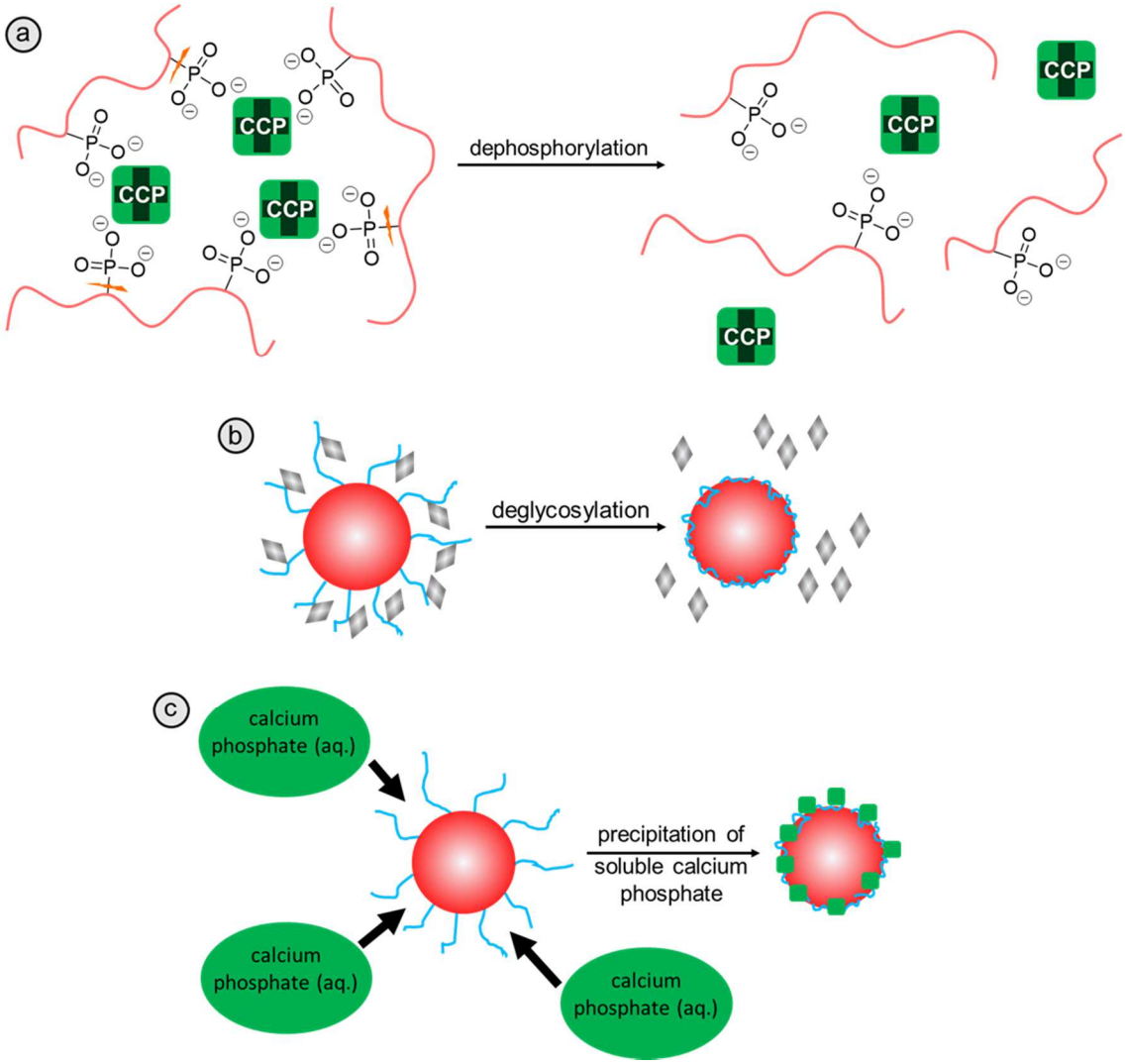


*Figure 13. Destabilization of casein micelles via heat: a) Dephosphorylation, b) deglycosylation, and c) precipitation of soluble calcium phosphate.*

Destabilization of casein micelles via enzymes has been used by mankind for thousands of years in cheesemaking. This reaction also occurs naturally in the stomachs of young mammals. As mentioned before, the protease chymosin is capable to specifically cleave the $Phe^{105}$-$Met^{106}$ bond in κ-casein.[81] This reaction is 1000-times faster than cleavage of any other peptide bond in caseins.[108] It follows first order kinetics and is diffusion controlled, because the casein micelle surface is very large compared to the size of a chymosin molecule.[109] The cleavage results in the release of hydrophilic caseino-macropeptide (see section 2.2.2). Casein micelles become hydrophobic and start to aggregate due to the lack of electrosteric stabilization (**Figure 14b**). Precipitation of casein occurs when about 90 % of the κ-casein molecules are cleaved.[110]

In addition, the stability of casein micelles is influenced by organic solvents in higher concentrations, e.g. ethanol, methanol, and acetone.[102,111,112] The mechanism of the solvent induced coagulation is still under discussion, but a collapse of the “hairy layer” can likely be assumed as the key factor. Unfavorable interactions of the caseinomacropeptide parts with poor solvents reduce drastically their free volume and result in destabilization of the entire micelle (**Figure 14c**). Coagulation of casein via organic solvents has no industrial significance and is therefore not further discussed in detail.

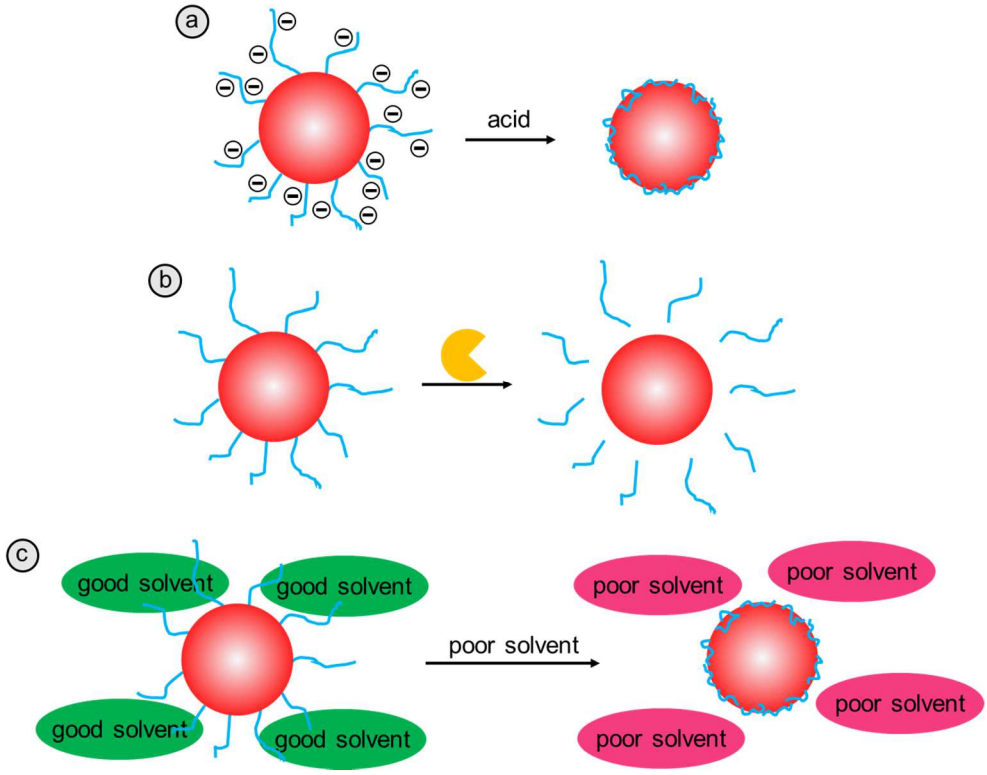


*Figure 14. Destabilization of casein micelles via a) acidification to isoelectric point, b) enzymatic cleavage of κ-casein, and c) interaction with poor solvents.*

### 2.2.6 Non-food applications of casein

The excellent films forming and adhesives properties of casein have been known and utilized throughout history of mankind. First verified non-food applications of casein were glues and paints in ancient Egypt.[69] Since then, non-food applications underwent noticeable changes. Up now, its use as binder in coating formulations and adhesives is still eminent. However, since casein is an everywhere present foodstuff, it is important to consider well influences on world's food supply regarding non-food applications of casein. On the other hand, as thousands of tons of milk are discarded every single day, e.g. due to mismatching governmental high standards for nutrients, negative impacts on food supply can easily be minimized, if not completely be ruled out.[113] Use of casein for non-food applications from such sorted out resources would represent a convenient solution and would reduce food waste at the same time.

Following, applications of casein in coatings, adhesives and glues, fiber-based materials, plastics, and packaging materials are described as well as selected potential applications in near future.

#### Coatings

Casein is ideally suited as binder in coating formulations. In addition to its good film-forming behavior, the availability of segments with different polarities and its very flexible protein chains make casein a very good wetting agent for pigments and inks. Thus, casein-based paints and coatings were frequently used in decorative paintworks independently of time.

In the last decades, application of casein decreased, e.g. in paper and board coatings, mainly due to high costs of purified casein. Nonetheless, it is still used in high quality paper finishing.[69] In connection with the rising demand for replacement of petroleum-based polymers by renewable materials, casein is gaining interest as polymer for modern coating formulations again. Noteworthy is its potential use in emulsifier-free emulsion polymerizations in combination with synthetic polymers, such as acrylates, to obtain environmentally friendly waterborne binders.[25,114] These hybrid binders combine the biocompatibility and good adhesive properties of casein with mechanical strength of synthetic polymers.

#### Adhesives and glues

At the beginning of the 20$^{th}$ century, casein based glues were commonly applied in exterior and interior woodworking.[115–117] The good heat and moderate moisture resistance of casein combined with its good substrate penetrability,

cold curing ability, and strong adhesion to cellulose were essential for this purpose. Often, casein was crosslinked with formaldehyde to improve its water stability. This technique has been used for decades and still is.[118] Worth of mentioning is also the frequent use of casein glues in the bottle labeling industry.[119] Of special advantage is the easy removal of the bottle label by warm water before glass recycling.

Today, casein glues and adhesives have almost completely been replaced by synthetic pendants, due to their lower prices and superior properties. Some casein glues are still used in labeling and interior woodworking, e.g. for lumber laminating, millwork, and even as adhesive in fire doors.[117,120,121]

**Fibers**

During the 20th century, casein was also processed into fibers, mainly to replace natural fibers in clothing. For instance, in the 1930s, Ferretti developed a novel spinning process for the manufacture of water insoluble casein fibers.[122] Such fibers were generally applied in combination with other fibers in clothing industry, such as cotton or later with synthetic fibers. Especially during the Second World War, casein fibers were increasingly used as substitute for cotton or wool, due to shortage of raw materials.

Nowadays, use of casein fibers in clothing materials has been decreased as a consequence of competing synthetic fibers. Nevertheless, there is still a commercially available casein fiber on the market which is called “Chinon®”.[123] This fiber is processed into nightwear, ties, scarves, and blouses.

**Plastics**

In the late 19th and early 20th century, casein was also used as raw material for the manufacture of rigid plastics. Processing was mostly performed via high pressure extrusion and crosslinking with formaldehyde. Casein-made plastics were available in many countries under many trade name like “Galalith®” (Germany and France), “Erinoid®” (UK), “Casolith®” (Netherlands), and “Aladdinite®” (USA).[69,124] Popular manufactured plastics were mostly clothing items, such as hat pins, buttons, brooches, umbrella handles, and cigarette holders. These products found high sales probably due to casein’s ability to optically imitate ivory.[123] Today, casein plastics lost their importance completely.

## Forward-looking and future applications

In addition to its rediscovered use as binder in conventional coatings, casein is a promising material for packaging applications and gains great importance as encapsulation and coating material in life sciences.

Renewable and biodegradable packaging materials are of growing interest at the moment. Here, casein greatly provides the required features. It can easily be processed into films, exhibits biodegradability, and has good barrier properties against non-polar gases.[125,126] Unmodified casein films are edible, transparent, and odorless.[14] All these properties fit perfectly for applications in the food packaging sector. A limiting factor is the conventional preparation of casein films. Predominant techniques are solution casting and spin-coating processes. These techniques are inadequate for the continuous processing of large packaging foils. To overcome this, Kozempel and Tomasula developed in 2004 a process for the manufacture of continuous casein films for packaging.[127] Casein solutions were sprayed continuously onto polyethylene or Mylar belts and were dried by heated air. Processed films could easily be removed from the belts after drying and had promising properties with respect to packaging applications. This allows for a broad applicability in future.

Additional applications of casein will probably focus on the biomedical sector. Biocompatible coatings for implants and nutrient and drug delivery systems are of special interest. For instance, casein has successfully been applied as novel coating material for tablets, providing sustained drug release properties.[128] Also drug delivery systems using casein as encapsulation material seem to be promising. Rutin was exemplarily encapsulated by a casein/pectin composite, yielding nano-complexes, which showed a controlled drug release under gastric conditions.[129] In addition, casein can be crosslinked with naturally occurring genipin to yield hydrogels.[130] Such hydrogels could be loaded with bovine serum albumin and also exhibited a controlled drug release behavior. Coating of implants with casein or casein composites is another potential application in life sciences. In 2015, Qin and coworkers successfully applied chitosan/casein composite coatings to Co-Cr-Mo orthopedic implants.[131] Deposited coatings showed auspicious properties, especially with respect to biocompatibility.

Summarizing, it can be expected that the number of applications of casein in the medical and packaging sector as well as in conventional coating applications will steadily increase in near future.

## 2.3 Enzymes

### 2.3.1 Importance of enzymes for modern chemistry

Enzymes often catalyze only one reaction and/or are specific to one substrate. Their use in chemical reactions offers versatile benefits compared to conventional catalysts. This leads to their great industrial importance for chemical, food, and pharmaceutical processes. Enzymes allow for the synthesis of well-designed products, which are not (or at least very ineffectively) synthesizable by conventional methods, while providing high catalytic activities and high turnover numbers.[132] Their high selectivities, including high enantio-, regio-, and chemoselectivity, enable a full control of the conducted reaction.[133] Enzymes lower the activation energy of particular reactions, due to stabilization of the transition state via an enzyme-substrate complex.[134] Therefore, *in vitro* enzymatic reactions can be carried out under mild conditions with respect to temperature, pressure, solvent, and p*H* of medium. This, combined with the high regioselectivity, allows for the preservation of functional groups.[135] In addition, enzymes are non-toxic and sustainable, since they are produced by living organisms. Reuse of enzymes after performed reactions can be accomplished by immobilization of the enzyme onto suitable support materials.

Decades ago, enzyme-catalyzed reactions were only frequently used by specialized groups in biochemistry. Over the last years, use of enzymes for special synthetic purposes became more and more popular in numerous fields of applied sciences. The number of commercially available enzymes is continuously increasing and novel methods in biotechnology, such as genetic engineering, allow for the production of pure and highly reactive enzymes at low prices.[132] Typical examples for the application of enzymes in chemistry are at the moment the synthesis of macromolecules, such as polyesters and polyphenols, and the production of biopolymers from natural resources. Lipases, such as the frequently used immobilized *Candida antarctica* lipase B (Novozym 435), are studied and applied in chemoenzymatic syntheses of polyesters, polycarbonates, and polyphosphates, providing tailor-made polymers.[136–138] Moreover, commercially available peroxidases, such as horseradish peroxidase and soybean peroxidase, are successfully used for the polymerization of phenols and bisphenols.[132,139]

Nowadays, enzymes are essential for many processes in modern chemistry and it can be expected that their use and importance will steadily increase in the future.

### 2.3.2 Chymosin

Chymosin (EC 3.4.23.4), which is also called rennin, is an aspartic protease and belongs to the class of endo-peptidases. It resembles pepsin regarding its proteolytic properties. Native chymosin consists of 323 amino acids and has a molecular weight of 30,700 g/mol.[140] It is a monomeric enzyme and exhibits a diameter of about 5–6 nm (PDB code 4AA8), since it is not a perfect sphere-like particle (**Figure 15**). Its primary structure is displayed in **Figure A-82**.

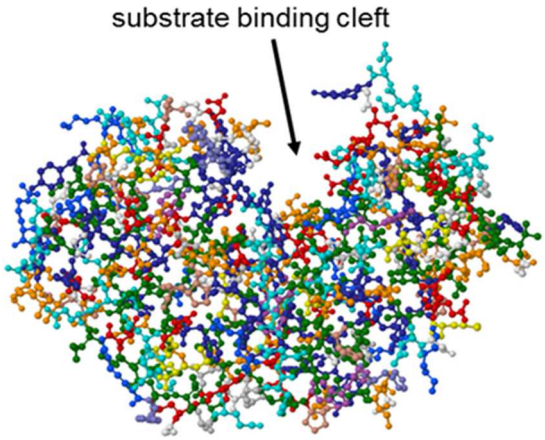


*Figure 15. 3D-model of bovine chymosin. Graphic refers to Newman et al.*[141]

Chymosin is produced as an inactive precursor, called prochymosin, in the stomachs of all nursing mammals. Prochymosin is transformed into active chymosin at acidic p*H* by proteolysis of the N-terminal, either by the action of pepsin or by autocatalysis.[140,141] Three major types of calf chymosin exist, i.e. type A, B, and C. Type A and B are very similar and differ only in one single amino acid residue at position 243 (Asp or Gly), whereas chymosin of type C is a degradation product of type A.[142]

Chymosin, like all endopeptidases, cleaves preferably peptide bonds in the inner region of protein chains away from the N- and C-terminals. As mentioned before, it specifically cleaves the $Phe^{105}$-$Met^{106}$ peptide bond in κ-casein. This results in the formation of hydrophobic para-κ-casein and hydrophilic caseinomacropeptide. The substrate binding cleft of chymosin (Figure 15) is formed by its two lobes. Both contain an aspartic acid residue which participate in the cleavage reaction. The distance between the two amino acid residues ($Asp^{32}$ and $Asp^{215}$) accounts for 3.1 Å.[141] The general cleavage mechanism of peptide bonds is shown in **Figure 16**. It can be considered as an acid/base catalysis with water participating in the reaction.

The isoelectric point of chymosin is at p*H* 4.6.[143] It is most stable between p*H* 5.3 and 6.3, but it is also relatively stable at lower p*H* values down to p*H* 2.[144] Its proteolytic activity strongly depends on the surrounding p*H* value. Like other aspartic proteases, chymosin exhibits its highest activity under acidic conditions, i.e. p*H* 3–4.[140] In literature, it is mentioned that chymosin is most

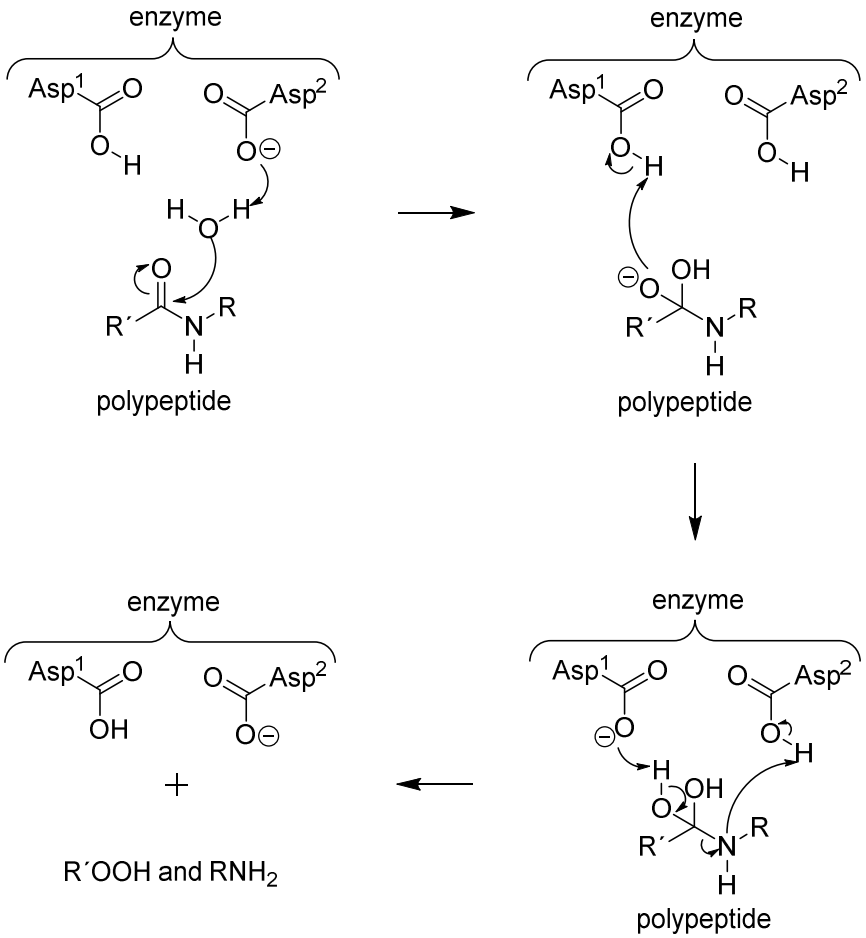


*Figure 16. Cleavage mechanism of peptide bonds via chymosin. The mechanism refers to Rao et al.*[140]

active at p*H* 3.5–3.7.[145,146] However, chymosin is only moderately stable in this range of p*H*, resulting in a rapid loss of activity. This is assumed to be caused by its autoproteolysis.[144] Consequently, compromises must be made in practice to manage the reactivity and stability of chymosin. With respect to temperature, calf chymosin shows the highest activity at 40 °C and becomes inactive at temperatures higher than 56 °C.[147] Nonetheless, some recombinant types of chymosin can be stable up to 60 °C.[148]

Due to the world's increasing cheese production, high amounts of chymosin are consumed every day. In the past, chymosin has solely been extracted from calf stomachs. Based on the declining number of slaughtered calves and the increasing industrial consumption of chymosin, alternative resources are explored. Most promising is the use of recombinant chymosin.[149] Several microorganisms, such as bacteria and fungi, can be genetically modified to produce chymosin, satisfying the growing need of this important enzyme.[150–152]

### 2.3.3 Immobilization of enzymes

#### 2.3.3.1 General remarks

In the last decades, much effort has been invested in the improvement of conventional and the development of novel immobilization techniques for enzymes.[153–155] This has led to a wide-ranging knowledge about advantages and obstacles connected to this specific field of biotechnology.

Immobilization of enzymes makes bio-catalyzed processes particularly economical by improving their performance under optimal process conditions, e.g. under harsh acidic or alkaline environments, in the presence of organic solvents, or at elevated temperatures. Immobilized enzymes are stable for long periods of time and can be easily recycled after reaction.[156,157] The use of immobilized enzymes is therefore of special importance for industrial scale, although the larger percentage amount of enzyme-catalyzed reactions is still performed with free, soluble enzymes.[158]

Reactivity and selectivity of enzymes are properties which need to be carefully considered. Improvement of enzyme stability may be accompanied by a decrease of activity and selectivity.[154] Changes in the orientation and conformation of enzyme molecules during the immobilization process are crucial points. Enzymes, exhibiting an orientation with their active site towards the support surface, show reduced reactivities and selectivities compared to their free forms.[159] In case of enzymes with two or more conformational forms, like lipases, the more active form (open cleavage site) can be stabilized by using detergents. This ensures coupling of the enzyme in the right orientation.[160] Of particular note is the immobilization of multimeric enzymes. Here, subunits need to be crosslinked in some cases. This results in higher stabilities, because dissociation of enzyme subunits is prevented.[161] **Figure 17** illustrates particular structural issues involved in the immobilization of enzymes.

As a special tool of bioengineering, enzymes can be modified via mutagenesis to enhance their properties under particular conditions.[162,163] Especially mentionable is the opportunity to control the orientation of enzyme molecules during the immobilization process. To this, the necessary exchange of particular amino acid residues in the peptide chain can be accomplished either by random or site-directed mutagenesis.[164]

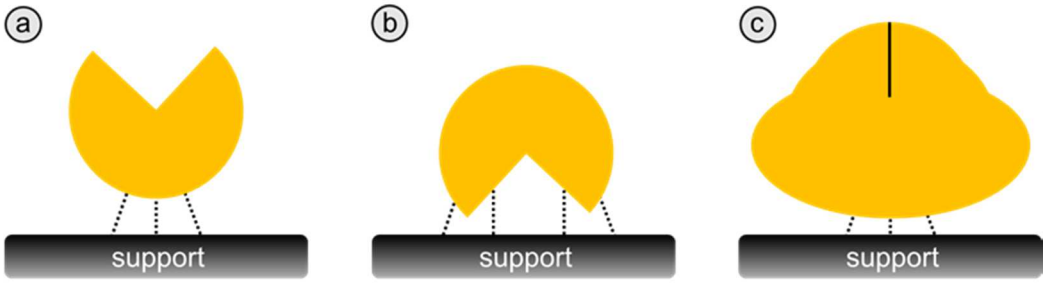


*Figure 17. Efficient and inefficient orientation or conformation of enzyme after immobilization. a) Efficient and b) inefficient orientation of enzyme towards support surface during immobilization and c) conformational changes of enzyme structure, resulting in non-reactive enzyme.*

Nevertheless, if the immobilization method is carefully chosen and properly applied, residual enzyme reactivities and selectivities can be obtained, which are similar or even higher compared to free native forms.[165,166] Commonly applied immobilization techniques for enzymes encompass reversible and irreversible methods with respect to ease of de-immobilization and methods which can be categorized between the latter ones (**Figure 18**).[154]

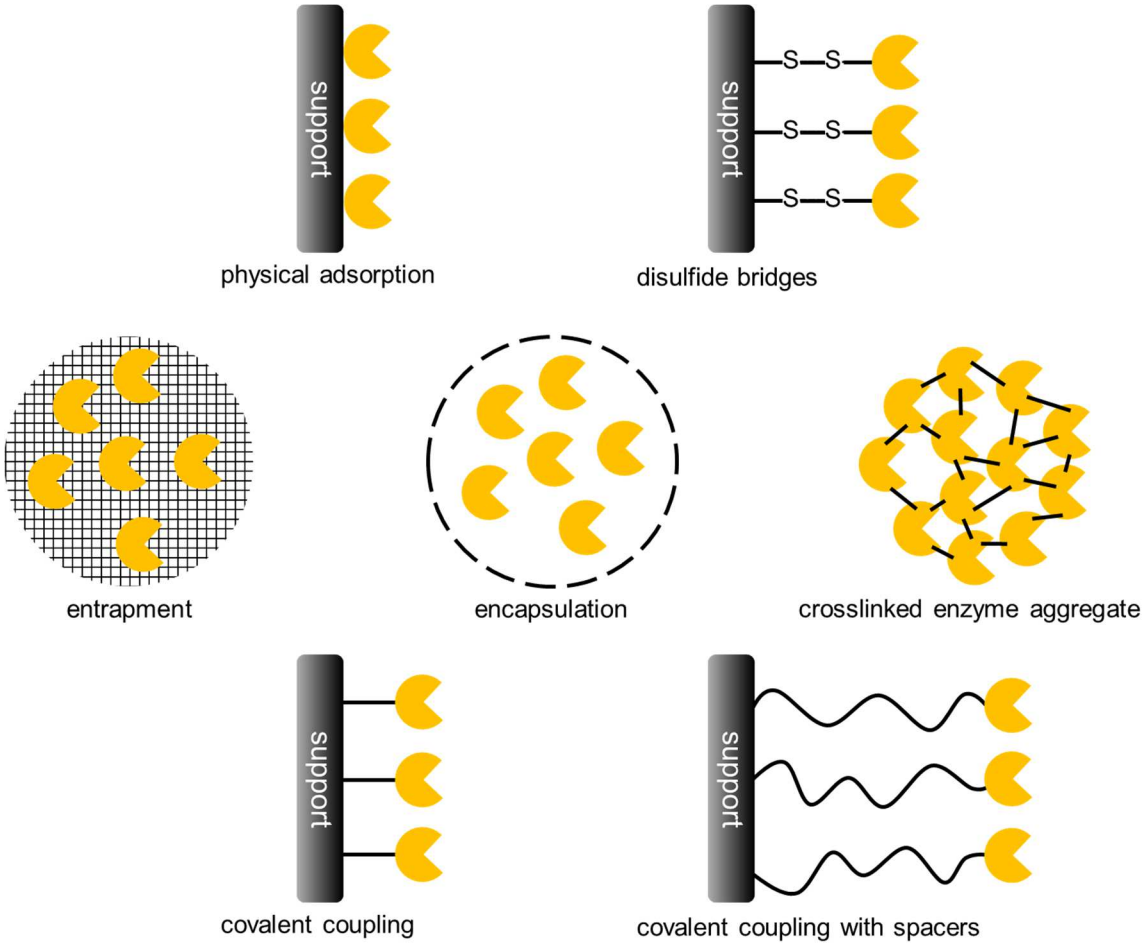


*Figure 18. Overview on commonly applied immobilization techniques.*

#### 2.3.3.2 Reversible immobilization methods

The reversible immobilization preserves usually the conformational shape of the enzyme and provides good enzymatic activity and performance.[167] Moreover, the immobilized enzyme can be detached from the support under mild conditions. This allows for a repetitive loading of a once used support with ease, when the enzymatic activity is strongly decreased.

The simplest method for reversible immobilization of enzymes onto a support surface is the physical adsorption. Here, the stability is provided by weak, non-specific interactions, i.e. van der Waals forces, hydrophobic interactions, and hydrogen bonds.[168] Adsorption of enzymes via specific interactions can be obtained through ionic linkages, e.g. supports can be coated with polyethylenimine, providing high stabilities of reversibly attached enzyme molecules.[169] A more sophisticated reversible method is represented by the formation of disulfide bonds between the enzyme and the support surface. The resulting bond is covalent and stable in non-reducing environments.[170] Nevertheless, if desired, the covalent bond can be easily broken under mild conditions by action of low molecular thiol reagents, such as dithiothreitol.[171]

Physical adsorption of enzymes can be generally achieved by immersion of the support into an enzyme solution. During the incubation, enzyme molecules diffuse to the support and adsorb. As an alternative way, enzyme solutions can also be poured onto the support, allowing to dry and to provide adsorption of enzyme. Non-specifically adsorbed enzyme molecules can be removed afterwards by intense rinsing.[172]

The reversible immobilization of enzymes onto supports is a very convenient method, but has the drawback that leakage of enzyme into solution is likely.[154] Diffusing enzyme cannot easily be recovered and contamination of products may result. On the other hand, reversible methods have the lowest costs of all immobilization methods, lack the usage of additional chemicals for enzyme attachment, are suitable for almost all enzymes, and preserve usually the enzymatic activity. Thus, these methods are especially interesting and frequently used in industrial approaches.[173,174]

#### 2.3.3.3 Covalent immobilization methods

Attachment of enzyme molecules via covalent bonds, especially via multipoint covalent attachment, is irreversible and provides a rigidification of the enzyme, more precisely, its conformational structure on the support.[175,176] This enables the highest possible thermal and chemical stabilities and allows for long periods of usage, while leakage of enzyme is prevented.[177]

Multipoint covalent coupling requires highly activated supports. This provides a high density of reactive groups on the support surface, which can react with available functional groups of the enzyme. In most cases, these groups are represented by amino groups of the enzyme's N-terminal or lysine residues, but also other functional groups, e.g. additional amino groups or thiol, phenolic, and imidazole groups are known to react with activated surfaces.[165] Consequently, multiple coupling is often connected to long immobilization times, because arrangement of many functional groups is supposed to take place. Following, the most commonly used covalent immobilization methods for enzymes are described in detail, i.e. coupling via epoxy groups and via pre-activated supports with glutaraldehyde.

**Covalent attachment via epoxy groups**

Supports which are activated with epoxy groups are very adequate for immobilization of enzymes through (multipoint) covalent coupling, providing high enzyme activity and stability.[178,179] Such immobilization reactions are usually carried out at neutral p*H* and high ionic strength (e.g. 1 M buffer). Here, immobilization of enzyme takes place via a two-step mechanism.[155,176] First, physical adsorption of enzyme occurs through hydrophobic interactions between non-polar regions of the enzyme and the support, i.e. the aliphatic chain under the epoxy group. This adsorption is favored at high ionic strength.[180] Subsequently, a covalent bond is formed between the adsorbed enzyme and neighboring epoxy groups. Also multipoint coupling is possible, provided that sufficient functional groups are available underneath the enzyme with the right orientation. Multiple binding can be enhanced by increasing p*H* value, e.g. up to p*H* 10.[176] This is based on higher activities of lysine residues at alkaline p*H* values. **Figure 19** shows the respective reaction scheme.

The good feasibility and properties of enzyme immobilization via epoxy groups are also apparent by the fact that carrier materials, namely Eupergit® and Sepabeads® are commercially available.[181,182] These support materials are

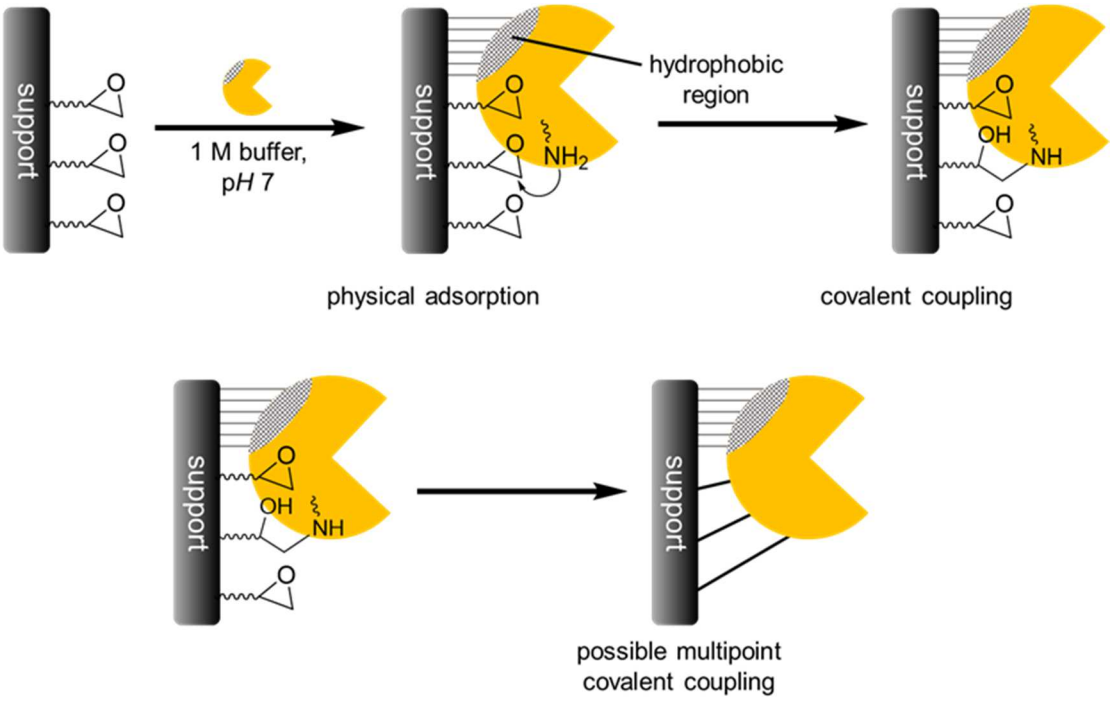


*Figure 19. Mechanism of covalent immobilization of enzymes via epoxy groups.*

macroporous acrylate spheres, bearing epoxy propyl residues on the surface as well as inside the pores. Such carriers are frequently used for industrial purposes. In addition, plane supports, exhibiting a large area for attachment of enzymes, are accessible by silylation of glass slides. To this, (3-glycidoxypropyl)trimethoxysilane (GLYMO) can be used to functionalize glass supports, providing sufficient epoxy groups on the surface.[183]

**Covalent attachment via glutaraldehyde**

Glutaraldehyde (pentanedial) is a versatile crosslinking agent and is frequently used in enzyme immobilization techniques, yielding very stable products.[184–187] It is a 5-carbon aliphatic dialdehyde and highly reactive. It has the ability to react with itself and with different functional groups of amino acid residues, i.e. predominantly with primary amino groups, but also with thiol, phenolic, and imidazole groups.

The crosslinking chemistry of glutaraldehyde depends on the particular applied immobilization method. It is able to form inter- and intramolecular enzyme crosslinks in absence of a support surface. The manufacture and application of these so-called “crosslinked enzyme aggregates” (CLEA) presents a new type of carrier-free biomolecule immobilization.[188,189] Furthermore, the stability of single enzyme molecules can be improved by the introduction of intramolecular

crosslinks via glutaraldehyde. This technique is also frequently used to prevent dissociation of subunits from multimeric enzymes.[190,191]

Mainly, glutaraldehyde is applied in enzyme immobilization in connection with a support. Aminated surfaces are activated by glutaraldehyde into a highly reactive surface for coupling of biomolecules. In this manner, glutaraldehyde functions as a crosslinker between the enzyme and the support surface.[192] Also enzymes, which are already immobilized on supports, can be treated with glutaraldehyde to enhance their stability.[193–195] **Figure 20** illustrates the different types of immobilization via glutaraldehyde.

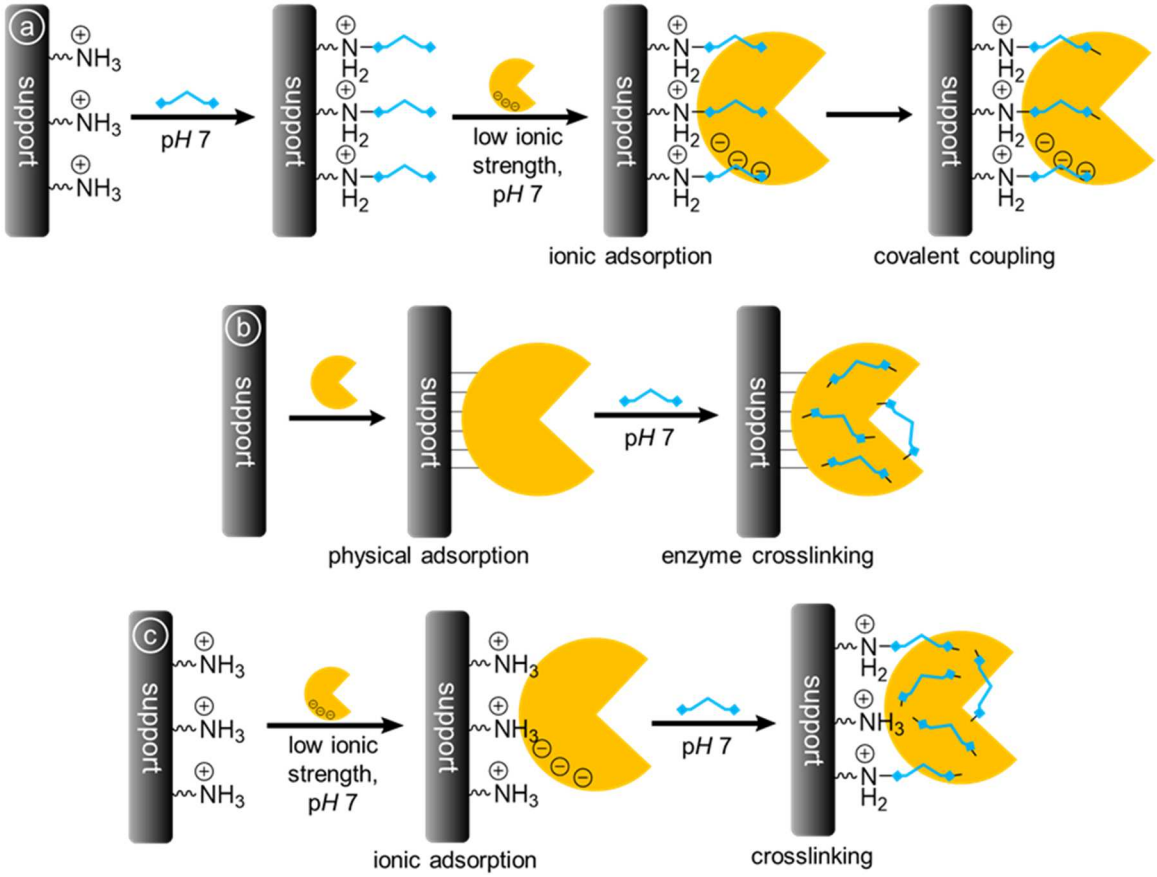


*Figure 20. Commonly applied immobilization methods of enzymes via glutaraldehyde (∿). a) Activation of amino-functionalized support and subsequent enzyme coupling. b) Crosslinking of previously adsorbed enzyme. c) Crosslinking of adsorbed enzyme plus formation of enzyme-support bonds.*

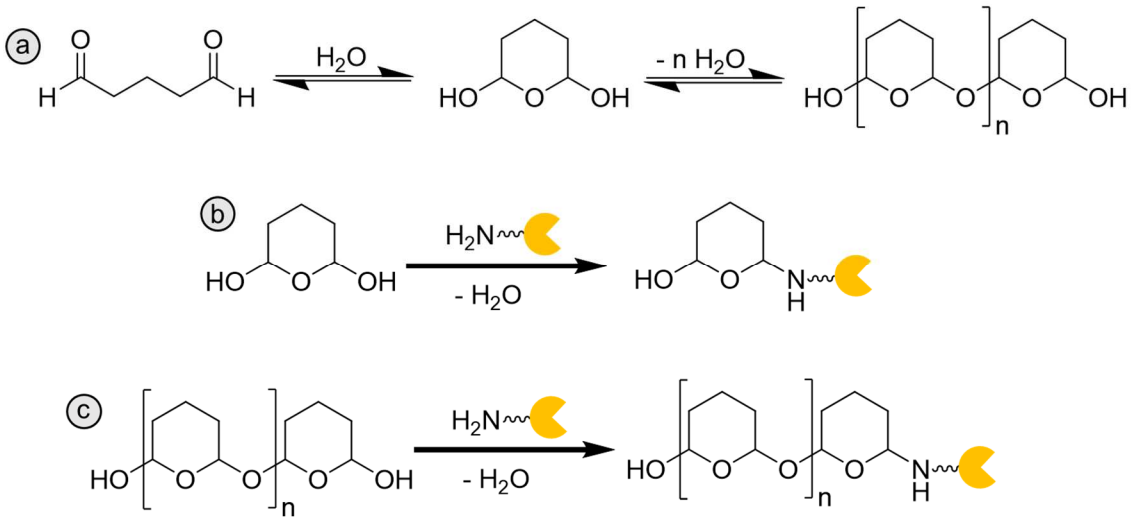


*Figure 21. Immobilization reactions of glutaraldehyde with enzymes under acidic or neutral conditions. a) Formation of (oligomeric) heterocycles. Enzyme coupling via b) heterocycle and c) oligomeric heterocycle of glutaraldehyde.*

The crosslinking chemistry as well as the molecular structures of glutaraldehyde in solution are not fully explained and are still under investigation.[185] It is well known that glutaraldehyde forms six-membered heterocycles and also oligomeric structures of them in aqueous solution under acidic or neutral conditions. Researchers assume that the crosslinking chemistry of glutaraldehyde is based on these (oligomeric) heterocycles by reaction with free amino groups of biomolecules.[186] In contrast to this, formation of imine groups via reaction of glutaraldehyde with free amino groups is unlikely, due to the high stability of immobilization products under acidic p*H*.[196] The versatility of the glutaraldehyde based crosslinking chemistry is summarized in **Figure 21**.

Briefly, glutaraldehyde is a very important crosslinking reagent, which has been used for a long time in biotechnology and still will be in future. Its highly stable immobilization products as well as its compatibility and applicability in new immobilization methods, such as the formation of CLEAs, make it an indispensable immobilization tool.

Genipin, a natural crosslinking reagent, might compete with glutaraldehyde in future with regard to biotechnological applications (**Figure A-83**). Genipin is known to react with accessible amino groups of biomolecules and can be isolated from the fruits *Genipa americana* and *Gardenia jasminoides Ellis*.[197] It has successfully been used for crosslinking collagen and gelatin, soy protein isolate, and especially chitosan.[32,53,197] Compared to glutaraldehyde, genipin exhibits slower reaction rates, but it is about 10,000-times less cytotoxic.[198]

The cytotoxicity of glutaraldehyde is based on its highly reactive nature and its ability to react with important endogenous proteins, such as DNA-proteins. Glutaraldehyde-crosslinked biopolymer adducts, which show leaching of non-reacted or degraded glutaraldehyde molecules, are likewise cytotoxic.[199,200] Therefore, crosslinking and immobilization reactions with glutaraldehyde must ensure, that only reacted and stable products are formed.

The reaction mechanism of genipin is well understood and also its use in the immobilization of enzymes has already been examined.[197,201] Such immobilization reactions were studied with chitosan-based supports so far and residual enzyme activities of more than 100 % compared to native forms could be achieved.[202–204]

These results support that genipin is a potential and environmentally friendly alternative for glutaraldehyde in enzyme immobilization techniques. On the other hand, the applicability of genipin in industrial processes in combination with frequently used support materials, such as Sepabeads®, still needs to be evaluated.

#### 2.3.3.4 Encapsulation and entrapment of enzymes

Encapsulation and entrapment of enzymes lack the need of a support surface and have similar effects on enzymatic properties. The most important one is that the structural shape of the native enzyme remains unaltered, yielding activities similar to free forms, while no leakage takes place.[205,206] Entrapment is achieved via embedment of enzyme molecules into a polymeric network, such as an organic polymer or sol-gel.[207,208] On the other hand, encapsulation is obtained by the formation of porous hard shells, usually formed by organic polymers or silicates, around an assembly of enzyme molecules.[209,210]

Encapsulation and entrapment provide good enzyme stabilities, because direct contact of enzyme with the surrounding medium is prevented and negative effects, e.g. by gas bubbles or organic solvents, are minimized.[153] Nonetheless, these techniques are often accompanied by severe drawbacks, such as low enzyme loading and mass transfer limitations.[211] In addition, these techniques have no significant importance for the purposes of this study and are therefore not further described in detail.

## 2.4 Nanostructuring

### 2.4.1 Conventional nanostructuring methods

Nanostructuring of surfaces is a challenging field of modern technologies and is especially important for medical, sensory, and nanoelectronic applications. Nanostructures are widely defined as those structures, which show dimensions smaller than 100 nm.[212] Commonly, enhanced methods of reliable microstructuring techniques are applied.[213–217] Techniques based on biological principles, such as biological self-assembly, are of special importance, if structuring with biomolecules is considered and preservation of biological functionalities is essential.[218]

Conventional methods for nanostructuring are predominantly based on lithography and scanning probe techniques. Methods, dealing with the deposition of particles from the gas phase and etching techniques play a minor role and are widely used as supporting techniques, especially in connection with lithography. **Figure 22** gives an overview about these techniques.

In nanolithography a resist layer is applied on the support, in order to generate a mask (**Figure 22a**). By this, a broad variety of surface materials can be patterned. Organic polymers represent the most frequently used material for masks. The structuring is based on altered solubilities of the polymers in the surrounding media upon local exposure to electromagnetic radiation. To achieve structures in the nanometer scale, radiation with wavelengths smaller than visible light is required. Suitable are UV light and X-rays, enabling the structuring of photoresists in the medium and lower nanometer scale.[219–221] In addition, also electron or ion beams can be applied to induce chemical changes in the resist layer.[222–224] Such techniques allow for highly accurate structuring, since particle beams can be focused down to 1 nm.[212]

Generally, high lateral resolutions can be obtained by lithography techniques. However, these techniques are tailor-made for synthetic polymers, which withstand the high energetic light and particle beams. If structuring of surfaces with biopolymers is considered, direct lithography techniques quickly reach their limits, since biomolecules tend to undergo denaturation upon exposure to high energetic irradiation and organic solvents.

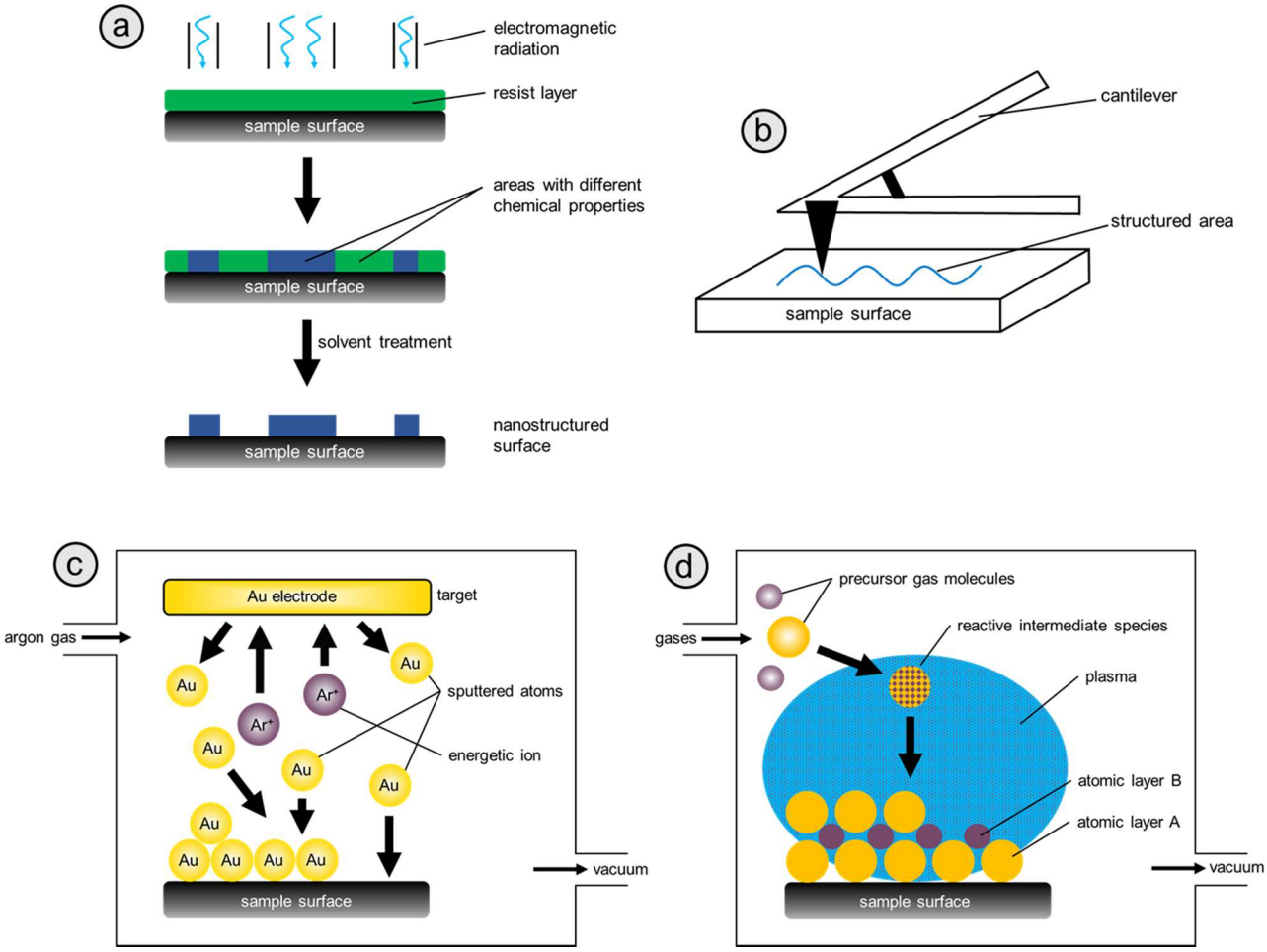


*Figure 22. Conventional techniques for nanostructuring of surfaces. a) Nanolithography process, b) structuring via AFM, c) physical vapor deposition, and d) chemical vapor deposition.*

A very useful tool for structuring of surfaces, especially in the nanometer scale, is the application of scanning probe techniques, such as atomic force microscopy (AFM) or scanning tunneling microscopy (STM). Both techniques offer very high lateral resolutions. In AFM-based techniques (**Figure 22b**), the interaction of the tip with the sample surface can be used to generate structures instead of imaging the surface's topology. Structure formation includes movement of weakly bound particles on the surface, addressment of individual nanoparticles, and direct scratching into the surface material.[225,226] Manipulation and deposition of particles range from single atoms to even biological molecules, such as DNA.[217] Principle and scope of STM techniques are similar to those of AFM techniques, but they are less frequently used due to material restrictions and extensive sample preparation.[227–229]

Subsuming, scanning probe techniques are very valuable for the precise structuring of surfaces in the nanometer scale and even in the subnanometer scale. AFM techniques are applicable to a wide variety of chemical substances,

and are even compatible with biomolecules. Nevertheless, structuring via scanning probe techniques requires long periods of time, especially if structuring of larger surface areas is attended. This makes this technique very uneconomical and impractical for industrial processes.

Techniques based on the deposition of particles from the gas phase are commonly applied for the formation of well-defined, continuous thin layers on different support materials. Two approaches are distinguished, i.e. physical or chemical vapor deposition (**Figure 22c and 22d**). In physical vapor deposition, the target is activated by a plasma with inert ions, e.g. argon ions. The activated target dissociates and particles deposit onto a given surface.[230,231] In chemical vapor deposition, precursor chemicals are added to the gas phase, to start the deposition process via plasma activation. Structure-forming species are formed *in situ* on the sample surface by chemical reactions.[214,232]

Physical and chemical vapor deposition techniques exhibit a high vertical resolution, but have no lateral resolution and are restricted to inorganic materials, e.g. metals or metal oxides. Direct structuring with other substances, such as biomolecules, has not yet been mentioned in literature and is probably incompatible.

### 2.4.2 Structuring with biomolecules

The previously described techniques are predominantly applied in nanostructuring with inorganic materials and synthetic polymers, and are often limited to those.[212] Structuring of surfaces with biomolecules is usually very challenging and often connected to obstacles. Biopolymers are, in general, more sensitive with respect to occurring conditions of conventionally applied methods, compared to inorganic materials and synthetic polymers. Possible factors are thermal or mechanical stress and exposure to irradiation and organic solvents. Especially structuring with proteins is complicated, because they are particularly sensitive. Nevertheless, (nano)structuring with biomolecules is of great importance, e.g. in life sciences. Thus, techniques must be used, which preserve integrity and biofunctionality of biomolecules and allow for a structuring in reasonable periods of time.

A technique for the nanostructuring with DNA, that is present everywhere in literature in recent days, uses the ability of biomolecules to undergo self-assembly.[218,233–235] This technique is called “DNA origami” and was

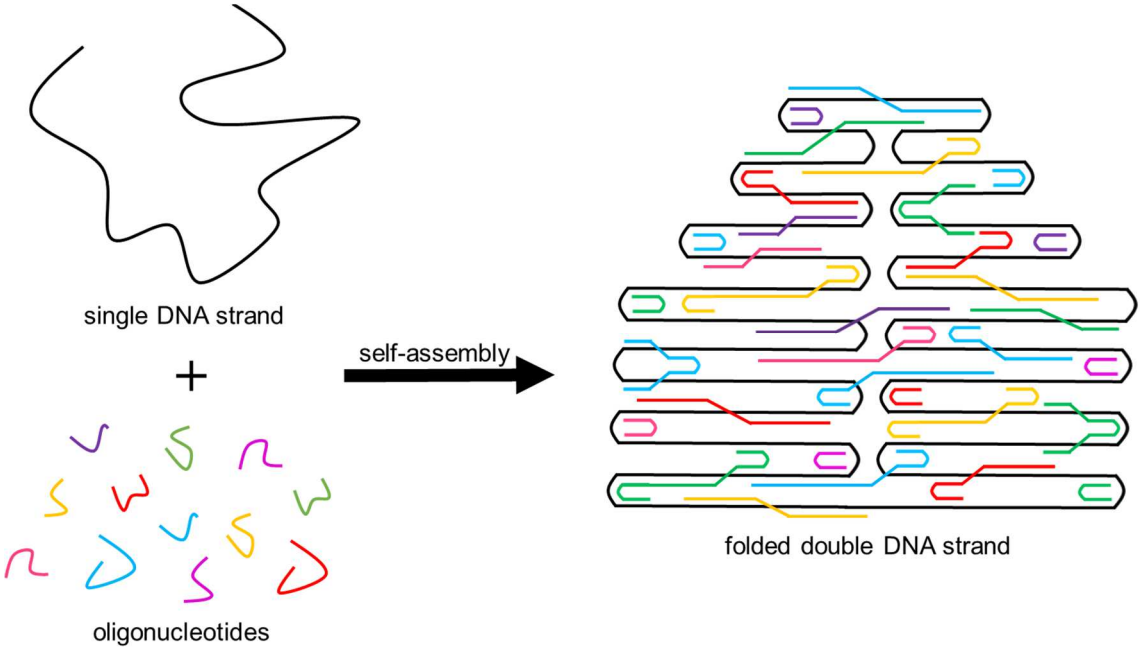


*Figure 23. Principle of DNA origami. Modified after Rothemund*.[218]

invented by Paul Rothemund in 2006. It is suitable for folding DNA in arbitrary structures with dimensions less than 100 nm. The general process is shown in **Figure 23**. Typically, simple 2D geometries can be generated, such as squares, stars, smileys, and triangles. In addition, 3D DNA structures are also accessible, which might be used as containers for drug delivery systems in near future.[234,236,237] The principle of DNA origami is based on the use of a single viral DNA strand as a scaffold for the assembly of additional hundreds of short oligonucleotides into desired forms. Folding into the particular shapes is driven by the formation of hydrogen bonds between single nucleic bases. Number and manner of bond formations are predictable via computer calculations, enabling the formation of various geometries. Self-assembly of the DNA nanostructures occurs in solution and their deposition on surfaces happens randomly.[238] Therefore, DNA origami needs to be combined with other methods, such as lithography or AFM techniques, to structure surfaces.

The self-assembling properties of biomolecules connected to structuring are not restricted to DNA molecules, but can also be used to achieve nanostructured protein geometries.[239] The main drawback also exists here; deposition of such protein nanostructures on samples results in arbitrary patterns. Combinations of biological self-assembly and photolithography are known as well.[240] By this, selective deposition of antibodies via self-assembly, connected to photo-activation of bound ligands, has been investigated. Here, avidin was immobilized on a silanized support and was subsequently modified with a

photo-activatable biotin analogue, called photo-biotin. Selected areas were then exposed to light, enabling site-specific coupling of antibodies via bioaffinity interactions. This method overcomes the drawback of random deposition and exhibits potential applications in the development of biosensors, but is limited to the micrometer scale.

Additional methods, used for structuring with biopolymers, especially proteins, are based on lithography or AFM techniques.[241–243] AFM techniques can be used to manipulate and arrange single biomolecules as well as macromolecular structures on surfaces in patterns.[244,245] Obtained structures had dimensions of a few nanometers up to several hundred micrometers. Taking advantage of the bioactivity of enzymes also presents an attractive opportunity for structuring with biomolecules.[246] Takeda *et al.* used an enzyme-immobilized AFM tip to alter the structure and the properties of a peptide layer. They called this novel technique “enzymatic lithography”. *Staphylococcal* serine V8 protease was covalently bound to an AFM tip and was used to specifically digest the protein layer via scanning the surface. Only scanned areas were manipulated and exhibited an altered biological structure. This technique enables a high lateral resolution in the nanometer scale and may have a certain potential for the development of biobased electronic chips and biosensors.

Summarizing, self-assembly methods exhibit a high precision to obtain nanoscaled biological structures, but their deposition on surfaces underlies arbitrary factors. Lithography techniques seem to be essential in nanostructuring, but are more beneficial, if used as pre-structuring or supporting method, as direct lithographic approaches are not compatible with biopolymers. In contrast to this, AFM techniques are highly compatible with biomolecules and achieve high resolutions. Nevertheless, they are very inappropriate in industrial scale, since non-efficiency, regarding spent time, money, and energy, is obvious, especially if structuring of large support areas or quantities is intended.

On the other hand, the use of enzymes for biostructuring seems to be a very attractive opportunity to circumvent obstacles. Processes could be performed in reasonable time periods and under mild conditions, while no necessity of irradiation, pressure, and solvents is required. This would particularly preserve biofunctional properties. Thus, specific incorporation of enzymes into structuring methods may present a highly economical and ecological solution. To this, enzymes need to be present on the surface in an immovable form exactly there, where deposition and formation of biological (nano)structures is desired.

## 2.5 Concept of the Enzyme Mediated Autodeposition

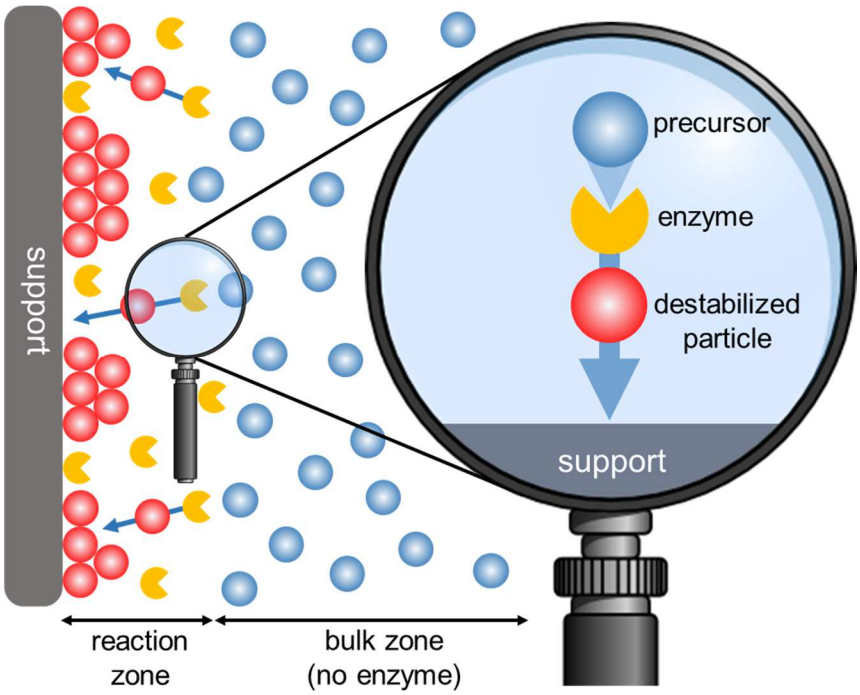


*Figure 24. Principle of the Enzyme Mediated Autodeposition.*

The Enzyme Mediated Autodeposition (EMA) is inspired by both, naturally occurring biological principles, such as milk clotting, as well as by industrially widespread deposition techniques for coatings, like conventional electrodeposition and autodeposition techniques.[247–249] These techniques are realized as easy-to-perform dip coating processes and offer a high control over particle deposition and the final film formation. This is triggered by the specific destabilization of film-forming particles in direct proximity to the support surface via electrolysis of water or dissolving iron ions. However, these processes are connected to several drawbacks and restrictions, such as energy consumption, limitation to metallic support materials, corrodibility of supports, and incompatibility with biological particles.

The EMA combines the advantages of the above mentioned techniques with the applicability of various support materials and the controlled deposition of biobased and bioinspired particles. Key factor of this process is the use of enzymatic reactions to generate destabilized film-forming particles and to induce their deposition. To this, the enzyme needs to be immobilized onto the support surface first, which is then considered to be coated. The immobilization of enzyme allows for a high control of the deposition process and makes this novel kind of material design applicable. **Figure 24** illustrates the general process of the Enzyme Mediated Autodeposition.

The area with enzyme activity is defined as the reaction zone. Precursor particles which enter this area are converted by the enzyme into a destabilized form and deposit onto the surface. Size of the reaction zone depends on the used immobilization method, which directly influences mobility and flexibility of the enzyme. This determines the amount of deposited particles as well as appearance of the formed structures. Relevant immobilization methods are physical and/or ionic adsorption and covalent coupling techniques. These are expected to have different effects on the size of the reaction zone. Immobilized enzyme is assumed to stay active, until it is covered by destabilized particles. Therefore, a self-limiting character of the process is presumed.

The versatility of the process allows realization of both top-down and bottom-up approaches. The *in situ* synthesis of film-forming particles based on dissolved monomers is a prominent example of the bottom-up approach. Here, increase in molecular weight leads to a destabilization of the entire particle after reaching a threshold and controlled deposition takes place. An important example for such a bottom-up approach is the enzyme-catalyzed *in situ* synthesis and deposition of melanin.[250,251]

Top-down approaches are characterized by the presence of stabilized film-forming particles right from the start of the deposition process. Their destabilization occurs via enzymatic cleavage reactions. The system, investigated in this study, is the most prominent example of this approach. It is based on the enzyme chymosin and the milk protein casein. Casein micelles are cleaved by immobilized chymosin inside the reaction zone. By this, the water solubility of the casein micelles is changed. They become hydrophobic and subsequently deposit onto the support. Unintended and uncontrolled aggregation of cleaved casein, followed by precipitation in the bulk phase, is excluded due to immobilization of enzyme. Non-cleaved casein micelles remain water soluble and do not contribute to the resulting protein coating.

Previous studies have proved the high application potential of the EMA.[252,253] Results showed that appearance of deposited structures in fact strongly depends on the used enzyme immobilization method. Parameters, influencing particle deposition and film formation, can easily be adjusted and controlled by choice and variation of the applied method. This enables the formation of well-defined biological films and structures. It can be expected that the number and variety of accomplishable structures has virtually no limits and that the Enzyme Mediated Autodeposition has great potential to open up new perspectives in coatings science and technology.

# 3 Experimentalia

## 3.1 Materials

### (3-Aminopropyl)triethoxysilane (APTES)

APTES was purchased from ABCR (Karlsruhe, Germany) and was used without further purification for silylation of glass supports and enzyme carriers. The alkoxysilane was stored at room temperature under protective nitrogen atmosphere.

### (3-Glycidoxypropyl)trimethoxysilane (GLYMO)

GLYMO was also obtained from ABCR (Karlsruhe, Germany) and was used without further purification for the functionalization of glass supports and enzyme carriers. GLYMO was stored at RT under gas atmosphere, using nitrogen.

### Buffer solutions

Phosphate buffer solution (1 M, p*H* 7.4) was obtained from SIGMA-ALDRICH (Steinheim, Germany) and was used for covalent immobilization reactions of chymosin. Additional buffer solutions for enzymatic activity assays were prepared in the range of p*H* 1.2–12.0 by using chemicals of technical grade.

KCl/HCl buffer was prepared by mixing a 0.2 M KCl solution with 0.2 M hydrochloric acid. This buffer was used for measurements of enzymatic activities at p*H* 1.2 and p*H* 2.0. Phosphate/citrate buffer was used for examinations in the range of p*H* 3.0–8.0. These buffers were prepared by mixing a particular volume, e.g. 20 mL, of 0.2 M disodium hydrogen phosphate solution with 0.1 M citric acid. For examinations at p*H* 9.0, a sodium borate/HCl buffer was used. To this, 4.77 g (12.5 mmol) sodium borate were mixed with 0.1 M HCl (46 mL). The buffer system at p*H* 10.0 was obtained by mixing 4.77 g (12.5 mmol) sodium borate with 0.1 M NaOH (183 mL). Glycine/NaCl/NaOH buffer systems were used for p*H* values of 11.0 and 12.0. To this, 7.85 g glycine and 6.28 g glycine, respectively, were added to 4.9 g NaCl and 100 mL NaOH solution (1 M).

**Casein**

Casein, obtained from bovine milk, was purchased from SIGMA-ALDRICH (Steinheim, Germany) as purified powder. This casein powder, containing all four major casein components ($\alpha_{s1}$-, $\alpha_{s2}$-, β-, and κ-casein), was used throughout the conducted studies and experiments.

**Chymosin**

Chymosin from calf stomach was purchased from SIGMA-ALDRICH (Steinheim, Germany) and was used for experiments without further purification. The amount of chymosin accounted for 62 wt% of the solid content. Chymosin activity was 42 units/mg solid, as indicated by SIGMA-ALDRICH. The enzyme was stored in a freezer at -20 °C, in order to prevent denaturation of the enzyme over a long storage time.

**Diepoxy-PEG-spacers**

Diepoxy-PEG-spacers with molecular weights of 10.000 g/mol and 20.000 g/mol were obtained from CREATIVE PEGWORKS (Winston-Salem, USA). Polydispersity of diepoxy-PEG-spacers was 1.05, as indicated by the manufacturer. PEG-spacers were stored in a freezer at -20 °C.

**Glutaraldehyde**

Glutaraldehyde was purchased from SIGMA-ALDRICH (Steinheim, Germany) as 50 wt% aqueous solution, which was stored in a refrigerator at 5 °C.

**Hemoglobin**

Bovine hemoglobin was obtained from SIGMA-ALDRICH (Steinheim, Germany) and was used without further purification as substrate for enzymatic activity assays of chymosin and rennet. It was stored in a refrigerator at 5 °C.

**Microscope cover glasses**

Microscope cover glasses with dimensions of 18 mm *x* 18 mm were purchased from CARL ROTH (Karlsruhe, Germany) and were used as support materials for immobilization of enzyme and casein deposition experiments.

**Microscope slides**

Microscope slides with dimensions of 75 mm *x* 26 mm were obtained from VWR (Darmstadt, Germany) and were used as glass supports for immobilization reactions and casein deposition.

### Rennet

Rennet is a commercially available enzyme mixture of chymosin and pepsin and is often used in cheesemaking. Pepsin is, just as chymosin, an aspartic protease and exhibits its highest activity at p*H* 1.0–2.0.[140] Like chymosin, pepsin preferably cleaves peptide bonds between hydrophobic amino acids. However, it is not known to specifically cleave the chymosin-sensitive peptide bond in κ-casein.

In this study, calf rennet powder from RENCO NEW ZEALAND (Eltham, New Zealand) was provided by the European supplier BICHSEL AG (Grosshöchstetten, Switzerland) and was used as enzyme for casein deposition reactions via physically adsorbed enzyme. The enzyme content of the obtained rennet powder accounts for at least 96 wt% of chymosin, as indicated by the supplier. The total enzyme content of the provided calf rennet powder was 1.6 wt%, as detected by thermogravimetric analysis. Commonly, NaCl is used in enzyme formulations in high amounts to enable an easy dosing, better dispersibility, and long term stability of the enzyme. In order to enhance the efficiency of conducted deposition experiments, the enzyme content of the rennet powder was significantly increased by reduction of the salt content via ultrafiltration. Unpurified calf rennet powder was dissolved in DI water at a concentration of 100 g/L and was centrifuged three times at 5,000 x g and 25 °C for 2 h, using Amicon® Ultra-15 Centrifugal Filter Devices with a cutoff of 3,000 g/mol. After ultrafiltration, the enzyme content was increased up to 67 wt%. The concentrated calf rennet powder was stored in a refrigerator at 5 °C.

An additional microbial rennet powder, i.e. rennet from *Mucor miehei*, was purchased from SIGMA-ALDRICH (Steinheim, Germany) and was used as a reference for enzymatic activity assays via determination of milk clotting time. The microbial rennet powder was stored in a freezer at -20 °C.

**All other chemicals which were used in the experiments and which are not mentioned above were of technical grade and used without further purification.**

## 3.2 Experimental procedures and syntheses

### 3.2.1 Investigation of properties of chymosin

**Determination of enzymatic activity of chymosin in dependence on p*H* and temperature**

The enzymatic activity of native chymosin was investigated with hemoglobin as substrate in dependence on p*H* and temperature. To this, two independent series of measurements were conducted.

The p*H* dependence was investigated at 40 °C in a range of p*H* 1.2–12.0. KCl/HCl buffers were used for test samples at p*H* 1.2 and 2.0. For p*H* 3.0–7.0 $Na_2HPO_4$/citric acid buffers were used. Sodium borate/HCl buffers were prepared for p*H* values of 8.0 and 9.0 and a sodium borate/NaOH buffer was used for p*H* 10.0. For p*H* 11.0 and 12.0 glycine/NaCl/NaOH buffers were prepared. Hemoglobin solutions with a concentration of 1 % (w/v) were obtained by dissolving hemoglobin at the particular p*H* value at 25 °C in an ultrasonic bath (100 % effectiveness) for 15 min. Enzymatic test reactions were started by the addition of 250 µL chymosin solution (0.1 % (w/v), 9.2 U) to 500 µL hemoglobin solution. Reactions were carried out in small vessels for 10 min in a water bath at 40 °C. After that, reactions were stopped by the addition of 500 µL trichloroacetic acid solution (10 % (w/v)) and vessels were allowed to stand at RT for 5 min. Reaction mixtures were then centrifuged at 13.000 rpm for 15 min. 1 mL of colorless supernatant was removed and absorbance was measured at 325 nm, using an UV/Vis spectrophotometer. Relative absorbance of test samples was calculated by comparison with control samples. These were prepared with the same approach, except that addition of enzyme solution took place after the addition of trichloroacetic acid solution. All test and control samples were measured in triple determination.

Temperature dependence of enzymatic activity was investigated from 20–70 °C in increments of 10 °C, using the hemoglobin test. All test samples were prepared at p*H* 3, using $Na_2HPO_4$/citric acid buffer. Measurements were performed for 10 min at the particular temperature in a water bath. Preparation of hemoglobin and enzyme solutions as well as processing of assays were carried out as described above.

### Comparison of enzymatic activity of used enzyme formulations

Photometrical determination and comparison of enzymatic activities of used enzyme formulations were performed via the hemoglobin test as described above. The reactions were merely carried out for 5 min instead of 10 min.

Examination of enzyme activity via determination of milk clotting time was performed accordingly to quality tests, used by SIGMA-ALDRICH. Therefore, a 10.4 % (w/v) solution of nonfat dry milk powder with 10 mM $CaCl_2$ was prepared. At first, clotting time of a rennet reference (rennet from *Mucor miehei*) was determined. 10 mL milk powder suspension was incubated at 30 °C in a water bath for 45 min. Then, 1 mL of a 0.1 % (w/v) rennet reference solution was added under gentle swirling of the flask. Clotting time was determined, when a white-translucent semi-liquefied film appeared on the side of the flask above the milk suspension. This reference clotting time was compared to clotting times of chymosin and rennet samples. These were determined in the same manner as before, except that 1 mL of a 0.005 % (w/v) enzyme solution, prepared from a 1 mg/mL stock solution, was used. Thus, the dilution factor was 20.

### Determination of number size distributions of used enzyme formulations and zeta potential of chymosin

Number size distributions at p*H* 3 and p*H* 7 of used enzyme formulations, i.e. chymosin and rennet, were obtained via DLS measurements. 0.1 % (w/v) enzyme solutions were prepared with chymosin and rennet. Adjustment of p*H* was achieved with 0.5 M KOH and 0.5 M HCl. Samples were filtered before DLS measurements with a 5 µm filter device. Maximal diameters were expressed by number mode values for the particular distributions. Zeta potential of chymosin (0.1 % (w/v)) was measured via DLS, using autotitration. Average zeta potentials were determined in triple.

### 3.2.2 Investigation of properties of casein

**Determination of zeta potential and sizes of casein micelles in dependence on p*H***

Solubility of casein was examined in dependence on p*H* value via determination of zeta potential and casein micelle size. A casein dispersion (1 g/L) was prepared by mixing 0.2 g with 200 mL deionized water at 50 °C under stirring. After 1 h, the resulting mixture (p*H* 4.5) was acidified with conc. HCl to p*H* 3.0 and stirred for further 3 h. Before DLS measurements, the casein dispersion was filtered, using a hydrophilic 5 µm syringe filter, to remove dust and other interfering particles. Zeta potential and micelle sizes were determined in p*H* increments of 0.5 via DLS, using autotitration. Average values were calculated from triple determination of number mean values. The preparation of a casein dispersion at p*H* 6.7 was conducted as described above, except for adjustment of p*H* with 5 M KOH. Shelf life of a casein dispersion (10 g/L, p*H* 3.0) was performed by repetitive determination of the average micelle size over five days. The dispersion was stored in a refrigerator and heated up to 40 °C for at least 30 min before DLS measurement.

**Determination of sizes of casein micelles and viscosity in dependence on casein concentration**

Preparation of casein dispersions with varying concentrations was performed as described above. Concentrations were 1, 5, 10, 20, 25, 30, and 50 g/L. All dispersions were adjusted to p*H* 3.0 with conc. HCl, filtered, and number mean diameters were determined via DLS in triple.

Additionally, viscosity measurements were performed with the dispersions, using a Mikro-Ostwald viscometer. To this, the viscometer was placed in a water bath at 25 °C and flow time was automatically determined with an optical sensor (light barrier). In triple determined flow times were used to calculate kinematic viscosities. These were converted into dynamic viscosity values by taking the density of the particular dispersion into account.

### 3.2.3 Synthesis and characterization of casein coatings via physically adsorbed enzyme

**Autodeposition procedure of casein films with adsorbed chymosin**

Microscope slides were cut into smaller pieces (15 mm *x* 75 mm) and cleaned with EtOAc and deionized water. Physical adsorption of chymosin was achieved by drying 600 µL of a chymosin solution in DI water (3 g/L, 66.4 U) on a particular area (15 mm *x* 25 mm) of the glass support. After enzyme adsorption, the support was washed with DI water to remove non-specifically adsorbed chymosin.

Subsequently, the functionalized support was placed in a holder and submerged in 20 mL of an aqueous casein dispersion (varying concentrations) at p*H* 3 and 40 °C. Deposition reactions were stopped after a predetermined time by removing the samples from the casein dispersion. Glass supports with the adherent protein film were washed in deionized water to remove non-cleaved casein and were dried. **Figure 25** illustrates the general dip coating process for casein deposition on enzyme-functionalized supports.

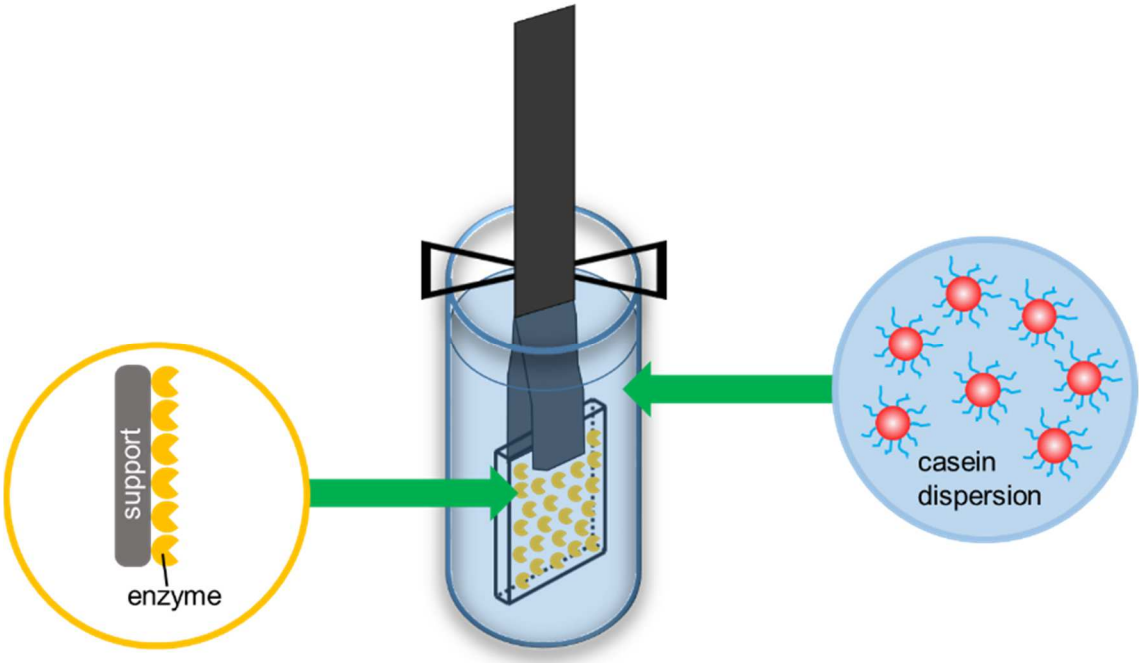


*Figure 25. Dip coating process for casein deposition.*

### Determination of film thickness

Atomic force microscopy was used for the determination of the film thickness of deposited casein coatings in dependence on deposition time, p*H* value, and casein concentration. To this, a cut was made with a scalpel into the protein coating down to the support surface. Height profiles of the cut-region were obtained by measuring the sample's topography (**Figure 26**). Height differences were detected by investigation of section lines with a length of 10 µm, crossing the glass surface of the cut and the surface of the continuous casein film. All height profiles were obtained in triple determination. Height data were used to calculate average film thicknesses of the protein coatings. Dependence of deposition time was examined in the range of 5–150 min, p*H* dependence from p*H* 2 to p*H* 8, and dependence of casein concentration was investigated at 1–20 g/L.

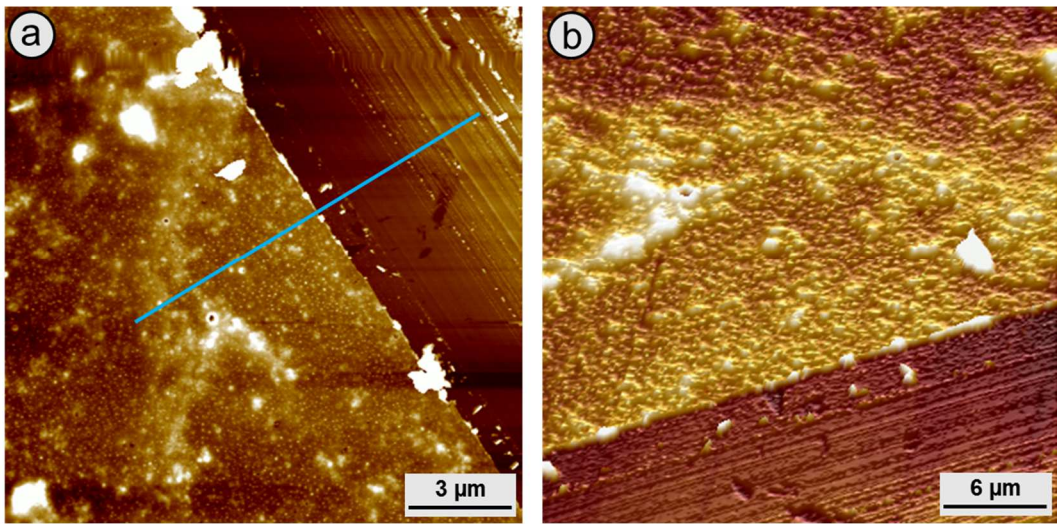


*Figure 26. Determination of film thickness of casein films via AFM: a) 2D and b) 3D view. Height profiles were obtained across section lines with a length of 10 µm, as indicated by the blue line. The presented casein coating was obtained at pH 3 after a deposition time of 20 min, using a casein concentration of 15 g/L.*

### Determination of properties of deposited casein coatings

Applicability of sterilization processes of deposited casein films was performed by treatment with UV radiation and at elevated temperature. Before proceeding, cleaved casein films were deposited as described above, using a casein concentration of 10 g/L and a deposition time of 60 min. Sterilization via UV radiation was achieved by using an Aktiprint mini 12 from TECHNIGRAF. Films were irradiated ten times with UV light at a power of 80 W/cm, using a belt speed of 3 m/min. Temperature sterilization was carried out by heating casein

films at 100 °C for 20 min. After particular treatment, protein coatings were washed in DI water, dried, and integrity of the films was examined via SEM.

Mechanical properties of casein coatings were investigated via AFM. Film hardness was indirectly measured via deformation measurements. In addition, DMT-moduli (Derjaguin-Muller-Toporov model) of the processed films were determined by using PeakForce QNM (Quantitative NanoMechanics) mode. Average deformation and modulus values were obtained for the particular casein coatings by examination of areas of 5 µm *x* 5 µm at a constant peak force of 7.6 nN.

Determination of resistance to organic solvents of deposited casein films was conducted visually, using light microscopy. Dry cleaved casein films were immersed in particular organic solvents, i.e. ethanol, ethyl acetate, toluene, and tetrahydrofuran, and dissolution was examined qualitatively at 20-fold magnification, using a Labophot-2 light microscope. Samples were compared to non-cleaved casein films as the reference. All samples were analyzed in triple determination.

**Pressureless gluing of two supports via EMA**

Supports (glass, Ti, and galvanized steel) were cut into smaller pieces, i.e. 25 mm *x* 75 mm. Cleaning of the supports was conducted with EtOAc in an ultrasonic bath for 45 min, followed by washing with DI water. 625 µL of an aqueous rennet solution (25 g/L, 595 U) was trickled onto an area of 25 mm *x* 25 mm and dried.

After that, two support slides with adsorbed enzyme were placed in special holders and fixed. A variable amount of bar spacers with a thickness of 125 µm each was used to adjust the particular distance between the slides. Following, the two supports were immersed into a casein dispersion (varying concentrations from 1 g/L up to 20 g/L, 200 mL) at 40 °C and p*H* 3 for 80 min. After the cleavage reaction, the adhered supports were washed in DI water to remove non-cleaved casein and were dried. Drying was performed in open air with the supports still vertically fixed in the holders.

### 3.2.4 Synthesis of casein films and structures via covalently immobilized enzyme

**Immobilization of chymosin via GLYMO**

Microscope cover glasses (18 mm *x* 18 mm) and Si-wafers (10 mm x 10 mm) were cleaned previously to the silylation step via a combination of alkaline and acid treatment. This combination is known to be most effective to remove organic and inorganic contaminations from glass supports and Si-wafers.[254] Supports were placed in a crystallizing dish, covered with a watch glass, allowing stirring of the cleaning solution with a magnetic stirrer. Alkaline cleaning was performed in a mixture of 25 wt% ammonia solution, 35 wt% hydrogen peroxide solution, and deionized water, using a volume ratio of 1:1:5. The mixture was heated up to 80 °C and kept at this temperature for 5 min. The cleaned supports were then thoroughly rinsed with DI water and subsequently subjected to acidic cleaning. Cover glasses and Si-wafers were immersed into a mixture of concentrated hydrochloric acid, 35 wt% hydrogen peroxide, and DI water in a volume ratio of 1:1:5. The mixture was heated up to 80 °C for 5 min. Supports were again intensively rinsed with DI water and dried at 120 °C for 30 min.

Modification of the cleaned supports for enzyme immobilization was achieved with GLYMO in an EtOH/$H_2O$ 80:20 (w/w) mixture at a GLYMO concentration of 10 wt% under alkaline conditions, using 1 wt% triethylamine. The reaction mixture was gently stirred at 25 °C for 2 h and was allowed to stand unstirred for further 10 min. Functionalized glass supports were thoroughly rinsed with EtOH and DI water to remove non-specifically adsorbed GLYMO. Subsequently, washed supports were cured at 110 °C for 1 h, rinsed with copious amounts of EtOH and DI water, and dried.

Immobilization of enzyme was carried out at p*H* 7 in 100 mL phosphate buffer solution at high ionic strength (1 M buffer) and low ionic strength (25 mM buffer). The different ionic strengths were chosen to yield varying degrees of enzyme aggregation. Enzyme immobilization reactions via epoxy groups are commonly conducted at high ionic strength, e.g. 1 M buffer concentration. Here, the first reaction step, i.e. the hydrophobic adsorption of the enzyme onto the support, is favored (see section 2.3.3.3). At low ionic strength this step is inhibited and aggregated enzyme structures are formed.

An amount of 6 mg chymosin formulation (221.4 U) was dissolved in 1 mL DI water and was added to the particular immobilization buffer. The immobilization

process was performed under gentle stirring at 25 °C. Progress of enzyme coupling was followed by taking samples (500 µL) from the supernatant, which were mixed with 1 % (w/v) hemoglobin solution (500 µL) to examine residual enzyme activity. Assays were carried out at 40 °C for 30 min at p*H* 3.5 and stopped by the addition of 10 % (w/v) trichloroacetic acid (500 µL). Samples were centrifuged at 13.000 rpm for 15 min and absorbance was measured at 325 nm and compared to control samples. Immobilization reactions were stopped after 96 h and modified glass supports were intensively washed with DI water to remove non-covalently bound chymosin and dried. Progress of enzyme immobilization is shown in **Figure A-84**.

Residual activity of covalently immobilized chymosin was quantitatively determined by use of Sepabeads EC-EP. This is mainly because the verification of enzyme activity of bound chymosin onto the cover glasses was not possible, due to the high ratio of support surface to bound enzyme. Immobilization of chymosin onto Sepabeads at high ionic strength was performed analogously to the use of glass supports, except for little modification.

Sepabeads EC-EP were washed 10-times with deionized water, using a Büchner flask and a glass filter (size 2). Immobilization solution was prepared by dissolving 20 mg (778.0 U) concentrated rennet formulation in 1 M phosphate buffer (20 mL). The p*H* value was adjusted to p*H* 7.0 with 5 M HCl and 2.22 g of washed and dried Sepabeads EC-EP were added. The suspension was then gently stirred for 96 h at 25 °C. Afterwards, the suspension was filtered and the enzyme carriers were washed 3-times with copious amounts of DI water. The hemoglobin test was performed as described hereafter to determine the residual chymosin activity. 224 mg of dried Sepabeads, containing 2 mg rennet, were dispersed in 500 µL DI water. The enzymatic cleavage reaction was started by the addition of 1000 µL hemoglobin solution (1 % (w/v), p*H* 5.0) and was carried out at 40 °C for 30 min under gentle stirring. The reaction was stopped by the addition of 10 % (w/v) trichloroacetic acid (1000 µL). The reaction vessels were left at room temperature for 5 min and were then centrifuged for 15 min at 13.000 rpm.

Enzymatic activity was determined by measuring the absorbance of 1 mL supernatant at 325 nm. Absorbance values were determined in triple and compared to reference samples, representing full enzymatic activity of free native enzyme. These reference samples were prepared in the same manner, except that 2 mg (77.8 U) concentrated rennet were dispersed in 500 µL DI water.

**Immobilization of chymosin via APTES/glutaraldehyde**

Cover glasses and Si-wafers were cleaned analogously to previous experiments, regarding the immobilization of chymosin via GLYMO.

Silylation of the cleaned supports was obtained by immersion into an EtOH/$H_2O$ 80:20 (w/w) solution at an APTES concentration of 10 wt%. Since APTES is able to catalyze the hydrolysis reaction of the ethoxy groups and following condensation reactions between neighboring hydroxyl and alkoxy groups by its amino group, no addition of a base in catalytic quantities was necessary. Except for this, the residual experimental procedure for the functionalization with APTES was carried out as described for the modification with GLYMO (see above).

Activation of the silanized supports with glutaraldehyde was conducted in 200 mM phosphate buffer (80 mL) and 50 % (v/v) glutaraldehyde solution (34.3 mL). The p*H* value was adjusted with 0.2 M HCl to p*H* 7.0 and the reaction was carried out at 25 °C for 17 h under gentle stirring. Subsequently, the activated cover glasses were washed in 25 mM phosphate buffer solution and then thoroughly rinsed with deionized water and dried.

Immobilization of enzyme onto the activated glass supports was carried out in the same manner as for the procedure with epoxy-activated supports at low ionic strength (25 mM buffer concentration). The immobilization progress was also followed by taking samples from the supernatant and determination of the residual enzymatic activity via the hemoglobin test (**Figure A-85**). The reaction was stopped after 48 h and supports were intensively rinsed with DI water and dried.

As conducted before, the residual enzymatic activity of via APTES/glutaraldehyde covalently bound chymosin was investigated with Sepabeads. Sepabeads of the type EC-EA were washed 10-times with DI water, using a Büchner flask and a glass filter (size 2). 7 g of washed and dried Sepabeads EC-EA were suspended in 20 mL of a 15 % (v/v) glutaraldehyde solution, which was prepared by mixing 200 mM phosphate buffer (14 mL) with 50 % (v/v) glutaraldehyde solution (6 mL). The p*H* value was adjusted to p*H* 7.0 with 5 M HCl and the reaction mixture was gently stirred for 17 h at 25 °C. Activated Sepabeads EC-EA were filtered and washed 3-times with 25 mM phosphate buffer and copious amounts of DI water. The immobilization reaction was carried out in 25 mM phosphate buffer solution (20 mL). An amount of 20 mg (778.0 U) concentrated rennet formulation and 6 g of dried enzyme

carriers, activated with glutaraldehyde, were added. The p*H* value was set to p*H* 7.0 and the suspension was stirred for 48 h at 25 °C. After filtration of the suspension, the enzyme-functionalized Sepabeads were washed 3-times with DI water and dried.

Examination of the residual enzymatic activity was performed analogously to the use of Sepabeads EC-EP, except that an amount of 602 mg Sepabeads EC-EA, containing 2 mg (77.8 U) enzyme, was tested for activity and that reactions were carried out at p*H* 3.

**Immobilization of chymosin via diepoxy-PEG-spacer**

Cleaned cover glasses (18 mm *x* 18 mm) were first modified with APTES as described above. The availability of amino groups allowed for the succeeding attachment of the used diepoxy-PEG-spacers. To this, a spacer solution (400 µL) was dried onto the amino functionalized support surface over 24 h. In case of using the large PEG-spacers (20.000 g/mol) the concentration of the solution was 0.25 g/L, while for the small spacers (10.000 g/mol) a concentration of 0.125 g/L was used. These concentrations correspond to two PEG molecules per hydroxyl group of the glass surface, if a density of 5 OH-groups per nm² is assumed. The excess of spacer molecules reduces the probability of double attachments and thus, insufficient chymosin immobilization. The particular spacer solutions were obtained by dissolution of the respective diepoxy-PEG-spacer in 0.1 M phosphate buffer solution and adjustment to p*H* 8.0 with 5 M KOH. After covalent coupling of epoxy terminated PEG-spacers, modified cover glasses were thoroughly rinsed with DI water and dried.

Covalent immobilization of chymosin was achieved in the same manner as described for the procedure without the use of spacer molecules (see above). Immobilization reactions were carried out for both spacer types at high (1 M buffer) and low ionic strength (25 mM buffer), to obtain different degrees of enzyme aggregation.

**Deposition of casein onto enzyme-functionalized supports**

Deposition of casein was achieved in an analogous manner for all three covalent immobilization methods. Enzyme-functionalized glass supports were immersed into 20 mL casein dispersion (10 g/L) at p*H* 3 and 40 °C for 2 h. After casein cleavage and deposition, the supports were washed in DI water as conducted in previous experiments to remove non-cleaved casein and were eventually dried.

### 3.2.5 Synthesis of nanostructured surfaces via EMA

**Prepatterning of supports via Nanosphere Lithography**

Silicon wafers with native $SiO_2$ layer were pretreated by oxygen plasma (Oxford Instruments PlasmaLab 80 plus) with 2 sccm $O_2$ and 8 sccm Ar at 75 mTorr with 50 W RF power for 5 min. For the formation of patterned platinum films with antidots a monolayer of PS spheres was deposited onto the $SiO_2$ surface by doctor blade technique. A 40 µL droplet of the colloidal suspension was placed onto the surface and moved over it, using a hydrophobic blade at constant velocity. This preparation was performed in air under 50 % RH, while annealing the Si-wafer to 26 °C. Hexagonally dense packed PS sphere masks were formed.

For final mask modification, the self-assembled PS-sphere monolayer was treated in an oxygen plasma as described above. This led to a partial removal of PS and thus, resulted in shrinking of the spheres. The degree of shrinkage can be adjusted by variation of the duration of plasma treatment. For antidots with larger diameter PS spheres with an initial diameter of 618 nm were deposited on the support and shrunk in the applied plasma for 5 min, while for smaller antidots 220 nm PS spheres were shrunk for 1.5 min.

The modified spheres then acted for Nanosphere Lithography as a shadow mask during the sputter deposition of platinum. This was conducted in an “ISI PS-2” coating unit for 60 s at 1.2 kV and 20 µA under argon atmosphere (0.1 Torr). Spheres were subsequently removed with THF in an ultrasonic bath to yield prepatterned supports for enzyme immobilization.

**Covalent immobilization of chymosin and subsequent casein deposition**

The functionalization of the accessible native oxide layer of the used Si-wafers was achieved by modification with GLYMO. The experimental procedure was conducted as described in 3.2.4. Subsequently, chymosin was covalently immobilized onto the modified prepatterned supports in the same manner as described before, using an immobilization buffer with high ionic strength (1 M phosphate buffer).

Prepatterned supports with covalently immobilized chymosin were immersed into 20 mL casein dispersion (1 g/L) at p*H* 3 and 40 °C for 2 h. After casein cleavage and deposition, supports were washed in DI water, in order to remove non-cleaved casein and were dried.

## 3.3 Analytical methods

### Atomic force microscopy

AFM measurements were performed on a Dimension Icon PT from BRUKER. Detection of topology of samples was conducted in ScanAsyst mode, i.e. a PeakForce Tapping mode, which allows for high resolution imaging by an automatic setting of AFM parameters. Mechanical properties, such as deformations and DTM moduli, of processed samples were determined via PeakForce QNM (Quantitative NanoMechanics) mode.

### Contact angle measurements

Contact angle measurements of sessile drops were performed using a Contact Angle Measuring System G10 from KRÜSS. Contact angles were measured one second after placing the drop onto the support. All reported contact angles are average values, calculated from three single measurements.

### Dynamic light scattering

DLS measurements were conducted on a Zeta Nano-ZS from MALVERN INSTRUMENTS. By DLS measurements, sizes of casein micelles and chymosin molecules were determined in aqueous dispersions and solutions. Number mean values, obtained by triple determination, were used for the characterization of particles.

### Ellipsometry

Ellipsometry was performed with an EP3-SW device from NANOFILM TECHNOLOGY. This spectroscopic technique was used to determine the layer thickness of alkoxysilanes on glass supports.

### Hemoglobin test

Hemoglobin tests were carried out to determine enzymatic activity of chymosin. Hemoglobin was used as substrate. It is cleaved by chymosin, resulting in the formation of components, which are soluble in trichloroacetic acid. The amount of soluble products upon cleavage was measured photometrically. Tests were performed according to Mezina and coworkers, except for small modifications.[146]

### Light microscopy

Resistance to organic solvents of deposited casein coatings was investigated via light microscopy, using a Labophot-2 from NIKON. Films were examined at 20-fold magnification for imaging.

### Measurement of adhesive strength

Adhesive strengths of agglutinating casein layers were measured with an Epprecht twistometer by application of torsion force. Values were measured three times for samples with a plate distance of 125 µm.

### Scanning electron microscopy

SEM measurements were performed, using a ZEISS Neon 40 scanning electron microscope equipped with an EDX-detector. Images of samples were obtained by applying the InLens-detector (detection of secondary electrons) and the SE-detector (detection of secondary and backscattered electrons) at an acceleration voltage of 2 kV. In addition, EDX-spectra were also obtained at particular acceleration voltages.

SEM images of prepatterned supports for nanostructuring experiments via EMA were obtained by using a JEOL JSM-6300F scanning electron microscope. The applied acceleration voltage was 5 kV.

### UV/Vis spectroscopy

Absorbance measurements were performed on a Genesys 20 spectro-photometer from THERMO FISHER SCIENTIFIC. Samples for enzymatic activity assays, using hemoglobin as substrate, were measured at 325 nm.

### Viscometry

For determination of dynamic viscosity of casein dispersions with varying concentration Mikro-Ostwald viscometers were used. For concentrations up to 30 g/L a Mikro-Ostwald viscometer type Ic and for a concentration of 50 g/L a Mikro-Ostwald viscometer type II was used.

### X-ray photoelectron spectroscopy

XPS measurements were performed with an Omicron ESCA+ system from OMICRON NANOTECHNOLOGY at an energy of 50 eV for survey spectra and 25 eV for element spectra. As internal reference, the C1s peak (BE = 285 eV) was used for calibration in all obtained spectra. Measurements were performed at a base pressure of $<5 \cdot 10^{-10}$ mbar and under a take-off angle of the detected photoelectrons of 60° with respect to the surface plane.

# 4 Results

## 4.1 Introduction

The main goal of this study is the evaluation of a groundbreaking process for the controlled formation of biobased coatings and structures, i.e. the Enzyme Mediated Autodeposition. Special emphasis will be placed on particular types of enzyme immobilization and their related deposition structures. It is intended to achieve a growing level of precision, ranging from the deposition of continuous coatings to the addressment of single particles. **Figure 27** provides a detailed overview on the conducted investigations and experiments.

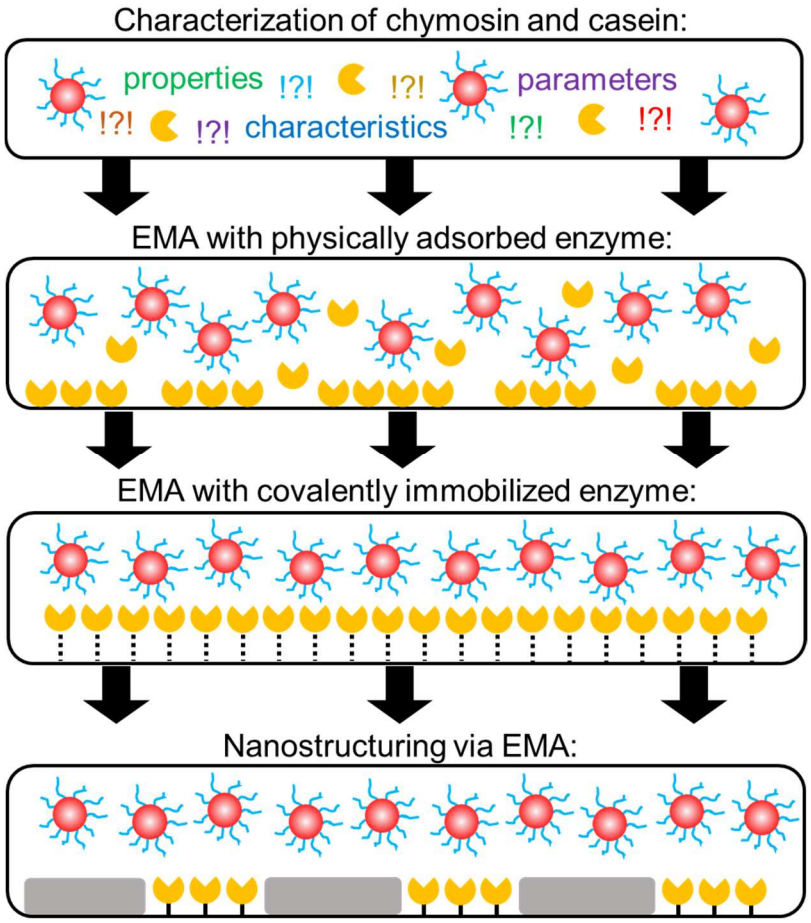


*Figure 27. Schematic outline of the conducted investigations and experiments of the EMA, using casein and chymosin. Dashed lines represent different covalent immobilization methods for chymosin. Short lines illustrate a short covalent linkage of the enzyme.*

At first, comprehensive investigations on the properties of the components of the used system, which is based on the enzyme chymosin and the milk protein casein, are made. Knowledge about the characteristics of these biomolecules is of essential importance for succeeding experiments.

After that, the EMA of casein with physically adsorbed chymosin will be considered. This reversible immobilization method is the most straightforward one and is very efficient with respect to used resources and time efficiency. It can be expected that this immobilization method and following casein deposition experiments will yield important results and fundamental knowledge about the general feasibility and functionality of the EMA. Certain importance will also be attached to potential limitations of the investigated system, regarding attainable film thicknesses and materials compatibility. Moreover, mechanical and physico-chemical properties of the resulting casein layers will be determined and evaluated.

Subsequent experiments will deal with the application of more complex and irreversible immobilization methods for chymosin. Here, individual results depending on the type of attachment and mobility of the enzyme are assumed. Investigations will comprise covalent immobilization methods, which are commonly applied in industry, i.e. tethering onto supports which have epoxy groups or are activated with glutaraldehyde. Additional experiments will consider enzyme coupling via spacer molecules, which is assumed to show beneficial influences on the mobility of the immobilized enzyme and thus, on the resulting casein deposition structures.

As the final highlight, the limitations of the EMA with respect to the structuring of surfaces will be examined. It can be expected that the EMA exhibits a great potential for the controlled, site-specific deposition of biomolecules. This is assumed to be applicable on the nanometer scale, because enzymes operate on the ångström level and previous experiments confirmed a high controllability of the overall process.[252,253] Thus, the highest possible precision of EMA in connection with the used system, i.e. the selective addressment of single casein micelles, will be a major goal.

## 4.2 Characterization of chymosin and casein

### 4.2.1 Overview

In order to achieve knowledge about the system chymosin and casein, relevant properties of the components, i.e. dispersibility, stability, particle size, and activity were examined. This allows for the precise determination of process parameters of succeeding deposition experiments.

### 4.2.2 Properties of chymosin

#### 4.2.2.1 Enzymatic activity of chymosin in dependence on p*H* and temperature

The examination of the p*H* dependence of chymosin activity was performed photometrically, using hemoglobin as substrate. The results are presented in **Figure 28**. Obtained data show that the used chymosin formulation exhibits its highest activity at p*H* 3. This is in good accordance to values found in literature, where the highest activity is indicated at p*H* 3–4.[140] Also references can be found which indicate the highest activity at even lower p*H* values, e.g. 2.8.[255] Nonetheless, in literature, the highest activity of chymosin is often indicated in the range of p*H* 3.5–3.7.[145,146] However, chymosin is only moderately stable in this region and tends to undergo autoproteolysis.[144] This seems to be consistent with the determination of the highest enzyme activity and should constitute the reason for its allegedly shifted nature. It can be stated that the used chymosin has its highest activity at p*H* 3 under the performed test conditions. Additionally, chymosin is very stable at p*H* 3.[256] This is especially important for potential applications, which require long reaction times.

Below p*H* 3 chymosin rapidly loses enzymatic activity. With increasing p*H* value (p*H* > 3), activity of chymosin also significantly decreases. Chymosin loses about 85 % of its activity up to p*H* 7 compared to p*H* 3. In the alkaline range of p*H*, chymosin is inactive. This p*H* dependence is based on the occurring denaturation of the enzyme at unfavorable p*H* values. Possible reasons are a partial dissolution of peptide bonds or certain conformational changes of protein segments, resulting in inactivity. Most plausible seems a p*H* induced interference of the cleavage mechanism (Figure 16). In the active state, one of the two aspartic amino acid residues is deprotonated, while the other one is

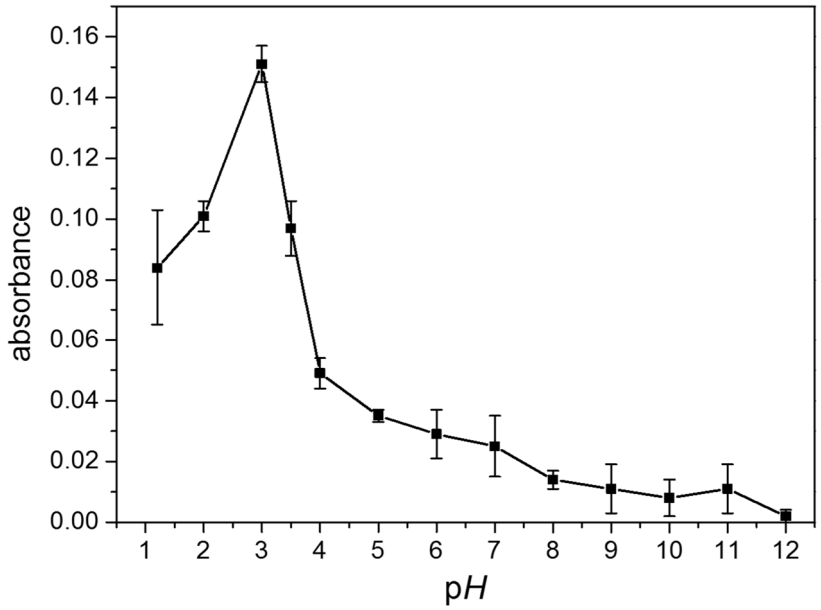


*Figure 28. Enzymatic activity of chymosin in dependence on pH at 40 °C. Lines are not based on mathematical calculations and serve as visualization. Data are listed in Table A-12.*

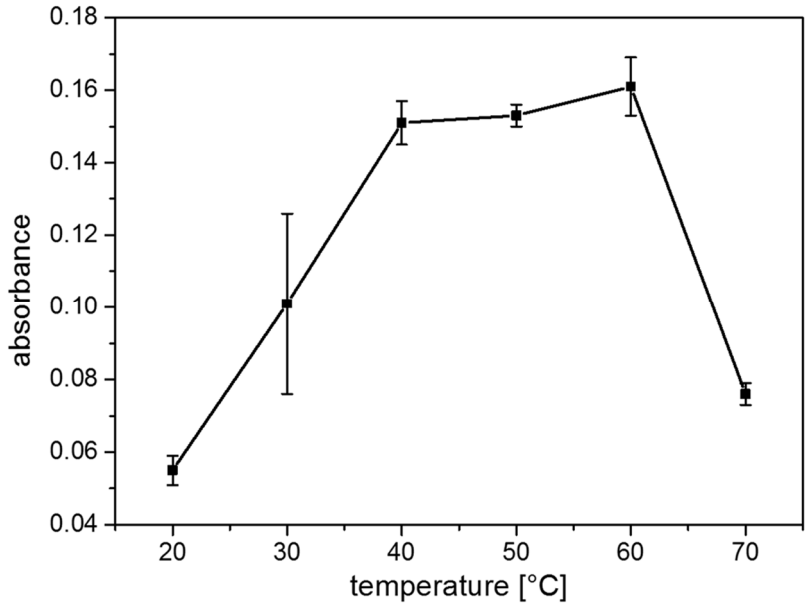


*Figure 29. Chymosin activity in dependence on temperature. Measurements were conducted at pH 3. Lines serve as visualization only. Data are shown in Table A-13.*

not. Changes in p*H*, i.e. lower or higher than p*H* 3, would disrupt this equilibrium state either by deprotonation or protonation of both carboxylic groups at the same time and thus, would cause failure of the cleavage reaction.

**Figure 29** shows the enzymatic activity of chymosin dependent on temperature. Measurements were performed at p*H* 3. With increasing temperature, i.e. 20–40 °C, the enzymatic activity also increases significantly. Additional rise in temperature up to 50 °C and 60 °C yields only little improvement, as indicated by the almost steady absorbance in this region. Standard deviations of the absorbances even cover same values.

Further elevation of temperature up to 70 °C leads to a drastic decline of cleavage activity. This is probably based on a temperature induced denaturation of chymosin. The obtained values are consistent with literature data.[147] The highest chymosin activity is indicated at 40 °C, but relevant high activities are also measureable up to 56 °C. At even higher temperatures, chymosin shows no activity. The highly reactive nature of chymosin at 40 °C is plausible and was expected, since the average internal body temperature of cows is about 39 °C.

Although slightly higher activities were determined at 50 °C and 60 °C compared to 40 °C, it seems highly recommendable to perform experiments with chymosin at 40 °C. Here, its activity is very high and denaturation of peptide chains due to elevated temperatures is restricted. This is especially important for long term experiments.

#### 4.2.2.2 Comparison of enzymatic activity of used enzyme formulations

A comparison between the two used enzyme formulations, i.e. chymosin and rennet, was performed in order to ensure that both exhibit sufficient activity to conduct experiments with comparable and reproducible results. To this, two independent enzymatic activity tests were applied, i.e. hemoglobin test and determination of milk clotting time.

Equal amounts of enzyme molecules were used in the hemoglobin test to cleave a distinct number of substrate molecules. The duration of the cleavage reaction was 5 min for both samples. Consequently, the resulting absorbance values can be directly compared. The parameters and results of the hemoglobin test are shown in **Table 3**.

*Table 3. Hemoglobin test results of chymosin and rennet solution.*

| Enzyme formulation: | Enzyme content: | Concentration: | Absorbance: |
|---|---|---|---|
| Chymosin: | 62 wt% | 0.1 % (w/v) | 0.065 ± 0.002 |
| Rennet: | 67 wt% | 0.09 % (w/v) | 0.063 ± 0.001 |

In addition to the hemoglobin test, enzymatic activity was also investigated by measuring the time which is required by the enzyme to clot a certain volume of milk. This kind of assays are often used in industry and by manufacturers and distributors of enzyme formulations.

Enzymatic activity via determination of clotting time was calculated using the following equation:

$$\frac{\text{Units}}{\text{mL enzyme}} = \frac{(t_1)(df)}{(t_2)(V_e)}$$

Here, $t_1$ is defined as the clotting time of enzyme standard, df is the dilution factor, $t_2$ is the clotting time of the enzyme sample, and $V_e$ is the volume of the used enzyme sample.

Clotting time for the enzyme standard was 1.42 min and clotting times were 0.77 min and 0.73 min for chymosin and rennet solutions, respectively. This yields:

Chymosin:

$$\frac{1.42\ \text{min} \cdot 20}{0.77\ \text{min} \cdot 1\ \text{mL}} = 36.9\,\frac{\text{Units}}{\text{mL solution}} = 36.9\,\frac{\text{Units}}{\text{mg solid}} = 59.5\,\frac{\text{Units}}{\text{mg chymosin}}$$

Rennet:

$$\frac{1.42\ \text{min} \cdot 20}{0.73\ \text{min} \cdot 1\ \text{mL}} = 38.9\,\frac{\text{Units}}{\text{mL solution}} = 38.9\,\frac{\text{Units}}{\text{mg solid}} = 58.1\,\frac{\text{Units}}{\text{mg rennet}}$$

The used chymosin formulation exhibits 59.5 units/mg enzyme, while the rennet formulation has an activity of 58.1 units/mg enzyme. Both tests show similar results, meaning that both formulations have nearly the same enzymatic activity. As a consequence, the used chymosin and rennet formulations can be applied compatibly for experiments, ensuring reproducible results and conclusions.

### 4.2.2.3 Size distributions of used enzyme formulations and zeta potential of chymosin

To verify the presence of single chymosin molecules in enzyme solutions used throughout the experiments, DLS measurements were performed with both enzyme formulations, i.e. chymosin and rennet formulations.

The obtained number size distributions are shown in **Figure 30**. The graphs confirm that indeed predominantly single enzyme molecules are present for both enzyme solutions. Number mode values for chymosin solutions are 5.6 nm and 5.7 nm at p*H* 7 and p*H* 3, respectively. For rennet solutions number mode values are 4.9 nm and 5.1 nm at p*H* 7 and p*H* 3, respectively. These values represent single enzyme molecules and are in good accordance to the diameter of a single chymosin molecule which is about 5-6 nm (PDB code 4AA8). Presence of single enzyme molecules is therefore ensured, when enzymatic reactions are carried out at p*H* 3 or immobilization of chymosin onto support surfaces is considered. Such immobilization reactions are usually performed under neutral conditions.[155] At these conditions the N-terminal amino group is not protonated and coupling reactions proceed most likely via this amino group.

**Figure 31** illustrates the zeta potential of dissolved chymosin molecules in dependence on p*H*. The isoelectric point of chymosin is at p*H* 4.6. This is the same value as found in literature.[143] Chymosin is electrostatically stable

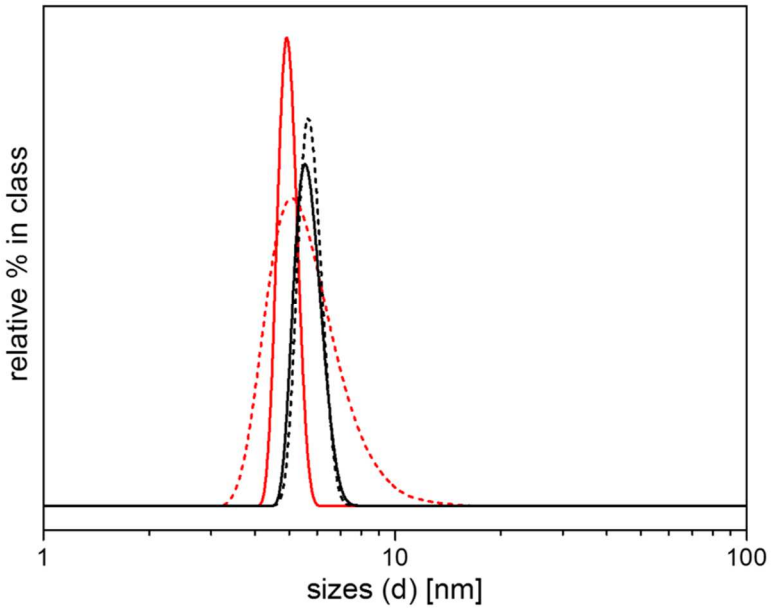


*Figure 30. Number size distributions of chymosin solutions at pH 7 (—) and at pH 3.0 (·····) and of rennet solutions at pH 7 (—) and at pH 3.0 (·····). Data are listed in Table A-14.*

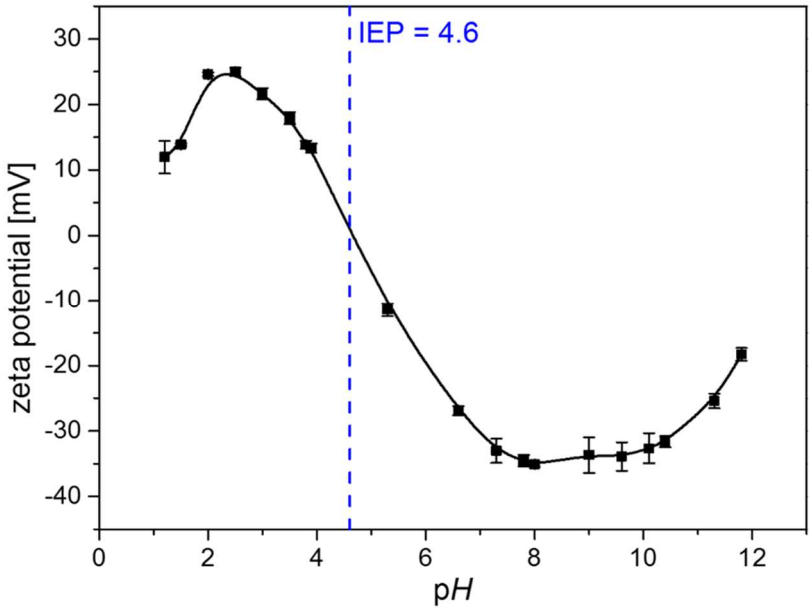


*Figure 31. Zeta potential of chymosin molecules in dependence on pH. Lines are for visualization of zeta potential course only. Data are shown in Table A-15.*

between p*H* 1.8 and p*H* 3.2 and between p*H* 6.0 and p*H* 11.7 (|ζ| ≥ 20 mV). At p*H* values lower than p*H* 1.8 and higher than p*H* 11.7, the enzyme is not electrostatically stable. This is probably based on a promoting denaturation due to hydrolysis of peptide bonds or conformational.

To conclude, performing deposition experiments of casein at p*H* 3, as it is intended due to the highest activity of chymosin, ensures in addition to the presence of molecular enzyme also electrostatically stable enzyme. This matches the targeted requirements for the planned deposition experiments.

### 4.2.3 Properties of casein

#### 4.2.3.1 Size and zeta potential of casein micelles in dependence on p*H*

**Figure 32** displays the dependence of the casein micelle size and zeta potential from the particular p*H* value. The diameter of casein micelles increases around the IEP, i.e. at p*H* 4.9. This is in accordance to the decreasing zeta potential in this range (p*H* 4.0–6.0). Destabilization and aggregation of casein micelles occur due to a collapse of the “hairy layer”. On the other hand, micelles are electrostatically stable at p*H* 2.2–4.0 and 6.0–11.8 (|ζ| ≥ 20 mV). An additional entropic stabilization of micelles, which definitely exists, is not considered here.

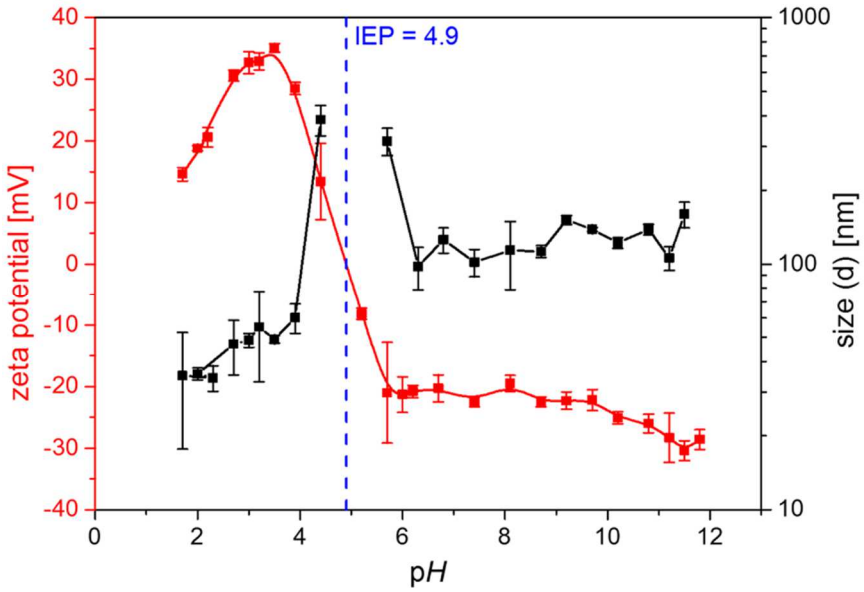


*Figure 32. Casein micelle size (—) and zeta potential (—) in dependence on pH. Casein concentration was 1 g/L and temperature was 25 °C. Lines serve as visualization only. Data are shown in Table A-16.*

Casein micelles show diameters between 100 and 150 nm above p*H* 6. Below p*H* 4, the diameter is significantly smaller than 100 nm, accounting for about 35–60 nm. This is probably based on an acid induced partial dissolution of CCP in the micelle interior, which leads to the formation of smaller micelles. The differences in the casein micelle size with varying p*H* value are also apparent by consideration of size distributions.

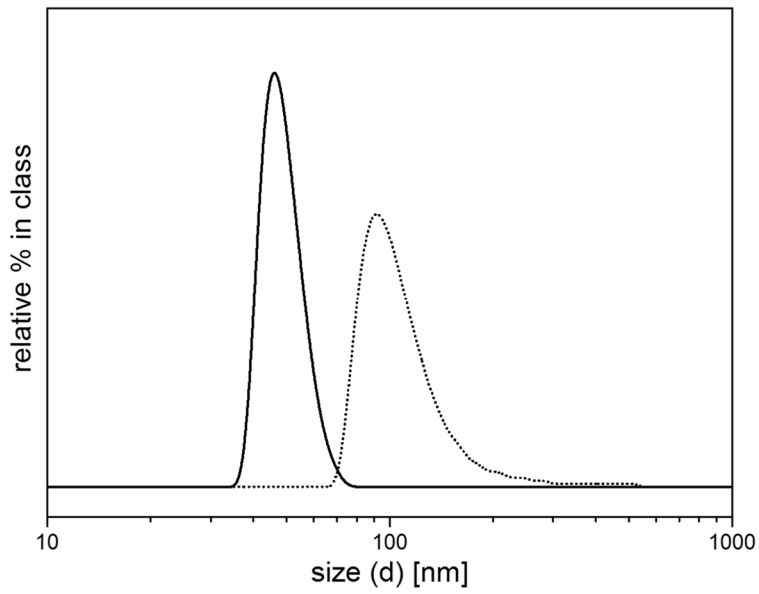


*Figure 33. Number size distributions of dispersed casein micelles (1 g/L, 25 °C) at pH 3.0 (—) and pH 6.7 (·····). Data are listed in Table A-17.*

**Figure 33** shows number size distributions of casein micelle sizes at p*H* 3.0 and p*H* 6.7. At p*H* 3.0 casein micelles exhibit diameters of about 40–80 nm with a number mean value of 49 nm. At p*H* 6.7, i.e. the p*H* value of native milk, casein micelles have notably larger diameters. Here, diameters are mainly between 70 nm and 200 nm with a number mean value of 114 nm. In addition, some micelles have diameters up to 500 nm. The determined diameters at the p*H* of milk are in good correspondence with values found in literature. Mean diameters of about 120 nm or 105 nm are mentioned.[87,257] Also the presence of very large casein micelles with diameters up to 500 nm is recorded in literature.[87]

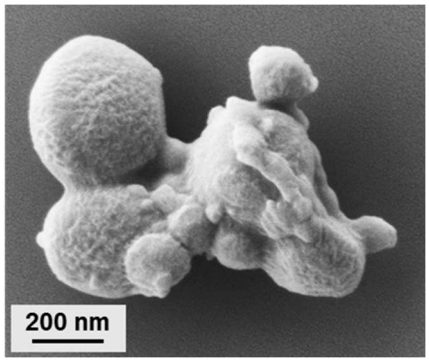

*Figure 34. SEM image of casein micelles at pH 3.0.*

Considering the synthesis of casein and its natural purpose, i.e. simple nutrition, there exists no reason for casein micelles to appear as monodisperse system. The varying micelle size is also apparent by visualization via SEM (**Figure 34**). Single micelles have diameters of more than 200 nm at p*H* 3, while indeed the majority exhibits diameters smaller than 100 nm. With regard to the controlled deposition of casein to yield defined protein layers, use of dispersions at p*H* 3 is favored. Here, the number size distribution is narrower and the number mean micelle diameter accounts for less than half of the diameter at p*H* 6.7. In addition, the presence of very large micelles with diameters up to 500 nm, which would have interfering effects during particle deposition and film formation, is diminished.

It can be stated that casein dispersions at p*H* 3 are still polydisperse systems, but provide better features for a controlled deposition. This constitutes an additional benefit, taking into account that chymosin is most active at this value.

Stability of casein micelles at p*H* 3 was further investigated and verified by evaluation of shelf life. To this, changes in size of a casein dispersion, which was stored in a refrigerator, was observed over five days. The results are shown in **Figure 35**. Altering of casein dispersions due to long storage times might cause non-reproducible experimental results. Nevertheless, the diagram shows that casein micelles stay stable under acidic conditions for at least five days. No significant changes or dissolution of micelles occurred over this time. Therefore, dispersions were only stored at maximum for five days in a refrigerator.

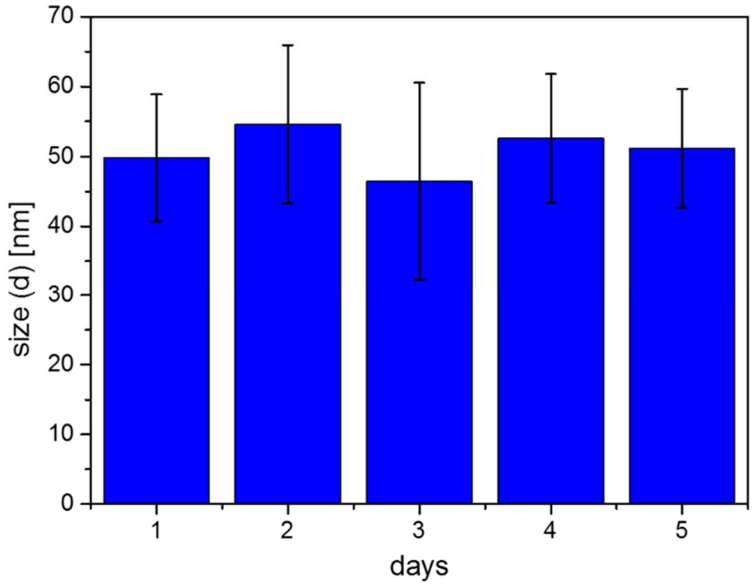


*Figure 35. Investigation of shelf life of casein dispersions (10 g/L) at pH 3.0. Data are shown in Table A-18.*

#### 4.2.3.2 Viscosity and size of casein micelles in dependence on casein concentration

It is important to know influences of the casein concentration on the micelle size and the dispersion viscosity. Thus, casein dispersions with 1, 5, 10, 20, 25, 30, and 50 g/L were examined at p*H* 3 via DLS and viscosity measurements (**Figure 36a and 36b**). Figure 36a shows that the micelle size is nearly constant up to 10 g/L, exhibiting diameters of about 50 nm. Higher concentrations up to 30 g/L result in an increase of the micelle diameter up to 70 nm. Even higher amounts of casein up to a concentration of 50 g/L yield very large aggregated casein particles of about 450 nm. Connected to the formation of well-designed protein layers the incorporation of small film-forming particles is rather desired.

The influence of the casein concentration on the viscosity is displayed in Figure 36b. The exponential growth is typical for casein dispersions.[258] Up to a concentration of 10 g/L the dynamic viscosity is close to 1 mPa·s, enabling an easy practical use. Increasing the casein concentration up to 20 g/L results in a viscosity of about 2 mPa·s. Higher casein concentrations of about 25 g/L and 30 g/L further increase the viscosity to about 2.3 mPa·s and 2.7 mPa·s, respectively. This indicates that influence of casein particle size is less significant on viscosity than the amount of particles. Very high viscosities of about 13 mPa·s are obtained at a concentration of 50 g/L, inhibiting an easy handling of dispersions.

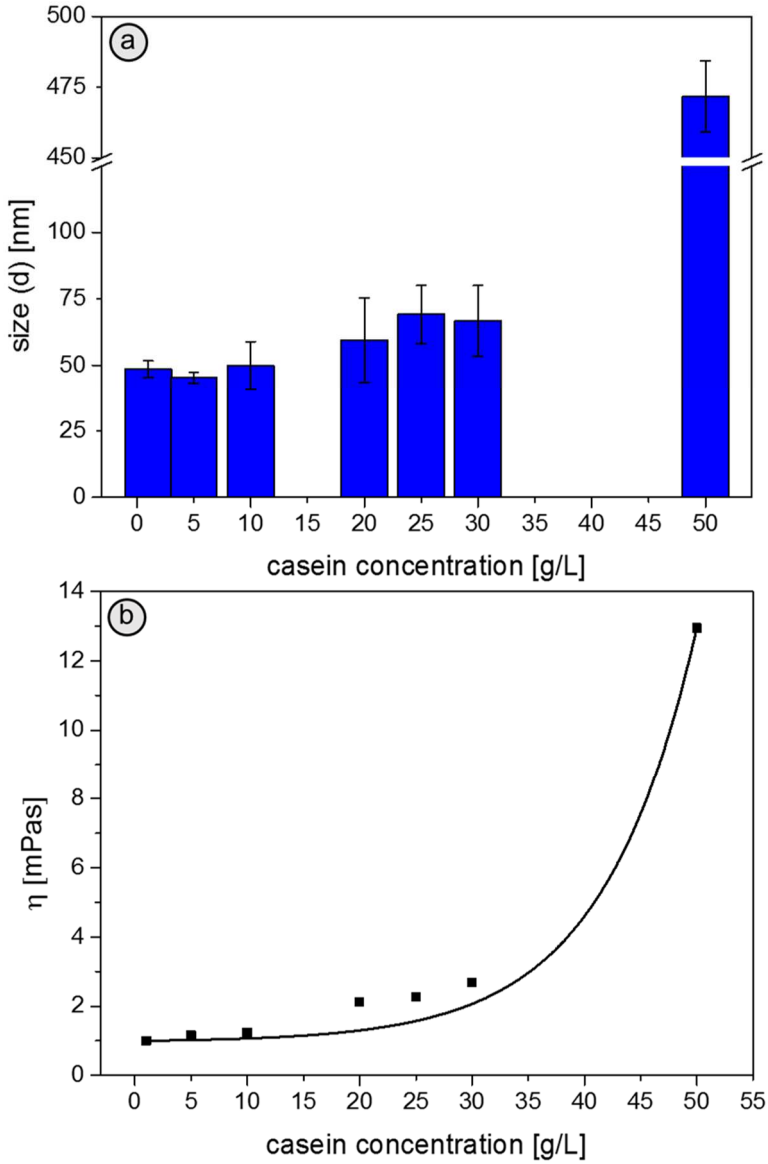


*Figure 36. a) Casein micelle sizes and b) viscosities of casein dispersions dependent on casein concentration (pH 3, 25 °C). Data are listed in Table A-19.*

### 4.2.4 Conclusion

Chymosin and casein were investigated to determine parameters, which realize presence of stable and active particles, enabling the controlled deposition of casein onto surfaces. Chymosin is most active at p*H* 3 and shows high activity at 40 °C. It is electrostatically stable at p*H* 3 and p*H* 7. Conduction of deposition experiments at p*H* 3 is therefore reasonable. Additionally, immobilization of chymosin is feasible at p*H* 7. Casein dispersions are electrostatically stable at p*H* 3, exhibit micelle diameters of about 50 nm, and can be stored for at least five days. Casein concentrations up to 10 g/L provide low viscosities of about 1 mPa·s. This ensures an easy practical use of dispersions, while impacts on the diffusion behavior of additional particles, such as chymosin, are minimized.

## 4.3 Controlled formation of continuous casein coatings

### 4.3.1 Overview

This section deals with the formation of continuous casein coatings via the Enzyme Mediated Autodeposition, using adsorbed chymosin. Results were published in “Journal of Biotechnology”, “Progress in Organic Coatings”, and “International Journal of Adhesion and Adhesives”.[259–261]

First, results of initial experiments are discussed, which verified the high potential of the EMA and enabled the development of a deposition and film formation mechanism. Secondly, the features of enzymatically deposited casein coatings are described in comparison to conventionally processed casein coatings. Control of the deposition process is investigated in detail with respect to different parameters, i.e. deposition time, p*H* value, and casein concentration. The experimental procedures of these influences were conducted by ELKE TERBORG, who deserves my gratitude for her excellent work. Finally, the pressureless gluing via EMA is introduced as a potential application.

The use of adsorbed enzyme presents the most convenient immobilization method for the controlled formation of continuous casein coatings. Physical immobilization is achieved by drying an enzyme solution onto the support surface. This represents a reversible immobilization method. Desorption and subsequent diffusion of chymosin into solution is likely upon immersion into a casein dispersion. **Figure 37** illustrates the concept of the Enzyme Mediated Autodeposition, using adsorbed enzyme.

Due to diffusion of chymosin, cleavage of casein micelles occurs not only in very close proximity to the support surface, but also in greater distance. This distance expands with proceeding reaction time and as a consequence, the reaction zone is enlarged by this value.

Diffusing chymosin is not readily covered by cleaved casein after immersion into the protein dispersion. With increasing diffusion pathways, the amount of cleaved and deposited casein micelles also increases. Therefore, a delayed self-termination of the process is assumed. Deposition of casein stops either when the enzyme molecules are embedded within the cleaved casein film or micelles are cleaved in such a distance to the support surface that they do not contribute to the resulting coating and precipitate.

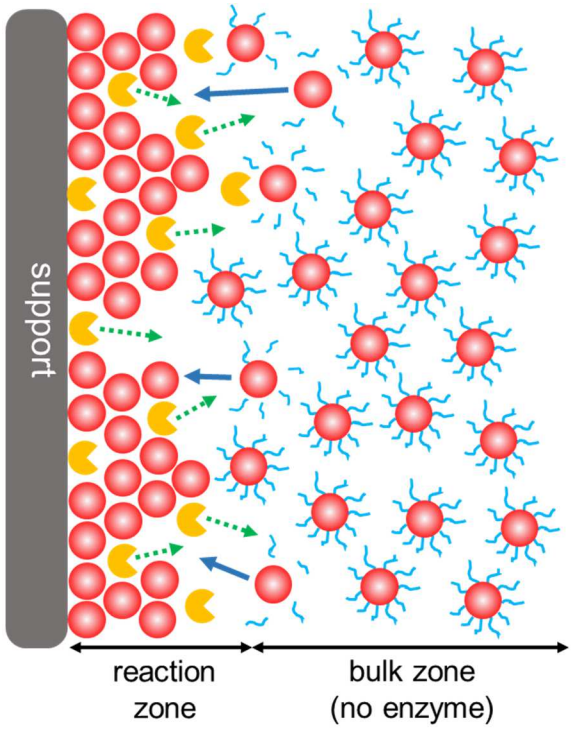


*Figure 37. Concept of EMA, using adsorbed enzyme. Diffusion of enzyme is indicated by green dot-arrows. Deposition of destabilized micelles is shown by blue arrows.*

### 4.3.2 Film formation of casein and deposition of continuous coatings


*Figure 38. Casein film obtained via solution casting.*

Exemplarily, the good film-forming behavior of the used casein dispersions was tested at first and confirmed under ambient conditions via solution casting, using a dispersion with a casein concentration of 10 g/L (p*H* 3). By this, flexible, transparent, and taste- and odorless polymer films were easily obtained (**Figure 38**). This quick experiment indicates, why casein has been used so successfully throughout history of mankind in gluing and coating applications, as handling and preparation of the obtained films is very simple. It is assumed that this good film-forming behavior also occurs, if the controlled deposition of casein micelles on supports is intended via immobilized chymosin. In addition, the major drawback of native casein films also becomes obvious. Contact of the processed films with

moisture leads to fast degradation and makes understandable why casein films were mostly used in interior applications.

Deposition experiments indeed show, that immersion of supports with reversibly immobilized enzyme into protein dispersions yields continuous casein coatings. **Figure 39** shows SEM images of such obtained casein films, which are homogeneous and show sporadically occurring cavities (**Figure 39a**). These cavities are probably based on retained water which evaporated after film formation.

The resulting surface topography is very significant. Deposited films exhibit a high roughness, as shown in **Figure 39b**. This leads to high standard deviations of film thicknesses, regarding thin casein layers, but becomes less significant with increasing film thickness. **Figure 39c** and **39d** show that either time of reaction or protein concentration have a direct impact on the resulting film thickness, which accounts here for several hundred nanometers. Increases in time of reaction and/or casein concentration favor the deposition of higher casein thicknesses.

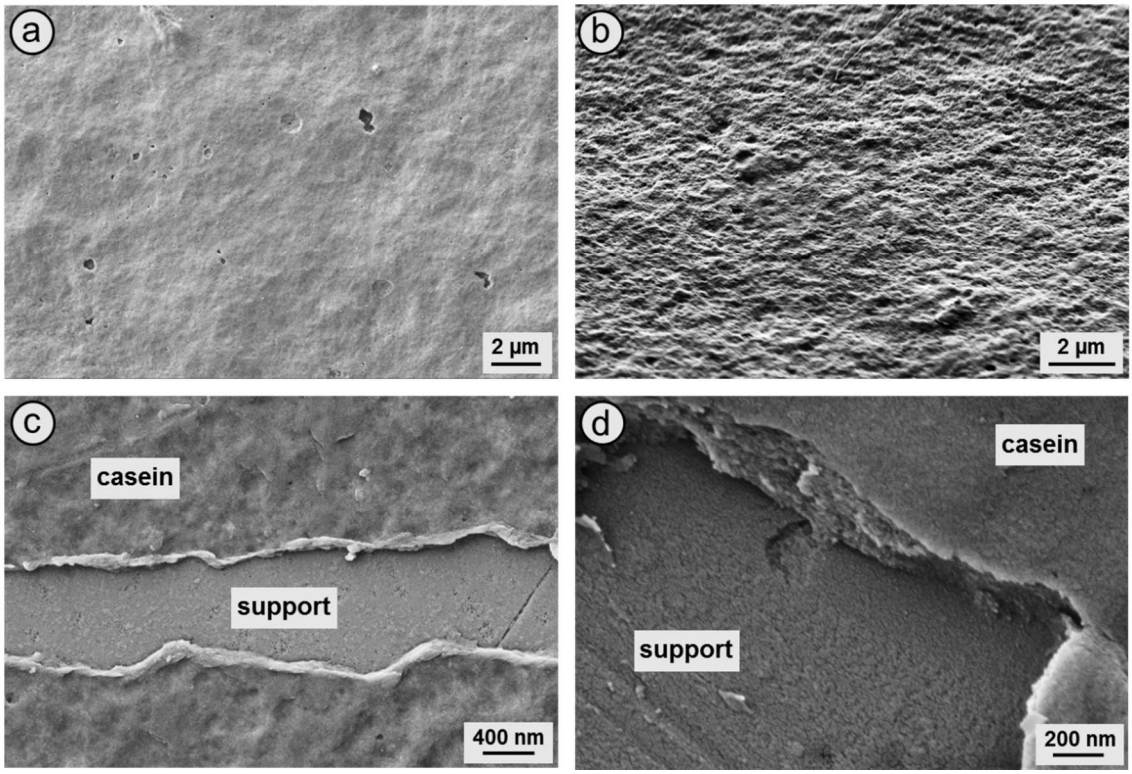


*Figure 39. SEM sample images of casein coatings obtained via EMA, using adsorbed enzyme. a) Top view on casein coating, b) view at tilted angle of 54°, c) and d) views on scratches in casein coatings. Conditions: a) c (casein) = 10 g/L, $t_D$ = 60 min, pH 3; b) c = 10 g/L, $t_D$ = 90 min, pH 3; c) c = 20 g/L, $t_D$ = 60 min, pH 3; d) c = 10 g/L, $t_D$ = 90 min, pH 3.*

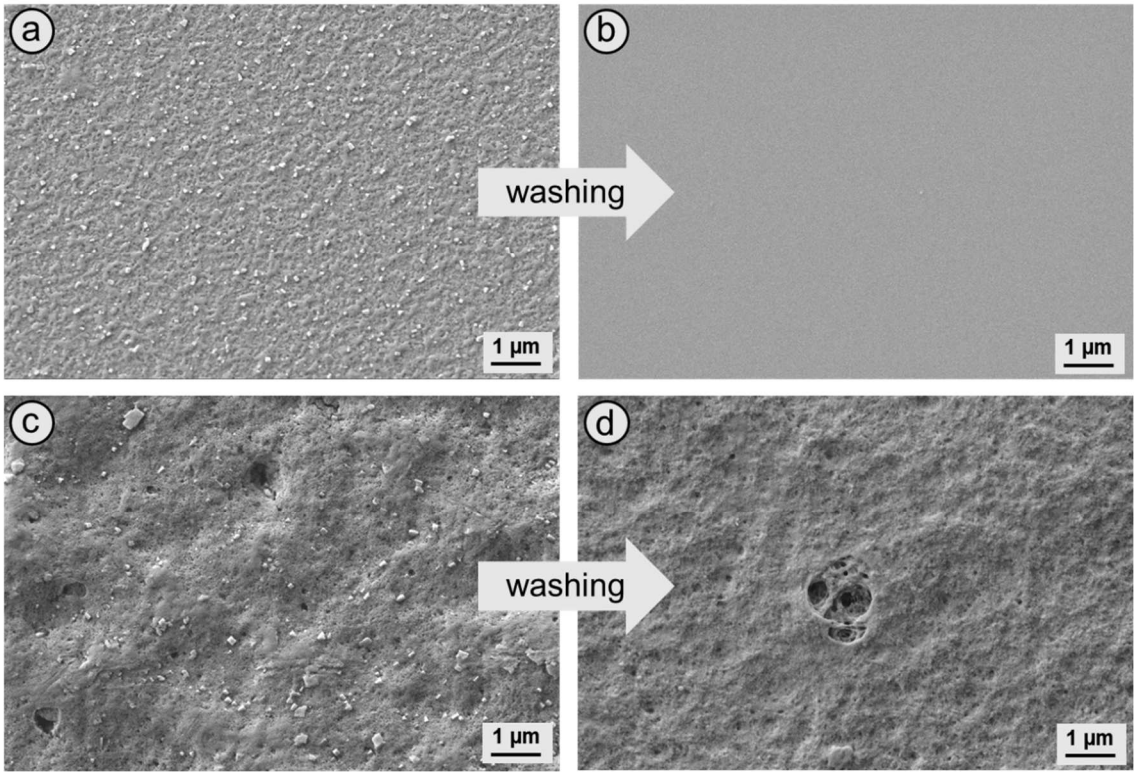


*Figure 40. Water stability of cleaved and non-cleaved casein films. Casein coating obtained via solution casting a) before and b) after washing in DI water. Casein coating obtained via EMA with adsorbed chymosin c) before and d) after washing in DI water.*

Due to cleavage of κ-casein, casein micelles become hydrophobic and deposit onto the support. Consequently, the polarity of formed casein coatings is significantly decreased compared to conventional, non-cleaved ones. The improved water stability is verified by washing in deionized water. Enzymatically deposited casein coatings withstand washing, while non-cleaved films can easily be removed by this. **Figure 40** illustrates this increased water stability by means of SEM images, which were obtained before and after the washing procedure.

Both casein coatings were obtained from the same dispersion (10 g/L, p*H* 3). Prior to the washing procedure, no significant differences are visible (**Figure 40a** and **40c**). Both images show continuous protein layers with salt crystals (predominantly NaCl) occurring on the surface, which result from the p*H* adjustment as well as from the casein formulation itself. After the washing procedure, the higher water stability of cleaved casein films compared to non-cleaved ones is obvious (**Figure 40b** and **40d**). Non-cleaved casein is easily removed by immersion and washing in DI water. Due to the presence of

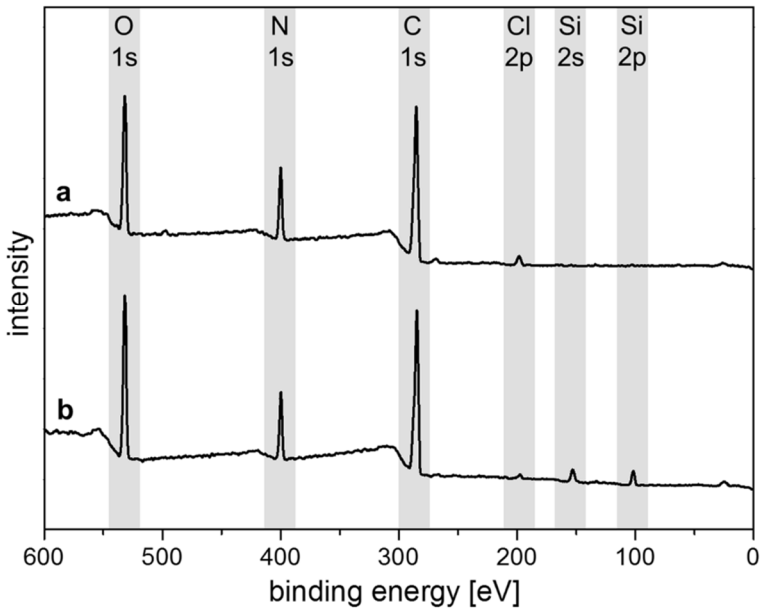


*Figure 41. XPS measurements of cleaved casein films a) before and b) after washing with DI water. Conditions: c (casein) = 10 g/L, $t_D$ = 40 min, pH 3.*

κ-casein, non-cleaved casein micelles have their intact, natural hydrophilic surface and are water dispersible. On the contrary, cleaved casein is not removed by DI water, due to increased hydrophobic properties. The enzyme mediated deposition and loss of κ-casein results in water-stable protein layers. Only the salt crystals and non-cleaved casein micelles, which were present on top of the cleaved casein, are removed.

The presence of an additional layer of non-cleaved casein on top of cleaved casein coatings has also been verified by XPS measurements (**Figure 41**). The spectra show an element composition that is consistent with protein structures, i.e. carbon, oxygen, and nitrogen. This composition is detected before and after the washing procedure. In addition, after washing in DI water silicon peaks, originating from the glass surface, are detected. This indicates that an additional layer of non-cleaved casein has been present previously to washing and has been removed by this. It can be stated that the cleaved casein film is very thin, as XPS measurements are highly surface specific.

### 4.3.3 Mechanism of particle deposition and film formation

Washing tests and the confirmed improved water stability of the deposited casein films as well as conducted XPS measurements imply that no non-cleaved casein micelles are present in the final layer, neither partially nor forming the upper layer itself. These findings allow for the development of a mechanism of particle deposition and film formation via EMA, using adsorbed chymosin, which is illustrated in **Figure 42**.

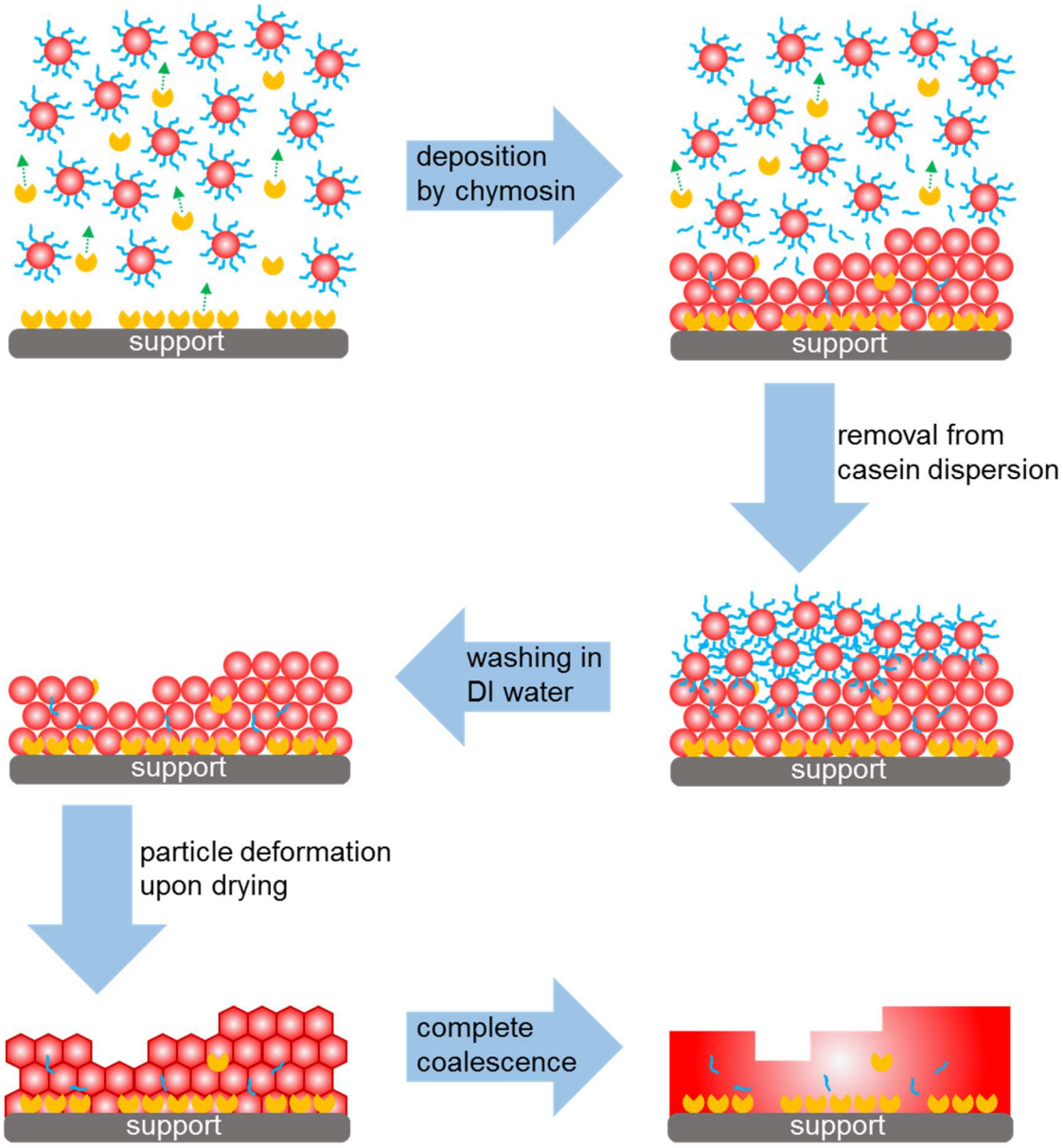


*Figure 42. Proposed mechanism of particle deposition and film formation via EMA with adsorbed enzyme.*

Casein micelles are cleaved by adsorbed chymosin close to the support surface. Additionally, diffusing enzyme molecules cleave micelles in a greater distance to the support. Cleaved micelles lose their previous water dispersibility, become instable, and eventually deposit onto the support. The degree of enzyme diffusion determines the number of deposited casein layers per area. Based on different diffusion pathways, the amount of deposited casein slightly varies in different areas. Enzyme molecules as well as free caseinomacropeptide molecules are covered by depositing micelles and are incorporated into the layer of adherent micelles.

During removal from the protein dispersion non-cleaved micelles adhere to cleaved micelles onto the support. Washing in DI water completely removes these non-cleaved micelles, while enzymatically treated micelles are not removed due to their increased hydrophobicity. Eventually, cleaved casein micelles undergo coalescence upon drying analogously to the well-studied film formation of polymer particles of aqueous dispersions.

The deposition of different amounts of cleaved casein micelles in different areas on the support results in locally varying film thicknesses and causes the roughness of the biocoatings, as detected before. This influence is apparent with regard to thin coatings and becomes relative at increased film thicknesses.

### 4.3.4 Properties of enzyme mediated casein coatings

Enzymatically deposited casein coatings were characterized by determination of their physico-chemical and mechanical properties and were compared to conventionally processed, non-cleaved casein coatings.

In order to quantify the increased hydrophobicity of enzyme mediated casein coatings, contact angles were determined. **Table 4** shows that cleaved films exhibit an about 20° higher contact angle compared to non-cleaved coatings. The high standard deviation, as detected for the conventional casein film, is

*Table 4. Contact angle measurements of cleaved and non-cleaved casein films.*

| Sample: | Contact angle in °: |
|---|---|
| Cleaned glass: | ≤ 3 |
| Conventional casein coating: | 54.7 ± 8.7 |
| Enzyme mediated casein coating: | 75.3 ± 1.1 |

based on a partial dissolution during the measurement. These results confirm the increased hydrophobicity and water stability of enzymatically deposited casein coatings. This is very important with respect to potential applications, because the low water resistance of native casein limited its use as coating material in the past.[68,69,262,263]

Moreover, light microscopic measurements demonstrated qualitatively that enzymatically deposited casein coatings exhibit an increased stability in organic solvents, such as ethanol and toluene, compared to conventionally processed ones.

Cleaved casein coatings are capable of surviving sterilization processes, using UV radiation or elevated temperatures. This was verified by investigation of their solubility behavior. Deposited films show no significant changes in water solubility after exposure to UV radiation or treatment with heat (100 °C for 20 min). SEM images verify the presence of intact coatings after the particular treatment and washing in water (**Figure 43**). The feasibility of sterilization shows that deposited casein films are applicable for medical purposes, e.g. coatings for implants or instruments. Here, use of sterilized materials is essential and is commonly performed with heat or UV radiation.[264–266]

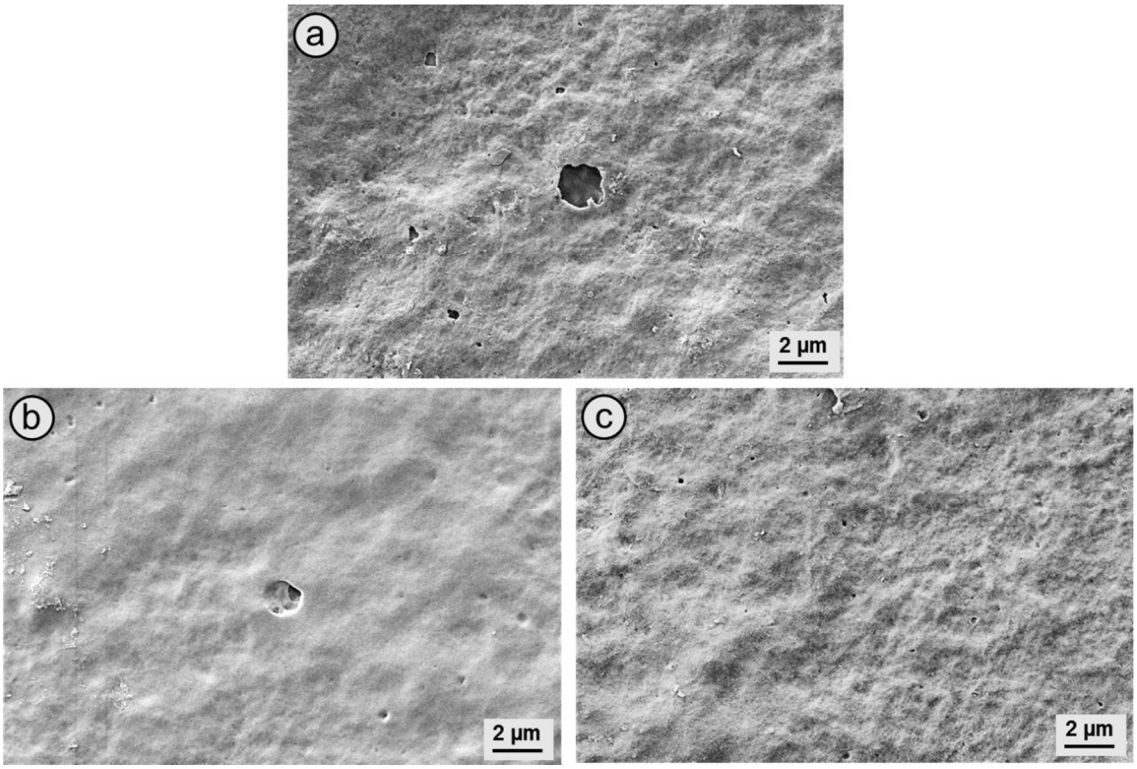


*Figure 43. SEM images of sterilized casein coatings. a) Reference casein film, i.e. no sterilization treatment. b) Casein coating after treatment with UV radiation and c) casein coating after temperature treatment at 100 °C.*

Obtained casein coatings also exhibit an enhanced flexibility compared to conventional ones. This has been verified by determination of DMT-moduli and film hardnesses. DMT-moduli of enzymatically deposited protein structures were about 1.2-1.4 GPa, independently of film thickness. Modulus of a non-cleaved reference sample, which was obtained via simple dip coating, was at 2.4 GPa. It is known that the elastic modulus of κ-casein is higher, due to the intense formation of strong intermolecular interactions, compared to the moduli of the other major caseins.[267] It is therefore reasonable that cleavage of κ-casein and subsequent removal of the hydrophilic part result in more flexible casein films.

Film hardness in dependence on the film thickness was examined indirectly via AFM by measuring the deformation of the processed casein films at a constant peak force (**Figure 44**). Results show no significant dependency of film hardness from the film thickness. All examined casein coatings exhibited nearly identical deformation values. For instance, deformation values of films exhibiting a low (d = 13.4 nm) and a high (d = 61.4 nm) thickness were 1.57 ± 0.01 nm and 1.58 ± 0.04 nm, respectively. Deformation values of the other processed protein films were in the same range, while the reference sample (non-cleaved film) showed a deformation of 0.86 ± 0.1 nm. Control measurements of blank glass surfaces showed a deformation of 0.09 ± 0.01 nm.

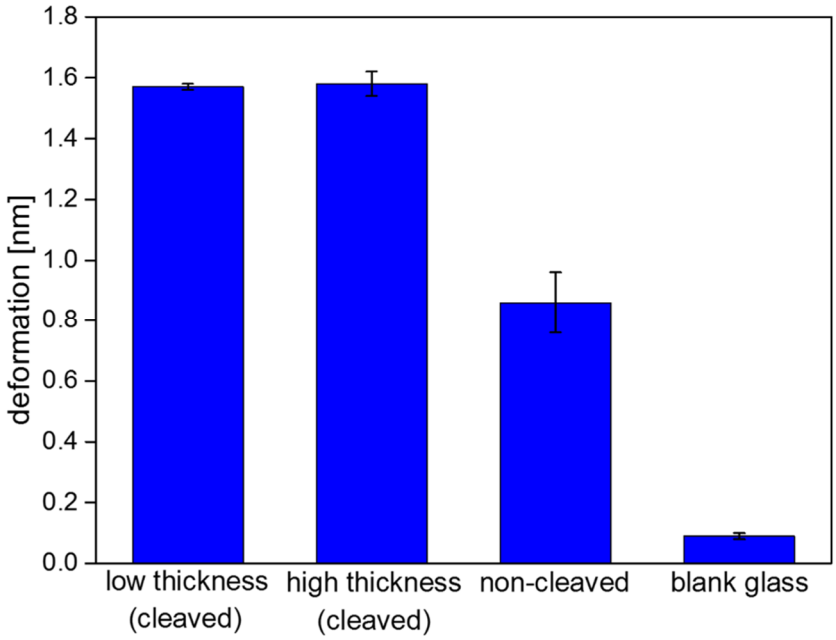


*Figure 44. Deformation of enzymatically deposited casein coatings in comparison to non-cleaved casein coatings and blank glass surfaces.*

The performed deformation measurements support the findings of the moduli determinations and also indicate that casein films obtained via EMA exhibit higher flexibilities compared to conventional casein coatings. The enhancement of flexibility presents an important improvement of processed casein coatings with respect to potential applications, which are commonly restricted due to the inherent brittleness of unmodified proteins.[268–270]

### 4.3.5 Control of deposition parameters

#### 4.3.5.1 Influence of deposition time

Reversibly immobilized enzyme tends to undergo diffusion and casein micelles are cleaved in greater distance to the support surface with ongoing reaction time. The amount of deposited casein increases until the chymosin molecules are covered with cleaved casein. Then, a limitation of the film growth, as it is known for the classical autodeposition process, is assumed to take place. To verify this feature of the EMA, the film thickness in dependence on the deposition time was measured via AFM. Time of reaction was varied between 5 and 150 min. The obtained results are shown in **Figure 45**.

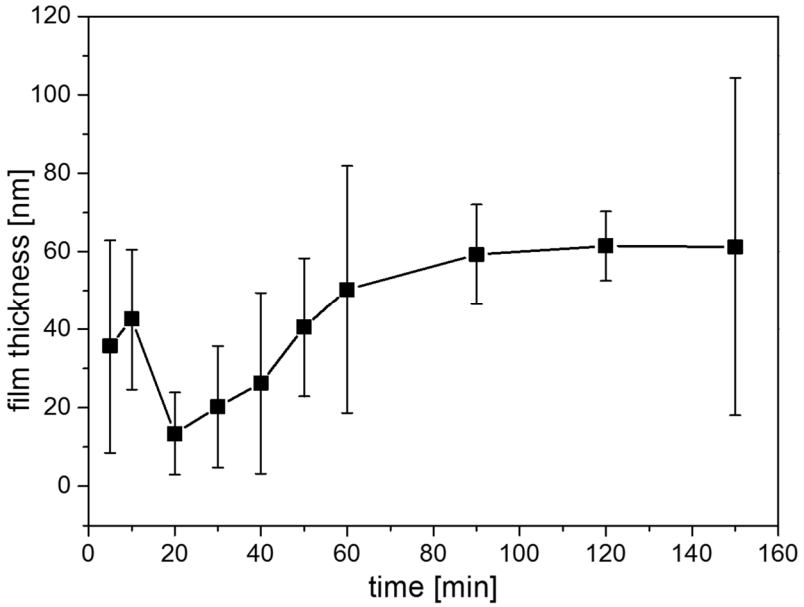


*Figure 45. Dependence of casein film thickness from deposition time at pH 3 and a casein concentration of 10 g/L. Lines serve for visualization and are not based on mathematical calculations. Data are shown in Table 5.*

As expected, higher film thicknesses are achieved with increasing reaction time. Longer diffusion ways of chymosin molecules lead to an increased amount of deposited casein micelles.

The ability of adsorbed chymosin to undergo diffusion was further verified by enzymatic activity tests of the aqueous solution after immersion of an enzyme-functionalized support into DI water for 60 min. Comparison with a reference sample, representing a degree of 100 % diffusion, yielded that 68 % of chymosin molecules underwent desorption from the support and diffused into solution. This supports the above made conclusions.

The relatively high film thicknesses at 5 and 10 min are based on the layer of reversibly adsorbed enzyme. As detected by SEM measurements, this layer is not negligible and contributes to the measured film thickness. Adsorbed chymosin partially diffuses into solution, resulting in a decreasing thickness up to 20 min reaction time. After this, deposition of casein micelles via enzymatic cleavage predominates and the film thickness increases continuously. Therefore, a reproducible minimum at 20 min is detected. Casein thickness increases up to a limitation of the film growth at 90 min. Here, the average film thickness accounts for about 60 nm. Nevertheless, film thicknesses up to 150-1000 nm on maximum are achievable, as detected via SEM measurements (Figure 39d and **Figure 46**).

These partially occurring areas with remarkably higher film thickness are intuitively found and examined during SEM measurements, but become less important during AFM measurements, which is a more objective method. Longer reaction times than 90 min provide no significant increase in

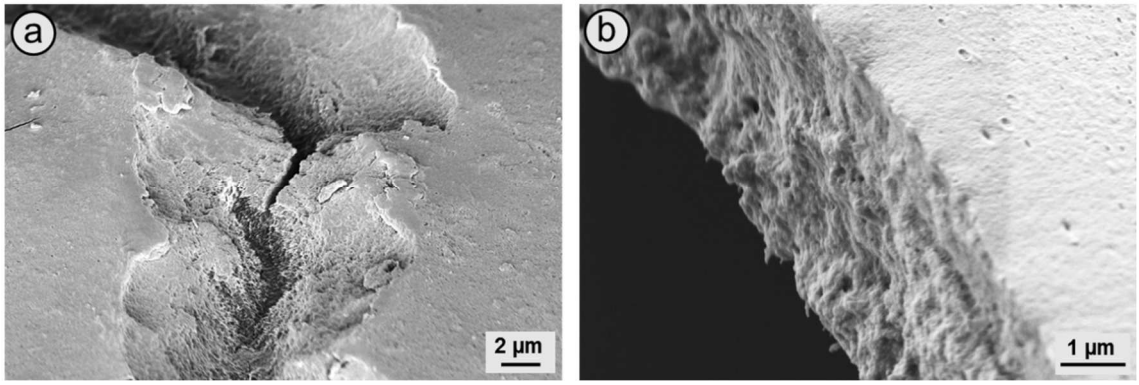


*Figure 46. SEM images of casein coatings with film thicknesses in the micrometer scale. Both protein films were obtained under equal conditions, i.e. at 40 °C, pH 3, $t_D$ = 90 min, and $c_C$ = 10 g/L.*

film thickness, as shown in Figure 45. Active enzyme molecules are no longer available in close proximity to the support surface, which could provide a proceeding deposition of casein micelles. Chymosin molecules are covered with cleaved micelles and are embedded into the protein film. On the other hand, chymosin that diffuses out of the reaction zone provides no effective deposition of cleaved casein, due to the high distance to the support surface. This is supported by an observed casein precipitation in the bulk phase at long reaction times.

The determined limitation of the film growth is similar to the trend of the film growth in the conventional autodeposition process. Here, an advanced reaction time is connected to longer diffusion pathways of metal ions which are inactivated by depositing polymer particles. This yields a similar limitation of the film growth as it could be observed for the enzyme mediated approach.

The high standard deviations of the determined film thicknesses are caused by the topographic appearance of the protein coatings (**Table 5**). AFM measurements show that the deposited casein films exhibit a significant roughness, regardless of deposition time. This explains the determined high standard deviations. **Figure 47** shows a 3D AFM image of a casein coating, to illustrate the differences in height and the resulting high roughness.

*Table 5. Film thicknesses of deposited casein coatings in dependence on deposition time.*

| Deposition time in min: | Film thickness in nm: |
|---|---|
| 5 | 35.7 ± 27.2 |
| 10 | 42.6 ± 17.9 |
| 20 | 13.4 ± 10.5 |
| 30 | 20.2 ± 15.5 |
| 40 | 26.3 ± 23.1 |
| 50 | 40.6 ± 17.9 |
| 60 | 50.3 ± 31.6 |
| 90 | 59.2 ± 12.8 |
| 120 | 61.4 ± 8.8 |
| 150 | 61.2 ± 43.1 |

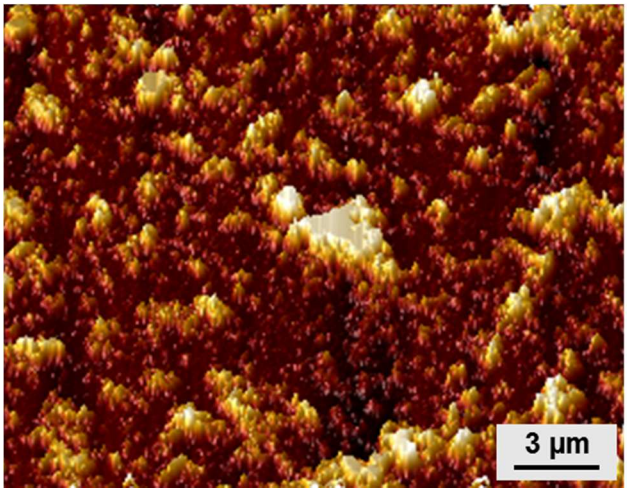


*Figure 47. Roughness of deposited casein coatings. The presented casein coating was obtained at pH 3 after a deposition time of 60 min, using a casein concentration of 10 g/L.*

A plausible reason for the high roughness of the deposited coatings is given by the polydispersity of casein micelles (Figure 33). Micelle sizes vary between 40 nm and 80 nm with a number mean value of 50 nm. Thus, particles with very different sizes are cleaved and deposited onto the support surface. In addition to this, even a small amount of additionally deposited particles on particular areas on top of the casein film has a significant impact on the resulting roughness (Figure 47).

It seems reasonable that the calculated standard deviations of the film thickness are in accordance to the size of a monolayer of deposited casein micelles. The obtained coatings would vary locally around this height. Therefore, it can be expected that a monolayer of casein micelles is about 15-20 nm in height and thicknesses vary about a multiple of this value, as shown above. This seems to be a verifiable thickness for a final monolayer of casein micelles, because their water content accounts for about 63 wt%.[87] Herein used micelles have a number mean diameter of about 50 nm and loss of water would result in layers, exhibiting a thickness in the assumed range, i.e. 15-20 nm.

### 4.3.5.2 Influence of p*H* value

Since the enzymatic activity of chymosin is strongly p*H* dependent, an effect on the EMA with casein must be presumed. As determined before in 4.2.2.1, the highest activity of chymosin is at p*H* 3, using hemoglobin as substrate. It is therefore assumed that casein deposition in the acidic range is more efficient compared to neutral or slightly alkaline conditions. Deposition experiments were conducted with varying p*H* values from p*H* 2 to p*H* 8, in order to verify this. The results are shown in **Figure 48**.

The determined film thicknesses meet with the expectations. Casein deposition at acidic p*H* values is indeed more efficient than in the alkaline range or around neutral p*H*. The highest film thicknesses are obtained in the range, where chymosin exhibits its highest activity, i.e. at p*H* 3.0–3.5. However, at p*H* 3.5 a remarkably higher thickness is achieved compared to p*H* 3.0, although chymosin is more active at the latter p*H* value, as determined with the hemoglobin test. A possible explanation for this is based on the use of different substrates for the enzyme. Enzymatic activity tests were performed with hemoglobin as substrate. Here, chymosin reacts with κ-casein. It is known that enzymes can have varying activities at different p*H* values with different substrates.[271] It can be assumed that the enzymatic activity of

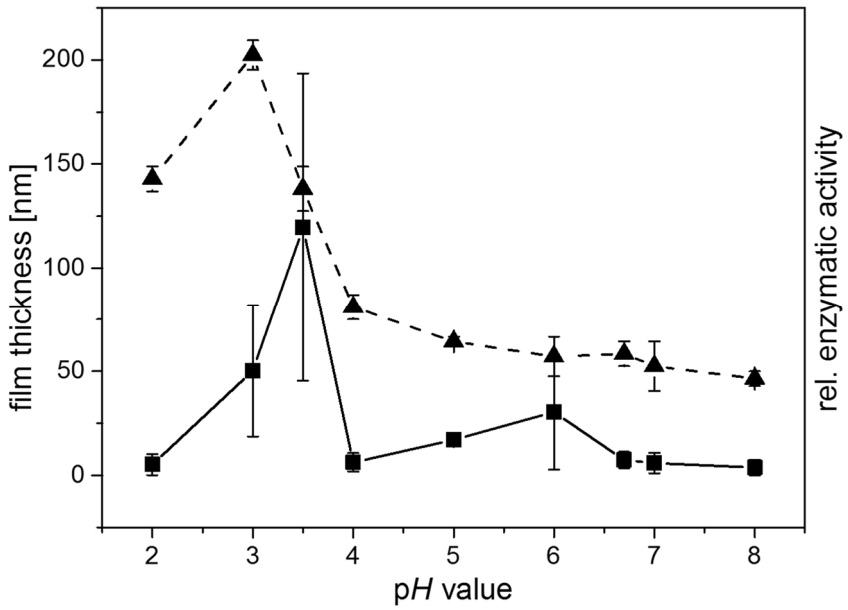


*Figure 48. Film thickness (■) of casein coatings in dependence on pH value at equal deposition times (60 min) and casein concentration (10 g/L). Relative enzymatic activity (▲) of chymosin in dependence on pH value. Lines are for visualization only. Data are listed in Table A-12 and A-20.*

chymosin with casein micelles is slightly different compared to hemoglobin. This explains the obtained higher film thickness at p*H* 3.5. Nonetheless, the film thickness at p*H* 3.0 is significantly higher compared to all other investigated p*H* values, indicating a successful and efficient casein deposition.

Since chymosin is barely active at neutral p*H* and in the alkaline range of p*H*, ultrathin casein films are deposited at these values. In cheesemaking, casein is precipitated by chymosin at the p*H* of milk, which is 6.7. Under these conditions κ-casein is strongly exposed and chymosin is able to reach the specific cleavage site at $Phe^{105}$-$Met^{106}$ easily.[272] A higher film thickness was therefore expected to appear at this p*H*, but this could not be confirmed via AFM measurements. Remarkably, at p*H* 6.0 a higher film thickness was determined compared to adjacent p*H* values. This supports that κ-casein in fact has an exposed state around the p*H* of milk, which facilitates cleavage of casein micelles.

Below the isoelectric point of casein, i.e. at p*H* 4.9, casein is positively charged, while glass is negatively charged down to about p*H* 2.[273,274] One could assume that deposition of casein micelles is driven by electrostatic interactions and not by the enzyme. To verify that deposition reactions were enzyme-catalyzed, casein deposition was further examined. Depositions were carried out at particular p*H* values, i.e. p*H* 3.0, p*H* 3.5, and p*H* 6.0, under the same conditions, except that no enzyme was used. AFM measurements yielded that no casein deposition at all was attainable without the presence of chymosin.

This confirms that protein deposition is initiated and controlled via enzymatic cleavage reactions. Electrostatic interactions between the glass support and dispersed casein micelles as initiating factor can therefore be ruled out. This is a very important conclusion and strengthens further the principle of the Enzyme Mediated Autodeposition.

### 4.3.5.3 Influence of casein concentration

As the third parameter, the concentration of the casein dispersion was varied in additional experiments from 1 to 20 g/L, to examine influences on the resulting film thickness (**Figure 49**).

The Michaelis-Menten theory predicts a zero order kinetic for enzyme-catalyzed reactions with respect to substrate concentration, if $[S] \gg K_M$.[275] The Michaelis constant $K_M$ for the cleavage of κ-casein by chymosin is about 0.5 mM, when κ-casein is present in intact casein micelles.[109,276] The κ-casein concentration in milk with a casein content of 25 g/L is 0.17 mM. This means that the enzymatic cleavage reaction does not follow zero order kinetics with respect to casein concentration in both, naturally occurring milk as well as in the herein investigated deposition experiments. It seems reasonable to assume in good approximation a first order kinetic for the cleavage reaction, as described in literature.[277]

The dependence on the casein concentration is reflected in the obtained results. AFM measurements clearly show the tendency that an increase in the casein concentration leads to higher film thicknesses. Enzyme molecules, which undergo diffusion and cover same pathways, are able to cleave more casein micelles in the same deposition time, if the number of micelles is increased.

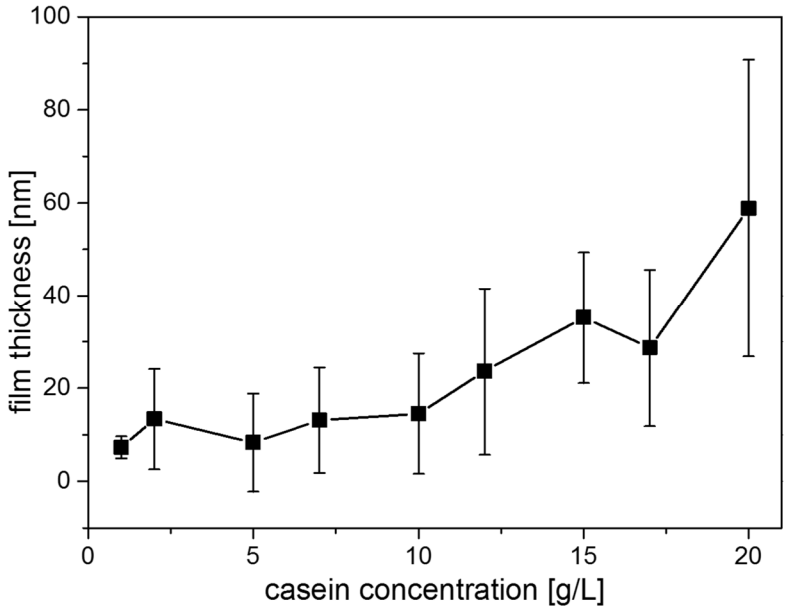


*Figure 49. Film thickness of casein coatings in dependence on casein concentration at pH 3 and equal deposition times (60 min). Lines are only intended for illustration. Data are listed in Table A-21.*

At the start of the reaction, all enzyme molecules are adsorbed on the support surface and diffusion starts to take place. Therefore, a depletion of intact micelles close to the support surface must be considered at this point. Consequently, the casein concentration directly influences the number of succeeding micelles which are available for deposition. This further increases the dependence of the deposition reaction on the protein concentration. On the other hand, an increased number of micelles might have a negative impact on the diffusion of chymosin molecules by hindering their mobility (see 4.2.3.2).

However, results verify the dependence of the deposition process on the casein concentration, according to investigations on the enzymatically induced coagulation of milk. The opportunity to cleave more casein micelles in the same time has a stronger impact on the film thickness than a potentially restricted enzyme diffusion due to an increased number of particles.

### 4.3.6 Pressureless gluing as potential application

In the fields of adhesives, there is also a growing demand for environmentally friendly alternatives, to replace fossil fuel-based adhesives. Especially biobased polymers have a high potential in this area. They exhibit competitive properties, such as fast reversible adhesion, strong resistance to weathering, and advanced underwater adhesion, as compared to synthetic adhesive polymers.[24,278]

Proteins play an important role in commonly applied biobased adhesives, due to their superior properties, compared to other bioadhesive materials, such as presence of versatile functional groups and highly flexible backbones.[279–281] Popular resources for proteins used as adhesives are soy protein, wheat-gluten, gelatin, and casein.[123,282–284] In particular, casein has been used throughout history of mankind for gluing, due to its very strong adhesion to manifold materials.[69]

Based on the Enzyme Mediated Autodeposition of casein, a pressureless gluing process has successfully been developed, using adsorbed enzyme (**Figure 50**). Two glass supports are functionalized with adsorbed chymosin in a distinct area and are immersed into a casein dispersion with a fixed distance in between. After the reaction time, a casein layer is formed only in the area with adsorbed enzyme, i.e. the lower part of the support. Vertical orientation of the supports excludes deposition of casein particles due to uncontrolled precipitation.

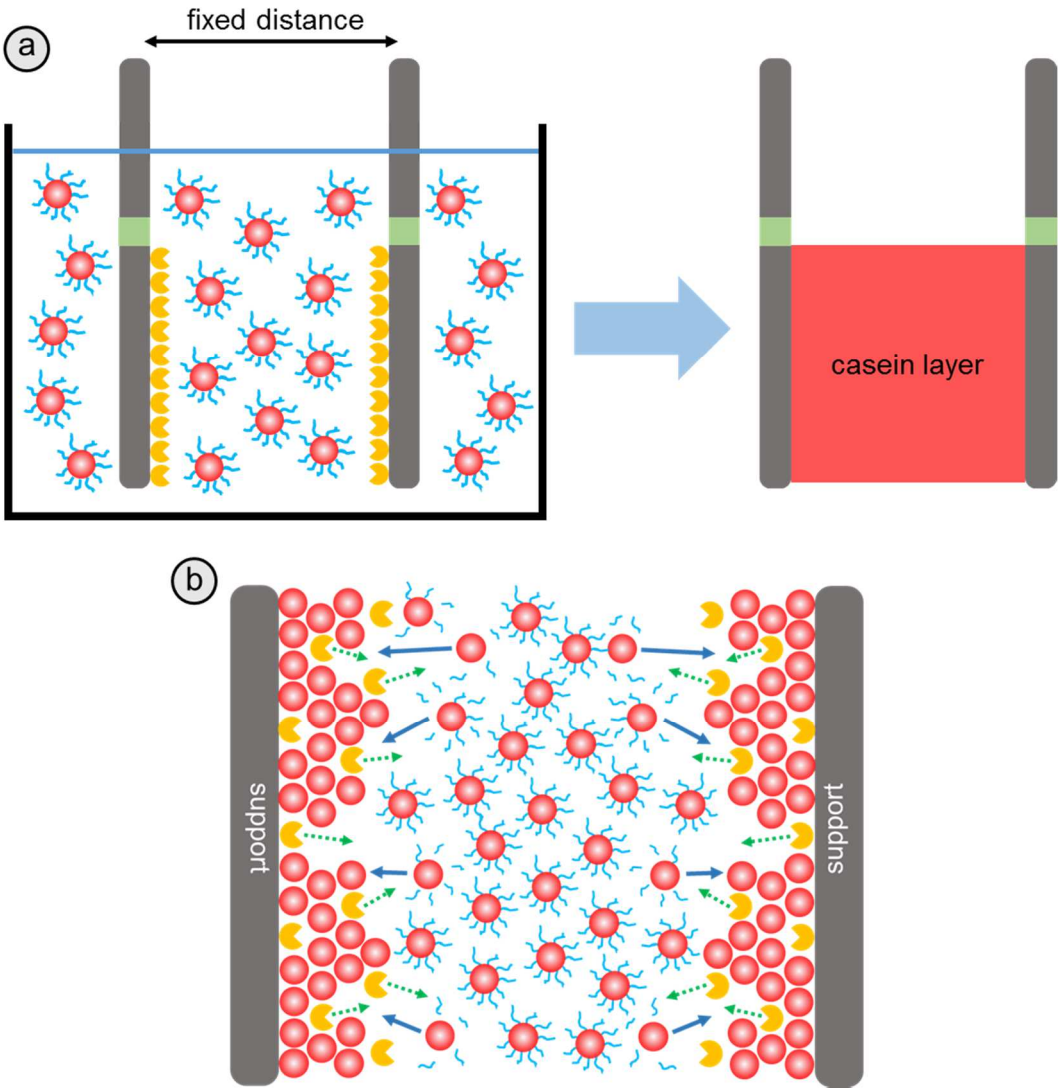


*Figure 50. Pressureless gluing application of EMA. a) Experimental setup and b) concept of gluing via EMA.*

If the casein layers extend far enough, gluing of the two supports results. To this, supports were first functionalized with enzyme, immersed into the casein dispersion, washed with DI water to remove non-cleaved casein, and dried.

Conglutination of support slides has been defined as successful, if the following conditions were achieved: First, supports need to stick together after removal from the holding devices and drying time. Secondly, the gluing must not show any failure upon application of slight mechanical stress.

**Table 6** summarizes the obtained results. Experiments confirm that successful conglutination occurs only in the areas, which are functionalized with chymosin, i.e. the lower parts of the slides. The enzymatic cleavage reaction of casein micelles can also be verified as the driving force, enabling control and feasibility

Table 6. Results of conglutination of supports via EMA.

| Distance in µm: | c (casein) in g/L: | c (chymosin) in g/L: | p*H*: | Result: |
|---|---|---|---|---|
| 125 | 20 | 25 | 3 | + |
| 250 | 20 | 25 | 3 | + |
| 375 | 20 | 25 | 3 | + |
| 500 | 20 | 25 | 3 | - |
| 250 | 20 | 25 | 3 | + |
| 250 | 10 | 25 | 3 | + |
| 250 | 5 | 25 | 3 | +/- |
| 250 | 1 | 25 | 3 | - |
| 125 | 20 | no enzyme | 3 | - |
| 125 | 20 | only NaCl | 3 | - |
| 125 | 20 | 25 | 12 | - |
| 250 | 20 | no enzyme | 3 | - |
| 250 | 20 | only NaCl | 3 | - |
| 250 | 20 | 25 | 12 | - |

of the process. Successful conglutination was observed up to a distance of 375 µm. Samples with a distance of 500 µm or higher were not conglutinated. For such high distances detachment of deposited casein could be observed, resulting in insufficient gluing. It can be assumed that this is caused by gravitation, as the layer becomes too heavy. If two layers meet before this happens, successful conglutination takes place.

Additionally, the casein concentration was varied to characterize the process further. Results show that concentrations down to 10 g/L yield a permanent conglutination of the support slides. Use of a casein concentration of 5 g/L showed variable results and appears to be a threshold. Even lower concentrations, e.g. 1 g/L, result in no conglutination of the supports at all.

To prove that the gluing is enzyme mediated, several reference samples were examined. Samples without the presence of any enzyme as well as samples with adsorbed salt (NaCl) showed no conglutination of supports after immersion

into a casein dispersion. Identical observations were also obtained, if enzyme-functionalized supports were immersed at a p*H* value, where chymosin is not active, e.g. p*H* 12. All reference samples confirm that the conglutination of supports is in fact only feasible and controllable by the enzymatic cleavage reaction.

Moreover, conglutination of titanium and galvanized steel supports was examined via the Enzyme Mediated Autodeposition, yielding similar results compared to the used glass supports. Especially the successful conglutination of titanium supports is very important with respect to potential applications, as Ti-based materials are frequently used as implants for medical purposes.[285–287]

In order to characterize the obtained adhesive casein layers, adhesion strength was measured with an Epprecht twistometer. The determined strength is 7.8 ± 1.4 MPa. This represents a relatively low value compared to other commonly used adhesives, based on synthetic polymers, such as polyurethane, epoxy, acrylic, or phenolic adhesives, which may have adhesive strengths up to 20-35 MPa.[288] The measured adhesion strength is probably based on the inherent brittleness of the protein layers, which is a commonly known issue of native casein.[289] However, the achieved adhesion strength of the deposited casein layers is much higher compared to conventional casein adhesive layers, which exhibit adhesion strengths of about 1.2 MPa.[290] This also indicates that via enzymatic cleavage of κ-casein and the resulting loss of κ-casein's polar part more flexible and less brittle casein layers are obtained.

A more detailed investigation of the adhesive casein layers via SEM revealed the presence of two distinctive areas. Representative SEM images of such layers, which were separated after conglutination are shown in **Figure 51**.

First, a continuous layer of casein covers the entire support surface. This is analogous to obtained results of casein film deposition on single glass supports. Secondly, a honeycomb-like structure is formed above the continuous film, which declines in thickness with increasing height. These structures are found on both conglutinated supports, indicating a structure as illustrated in **Figure 52**.

A complex pattern of walls is formed which connects the continuous protein films on the support surfaces. Explanations for the buildup of these structures are based on several aspects. Formation of a massive layer is unlikely, because depletion of casein particles between the supports occurs during the conglutination process. Casein supply from the bulk is also inhibited due to

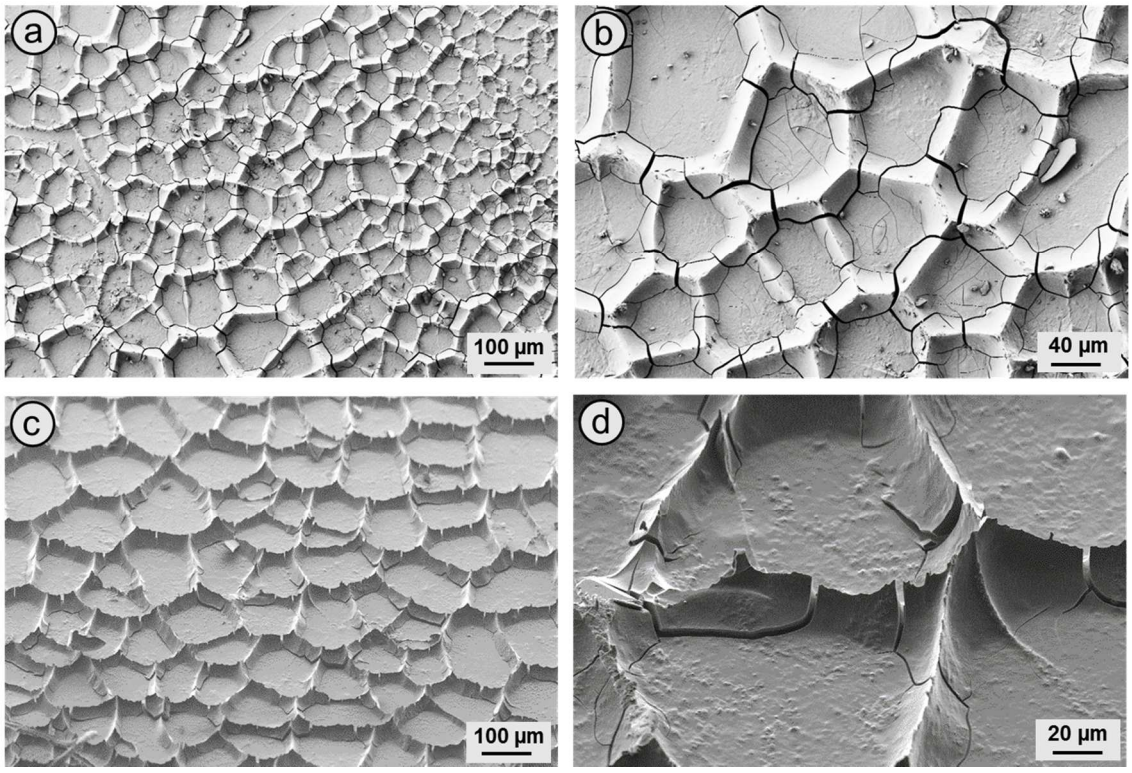


*Figure 51. SEM images of adhesive casein layers upon separation after conglutination. a) and b) top views and c) and d) views under tilt angle on adhesive layers.*

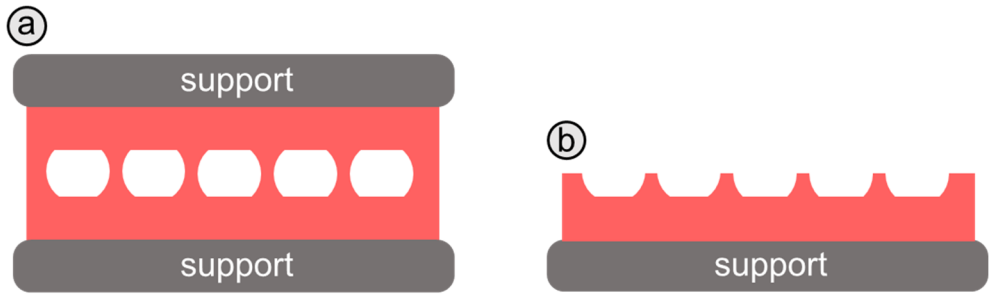


*Figure 52. 2D-model picture of adhesive casein layers a) before and b) after separation of the supports.*

blockage of the border areas. Additionally, buildup of the honeycomb-like structure is favored due to the different polarities of cleaved casein and water. This results in the formation of minimal surfaces. The observation of angles, frequently being in the range of about 120°, of three branching walls confirms the presence of these minimal surfaces.

Worth of mentioning is the much higher layer thickness, which can be up to about 375 µm, in comparison to the deposition of casein on single supports (up to about 1 µm, see 4.3.5.1). A possible explanation for this considers the presence of two neighboring supports as the reason. In experiments with a single support, cleavage reactions in the bulk phase have no contribution to the resulting protein layer. Cleaved micelles start to aggregate and eventually precipitate.

In the gluing approach, the distance between the two supports is very short compared to their dimension. Cleaved micelles in higher distances to the surfaces are trapped between them and thus, also deposit onto the supports instead of undergoing precipitation and sedimentation on the ground of the vessel. Indeed, this represents a decrease of control for a single film formation, but on the other hand, it is very beneficial for the pressureless gluing application.

### 4.3.7 Conclusion

The Enzyme Mediated Autodeposition, using adsorbed enzyme, enables the controlled formation of homogeneous and continuous casein coatings. Film thicknesses up to 1 µm are obtainable, as verified via SEM measurements. The reversible character of the immobilization method, the resulting enzyme diffusion, and the good film-forming behavior of casein are the dominating factors.

Deposited casein coatings exhibit superior properties compared to their conventional, non-cleaved counterparts. Cleaved casein films are resistant towards washing in DI water and exhibit an enhanced flexibility. This, in combination with the implementability of sterilization procedures (heat and UV radiation), enables versatile applications, where conventional casein coatings quickly reach their limits. Potential fields are medical as well as classical coating applications.

Control over the deposition process can easily be achieved by variation of reaction parameters, such as deposition time, p*H* value, and casein concentration. This allows for the formation of tailor-made protein multilayers. In addition, the physical adsorption approach of the EMA can even be modified into a pressureless gluing with biomolecules.

## 4.4 Site-specific addressing of casein particles

### 4.4.1 Overview

This section presents the results of the Enzyme Mediated Autodeposition which were achieved with covalently immobilized chymosin. Obtained findings confirm the high site-specificity of the process and were published in “Macromolecular Materials and Engineering” and “Journal of Coatings Technology and Research”.[291,292]

First, the applied enzyme immobilization methods, i.e. coupling via epoxy groups, using GLYMO, and coupling via APTES/glutaraldehyde are described with regard to support preparation and design of immobilized enzyme particles. Secondly, casein deposition on enzyme-functionalized supports is examined. Furthermore, the effect of spacer molecules on the mobility of covalently immobilized enzyme is investigated.

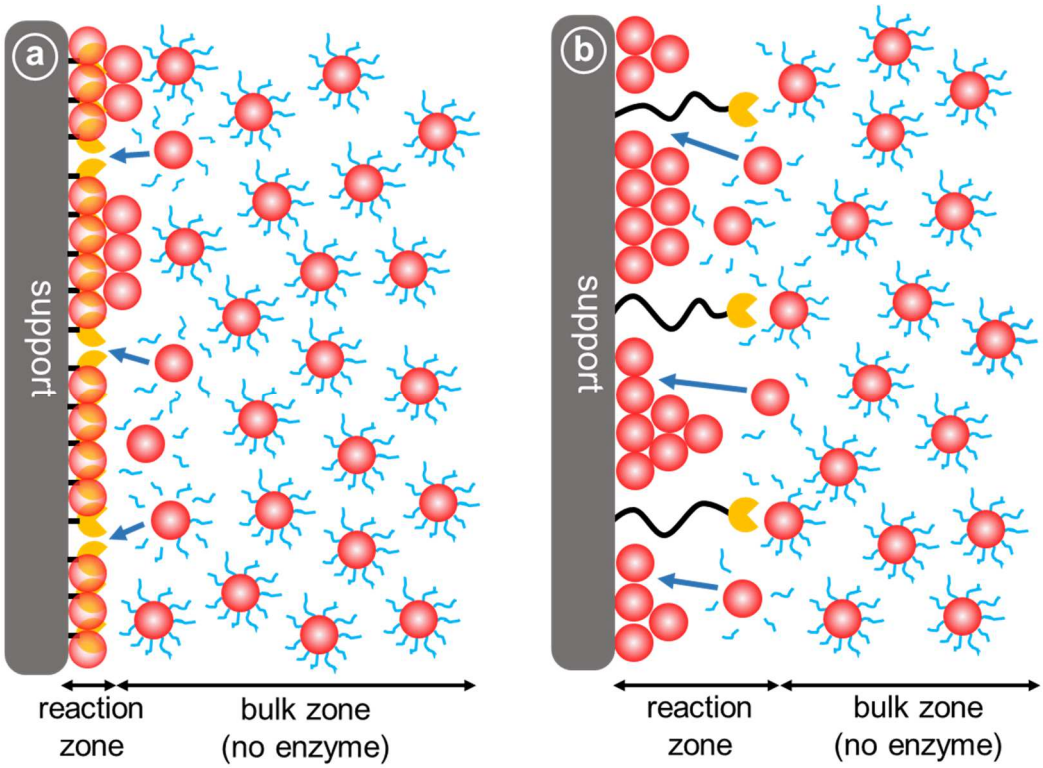


*Figure 53. Concept of EMA, using covalently immobilized enzyme. a) Short linkage for enzyme coupling and b) use of spacer molecules. Type of enzyme immobilization, especially length of linkage molecules, determines the size of the reaction zone.*

Covalent coupling presents an irreversible immobilization method, excluding enzyme diffusion. Therefore, it is assumed that the dimension of resulting casein layers is determined by the length of the covalent linkage. **Figure 53** shows the concept of the EMA, using covalently immobilized enzyme. Detailed illustrations of the three investigated coupling methods are displayed in **Figure 54**.

In case of a short linkage for enzyme coupling, e.g. via functionalization with GLYMO or glutaraldehyde, cleavage of casein micelles occurs only in very close proximity to the support surface, due to a minimal size of the reaction zone. It is therefore expected that immobilized enzyme is readily covered with cleaved casein micelles. Taking this into account, monolayers or at the maximum double layers of cleaved casein micelles should be deposited.

On the other hand, covalent coupling via a hydrophilic spacer molecule, such as PEG, is expected to enlarge the reaction zone by the spacer length, also increasing enzyme mobility and flexibility. This should increase the amount of deposited casein in dependence on the spacer length, while diffusion of enzyme is still restricted. As a consequence, different protein deposition patterns based on the particular immobilization method are expected to appear.

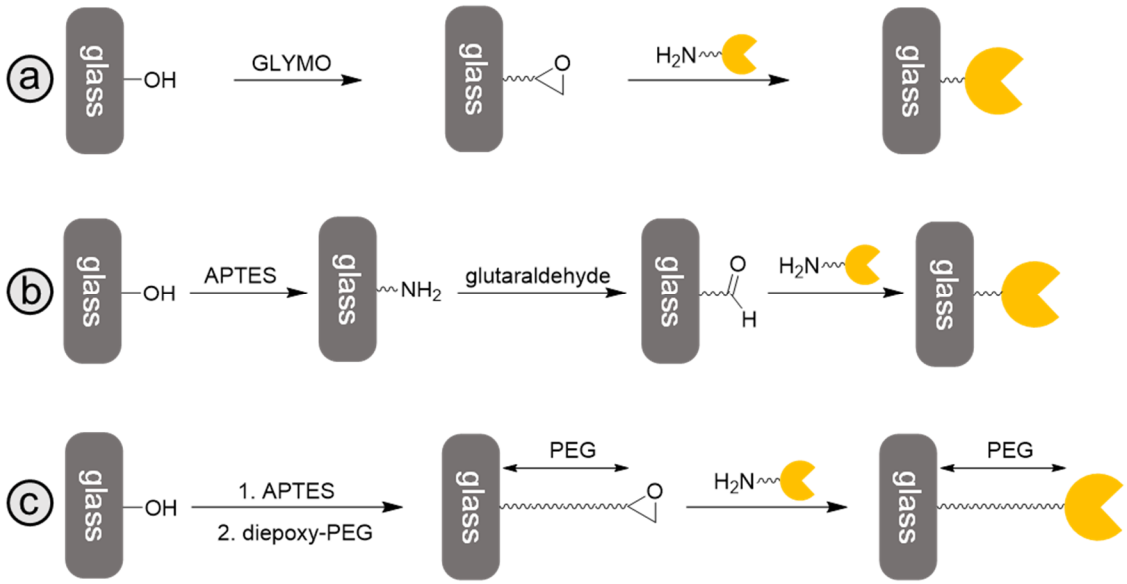


*Figure 54. Overview on applied covalent immobilization methods. a) Covalent immobilization via GLYMO and b) via APTES/glutaraldehyde, resulting in short linkages of chymosin. c) Covalent immobilization via diepoxy-PEG-spacer, using an amino-functionalized support surface.*

### 4.4.2 Preparation of supports for enzyme immobilization

Successful silylation of glass supports either with GLYMO or APTES was verified by ellipsometry, contact angle, and AFM measurements (**Table 7**).

Ellipsometry measurements provided a layer thicknesses of 5.4 ± 0.2 nm for GLYMO and 1.3 ± 0.2 nm for APTES under the applied conditions. Consequently, a GLYMO multilayer was achieved, since the thickness of a GLYMO monolayer is known to account for about 1.0 nm.[293] In literature, an APTES monolayer accounts for 0.7 nm.[294] Thus, a double layer of APTES on the glass supports can be assumed. The obtained contact angles are 69.4 ± 0.6° (GLYMO) and 60.3 ± 0.8° (APTES). Both contact angles are consistent with literature values.[183,295,296]

Roughness of silane layers was examined via AFM by determination of the arithmetic average $R_a$ values of the surface height deviations. $R_a$ values are 0.35 nm for GLYMO and 0.33 nm for APTES layers. Comparison of these values with the roughness of a cleaned glass surface ($R_a$ = 0.28 nm) yields the verification that very smooth silane layers were formed.

GLYMO-functionalized glass supports enable direct covalent binding of enzyme molecules via their surface epoxy groups. APTES layers need to be subjected to an activation step before enzyme coupling. Activation via glutaraldehyde yielded a contact angle of 62.7 ± 1.5°. Such small changes of contact angles for this modification step are known in literature.[297] Therefore, the activation via glutaraldehyde can be verified as successful.

*Table 7. Characterization of silanized glass surfaces. Thicknesses, contact angles, and roughnesses of GLYMO and ATPES layers are compared to cleaned glass surface.*

| Surface: | Layer thickness in nm: | Contact angle in °: | Roughness ($R_a$) in nm: |
|---|---|---|---|
| Cleaned glass | / | ≤ 3 | 0.28 |
| GLYMO | 5.4 ± 0.2 | 69.4 ± 0.6 | 0.35 |
| APTES | 1.3 ± 0.2 | 60.3 ± 0.8 | 0.33 |

### 4.4.3 Covalent immobilization of chymosin

#### 4.4.3.1 Binding via GLYMO

Successful covalent immobilization of chymosin onto GLYMO-functionalized glass supports was verified via contact angle, XPS, SEM, AFM, and EDX.

As mentioned in 2.3.3.3, the physical adsorption step of enzyme during immobilization is favored at high ionic strength (1 M buffer). Immobilization of chymosin at unfavorable conditions, e.g. at low ionic strength, should yield different immobilized chymosin structures. In order to investigate this, the immobilization reaction was also carried out with a 25 mM buffer concentration.

Coupling of hydrophilic chymosin results in lower contact angles, i.e. 61.1 ± 2.0° (1 M buffer) and 59.5 ± 1.6° (25 mM buffer), and thus, in a more hydrophilic surface compared to the GLYMO layer. Presence of enzyme molecules after the immobilization reaction is also confirmed by XPS measurements. **Figure 55** shows the particular XPS graphs before and after the immobilization. While no significant amounts of nitrogen could be detected regarding the GLYMO layer, nitrogen is detected in reasonable amounts after enzyme immobilization. Also increased amounts of carbon and lower amounts of silicon support this conclusion.

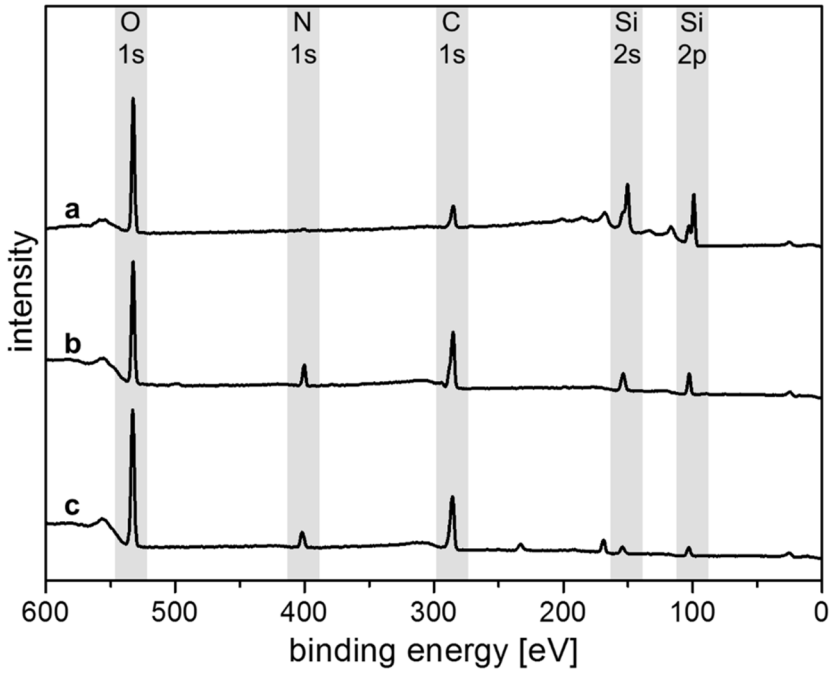


*Figure 55. XPS measurements of a) GLYMO-functionalized glass support, b) after enzyme immobilization at high ionic strength (1 M buffer), and c) after enzyme immobilization at high ionic strength (25 mM buffer).*

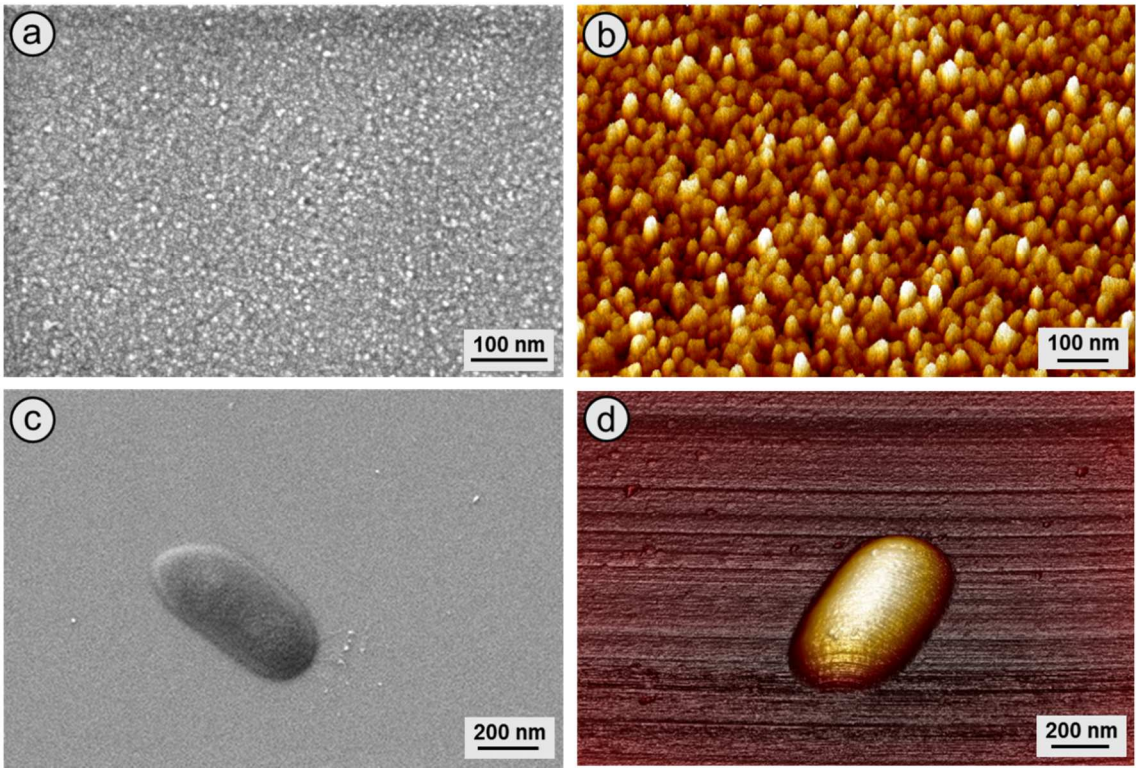


*Figure 56. SEM and AFM images of covalently tethered chymosin on epoxy-functionalized glass supports a) and b) after immobilization at high ionic strength (1 M buffer) and c) and d) after immobilization at low ionic strength (25 mM buffer)*

SEM and AFM images of the resulting enzyme particles after the respective immobilization process are shown in **Figure 56**. Diameters of enzyme structures at high ionic strength are about 6–25 nm. The diameter of a single chymosin molecule is about 5–6 nm (PDB code 4AA8). This indicates that single enzyme molecules were immobilized as well as small aggregated structures. Both SEM and AFM measurements display a homogeneous and dense distribution of enzyme on the support surface (**Figure 56a** and **56b**).

Monomolecular enzyme can easily be distinguished from the used Au/Pd sputter coatings for SEM measurements. SEM and AFM images, showing clearly the differences between immobilized chymosin and the sputter coating, are shown in the appendix (**Figure A-86**). A mistaking of sputter structures from immobilized enzyme can therefore be ruled out.

In contrast to the results at high ionic strength, large enzyme aggregates with sizes of several hundred nanometers were covalently attached at low ionic strength (**Figure 56c** and **56d**). Their predominant size is about 600 nm in length, 300 nm in width, and 120 nm in height. These aggregates are mostly

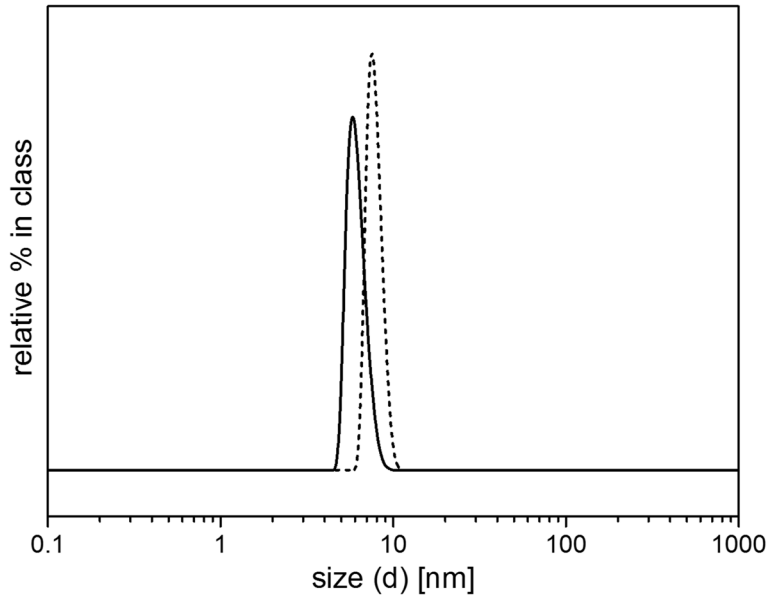


*Figure 57. Number size distributions of dissolved chymosin molecules in 25 mM buffer (—) and in 1 M buffer (·····). Data are listed in Table A-22.*

found in isolated form on the support. The formation of such aggregates is probably based on a reduction of the number of effective collisions between enzyme molecules and the hydrophobic matrix. After some chymosin molecules have underwent a successful immobilization, further enzyme molecules preferably attach to this nucleus and aggregation results.

These considerations are supported by DLS measurements (**Figure 57**). Sizes of dissolved chymosin molecules in the particular immobilization solutions correspond to single molecules. No aggregation of chymosin could be detected neither at 25 mM nor at 1 M buffer concentration. An aggregation of enzyme molecules previously to the immobilization step can therefore be excluded.

Identification of the aggregated structures as enzyme is also confirmed by EDX measurements, which could be performed due to the large dimension of the aggregates (**Figure 58**). The elemental composition of enzymes, i.e. carbon, nitrogen, and oxygen, is only found in the presumed areas of enzyme aggregates, while the support surface consists of silanized silicon dioxide. EDX measurements also confirm that the aggregates are found in isolated form.

Residual activity of covalently immobilized enzyme on epoxy-functionalized supports was determined with Sepabeads EC-EP, using monomolecular chymosin. Residual activity of chymosin was 46 % with respect to free native enzyme (100 % enzyme activity). This value is in accordance to literature values and is sufficient for the intended purposes, regarding the site-specific deposition of casein.[298]

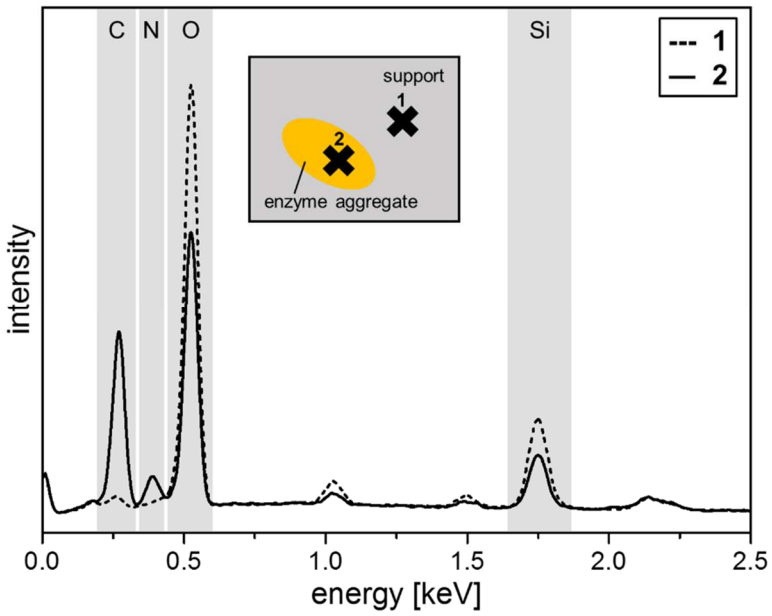


*Figure 58. EDX measurements of silanized glass surface after functionalization with large enzyme aggregates; EDX spectra of silanized surface (point 1) and of area with immobilized enzyme aggregate (point 2).*

#### 4.4.3.2 Binding via APTES/glutaraldehyde

Covalent immobilization of chymosin at low ionic strength (25 mM) onto APTES-functionalized glass supports, which were activated with glutaraldehyde, was confirmed via contact angle, XPS, and SEM measurements.

Coupling of enzyme increases the contact angle to 64.4 ± 2.0° (62.7 ± 2.0° after activation with glutaraldehyde), indicating a successful attachment. This is especially strengthened by performed XPS measurements (**Figure 59**). Consideration of the single graphs is more elaborate compared to the enzyme immobilization via GLYMO. Therefore, **Figure 60** shows for a better understanding the changes of the atom percentages of the particular immobilization steps.

Formation of the APTES layer provides an amino-functionalized surface. A nitrogen peak is therefore detected right from the start of the immobilization procedure. Oxygen and silicon are detected in high amounts, originating from the glass support as well as from the resulting silane layer. Carbon is also present in noticeable amounts, representing the three-carbon alkyl chain of APTES.

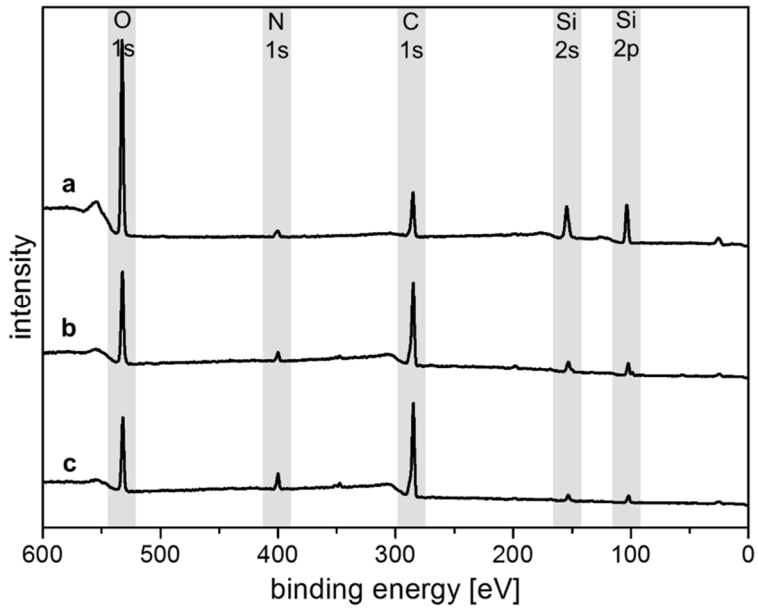


*Figure 59. XPS measurements of a) APTES-functionalized glass support, b) activated APTES layer with glutaraldehyde, and c) after enzyme immobilization.*

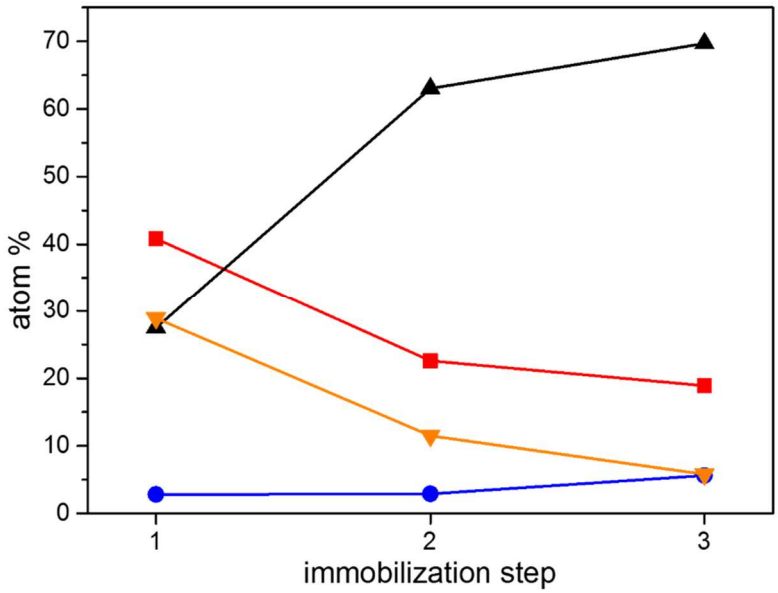


*Figure 60. Atom % of different steps during enzyme immobilization via APTES/glutaraldehyde. Step 1 = functionalization with APTES, step 2 = activation with glutaraldehyde, and step 3 = chymosin immobilization. ■ = oxygen, ● = nitrogen, ▲= carbon, and ▼= silicon. Data are shown in Table A-23.*

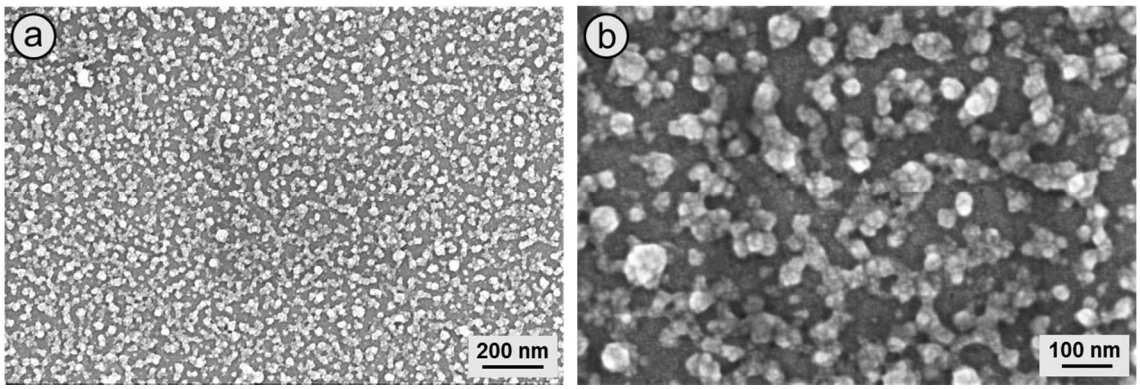


*Figure 61. SEM images of immobilized chymosin via APTES/glutaraldehyde at a) low and b) high magnification.*

Activation with glutaraldehyde yields an increased amount of carbon, while oxygen and silicon peaks decrease and the amount of nitrogen remains constant. This is in accordance to the attachment of glutaraldehyde or its (oligomeric) heterocycles to an amino-functionalized surface (see 2.3.3.3).

Coupling of enzyme to the activated support increases the amounts of carbon and nitrogen, whereas oxygen and silicon peaks further decline. This proves the successful covalent attachment of chymosin.

SEM measurements were conducted to visualize the immobilized chymosin structures (**Figure 61**). Structures exhibit diameters of about 40–80 nm and are homogeneously distributed on the support. In comparison to the immobilization via epoxy groups only small chymosin aggregates were immobilized.

The residual activity of via glutaraldehyde covalently immobilized chymosin was examined with commercially available Sepabeads EC-EA as support material. Chymosin was covalently tethered onto these aminated supports after activation with glutaraldehyde. Enzymatic activity was determined with the standardized hemoglobin test. This yielded a residual activity of 83 % with respect to free native enzyme (100 % enzyme activity). This activity is much higher compared to the one of chymosin, which was immobilized via epoxy groups. The reason for this is probably based on the use of glutaraldehyde or its oligomeric heterocycles as small spacer molecules. This provides a higher enzyme flexibility and consequently higher activities compared to the previously studied short epoxy linkage.

### 4.4.4 Casein deposition with covalently immobilized chymosin

#### 4.4.4.1 Deposition via monomolecular enzyme

Immersion of supports with covalently immobilized monomolecular enzyme (immobilization via GLYMO at high ionic strength) into a casein dispersion results in the deposition of continuous and homogenous cleaved casein films (**Figure 62**). Identity of the material as cleaved casein is proven by the high water stability, which is not found for non-cleaved casein films.

Deposited films exhibit a smooth surface and have film thicknesses of about 20–40 nm. Films with higher thicknesses than 40 nm are not achievable, regardless of deposition time. This is caused by the strong localization of enzyme to the support surface. Taking into account that a casein monolayer is assumed to be about 15–20 nm in height, monolayers or at the maximum double layers of cleaved casein are deposited.

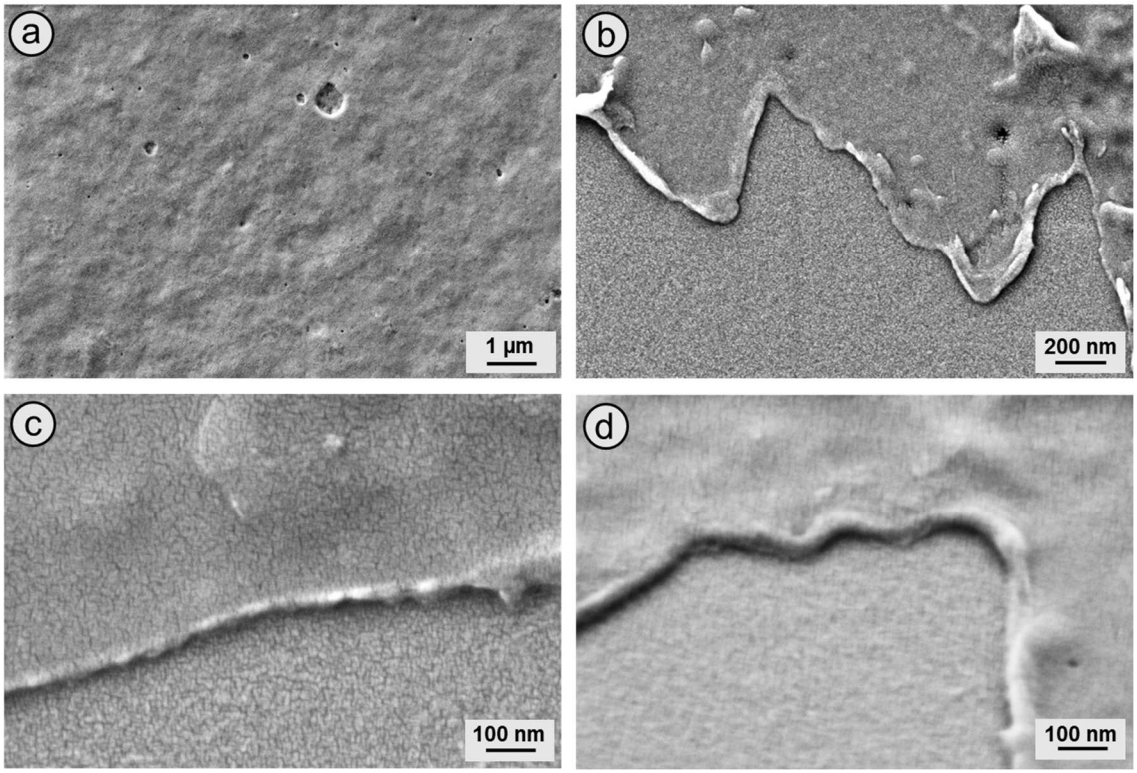


*Figure 62. SEM images of casein coatings via EMA, using via GLYMO covalently immobilized enzyme. a) Top view on casein coating, b) view at mechanical damage, c) and d) views at tilt angles for film thickness determination. Layer thickness in image c) is 20 nm and in image d) 40 nm. Casein deposition was achieved under equal conditions for all presented samples, i.e. $c_C$ = 10 g/L, pH 3, T = 40 °C, and $t_D$ = 120 min.*

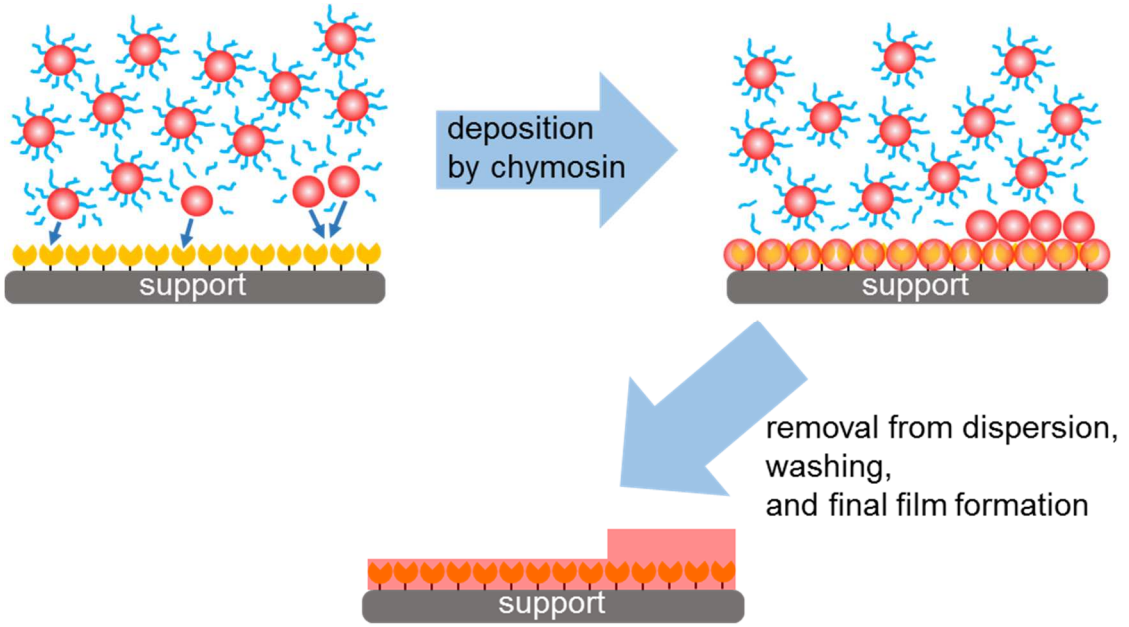


*Figure 63. Proposed deposition mechanism of particles via EMA, using via GLYMO covalently immobilized monomolecular enzyme (high ionic buffer concentration). Final film formation occurs analogously to Figure 42.*

Deposition of casein micelles appears site-specific on enzyme-functionalized areas only and is evenly distributed, where enzyme is homogenously present. Thus, even large area surfaces and objects with complex geometries can specifically be coated via this easy-to-apply process.

**Figure 63** illustrates the respective deposition mechanism. Cleaved micelles undergo coalescence upon drying and form a continuous protein film. Due to the chemical tethering of enzyme to the support, diffusion of chymosin molecules is prevented. It can be assumed that formation of double layers occurs, where several casein micelles are simultaneously cleaved and compete for the same space on the support during deposition. The formation of such areas with two layers of cleaved casein is also considered in the proposed mechanism.

The deposition process is self-terminating and stops, when tethered enzyme is covered with cleaved casein. This takes place after deposition of a monolayer or not more than a double layer of casein. Therefore, a highly improved vertical site-specificity is accomplishable in comparison to the deposition with reversibly immobilized enzyme, where increasing multilayers result with proceeding reaction time.

### 4.4.4.2 Deposition via small enzyme aggregates

The Enzyme Mediated Autodeposition, using via APTES/glutaraldehyde immobilized small enzyme aggregates (d = 40–80 nm), also yields continuous cleaved casein films. **Figure 64** shows SEM images of the obtained results. The presence of a continuous protein film is clearly visible from **Figure 64b**.

Interestingly, the enzyme aggregates are still recognizable under the casein film. The reason for this is based on the fact that the immobilized enzyme structures are much bigger compared to monomolecular enzyme, which was immobilized via GLYMO. Thus, even after casein deposition and film formation, these enzyme aggregates are detectable inside the protein film via SEM.

Contribution of the enzyme aggregates to the film thickness after the deposition reaction is not negligible this time. Casein layer thickness is calculated by subtraction of the size of the immobilized aggregates from the resulting structure heights, which account for 60–90 nm. This yields layer thicknesses in the range of a casein monolayer. Due to the strongly varying height, partial deposition of casein double layers is likely and needs to be taken into account, especially in gaps between neighboring aggregates.

The obtained results further strengthen the previous conclusion (4.4.4.1) that deposition of a casein monolayer or at the maximum of a double layer leads to self-termination of the deposition process, if covalently immobilized enzyme is used. **Figure 65** illustrates the modified deposition mechanism.

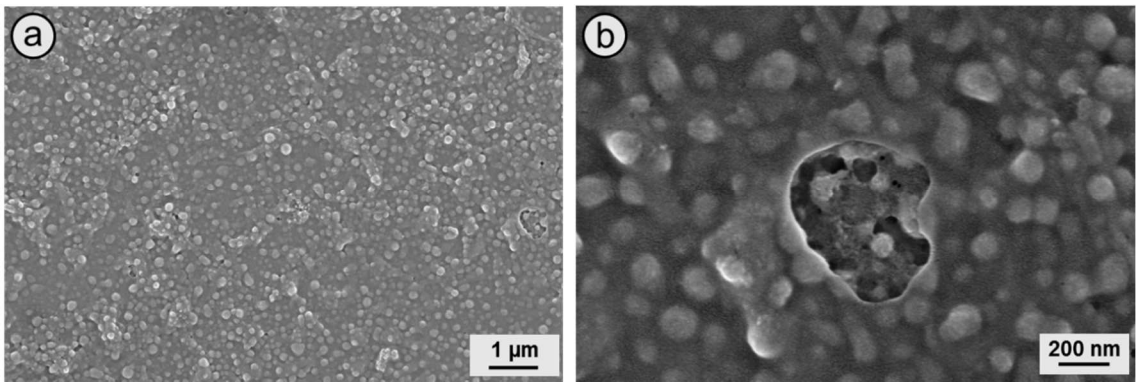


*Figure 64. SEM images of deposited casein coatings after enzyme immobilization via APTES/glutaraldehyde. Conditions for casein deposition: $c_C$ = 10 g/L, $t_D$ = 120 min, pH 3, and 40 °C.*

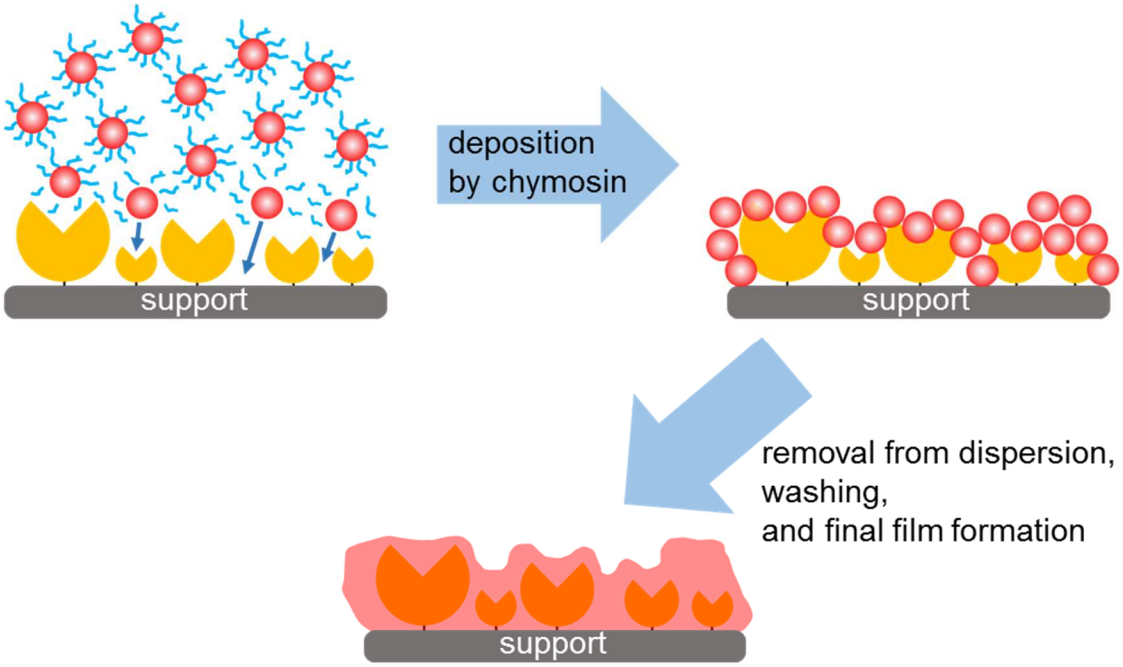


*Figure 65. Proposed deposition mechanism of particles via EMA, using via APTES/glutaraldehyde covalently immobilized small enzyme aggregates. Final film formation occurs analogously to Figure 42.*

#### 4.4.4.3 Deposition via large enzyme aggregates

Implementation of immobilized large chymosin aggregates (immobilization via GLYMO at low ionic strength) in EMA of casein results in highly site-specific deposition patterns of cleaved micelles. Dimensions of these patterns are in the nanometer scale. Cleaved micelles are only deposited in the direct surrounding of the aggregates. No deposition of protein particles apart from the aggregates takes place. The radius for deposition accounts for about 500 nm around the enzyme aggregate. **Figure 66** shows SEM and AFM images as well as illustration pictures of the results.

Cleaved micelles are also deposited on top of the aggregates. This is confirmed by detection of their heights before (120 nm) and after (160 nm) deposition. Similar heights are also measured for the deposited micelles around the aggregates, i.e. 20–40 nm. Single casein micelles or in individual cases overlapping micelles are deposited. This is in good accordance to previously described results, considering the deposition of mono- or double layers with covalently immobilized monomolecular chymosin (see 4.4.4.1).

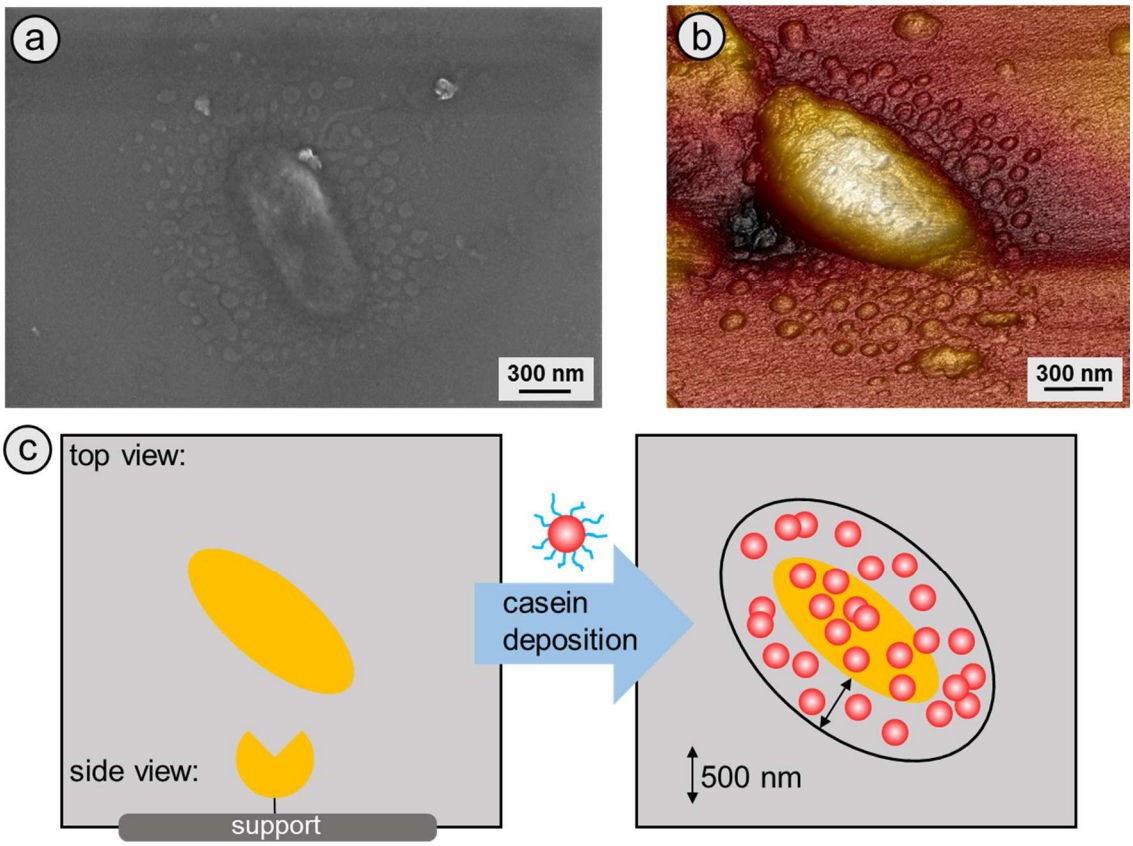


*Figure 66. a) SEM and b) AFM images of casein deposition patterns via large chymosin aggregates. c) Illustration pictures, explaining the obtained results. Conditions for casein deposition: $c_C$ = 10 g/L, $t_D$ = 120 min, pH 3, and 40 °C.*

The high site-specificity of the deposition reaction is confirmed by the occurring distinct radius of cleaved micelles around the aggregates. Unspecific adsorption of micelles on the support is excluded and their adhesion must be the consequence of the enzymatic cleavage reaction. This is further confirmed by additional deposition experiments (**Figure 67**). Reference samples at p*H* 12, where chymosin is nearly not active, show no deposition of casein and proof that participation of active chymosin in the deposition reaction is required.

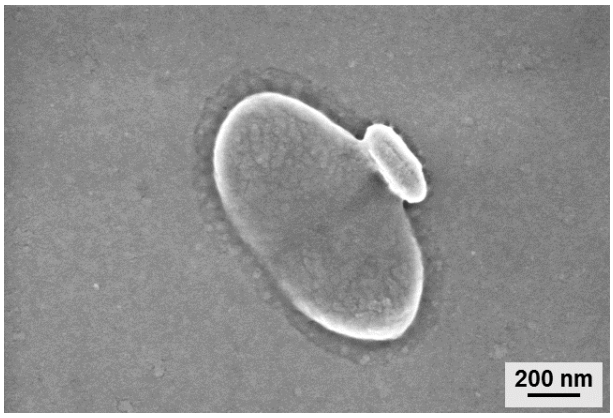


*Figure 67. SEM image of impracticable casein deposition after immersion of immobilized large enzyme aggregates into casein dispersion at pH 12.*

### 4.4.5 Effect of spacer molecules on casein deposition

Deposition experiments with reversibly immobilized chymosin showed that enzyme mobility influences directly the size of the reaction zone and the resulting casein deposition structures. Therefore, it can be assumed that the application of spacer molecules in covalent enzyme immobilization will change the appearance of the so far obtained deposition patterns. To this, diepoxy-PEG-spacer molecules were incorporated into the immobilization process (**Figure 53b** and **Figure 54c**). At first, chymosin has been covalently immobilized as monomolecular particles and as large aggregates, using diepoxy-PEG-spacers with a molecular weight of 20.000 g/mol.

PEG was chosen, because it exhibits an excellent water solubility and should therefore, enhance the mobility of immobilized enzyme. Generally, PEG has beneficial effects on the activity of covalently immobilized enzyme, if used as a spacer molecule.[299,300] The enzymatic activity is retained in most cases, but also higher activities compared to free native enzyme might be gained. The persistence length of a single PEG unit in water is 0.35 nm.[301] Thus, the reaction zone should be increased by about 160 nm, i.e. the persistence length of a PEG molecule with a molecular weight of 20.000 g/mol.

On the other hand, PEG is known to have protein-repelling properties, which at least have been demonstrated on the example of mammalian blood albumin.[302,303] Such interfering properties connected to casein would restrict a successful deposition. Nevertheless, the expected beneficial effects of PEG-spacers on the chymosin activity and mobility are decisive for the intended approach.

Successful binding of spacer molecules onto APTES-functionalized glass supports and subsequent enzyme coupling have been confirmed by contact angle and XPS measurements. The determined contact angles are shown in **Table 8**. Attachment of the PEG-spacer to the aminated support lowers the contact angle by about 6°. Since PEG is a very hydrophilic molecule, an even lower contact angle was expected. However, successful binding of the spacer is best confirmed by XPS measurements. **Figure 68** shows the detected C1s peaks before and after the reaction with the PEG-spacer.

*Table 8. Contact angles after different modification steps of chymosin immobilization via diepoxy-PEG-spacers.*

| Surface: | Contact angle in °: |
|---|---|
| Cleaned glass | ≤ 3 |
| APTES | 60.3 ± 0.8 |
| Diepoxy-PEG-spacer | 54.5 ± 0.4 |
| Chymosin (1 M buffer) | 62.7 ± 0.8 |
| Chymosin (25 mM buffer) | 60.2 ± 1.0 |

The comparison of the C1s peaks reveals that the peak after PEG functionalization is a combined peak from different carbon species. Deconvolution of this peak into the particular signals verifies the presence of a new C–O–C species at 286.5 eV. This peak originates from the ether bridges in the newly existing ethylene glycol units. The detected binding energy is in accordance to data found in literature for ether bonds in PEG.[304]

Coupling of enzyme results, accordingly to previous experiments, in contact angles of about 60°. Successful binding of chymosin is additionally verified via SEM and AFM measurements for both, monomolecular enzyme and large enzyme aggregates (**Figure 69**).

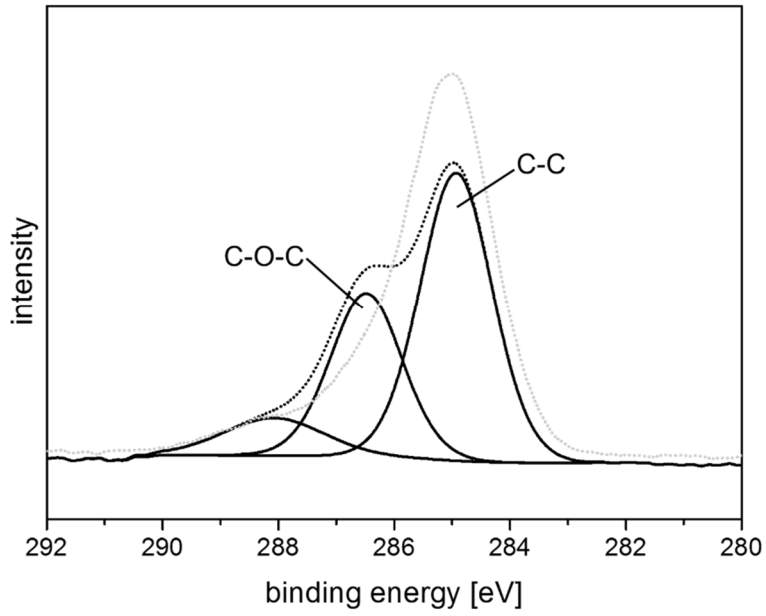


*Figure 68. XPS spectrum of carbon C1s peak before (·····) and after (·····) binding of diepoxy-PEG-spacer. The peak after functionalization can be deconvolved into multiple single signals (—).*

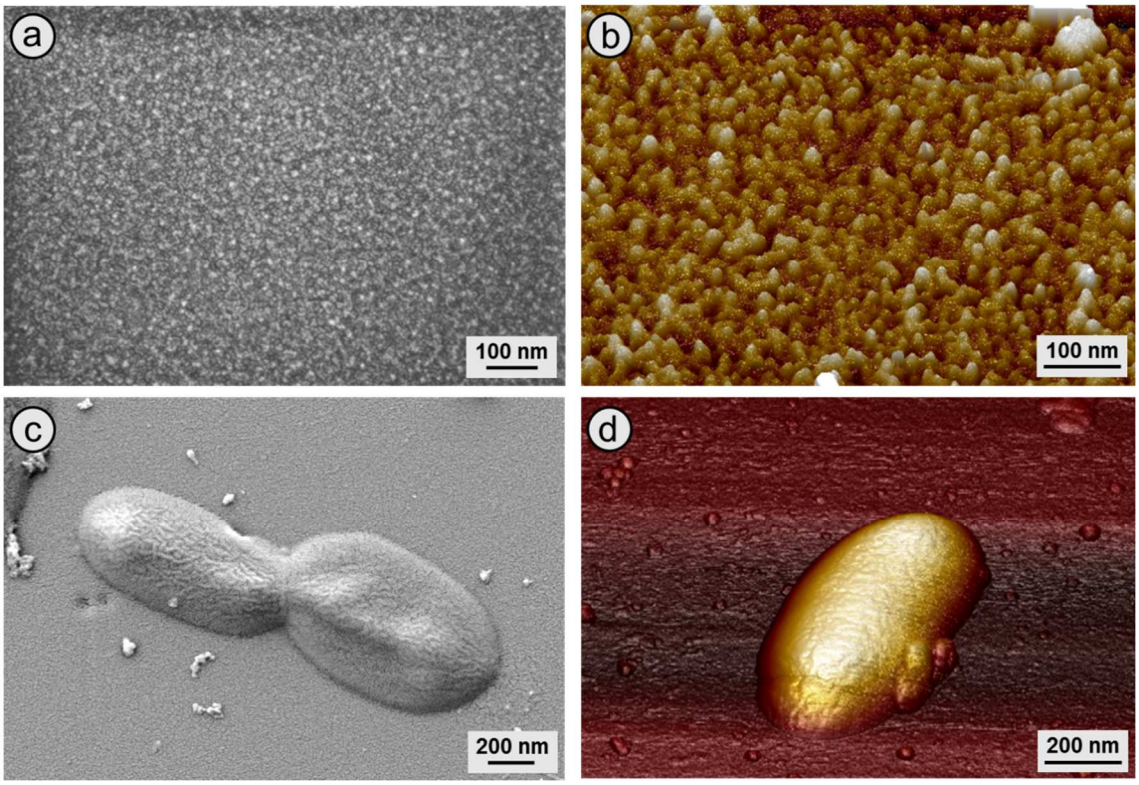


*Figure 69. SEM and AFM images of immobilized chymosin via diepoxy-PEG-spacer at high (1 M buffer) and low ionic strength (25 mM buffer). a) SEM and b) AFM images of immobilized enzyme at high ionic strength. c) SEM and d) AFM images of immobilized enzyme at low ionic strength.*

Results are very similar to previous experiments and enzyme particles exhibit sizes in the same range as before. Monomolecular enzyme particles and small aggregates have diameters of about 6-25 nm and are homogeneously distributed on the support surface. On the other hand, large enzyme aggregates account again for several nanometers in size and occur predominantly in isolated form on the surface.

The effect of the PEG-spacer molecules becomes apparent, when the enzyme-functionalized supports are immersed into a casein dispersion and autodeposition of protein micelles is initiated. In case of immobilized molecular enzyme, less deposition of casein takes place compared to experiments conducted without the use of spacer molecules. Although the enzyme is evenly distributed on the surface, only deposition of single particles takes place and no homogeneous casein films results. **Figure 70** reveals exemplarily these single casein micelles.

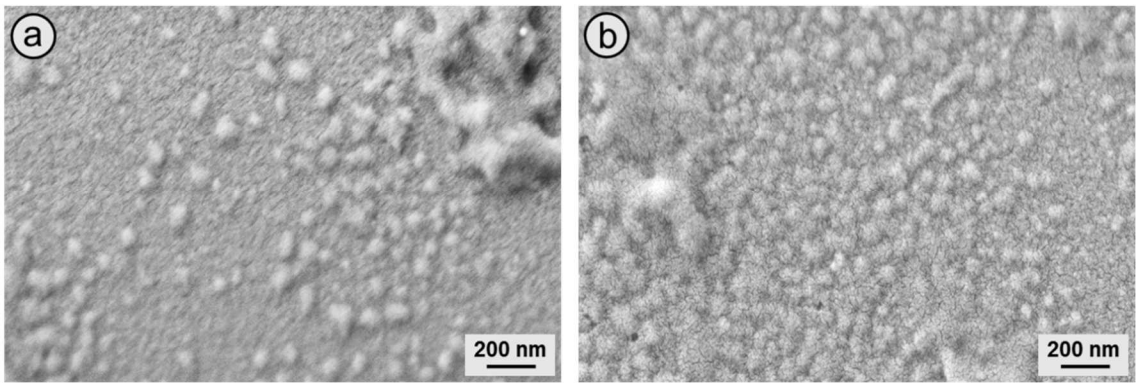


*Figure 70. SEM images of deposited casein structures, using diepoxy-PEG-spacers (20.000 g/mol) for immobilization of monomolecular enzyme. Conditions for casein deposition: $c_C$ = 10 g/L, $t_D$ = 120 min, pH 3, and 40 °C.*

It is obvious from the images that the critical amount of deposited micelles, necessary for coalescence of particles, is not accomplished. This is probably based on the protein-repelling properties of PEG. Consequently, PEG-spacers are not suitable for deposition reactions with molecular enzyme.

However, the use of PEG-spacers in combination with large enzyme aggregates shows the expected effects. Their incorporation enhances the mobility of immobilized enzyme and increases the amount of deposited casein. **Figure 71** illustrates the obtained findings.

The deposition radius is increased by the factor four compared to experiments conducted without spacers. This means that cleaved casein particles are found up to a distance of 2000 nm around the aggregate. In comparison to the outer radius, degree of deposition inside the inner radius (500 nm) is higher and partial coalescence of cleaved micelles is observed. Related to the height of the enzyme aggregates, which is about 120 nm, implementation of the spacers with a persistence length of 160 nm should at least double the size of the reaction zone. The increased amount of deposited casein confirms this assumed expansion.

Aggregates probably tend to “float” at higher distances in an aqueous environment. In consequence, destabilized micelles must pass a longer way, until they reach the support and deposit. This results in a broader distribution of protein particles on the support surface. Moreover, enzyme aggregates remain active for a longer time, until they are covered with cleaved casein.

Protein-repelling properties of the PEG-spacers are probably superimposed by presence of the large enzyme aggregates, which initiate the deposition of a high amount of casein micelles in the surrounding area.

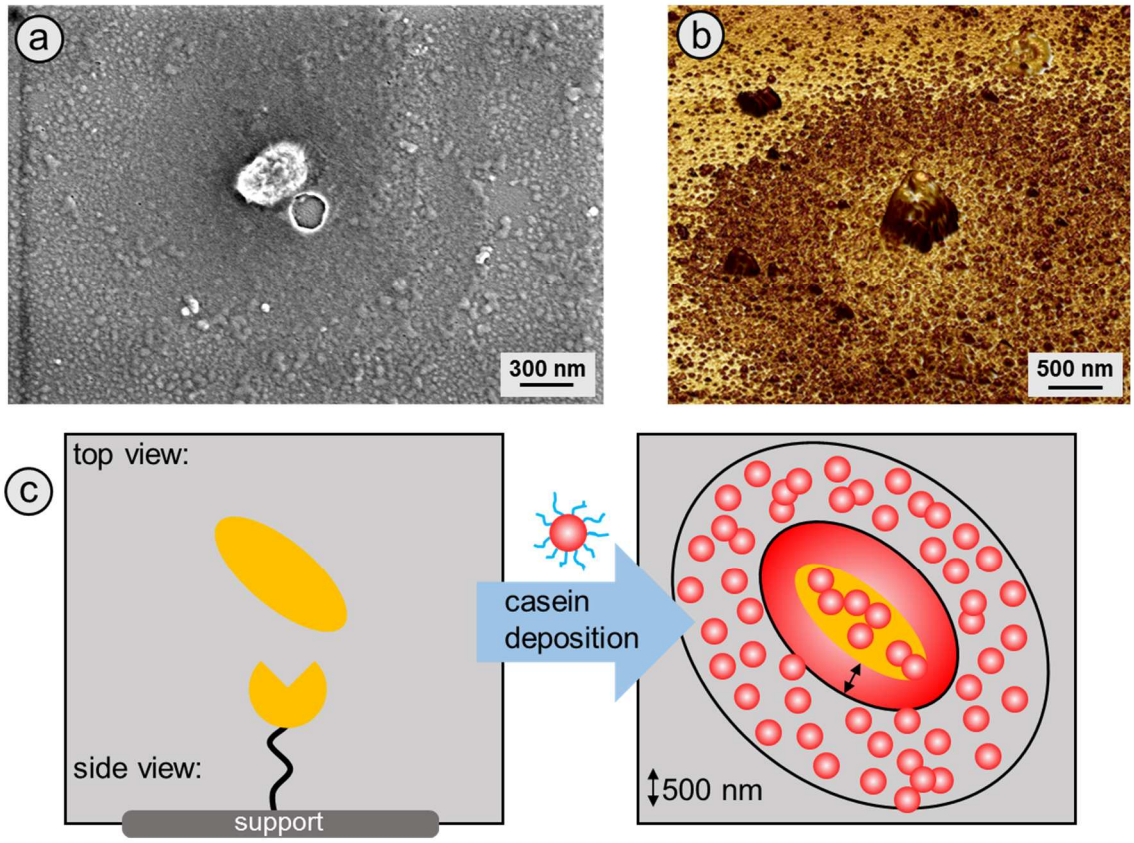


*Figure 71. a) SEM and b) AFM images of casein deposition patterns via large chymosin aggregates and use of PEG-spacer molecules (20.000 g/mol). c) Illustration pictures, explaining the obtained results. Conditions for casein deposition: $c_C$ = 10 g/L, $t_D$ = 120 min, pH 3, and 40 °C.*

Self-termination of the deposition process is delayed and the chymosin aggregate is able to cleave more micelles at equal reaction times, as compared to directly bound enzyme aggregates. A multipoint covalent attachment of the aggregates must be taken into account, but obviously does not significantly influence the mobility of the aggregate.

In order to obtain a more detailed view on the influences of spacer molecules, further experiments were performed under the same conditions, using diepoxy-PEG-spacers with a molecular weight of 10.000 g/mol. These spacer molecules exhibit a persistence length of about 80 nm in an aqueous solution and should increase the reaction zone by this length. It can be assumed that deposition structures of cleaved casein should appear, which can be categorized in between of the latter two experiments, i.e. use of directly bound enzyme and use of large PEG-spacer molecules (20.000 g/mol) for immobilization.

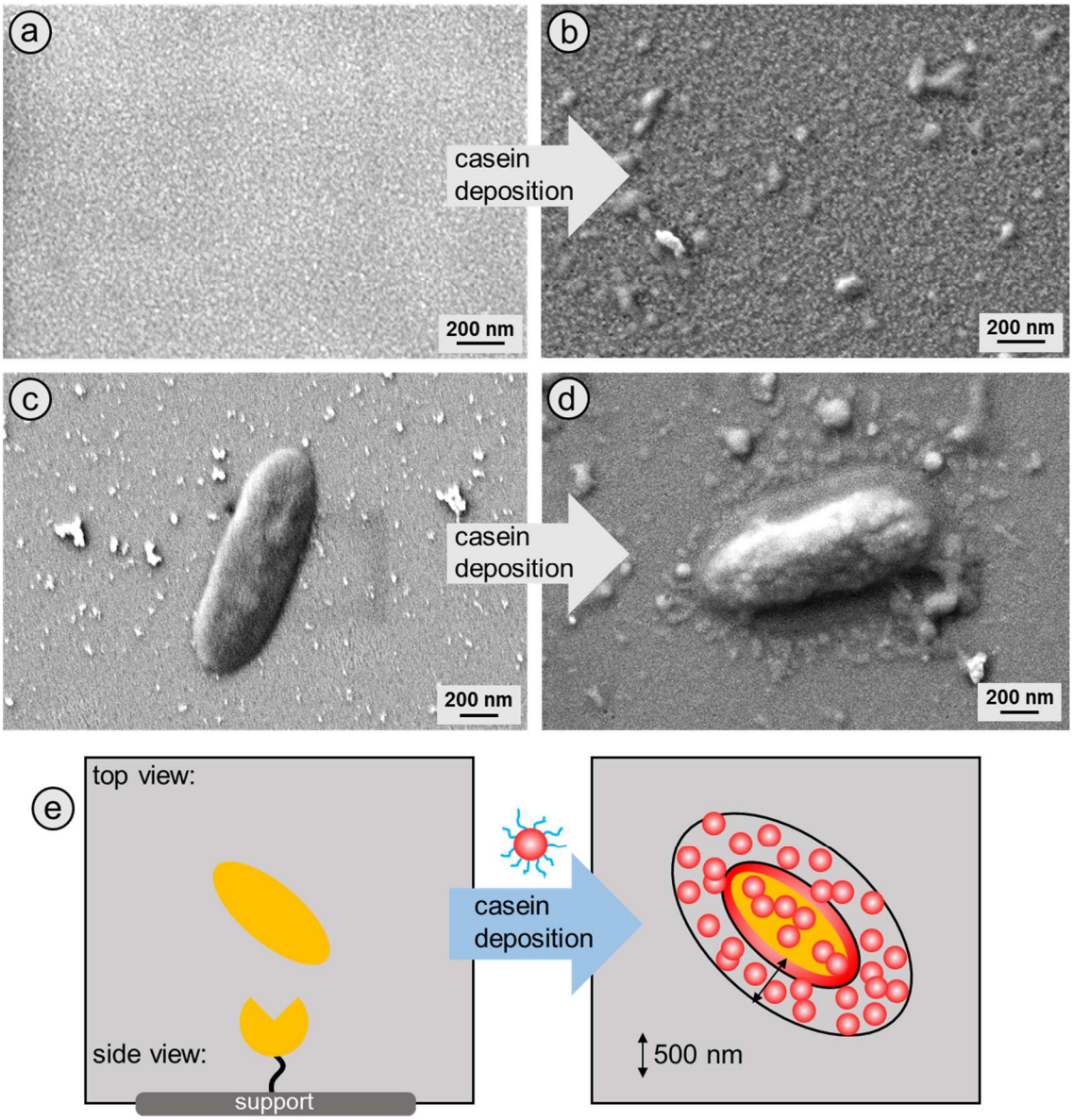


*Figure 72. SEM images of immobilized chymosin via small diepoxy-PEG-spacers (10.000 g/mol) and after casein deposition. a) Immobilized molecular chymosin and b) after casein deposition. c) Immobilized enzyme aggregates and d) after immersion into casein dispersion. e) Illustration pictures, explaining the results obtained with chymosin aggregates. Conditions for casein deposition: $c_C$ = 10 g/L, $t_D$ = 120 min, pH 3, and 40 °C.*

Chymosin was again immobilized at high and low ionic strength, to gain different degrees of enzyme aggregation. The obtained findings are shown in **Figure 72**. Using small PEG-spacer molecules, only a very small degree of casein deposition could be achieved with immobilized molecular chymosin. Single micelles and slightly coalesced protein structures were deposited (**Figure 72b**). The reason for this is probably again based on the protein-repelling properties of PEG, as this was also confirmed for the use of large

spacer molecules. The amount of deposited casein is lower compared to the previous experiments. It seems reasonable that this is caused by the lower flexibility of the immobilized chymosin molecules. This results in a smaller range of the reaction zone and thus, in the lower amount of deposited casein micelles.

The results, which were obtained with large chymosin aggregates, support this. The radius around the aggregates, where deposition of protein is detected, is much smaller compared to the one obtained with large spacer molecules. Here, the radius accounts for about 500 nm and is therefore equal to the one obtained with directly bound enzyme aggregates. Worth of mentioning is a small area in direct proximity to the aggregate (d = 100 nm), where coalescence of deposited micelles could be observed (**Figure 72d**). It can be assumed that in this area the amount of deposited protein was higher according to the remaining area around the aggregate and was higher compared to the deposition level, which was achieved with directly tethered chymosin aggregates (Figure 66). Coalescence of neighboring micelles could therefore take place.

### 4.4.6 Conclusion

The Enzyme Mediated Autodeposition, using covalently immobilized chymosin, enables highly site-specific deposition and film formation of casein. Chymosin was successfully immobilized via GLYMO and APTES/glutaraldehyde under varying conditions, yielding different degrees of enzyme aggregation.

Homogeneous distribution of tethered monomolecular enzyme and small aggregates results in the deposition of continuous casein coatings. The process is self-terminating after deposition of a casein monolayer or at the maximum of a double layer, regardless of deposition time. This high vertical site-specificity ensures that even large area surfaces and objects with complex geometries can specifically be coated via this easy-to-apply process.

The high lateral site-specificity of the EMA is verified by use of large enzyme aggregates. Deposition of casein took only place in distinct radii around the isolated aggregates. This opens up additional features of the EMA with regard to the targeted deposition of single particles on surfaces.

The influence of spacer molecules on the mobility of immobilized enzyme was verified by use of PEG-spacer molecules. Spacers increase the reaction zone by their persistence lengths and expand the deposition patterns. Nonetheless, PEG exhibits interfering protein-repelling properties. Therefore, future investigations will focus on other spacer polymers, such as polyurethanes.

## 4.5 Nanostructures via combination with lithographic methods

### 4.5.1 Overview

The findings of the above presented experiments show and confirm a high site-specificity of the Enzyme Mediated Autodeposition. Cleaved casein particles are deposited exactly there on the support, where immobilized enzyme is present. This leads to the conclusion that the EMA is predestinated for structuring of surfaces with biopolymers, especially on the nanometer scale. This section deals with the evaluation and verification of this approach. Obtained results are currently submitted and under review.

Structuring via EMA requires at first an immobilization of enzyme only in desired areas, which will later be covered by the biopolymer. For this purpose, the EMA is combined with the Nanosphere Lithography (NSL).[305,306] NSL is a cost-effective method for the patterning of surfaces on the nanometer scale. In addition, it is also suitable for the application on large scale areas. Prepatterning via NSL was conducted by KATHARINA BRASSAT, who deserves my gratitude for the prosperous collaboration.

Via NSL, hexagonally close packed monolayers of polymer particles are generated by self-assembly from colloidal suspensions, e.g. by dip coating, spin coating, or doctor blading.[307,308] Use of these convective self-assembly techniques leads to arrangement of the particles in close packed layers on the surface at the three-phase boundary, i.e. between the liquid colloidal suspension, the solid support, and the surrounding gas phase.[309] Motion of this three-phase boundary over the support yields large area monolayers. These particle monolayers act then as a shadow mask for support patterning. Different materials, like metals, oxides, or organic molecules, can be deposited onto the support through the mask openings, which are formed between neighboring spheres. For a triplet of close packed spheres, the mask has a triangular shape. Moreover, the shape of the masks can be generally modified by different treatments, such as thermal or plasma treatments.[310,311] This enables a high level of tailoring with respect to the achievable support patterns.

**Figure 73** illustrates the intended approach for the nanostructuring of surfaces via EMA in combination with NSL. Chymosin is covalently immobilized onto

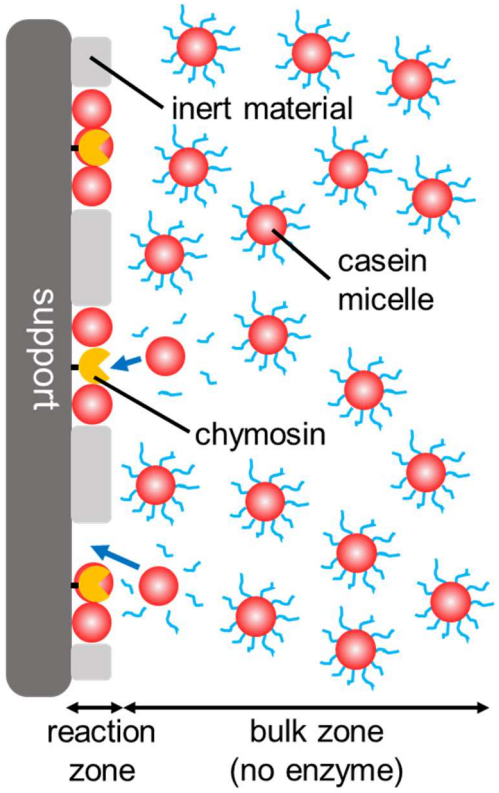


*Figure 73. Nanostructuring via EMA on the example of casein and chymosin.*

particular areas, which are accessible through prepatterning by NSL. The covalent immobilization approach allows for a determination of the reaction zone not only in vertical direction, but also in lateral direction. Cleavage of casein micelles and subsequent deposition of casein is assumed to appear only in the predetermined nanoscaled areas.

### 4.5.2 Support prepatterning via Nanosphere Lithography

$SiO_2$ surfaces are first modified by deposition of large-area monolayers of hexagonally arranged PS spheres. The polymer spheres are then shrunk in an oxygen plasma and a thin platinum film is deposited as inert material. PS sphere removal yields then freely accessible and hexagonally arranged $SiO_2$ dots (**Figure 74**).

Size of the dots and their distance to each other can be tailored by the dimension of the used polymer spheres and by the duration of the applied plasma treatment. The diameter of the resulting $SiO_2$ dots on the support is smaller than the diameter of the shrunk spheres. This is caused by the Pt film deposition. The sputter process is undirected and Pt atoms deposit from

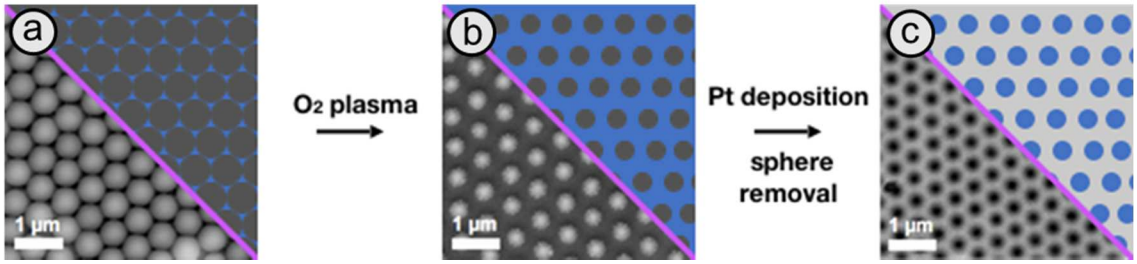


*Figure 74. SEM images and illustration pictures of NSL prepatterning steps. $SiO_2$ areas are visualized in blue, PS spheres in dark gray, and the Pt film in light gray. a) Self-assembled hexagonally close packed PS sphere monolayer, b) shrunk spheres after plasma treatment, and c) inert Pt film with freely accessible hexagonal $SiO_2$ dots.*

different directions onto the surface and thus, also in parts underneath the spheres. AFM topography measurements confirm the presence of a thicker Pt film in between dots and a decreasing film thickness towards the dots centers.

Two systems based on PS spheres with different sizes and different plasma shrinking parameters were investigated. This resulted in the formation of prepatterned supports with enzyme binding areas, exhibiting diameters of 170 nm and 50 nm. **Table 9** displays the respective system parameters.

*Table 9. Overview about parameters of obtained prepatterned Si-supports.*

| Parameters in nm: | System 1: | System 2: |
|---|---|---|
| Ø sphere before plasma: | 618 | 220 |
| Ø sphere after plasma: | 440 | 120 |
| Ø resulting $SiO_2$ dot: | 170 | 50 |
| Pt film thickness: | 13 | 8 |

### 4.5.3 Enzyme immobilization onto prepatterned supports

Only the surface of the dot's inner diameters, exhibiting no Pt deposition, consists of freely accessible $SiO_2$ and can be used as binding sites for chymosin. To this, the $SiO_2$ dots are functionalized with GLYMO.

Successful enzyme binding was verified via XPS and contact angle measurements. A decreasing contact angle from $69.2 \pm 0.6°$ (before) to $43.0 \pm 0.6°$ after the immobilization reaction confirms the presence of

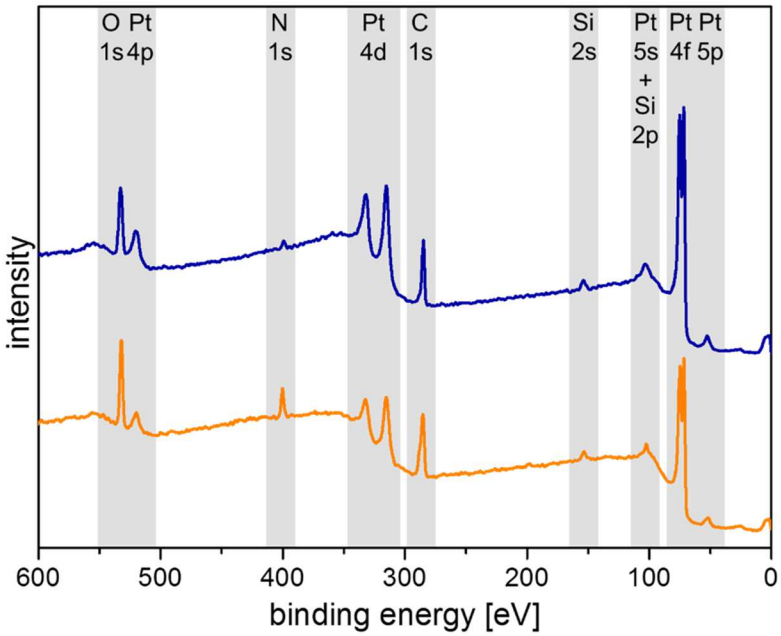


*Figure 75. XPS measurements of prepatterned support (—) and after enzyme immobilization (—).*

enzyme molecules. XPS survey spectra, which were obtained for the prepatterned and the enzyme-functionalized support, show significant changes in the elemental composition (**Figure 75**).

The accessibility of a native silicon oxide layer previously to the silylation step is confirmed by the blue graph. The maximum of the Si2s peak is at 153.8 eV, indicating the presence of silicon species in higher oxidation states, i.e. silicon oxide. Native silicon, on the other hand, has a binding energy of 150.5 eV.[312] After enzyme immobilization, increased amounts of carbon and especially nitrogen are detected.

Furthermore, a detailed view on the C1s peak additionally verifies the successful enzyme attachment (**Figure 76**). Evidently, the C1s peak after enzyme immobilization is a combined peak from different carbon species. Deconvolution of this peak into single three peaks confirms the presence of amine and amide species at 286.3 eV and 288.3 eV, respectively.[313,314] These peaks originate from the enzymatic peptide chains and were not detected for the prepatterned support. The presence of the carbon peak previously to silylation and enzyme coupling is probably based on the adsorption of low molecular hydrocarbons during storage of prepatterned supports and sample preparation for XPS measurements.

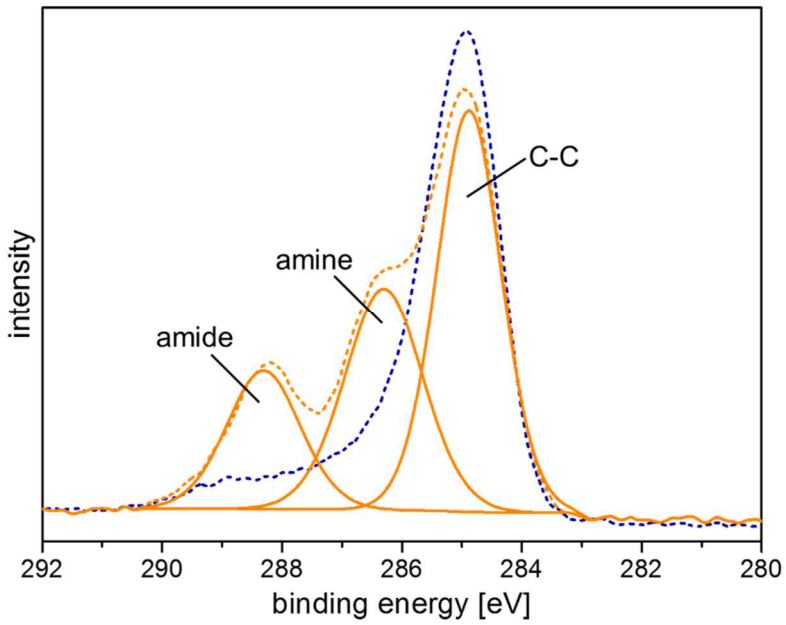


*Figure 76. XPS spectra of carbon C1s peak before (·····) and after (·····) enzyme immobilization for nanostructuring. The peak after functionalization can be deconvolved into multiple single signals (—).*

### 4.5.4 Nanostructuring via Enzyme Mediated Autodeposition

The specific immobilization of chymosin inside the $SiO_2$ dots enables the controlled deposition of single casein micelles in a very sophisticated manner, i.e. on the nanometer scale. **Figure 77** provides a detailed overview about the particular steps. The number of deposited micelles per dot depends on its size, or more precisely on the enzyme-functionalized area. It is assumed that if the diameter of the dots is in the range of single micelles, only one particle is deposited per dot. On the other hand, if the diameter is larger, compared to the size of a single micelle, several particles are deposited onto the enzyme-functionalized area.

In the first system, which has been investigated, the accessible dot diameter for casein deposition accounts for 170 nm. The number mean diameter of dispersed casein micelles at p*H* 3 is 50 nm. **Figure 78** shows 3D AFM height images of the conducted steps.

**Figure 78a** perfectly displays the periodic structure and the smooth shape of the hexagonally arranged dots. Also the decreasing Pt layer thickness, as well as the freely accessible $SiO_2$ areas, are clearly apparent. **Figure 78b** visualizes the state after chymosin immobilization. Small enzyme aggregates can be recognized inside the dots and are not found on the Pt film.

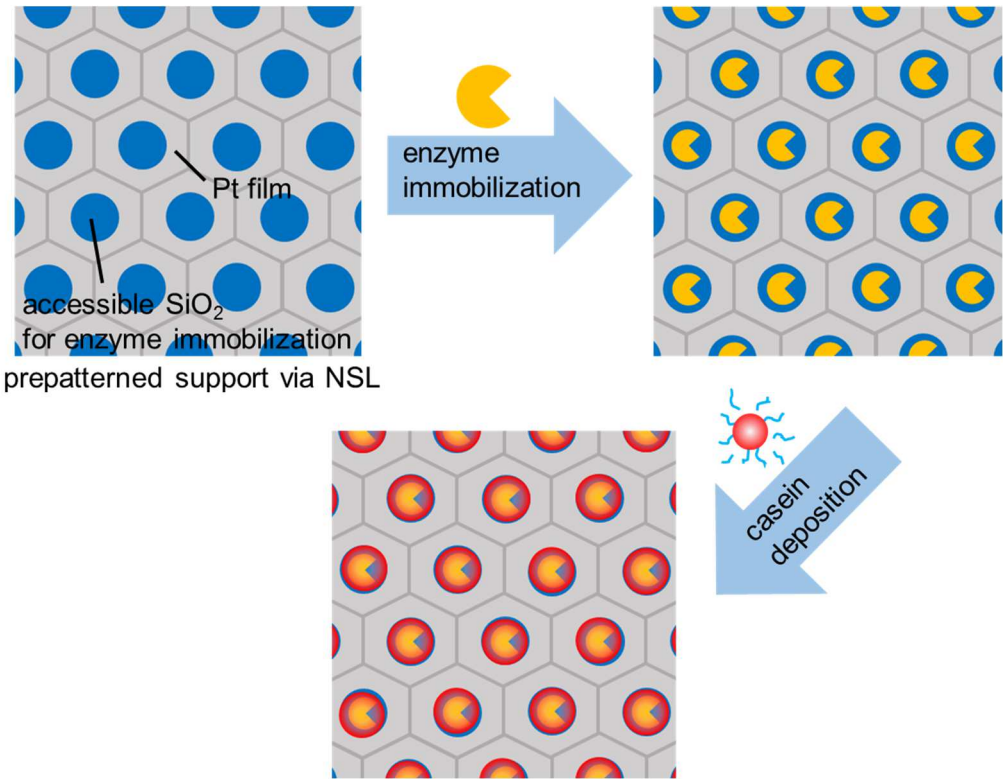


*Figure 77. Site-specific deposition of single casein micelles via EMA.*

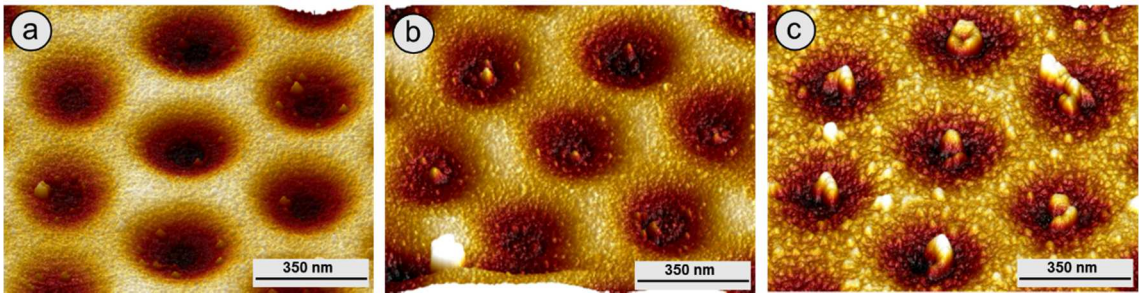


*Figure 78. 3D AFM height images of a) prepatterned support, b) after enzyme immobilization, and c) casein deposition, using 170 nm $SiO_2$ antidots. Casein deposition was achieved at pH 3 and 40 °C for 120 min with a casein concentration of 1 g/L.*

Enzyme mediated deposition of casein is shown in **Figure 78c**. The image verifies the specific addressment of cleaved casein micelles inside the antidot areas. The hexagonal patterning of the dots is still recognizable after the process. Immersion of control samples, which were prepatterned as described above, but which were not functionalized with enzyme, results in no deposition of casein micelles (**Figure A-87**). Immobilization of enzyme is therefore essential for the controlled and site-specific deposition. Adsorption of casein micelles due to electrostatic interactions can be ruled out.

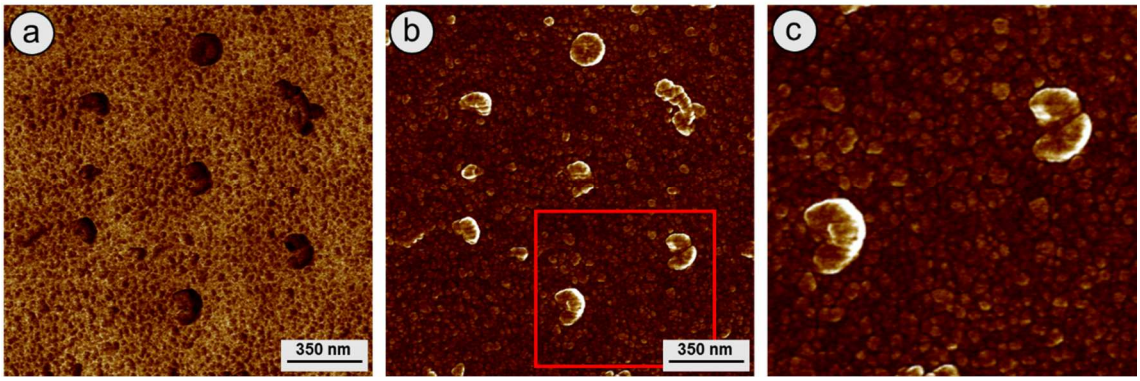


*Figure 79. AFM images of nanostructured supports with 170 nm dots. a) DMT-modulus, b) deformation sensor, and c) magnification of deformation image.*

The high site-specificity of the process is best displayed by AFM imaging of mechanical properties (**Figure 79**). Darker spots, imaging material with lower DMT-moduli compared to the Pt sputter layer, represent cleaved casein (**Figure 79a**). These particles are nearly perfectly arranged in the prepatterned hexagonal structure. Analogously, in deformation mode, brighter spots, outlining softer material compared to the Pt layer, likewise represent casein (**Figure 79b**).

Deposition of particles outside the dots is reduced to a minimal degree and thus, is negligible. Deposited casein particles are cleaved. First, this is confirmed by their resistance towards washing in DI water. Secondly, the DMT-modulus of the protein particles is about 1.0 GPa. This is in good accordance to values previously found for cleaved micelles, i.e. 1.2-1.4 GPa (see 4.3.4). In addition, this value is different from non-cleaved casein, which has a DMT-modulus of about 2.4 GPa and it is different from the modulus of the used PS spheres, which is about 1.6-1.7 GPa. This also excludes the presence of residual PS on the support surface.

As assumed, several micelles are deposited per dot in this experiment, as it can be clearly seen in **Figure 79c**. Single protein particles are well distinguishable. This further verifies the proposed mechanism of the Enzyme Mediated Autodeposition. Destabilized casein micelles cover the active enzyme areas, until all covalently immobilized chymosin is no longer able to reach and to react with additional micelles. As a consequence, this leads to the already mentioned self-termination of the process and thin layers of casein in the range of one or two monolayers result. Height differences in the AFM images confirm this assumption. Casein particles stick out of the dots by about $10 \pm 5$ nm (**Figure 78c**). By addition of the Pt film thickness (13 nm), this yields a protein structure thickness of about 18-28 nm. This value is in good accordance with

the previously determined thickness for a casein monolayer, which is about 15-20 nm in height. However, it must be taken into account that partially overlapping casein micelles were deposited, resulting in higher thicknesses than a monolayer.

The applicability of the investigated process in large scale is shown in **Figure 80**. This AFM height sensor image confirms a homogeneous distribution of cleaved casein micelles in the range of several micrometers on the prepatterned support. The displayed section (10 µm *x* 10 µm) exhibits 298 dots, taking defects into account. 257 dots show deposition of cleaved micelles inside. This yields a coverage density of 86.2 %. Thus, the method is suitable for large area applications, showing a good level of covering.

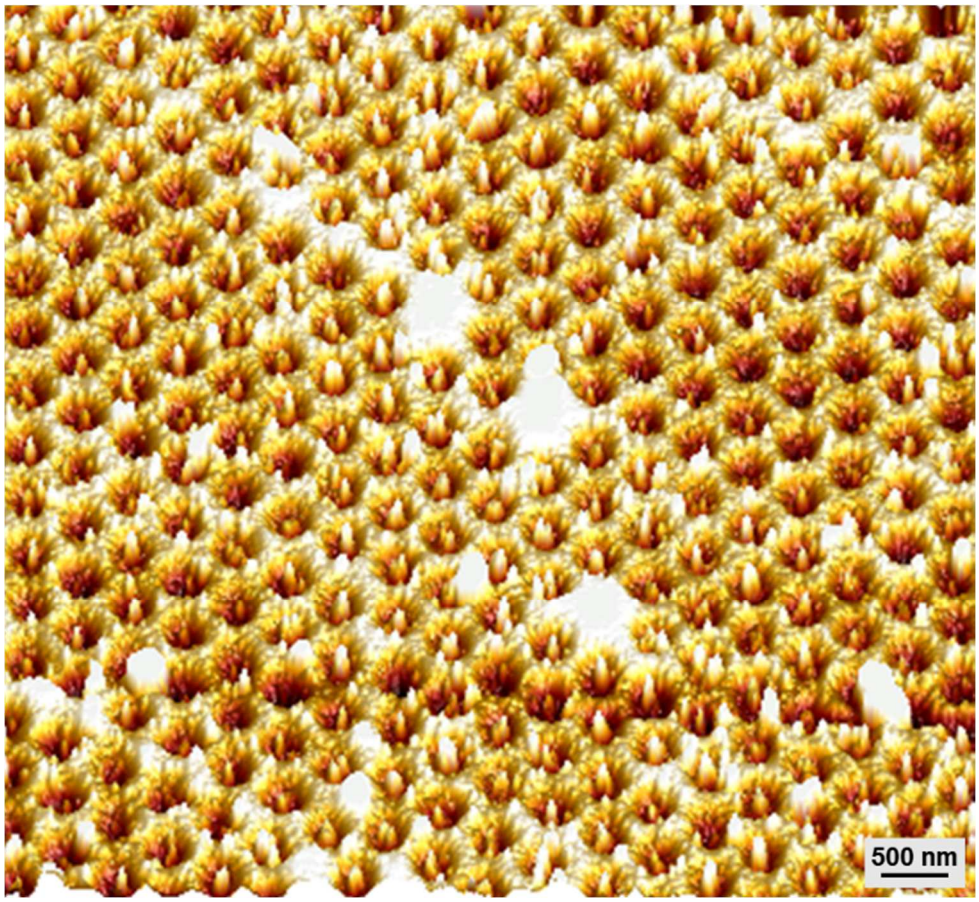


*Figure 80. 3D AFM image of large area structured by EMA. Casein deposition was achieved at pH 3 and 40 °C for 120 min with a casein concentration of 1 g/L.*

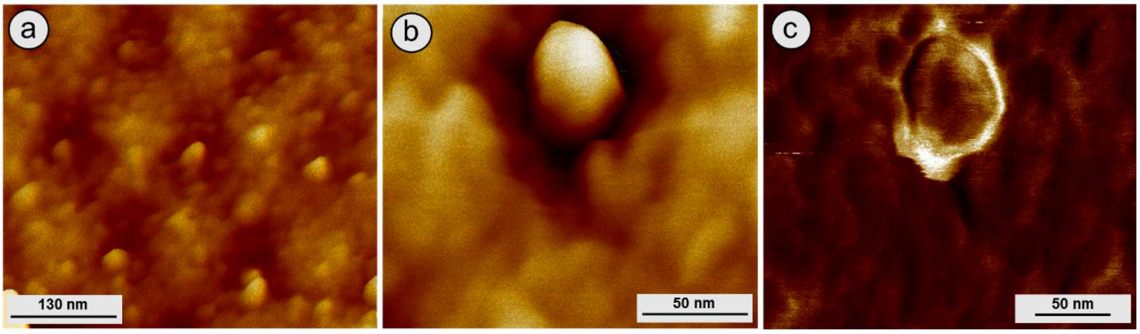


*Figure 81. AFM images of single particle deposition via EMA. a) 3D height image of hexagon, b) 3D height image of single dot, exhibiting one cleaved micelle, and c) respective deformation image. Casein deposition was achieved at pH 3 and 40 °C for 120 min with a casein concentration of 1 g/L.*

Controlled addressing of one single casein particle per dot represents the highest attainable specificity, using casein micelles. This can be achieved by using $SiO_2$ dots with diameters in the range of single micelles (system 2). Such dots with diameters of about 50 nm were obtained by use of small PS spheres (d = 220 nm; Table 9). **Figure 81** shows the obtained findings.

Deposited casein particles exhibit diameters of about 50-65 nm. This time, the active enzyme area per dot is completely covered by a single cleaved micelle. Deposition of additional protein particles is excluded. Micelles stick out of the dots by about 4-5 nm. Addition of the Pt film thickness, which accounts for 8 nm, yields a protein structure thickness of about 12-13 nm. This value corresponds well to a casein monolayer and further confirms the presence of only one single protein particle per dot.

### 4.5.5 Conclusion

The conducted deposition experiments represent the highest achievable precision for the addressment of casein micelles and verify the high specificity of the EMA down to the controlled structuring of surfaces on the nanoscale.

In combination with the Nanosphere Lithography it is easily feasible to structure large-scaled supports. Hexagonal patterns with active areas of 170 nm and 50 nm diameter were specifically coated with casein micelles. By this, multiple and single particle addressing was accomplished.

Prepatterning via NSL is accomplished with reasonable effort and does not require the presence of biomolecules. The final structuring with protein particles is realized by two consecutive simple dip coating process and thus, especially valuable. All biological functions of participating biomolecules are preserved.

# 5 Epilogue

## 5.1 Summary

In this study, the Enzyme Mediated Autodeposition on the example of casein and chymosin has been investigated with respect to applied enzyme immobilization methods, design of tethered enzyme particles, and resulting deposition structures of casein. A broad spectrum of deposition patterns, ranging from the controlled formation of continuous casein coatings to the specific deposition of single protein particles, was accomplished.

First, the system components chymosin and casein were examined and characterized with respect to optimal process conditions. Efficient enzyme immobilization was achieved under neutral conditions, ensuring the presence of molecular chymosin. It was found that optimal deposition conditions for EMA are at p*H* 3 and 40 °C, using casein concentrations up to 10 g/L. This provides the participation of stable particles, highly active enzyme, small casein micelles (d = 50 nm), and the application of protein dispersions with low viscosities.

Enzyme immobilization via physical adsorption was achieved by drying enzyme solutions onto glass supports. Incorporation of the enzyme-functionalized supports into the EMA process yielded homogeneous and continuous casein coatings. Variation of process parameters, such as deposition time, p*H* value, and casein concentration, enabled a high control of the deposition process. This method is the means of choice, if well-defined multilayers of protein, ranging up to several hundred nanometers, are envisaged.

In addition, the physical adsorption approach was further modified to conglutinate opposing enzyme-functionalized supports. This represents a pressureless gluing application with biomolecules and was tested successfully with glass, titanium, and galvanized steel supports.

Cleaved casein coatings showed several advantageous changes in the mechanical and physico-chemical properties, compared to conventional casein coatings. Enzymatically deposited casein exhibited a greatly improved water resistance. In addition, coatings had superior stabilities in organic solvents, such as ethanol and toluene, and were also capable of surviving sterilization processes (heat or UV radiation). Enhanced mechanical properties were verified by comprehensive AFM measurements. Cleaved casein coatings

showed lower DMT-moduli (1.2–1.4 GPa) and higher deformation (1.6 nm), compared to non-cleaved casein (2.4 GPa; 0.9 nm). As the inherent water sensitivity and brittleness of conventional casein coatings are their major drawbacks, the generation of water-stable and flexible coatings should highly extend non-food applications in everyday life.

Highest possible control in EMA is attainable via irreversible enzyme immobilization. This reduces the reaction zone to a minimum, while diffusion of enzyme is excluded. Chymosin was successfully immobilized via GLYMO and APTES/glutaraldehyde, yielding different degrees of enzyme aggregation. Homogeneously distributed monomolecular chymosin and small aggregates induced the deposition of ultrathin casein coatings. Self-termination took place after deposition of a casein monolayer or at the maximum of a double layer. This high vertical site-specificity ensures uniform coating of even large area surfaces and objects with complex geometries.

The high lateral site-specificity of the EMA was verified by incorporation of immobilized large enzyme aggregates. Deposition of single casein particles was only detected in direct surrounding of isolated aggregates within a distinct radius. This confirmed the high potential of the EMA for the nanoscaled deposition of single particles.

The effect of polymeric spacer molecules on the mobility of covalently immobilized enzyme was investigated with PEG-spacers. By this, the reaction zone as well as the amount of deposited casein was successfully increased, as verified by the extended deposition patterns of casein particles.

The unrivaled high site-specificity of the EMA enables the structuring of surfaces with biomolecules down to the nanometer scale. The EMA was therefore combined with a nano-scalable lithography technique, namely the Nanosphere Lithography. By this, hexagonal patterns with active areas of 170 nm and 50 nm were specifically coated with casein micelles. Multiple and single particle addressing was accomplished. This represents the highest achievable precision for the deposition of casein micelles and proves the capability of EMA for nanostructuring.

The Enzyme Mediated Autodeposition represents a next generation technique for the formation of well-defined biobased coatings and structures. The overall process is bioinspired, biocompatible, and transferable to all other systems, where an enzyme-catalyzed reaction changes the solubility of film-forming particles. Enzyme immobilization reactions as well as the final deposition

reactions are performed as easy-to-apply dip coating processes. No harsh conditions, such as use of organic solvents, high temperatures, or exposure to irradiation, are required. This preserves the biofunctionality of all participating substances. Large support surfaces even with complex geometries can be coated and structured in reasonable periods of time, providing tailor-made protein coatings with controllable film thickness or even the specific addressing of single particles on the nanometer scale. Appearance of the deposition structures is controlled by choice of the enzyme immobilization method. This directly determines the mobility and flexibility of the enzyme molecules. Consequently, the dimension of the reaction zone as well as the amount of deposited biomolecules can be adjusted.

## 5.2 Outlook

Some aspects of the Enzyme Mediated Autodeposition need to be further investigated. Incorporation of PEG as spacer molecule into the covalent immobilization of enzyme yielded only partially satisfying results, as the protein-repelling properties of PEG inhibited the optimal conduction of deposition experiments. Other water soluble spacer molecules, such as polyurethanes, which do not interfere with proteins need to be evaluated. In addition, genipin might be examined as an alternative coupling reagent for glutaraldehyde. Since genipin is naturally derived, the sustainable character of the overall process would be even more increased.

Of significant importance might also be the reversible formation of protective coatings. Deposited protein could be removed by a suitable solvent, while the immobilized enzyme remains in a bioactive state on the support. This would enable the repetitive deposition of protective protein layers, e.g. for the easy removal of contaminants in bioreactors.

An assignment of future investigations will also be the transfer of the concept of the EMA to other systems. Suitable are all systems, where an enzyme-catalyzed reaction changes the solubility of dispersed film-forming particles and induces their deposition. These systems might be of natural origin, like the system melanin and tyrosinase, or completely artificial.

With regard to all the beneficial properties and advantages, the Enzyme Mediated Autodeposition is at the moment an unrivaled process and will probably have revolutionary applications in biosensor technology, micro- and nanoelectronics, and especially in life sciences, such as implantology.

# Appendix

```
          10              20              30              40              50
VASVPLTNYL  DSQYFGKIYL  GTPPQEFTVL  FDTGSSDFWV  PSIYCKSNAC

          60              70              80              90             100
KNHQRFDPRK  SSTFQNLGKP  LSIHYGTGSM  QGILGYDTVT  VSNIVDIQQT

         110             120             130             140             150
VGLSTQEPGD  VFTYAEFDGI  LGMAYPSLAS  EYSIPVFDNM  MNRHLVAQDL

         160             170             180             190             200
FSVYMDRNG?  QESMLTLGAI  DPSYYTGSLH  WVPVTVQQYW  QFTVDSVTIS

         210             220             230             240             250
GVVVACEGGC  QAILDTGTSK  LVGPSSDILN  IQQAIGATQN  QYGEFDIDCD

         260             270             280             290             300
NLSYMPTVVF  EINGKMYPLT  PSAYTSQDQG  FCTSGFQSE?  ??????QKWI

         310             320
LGDVFIREYY  SVFDRANNLV  GLA
```

*Figure A-82. Primary structure of bovine chymosin. Data are based on Newman et al.*[141]

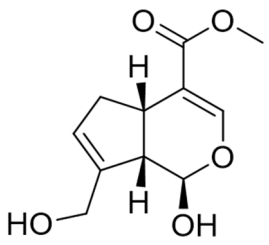


*Figure A-83. Molecular structure of genipin.*

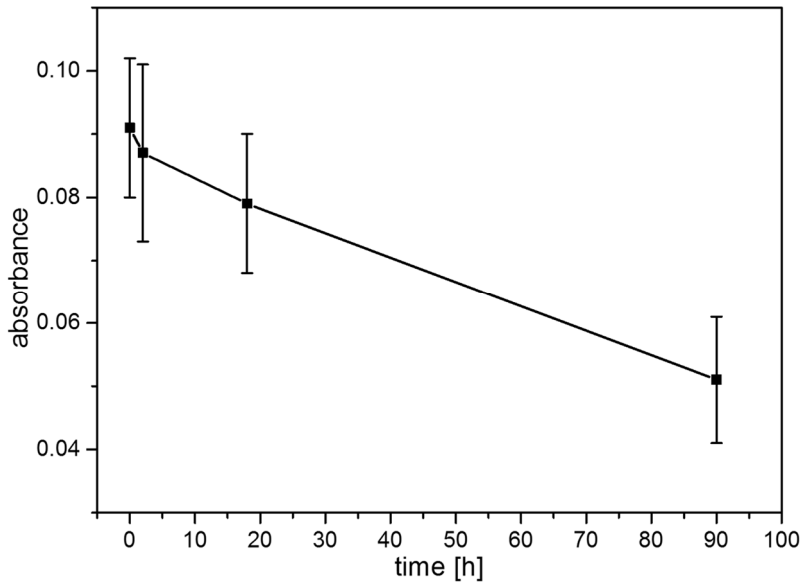


*Figure A-84. Immobilization process of chymosin on GLYMO-functionalized supports. Lines are for visualization only. Data are listed below.*

*Table A-10. Enzymatic activities for enzyme immobilization on GLYMO-functionalized supports.*

| Time in h: | Absorbance: |
|---|---|
| 0 | 0.091 ± 0.011 |
| 2 | 0.087 ± 0.014 |
| 18 | 0.079 ± 0.011 |
| 90 | 0.051 ± 0.010 |

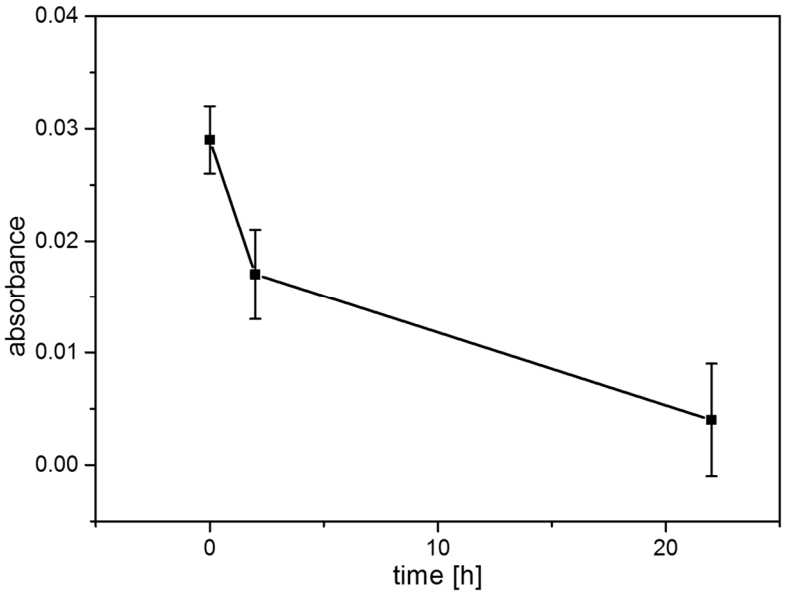


*Figure A-85. Immobilization process of chymosin on APTES/glutaraldehyde-functionalized supports. Lines serve visualization only. Data are listed below.*

*Table A-11. Enzymatic activities for enzyme immobilization on APTES/glutaraldehyde-functionalized supports.*

| Time in h: | Absorbance: |
|---|---|
| 0 | 0.029 ± 0.003 |
| 2 | 0.017 ± 0.004 |
| 22 | 0.004 ± 0.005 |

*Table A-12. Determination of pH dependence of chymosin activity.*

| p*H*: | Absorbance: |
|---|---|
| 1.2 | 0.084 ± 0.019 |
| 2.0 | 0.101 ± 0.005 |
| 3.0 | 0.151 ± 0.006 |
| 3.5 | 0.097 ± 0.009 |
| 4.0 | 0.049 ± 0.005 |
| 5.0 | 0.035 ± 0.002 |
| 6.0 | 0.029 ± 0.008 |

| | |
|---|---|
| 7.0 | 0.025 ± 0.010 |
| 8.0 | 0.014 ± 0.003 |
| 9.0 | 0.011 ± 0.008 |
| 10.0 | 0.008 ± 0.006 |
| 11.0 | 0.011 ± 0.008 |
| 12.0 | 0.002 ± 0.002 |

*Table A-13. Determination of temperature dependence of chymosin activity.*

| Temperature: | Absorbance: |
|---|---|
| 20 | 0.055 ± 0.004 |
| 30 | 0.101 ± 0.025 |
| 40 | 0.151 ± 0.006 |
| 50 | 0.153 ± 0.003 |
| 60 | 0.161 ± 0.008 |
| 70 | 0.076 ± 0.003 |

*Table A-14. Number size distributions of chymosin and rennet solutions.*

| Size (d) in nm: | Relative % (chymosin, neutral cond.) | Size (d) in nm: | Relative % (chymosin, p*H* 3) |
|---|---|---|---|
| 4.46 | 0 | 4.46 | 0 |
| 4.67 | 0 | 4.67 | 0 |
| 4.89 | 3.6 | 4.89 | 1.2 |
| 5.12 | 12.7 | 5.12 | 7.7 |
| 5.36 | 20.6 | 5.36 | 18.9 |
| 5.61 | 21.9 | 5.61 | 25.4 |
| 5.88 | 18.2 | 5.88 | 22.7 |

| | | | |
|---|---|---|---|
| 6.16 | 12.4 | 6.16 | 14.9 |
| 6.45 | 6.8 | 6.45 | 6.9 |
| 6.75 | 2.8 | 6.75 | 1.9 |
| 7.07 | 0.7 | 7.07 | 0.2 |
| 7.41 | 0.1 | 7.41 | 0 |
| 7.76 | 0 | 7.76 | 0 |
| 8.12 | 0 | 8.12 | 0 |
| Size (d) in nm: | Relative % (rennet, neutral cond.) | Size (d) in nm: | Relative % (rennet, p*H* 3) |
| 4.06 | 0 | 3.09 | 0 |
| 4.25 | 0 | 3.43 | 0 |
| 4.46 | 5.9 | 3.80 | 3 |
| 4.67 | 21.0 | 4.21 | 10.9 |
| 4.89 | 31.4 | 4.66 | 18.2 |
| 5.12 | 26.2 | 5.16 | 19.8 |
| 5.36 | 12.6 | 5.72 | 16.9 |
| 5.61 | 2.8 | 6.33 | 12.4 |
| 5.88 | 0 | 7.01 | 8.2 |
| 6.16 | 0 | 7.77 | 4.9 |
| 6.45 | 0 | 8.61 | 2.8 |
| 6.75 | 0 | 9.53 | 1.5 |
| 7.07 | 0 | 10.56 | 0.7 |
| 7.41 | 0 | 11.70 | 0.4 |
| 7.76 | 0 | 12.96 | 0.2 |
| 8.12 | 0 | 14.35 | 0.1 |
| 8.51 | 0 | 15.90 | 0 |
| 8.91 | 0 | 17.61 | 0 |

*Table A-15. Zeta potential of chymosin molecules in dependence on pH.*

| p*H*: | Zeta potential in mV: |
|---|---|
| 1.2 | 12.0 ± 2.5 |
| 1.5 | 13.9 ± 0.2 |
| 2.0 | 24.6 ± 0.3 |
| 2.5 | 25.0 ± 0.6 |
| 3.0 | 21.6 ± 0.9 |
| 3.5 | 17.9 ± 0.9 |
| 3.8 | 13.8 ± 0.6 |
| 3.9 | 13.3 ± 0.7 |
| 5.3 | -11.4 ± 1.0 |
| 6.6 | -26.9 ± 0.7 |
| 7.3 | -33.0 ± 1.9 |
| 7.8 | -34.5 ± 0.9 |
| 8.0 | -35.1 ± 0.4 |
| 9.0 | -33.7 ± 2.8 |
| 9.6 | -33.9 ± 2.2 |
| 10.1 | -32.6 ± 2.3 |
| 10.4 | -31.6 ± 0.9 |
| 11.3 | -25.4 ± 1.1 |
| 11.8 | -18.3 ± 1.0 |

*Table A-16. Determination of zeta potential and size of casein micelles in dependence on pH.*

| p*H*: | Zeta potential in mV: | Size (d) in nm: |
|---|---|---|
| 1.7 | 14.6 ± 1.1 | 35.0 ± 17.4 |
| 2.2 | 20.6 ± 1.6 | 34.3 ± 4.1 |
| 2.0 | 18.8 ± 0.4 | 35.6 ± 2.0 |
| 2.7 | 30.6 ± 0.9 | 47.0 ± 11.8 |
| 3.0 | 32.7 ± 1.8 | 48.7 ± 3.1 |
| 3.2 | 32.9 ± 1.4 | 55.1 ± 22.0 |
| 3.5 | 35.1 ± 0.7 | 49.2 ± 1.7 |
| 3.9 | 28.5 ± 1.0 | 60.2 ± 8.2 |
| 4.4 | 13.4 ± 6.2 | 385.6 ± 54.7 |
| 5.2 | -8.2 ± 0.9 | / |
| 5.7 | -21.0 ± 8.2 | 315.7 ± 39.7 |
| 6.0 | -21.3 ± 2.9 | 97.8 ± 19.2 |
| 6.2 | -20.8 ± 1.0 | 125.7 ± 14.8 |
| 6.7 | -20.3 ± 2.2 | 101.9 ± 13.1 |
| 7.4 | -22.5 ± 0.8 | 113.9 ± 35.1 |
| 8.1 | -19.5 ± 1.3 | 112.6 ± 6.4 |
| 8.7 | -22.5 ± 0.8 | 151.3 ± 6.6 |
| 9.2 | -22.3 ± 1.4 | 138.4 ± 2.3 |
| 9.7 | -22.2 ± 1.7 | 122.1 ± 6.2 |
| 10.2 | -25.1 ± 1.0 | 138.4 ± 7.0 |
| 10.8 | -26.0 ± 1.5 | 106.0 ± 11.8 |
| 11.2 | -28.3 ± 4.0 | 159.5 ± 19.0 |
| 11.5 | -30.4 ± 1.6 | / |
| 11.8 | -28.6 ± 1.6 | / |

*Table A-17. Number size distributions of casein micelles at pH 3.0 and pH 6.7.*

| Size (d) in nm: | Relative % at p*H* 3.0: | Relative % at p*H* 6.7: |
|---|---|---|
| 34.02 | 0 | 0 |
| 35.63 | 0 | 0 |
| 37.32 | 0.8 | 0 |
| 39.08 | 3.6 | 0 |
| 40.93 | 8.1 | 0 |
| 42.87 | 12.0 | 0 |
| 44.89 | 13.9 | 0 |
| 47.02 | 13.9 | 0 |
| 49.24 | 12.6 | 0 |
| 51.57 | 10.5 | 0 |
| 54.01 | 8.3 | 0 |
| 56.56 | 6.1 | 0 |
| 59.23 | 4.2 | 0 |
| 62.04 | 2.7 | 0 |
| 64.97 | 1.6 | 0 |
| 68.04 | 0.9 | 0 |
| 71.26 | 0.4 | 0.6 |
| 74.63 | 0.1 | 2.4 |
| 78.16 | 0 | 4.9 |
| 81.85 | 0 | 7.1 |
| 85.73 | 0 | 8.5 |
| 89.78 | 0 | 9.2 |
| 94.03 | 0 | 9.1 |
| 98.47 | 0 | 8.6 |
| 103.1 | 0 | 7.9 |

| | | |
|---|---|---|
| 108.0 | 0 | 6.9 |
| 113.1 | 0 | 6.0 |
| 118.5 | 0 | 5.0 |
| 124.1 | 0 | 4.2 |
| 129.9 | 0 | 3.4 |
| 136.1 | 0 | 2.8 |
| 142.5 | 0 | 2.2 |
| 149.2 | 0 | 1.8 |
| 156.3 | 0 | 1.5 |
| 163.7 | 0 | 1.2 |
| 171.4 | 0 | 0.9 |
| 179.5 | 0 | 0.8 |
| 188.0 | 0 | 0.6 |
| 196.9 | 0 | 0.5 |
| 206.2 | 0 | 0.5 |
| 216.0 | 0 | 0.4 |
| 226.2 | 0 | 0.3 |
| 236.9 | 0 | 0.3 |
| 248.1 | 0 | 0.3 |
| 259.8 | 0 | 0.2 |
| 272.1 | 0 | 0.2 |
| 285.0 | 0 | 0.2 |
| 298.5 | 0 | 0.1 |
| 312.6 | 0 | 0.1 |
| 327.4 | 0 | 0.1 |
| 342.9 | 0 | 0.1 |
| 359.1 | 0 | 0.1 |

| | | |
|---|---|---|
| 376.1 | 0 | 0.1 |
| 393.8 | 0 | 0.1 |
| 412.5 | 0 | 0.1 |
| 432.0 | 0 | 0.1 |
| 452.4 | 0 | 0.1 |
| 473.8 | 0 | 0.1 |
| 496.2 | 0 | 0.1 |
| 519.7 | 0 | 0.1 |
| 544.2 | 0 | 0 |
| 570.0 | 0 | 0 |

*Table A-18. Shelf life of casein dispersion at pH 3.*

| Days: | Size (d) in nm: |
|---|---|
| 1 | 49.8 ± 9.1 |
| 2 | 54.6 ± 11.3 |
| 3 | 46.4 ± 14.1 |
| 4 | 52.6 ± 9.2 |
| 5 | 51.2 ± 8.5 |

*Table A-19. Micelle size and viscosity of casein dispersions at pH 3.*

| Casein concentration in g/L: | Size (d) in nm: | Viscosity in mPa·s: |
|---|---|---|
| 1 | 48.7 ± 3.1 | 1.00 |
| 5 | 45.3 ± 2.0 | 1.16 |
| 10 | 49.8 ± 9.1 | 1.25 |
| 20 | 59.6 ± 15.9 | 2.11 |
| 25 | 69.2 ± 11.0 | 2.28 |

| | | |
|---|---|---|
| 30 | 66.7 ± 13.3 | 2.69 |
| 50 | 471.7 ± 12.6 | 12.95 |

*Table A-20. Film thickness of EMA with adsorbed chymosin in dependence on pH value.*

| p*H* value: | Film thickness in nm: |
|---|---|
| 2.0 | 5.2 ± 5.1 |
| 3.0 | 50.3 ± 31.6 |
| 3.5 | 119.4 ± 74.0 |
| 4.0 | 6.2 ± 4.5 |
| 5.0 | 17.0 ± 3.2 |
| 6.0 | 30.4 ± 27.5 |
| 6.7 | 7.3 ± 4.0 |
| 7.0 | 5.9 ± 5.0 |
| 8.0 | 3.7 ± 3.7 |

*Table A-21. Film thickness of EMA with adsorbed chymosin in dependence on casein concentration.*

| Casein concentration in g/L: | Film thickness in nm: |
|---|---|
| 1 | 7.3 ± 2.4 |
| 2 | 13.4 ± 10.8 |
| 5 | 8.3 ± 10.5 |
| 7 | 13.1 ± 11.3 |
| 10 | 14.5 ± 12.9 |
| 12 | 23.6 ± 17.9 |
| 15 | 35.2 ± 14.1 |

| | |
|---|---|
| 17 | 28.7 ± 16.8 |
| 20 | 58.8 ± 32.0 |

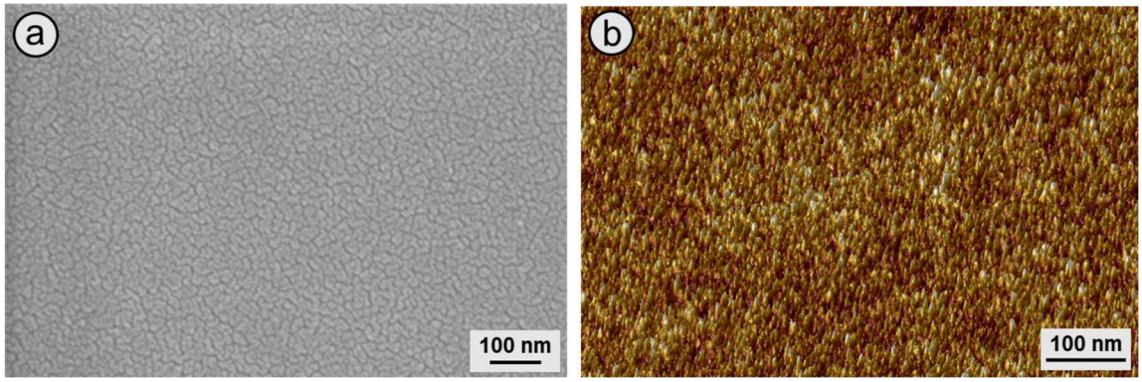


*Figure A-86. a) SEM and b) AFM images of used sputter coating.*

*Table A-22. Number size distributions of chymosin molecules in 25 mM and in 1 M buffer solutions for enzyme immobilization.*

| Size (d) in nm: | Relative % in 25 mM buffer: | Relative % in 1 M buffer: |
|---|---|---|
| 4.25 | 0 | 0 |
| 4.46 | 0 | 0 |
| 4.67 | 0 | 0 |
| 4.89 | 1.6 | 0 |
| 5.12 | 6.4 | 0 |
| 5.36 | 11.9 | 0 |
| 5.61 | 15.0 | 0 |
| 5.88 | 15.5 | 0 |
| 6.16 | 14.1 | 0 |
| 6.45 | 11.6 | 2.3 |
| 6.75 | 8.8 | 8.7 |
| 7.07 | 6.2 | 15.4 |

| | | |
|---|---|---|
| 7.41 | 4.1 | 18.4 |
| 7.76 | 2.5 | 17.7 |
| 8.12 | 1.3 | 14.6 |
| 8.51 | 0.6 | 10.5 |
| 8.91 | 0.2 | 6.7 |
| 9.33 | 0.1 | 3.6 |
| 9.77 | 0 | 1.5 |
| 10.23 | 0 | 0.4 |
| 10.72 | 0 | 0.1 |
| 11.22 | 0 | 0 |
| 11.76 | 0 | 0 |
| 12.31 | 0 | 0 |

*Table A-23. Atom% of particular chymosin immobilization steps via APTES/glutaraldehyde.*

| Atom species: | Atom % (APTES): | Atom % (APTES + glutaraldehyde): | Atom % (APTES + glutaraldehyde + enzyme): |
|---|---|---|---|
| Oxygen: | 40.8 | 22.6 | 18.9 |
| Nitrogen: | 2.8 | 2.9 | 5.6 |
| Carbon: | 27.5 | 63.0 | 69.7 |
| Silicon: | 28.9 | 11.5 | 5.8 |

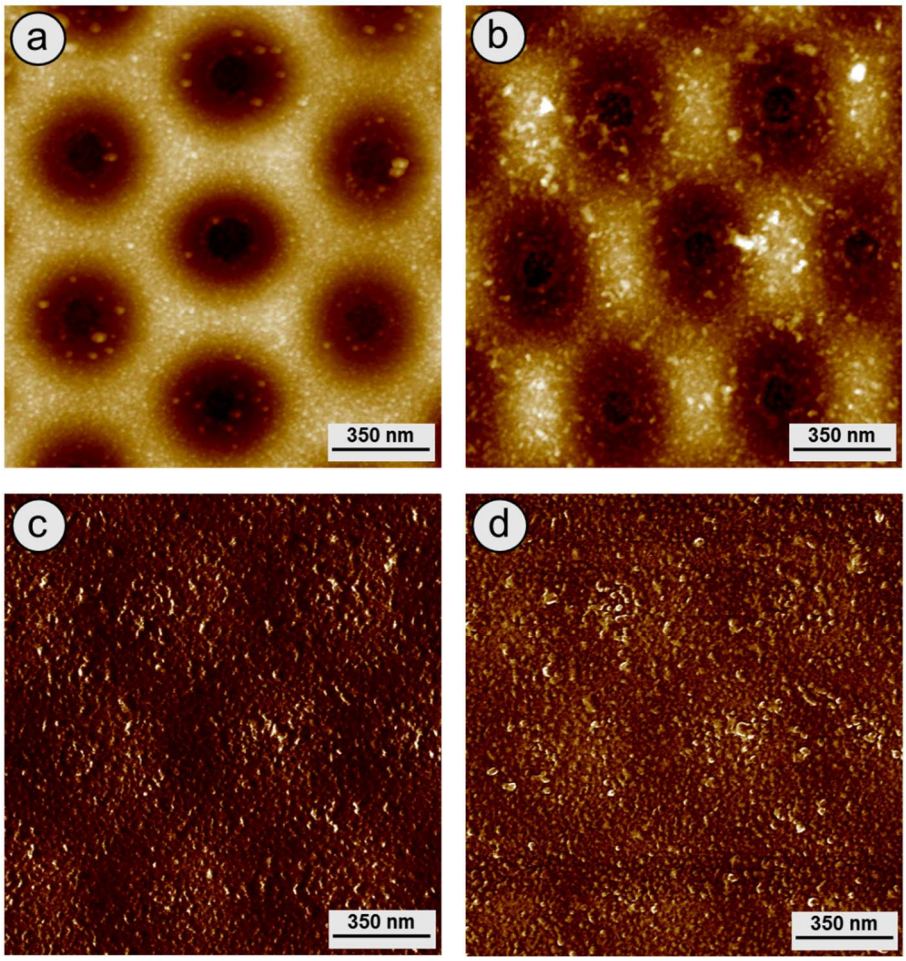


*Figure A-87. AFM images of a) prepatterned support and control samples after immersion into a casein dispersion: b) Height, c) DMT, and d) deformation sensor.*

## References


[1] M. Galià, L. M. de Espinosa, J. C. Ronda, G. Lligadas, V. Cádiz, *Eur. J. Lipid Sci. Technol.* **2010**, *112*, 87–96.

[2] J. T. P. Derksen, F. P. Cuperus, P. Kolster, *Prog. Org. Coat.* **1996**, *27*, 45–53.

[3] G. Schmidmaier, B. Wildemann, A. Stemberger, N. P. Haas, M. Raschke, *J. Biomed. Mater. Res.* **2001**, *58*, 449–455.

[4] S. Caillol, M. Desroches, G. Boutevin, C. Loubat, R. Auvergne, B. Boutevin, *Eur. J. Lipid Sci. Technol.* **2012**, *114*, 1447–1459.

[5] C. Johansson, B. Julien, I. Mondragon, P. Nechita, D. Plackett, P. Simon, D. G. Svetec, S. Virtanen, M. G. Baschetti, C. Breen, et al., *BioResources* **2012**, *7*, 2506–2552.

[6] A. D. Padhye, M. I. Chaudhari, *Paintindia* **2008**, *58*, 73–88.

[7] S. B. Goodman, Z. Yao, M. Keeney, F. Yang, *Biomaterials* **2013**, *34*, 3174–3183.

[8] N. M. L. Hansen, D. Plackett, *Biomacromolecules* **2008**, *9*, 1493–1505.

[9] S. R. MacEwan, A. Chilkoti, *Biopolymers* **2010**, *94*, 60–77.

[10] M. Garcia, M. N. Martino, N. E. Zanitzky, *Staerke* **2000**, *52*, 118–124.

[11] M. Z. Elsabee, E. S. Abdou, *Mater. Sci. Eng. C* **2013**, *33*, 1819–1841.

[12] Y. X. Xu, K. M. Kim, M. A. Hanna, D. Nag, *Ind. Crop. Prod.* **2005**, *21*, 185–192.

[13] A. Sionkowska, *Prog. Polym. Sci.* **2011**, *373*, 1254–1276.

[14] K. Khwaldia, C. Perez, S. Banon, S. Desobry, J. Hardy, *Crit. Rev. Food Sci. Nutr.* **2004**, *44*, 239–251.

[15] V. Morillon, F. Debeaufort, G. Blond, M. Capelle, A. Voilley, *Crit. Rev. Food Sci.* **2002**, *42*, 67–89.

[16] D. Ringe, G. Petsko, *Biophys. Chem.* **2003**, *105*, 667–680.

[17] K. L. Ngai, S. Capaccioli, N. Shinyashiki, *J. Phys. Chem. B* **2008**, *112*, 3826–3832.

[18] I. S. Arvanitoyannis, A. Nakayama, S. Aiba, *Carbohydr. Polym.* **1998**, *37*, 371–382.

[19] R. N. Tharanathan, *Trends Food Sci. Technol.* **2003**, *14*, 71–78.

[20] J. Velema, D. Kaplan, *Adv. Biochem. Eng. Biotechnol.* **2006**, *102*, 187–238.

[21] P. Ferreira, P. Alves, P. Coimbra, M. H. Gil, *J. Coat. Technol. Res.* **2015**, *12*, 463–475.

[22] J. K. Oh, D. I. Lee, J. M. Park, *Prog. Polym. Sci.* **2009**, *34*, 1261–1282.

[23] B. Zhou, Y. Hu, L. Jing, L. Bin, *Int. J. Biol. Macromol.* **2014**, *64*, 402–408.

[24] P. M. Favi, S. Yi, S. C. Lenaghan, L. Xia, M. Zhang, *J. Adhes. Sci. Technol.* **2014**, *28*, 290–319.

[25] M. L. Picchio, M. C. G. Passeggi, M. J. Barandiaran, L. M. Gugliotta, R. J. Minari, *Prog. Org. Coat.* **2015**, *88*, 8–16.

[26] R. Sothornvit, N. Pitak, *Food Res. Int.* **2007**, *40*, 365–370.

[27] L. Vermeiren, L. Heirlings, F. Devlieghere, J. Debevere, in *Nov. Food Packag. Tech.* (Ed.: R. Avhenainen), CRC Press LLC, Cambrige, **2003**, pp. 22–49.

[28] D. H. Bartlett, F. Azam, *Science (80-. ).* **2005**, *310*, 1775–1777.

[29] R. Jayakumar, M. Prabaharan, S. V. Nair, H. Tamura, *Biotechnol. Adv.* **2010**, *28*, 142–150.

[30] A. El-Ghaouth, R. Ponnampalam, F. Castaigne, J. Arul, *Hortscience* **1992**, *27*, 1016–1018.

[31] J. D. Bumgardner, R. Wiser, P. D. Gerard, P. Bergin, B. Chestnutt, M. Marin, V. Ramsey, S. H. Elder, J. a Gilbert, *J. Biomater. Sci. Polym. Ed.* **2003**, *14*, 423–438.

[32] M. C. Chen, C. T. Liu, H. W. Tsai, W. Y. Lai, Y. Chang, H. W. Sung, *Biomaterials* **2009**, *30*, 5560–5571.

[33] M. D. R. Moreira, M. Pereda, N. E. Marcovich, S. I. Roura, *J. Food Sci.* **2011**, *76*, 54–63.

[34] D. Hutchings, S. Clarson, A. Sakr, *Int. J. Pharm.* **1994**, *104*, 203–213.

[35] H. A. Shaaban, K. F. Mahmoud, M. A. Ibrahim, G. Ibrahim, *World Appl. Sci.* **2014**, *32*, 2092–2101.

[36] N. Maftoonazad, H. S. Ramaswamy, *LWT - Food Sci. Technol.* **2005**, *38*, 617–624.

[37] C. J. Tristram, J. M. Mason, D. B. G. Williams, S. F. R. Hinkley, *ChemSusChem* **2015**, *8*, 63–66.

[38] S. M. Notley, M. Norgren, *Langmuir* **2010**, *26*, 5484–5490.

[39] E. L. Hult, J. Ropponen, K. Poppius-Levlin, T. Ohra-Aho, T. Tamminen, *Ind. Crops Prod.* **2013**, *50*, 694–700.

[40] A. Ebringerova, Z. Hromadkova, T. Heinze, *Adv. Polym. Sci.* **2005**, *186*, 1–67.

[41] A. Ebringerova, T. Heinze, *Macromol. Rapid. Commun.* **2000**, *21*, 542–556.

[42] L. Day, M. A. Augustin, I. L. Batey, C. W. Wrigley, *Trends Food Sci. Technol.* **2006**, *17*, 82–90.

[43] P. R. Shewry, N. G. Halford, *J. Exp. Bot.* **2002**, *53*, 947–958.

[44] H.-J. Kersting, M. G. Lindhauer, W. Bergthaller, *Ind. Crops Prod.* **1994**, *3*, 121–128.

[45] H.-J. Kersting, W. Kempf, *Staerke* **1989**, *41*, 420–423.

[46] J. Irissin-Mangata, G. Bauduin, B. Boutevin, *Polym. Bull. (Berlin)* **2000**, *44*, 409–416.

[47] C. Guillaume, I. Schwab, E. Gastaldi, N. Gontard, *Innov. Food Sci. Emerg. Technol.* **2010**, *11*, 690–696.

[48] V. R. Sherman, W. Yang, M. A. Meyers, *J. Mech. Behav. Biomed. Mater.* **2015**, *52*, 22–50.

[49] M. C. Gomez-Guillen, B. Gimenez, M. E. Lopez-Caballero, M. P. Montero, *Food Hydrocoll.* **2011**, *25*, 1813–1827.

[50] L. L. Hood, *Adv. Meat Res.* **1987**, *4*, 109–129.

[51] C. Chaubaroux, E. Vrana, C. Debry, P. Schaaf, B. Senger, J. C. Voegel, Y. Haikel, C. Ringwald, J. Hemmerlé, P. Lavalle, et al., *Biomacromolecules* **2012**, *13*, 2128–2135.

[52] I. S. Arvanitoyannis, in *Protein-Based Film. Coatings* (Ed.: A. Gennadios), CRC Press, Boca Raton, **2002**, pp. 275–304.

[53] V. Chiono, E. Pulieri, G. Vozzi, G. Ciardelli, A. Ahluwalia, P. Giusti, *J. Mater. Sci. Mater. Med.* **2008**, *19*, 889–898.

[54] R. Shukla, M. Cheryan, *Ind. Crops Prod.* **2001**, *13*, 171–192.

[55] Y. C. Wong, T. J. Herald, K. A. Hachmeister, *Poult. Sci.* **1996**, *75*, 417–422.

[56] A. K. Kushwaha, P. S. Kawtikwar, *Int. J. Pharm. Technol.* **2013**, *5*, 2578–2593.

[57] P. F. Fox, in *Adv. Dairy Chem. 1 Proteins* (Eds.: P.F. Fox, P.L.H. McSweeney), Elsevier Academic Press, London, **2003**, pp. 1–18.

[58] J. A. O'Mahony, P. F. Fox, in *Adv. Dairy Chem. 1A Proteins Basic Asp.* (Eds.: P.L.H. McSweeney, P.F. Fox), Springer, New York, **2013**, pp. 43–85.

[59] J. J. Berzelius, *Schweiggers J. Chemie Phys.* **1814**, *1*, 261–280.

[60] J. R. Maynes, J. M. Krochta, *J. Food Sci.* **1994**, *59*, 909–911.

[61] L. Cisneros-Zevallos, J. M. Krochta, *JFS Food Eng. Phys. Prop.* **2003**, *68*, 176–181.

[62] T. C. McHugh, J. M. Krochta, *J. Acric. Food Chem.* **1994**, *42*, 841–845.

[63] C. Le Tien, C. Vachon, M. A. Mateescu, M. Lacroix, *J. Food Sci.* **2001**, *66*, 512–516.

[64] M. Schmid, K. Dallmann, E. Bugnicourt, D. Cordoni, F. Wild, A. Lazzeri, K. Noller, *Int. J. Polym. Sci.* **2012**, 1–7.

[65] A. O. Elzoghby, W. S. A. El-Fotoh, N. A. Elgindy, *J. Control. Release* **2011**, *153*, 206–216.

[66] S. K. Bajpai, M. Bajpai, F. F. Shah, *Des. Monomers Polym.* **2016**, *19*, 406–419.

[67] J. M. Krochta, A. E. Paylath, N. Goodman, in *Eng. Food* (Eds.: W.E.L. Spiess, H. Schubert), Elsevier Applied Science Publ. Co., London, **1990**, pp. 329–340.

[68] L. M. Bonnaillie, H. Zhang, S. Akkurt, K. L. Yam, P. M. Tomasula, *Polymers (Basel).* **2014**, *6*, 2018–2036.

[69] J. Audic, B. Chaufer, G. Daufin, *Lait* **2003**, *83*, 417–438.

[70] C. Holt, *Adv. Protein Chem.* **1992**, *43*, 63–151.

[71] H. M. Farrell, E. L. Malin, E. M. Brown, P. X. Qi, *Curr. Opin. Colloid Interface Sci.* **2006**, *11*, 135–147.

[72] C. Holt, J. A. Carver, H. Ecroyd, D. C. Thorn, *Joural Dairy Sci.* **2013**, *96*, 6127–6146.

[73] E. W. Bingham, H. M. Farrell, *J. Biol. Chem.* **1974**, *93*, 176–182.

[74] H. S. Rollema, C. G. De Kruif, *Prog. Biotechnol.* **2003**, *23*, 220–226.

[75] H. E. Swaisgood, in *Adv. Dairy Chem. 1 Proteins* (Eds.: P.F. Fox, P.L.H. McSweeney), Kluwer Academic/Plenum Publishers, New York, **2003**, pp. 139–187.

[76] W. N. Eigel, J. E. Butler, C. A. Erstrom, H. M. Farrell, V. R. Harwalker, R. Jenness, R. M. Whitney, *J. Dairy Sci.* **1984**, *67*, 1599–1631.

[77] A. F. Stewart, I. M. Willis, A. G. Mackinlay, *Nucleic Acids Res.* **1984**, *12*, 3895–3907.

[78] A. F. Stewart, J. Bonsing, C. W. Beattie, F. Shah, I. M. Willis, A. G. Mackinlay, *Mol. Biol. Evol.* **1987**, *4*, 231–241.

[79] A. Pisano, N. H. Packer, J. W. Redmond, K. L. Williams, A. A. Gooley, *Glycobiology* **1994**, *4*, 837–844.

[80] L.-J. Huang, J.-H. Lin, J.-H. Tsai, Y.-Y. Chu, Y.-W. Chen, S.-L. Chen, S.-H. Chen, *J. Chromatogr. A* **2014**, *1371*, 136–145.

[81] S. C. Burton, N. W. Haggarty, D. R. Harding, *Biotechnol. Bioeng.* **1997**, *56*, 45–55.

[82] M. D. Thompson, J. R. Dave, H. L. Nakhasi, *DNA* **1985**, *4*, 263–271.

[83] H. Zucht, M. Raida, K. Adermann, *FEBS Lett.* **1995**, *372*, 185–188.

[84] P. J. Atkinson, E. Dickinson, D. S. Horne, R. M. Richardson, *J. Chem. Soc. Faraday Trans.* **1995**, *91*, 2847–2854.

[85] K. Dangaran, P. M. Tomasula, P. Qi, in *Edible Film. Coatings Food Appl.* (Eds.: M.E. Embuscado, K.C. Huber), Springer Science + Business Media, New York, **2009**, pp. 25–56.

[86] D. G. Schmidt, *Neth. Milk Dairy J.* **1980**, *34*, 42–64.

[87] P. F. Fox, A. Brodkorb, *Int. Dairy J.* **2008**, *18*, 677–684.

[88] R. Gebhardt, C. Vendrely, U. Kulozik, *J. Phys. Condens. Matter* **2011**, *23*, 444201 (7pp).

[89] P. Walstra, *J. Dairy Sci.* **1990**, *73*, 1965–1979.

[90] J. A. Lucey, *J. Dairy Sci.* **2002**, *85*, 281–294.

[91] D. G. Dalgleish, *J. Dairy Sci.* **1998**, *81*, 3013–3018.

[92] P. Walstra, *Int. Dairy J.* **1999**, *9*, 189–192.

[93] C. G. De Kruif, T. Huppertz, V. S. Urban, A. V. Petukhov, *Adv. Colloid Interface Sci.* **2012**, *171–172*, 36–52.

[94] D. S. Horne, *Int. Dairy J.* **1998**, *8*, 171–177.

[95] D. S. Horne, *Curr. Opin. Colloid Interface Sci.* **2006**, *11*, 148–153.

[96] K. S. Mohammed, P. F. Fox, *Ir. J. Food Sci. Technol.* **1986**, *10*, 47–55.

[97] C. G. De Kruif, **2003**, *23*, 233–238.

[98] M. Mulvihill, M. B. Gufferty, *Int. Dairy Fed. [Spec. Issue] S.I.* **1995**, *9501*, 188–205.

[99] P. Walstra, *J. Dairy Sci.* **1979**, *46*, 317–323.

[100] C. Holt, D. S. Horne, *Neth. Milk Dairy J.* **1996**, *50*, 85–111.

[101] C. Holt, D. G. Dalgleish, *J. Colloid Interface Sci.* **1986**, *114*, 513–524.

[102] P. F. Fox, in *Adv. Dairy Chem. 1 Proteins* (Eds.: P.F. Fox, P.L.H.

McSweeney), Kluwer Academic/Plenum Publishers, New York, **2003**, pp. 1–48.

[103] H. Singh, *Int. Dairy Fed. [Spec. Issue] S.I.* **1995**, *9501*, 86–104.

[104] J. E. O'Connell, P. F. Fox, in *Adv. Dairy Chem. 1 Proteins* (Eds.: P.F. Fox, P.L.H. McSweeney), Kluwer Academic/Plenum Publishers, New York, **2003**, pp. 879–945.

[105] P. F. Fox, P. L. H. McSweeney, in *Cheese Chem. Phys. Microbiol.* (Eds.: P.F. Fox, P.L.H. McSweeney, T.M. Cogan, T.P. Guinee), Elsevier Academic Press, London, **2004**, pp. 1–18.

[106] S. Hildenbrand, *An. Asoc. Quim. Argent.* **1935**, *25*, 7B.

[107] J. A. Lucey, H. Singh, in *Adv. Dairy Chem. 1 Proteins* (Eds.: P.F. Fox, P.L.H. McSweeney), Kluwer Academic/Plenum Publishers, New York, **2003**, pp. 1001–1025.

[108] D. F. Waugh, *Disc. Faraday Soc.* **1958**, *25*, 186–196.

[109] D. B. Hyslop, in *Adv. Dairy Chem. 1 Proteins* (Eds.: P.F. Fox, P.L.H. McSweeney), Kluwer Academic/Plenum Publishers, New York, **2003**, pp. 839–878.

[110] K. W. Ruettimann, M. R. Ladisch, *Enzyme Microb. Technol.* **1987**, *9*, 578–589.

[111] D. S. Horne, in *Adv. Dairy Chem. 1 Proteins* (Eds.: P.F. Fox, P.L.H. McSweeney), Kluwer Academic/Plenum Publishers, New York, **2003**, pp. 975–999.

[112] R. Ye, F. Harte, *J. Dairy Sci.* **2013**, *96*, 799–805.

[113] D. S. Reay, E. A. Davidson, K. A. Smith, P. Smith, J. M. Melillo, F. Dentener, P. J. Crutzen, *Nat. Clim. Chang.* **2012**, *2*, 410–416.

[114] M. L. Picchio, R. J. Minari, V. D. G. Gonzalez, M. C. G. Passeggi, J. R.

Vega, M. J. Barandiaran, L. M. Gugliotta, *Macromol. Symp.* **2014**, *344*, 76–85.

[115] W. A. Hall, *Adhesive*, **1902**, US Patent 695,926.

[116] F. X. Govers, *Casein Glue*, **1905**, US Patent 799,599.

[117] A. Lambuth, in *Coatings Technol. Handb.* (Ed.: A.A. Tracton), CRC Press, Boca Raton, **2006**, p. 64/7-64/11.

[118] J. L. Audic, B. Chaufer, *Eur. Polym. J.* **2005**, *41*, 1934–1942.

[119] P. S. Columbus, R. T. Mason, *Labeling Adhesive*, **1968**, US Patent 3,376,148.

[120] L. A. De Graaf, P. Kolster, *Macromol. Symp.* **1998**, *127*, 82–90.

[121] B. Levecke, H. Lipkens, *Aqueous Adhesive Compositions, Preparing Adhesive Compositions and Labelling Containers*, **2012**, WO Patent 2012134281 (A2).

[122] A. Ferretti, *Ind. Text.* **1937**, *54*, 446–447.

[123] C. G. De Kruif, *Prog. Biotechnol.* **2003**, *23*, 259–263.

[124] G. H. Brother, *Ind. Eng. Chem.* **1940**, *32*, 31–33.

[125] H. Chen, *J. Dairy Sci.* **1995**, *78*, 2563–2583.

[126] M. Schou, A. Longares, C. Montesinos-Herrero, F. J. Monahan, D. O'Riordan, M. O'Sullivan, *LWT - Food Sci. Technol.* **2005**, *38*, 605–610.

[127] M. Kozempel, P. M. Tomasula, *J. Agric. Food Chem.* **2004**, *52*, 1190–1195.

[128] O. A. Diak, A. Bani-Jaber, B. Amro, *Food Bioprod. Process.* **2007**, *85*, 284–290.

[129] Y. Luo, K. Pan, Q. Zhong, *Int. J. Pharm.* **2015**, *486*, 59–68.

[130] F. Song, L. M. Zhang, C. Yang, L. Yan, *Int. J. Pharm.* **2009**, *373*, 41–47.

[131] L. Qin, H. Dong, Z. Mu, Y. Zhang, G. Dong, *Carbohydr. Polym.* **2015**, *133*, 236–244.

[132] M. Reihmann, H. Ritter, *Enzym. Synth. Polym.* **2006**, *194*, 1–49.

[133] A. M. Klibanov, *Nature* **2001**, *409*, 241–246.

[134] S. Kobayashi, A. Makino, *Chem. Rev.* **2009**, *109*, 5288–353.

[135] R. A. Gross, M. Ganesh, W. Lu, *Trends Biotechnol.* **2010**, *28*, 435–443.

[136] I. K. Varma, A. C. Albertsson, R. Rajkhowa, R. K. Srivastava, *Prog. Polym. Sci.* **2005**, *30*, 949–981.

[137] A. A. Ruediger, P. Hendil-Forssell, C. Hedfors, M. Martinelle, S. Trey, M. Johansson, *J. Renew. Mater.* **2013**, *1*, 124–140.

[138] S. Torron, M. Johansson, *J. Polym. Sci. Part A Polym. Chem.* **2015**, *53*, 2258–2266.

[139] H. Uyama, N. Maruichi, H. Tonami, S. Kobayashi, *Biomacromolecules* **2002**, *3*, 187–193.

[140] M. Rao, A. Tanksale, *Microbiol. Mol. Biol. Rev.* **1998**, *62*, 597–635.

[141] M. Newman, M. Safro, C. Frazao, G. Khan, A. Zdanov, I. J. Tickle, T. L. Blundell, N. Andreeva, *J. Mol. Biol.* **1991**, *221*, 1295–1309.

[142] D. E. Danley, K. F. Geoghegan, *J. Biol. Chem.* **1988**, *263*, 9785–9789.

[143] H. Schwander, P. Zahler, H. Nitschmann, *Helv. Chim. Acta* **1952**, *35*, 553–560.

[144] B. Foltmann, *Acta Chem. Scand.* **1959**, *13*, 1927–1935.

[145] B. Foltmann, *Compt. Rend. Trav. Lab. Carlsb.* **1966**, *35*, 143–231.

[146] M. N. Mezina, G. I. Lavrenova, M. I. Prokof'ev, V. V Starovoitova, V. I.

Ermolaev, V. Y. Chernyh, G. N. Balandina, S. S. Demidovich, *Biochemistry. (Mosc).* **2001**, *66*, 378–383.

[147] M. K. Walsh, L. Xiaoshan, *J. Dairy Res.* **2000**, *67*, 637–640.

[148] C. Merheb-Dini, E. Gomes, M. Boscolo, R. da Silva, *Food Chem.* **2010**, *120*, 87–93.

[149] M. Teuber, *Bull. Int. Dairy Fed.* **1990**, *251*, 3–15.

[150] J. S. Emtage, S. Angal, M. T. Doel, T. J. Harris, B. Jenkins, G. Lilley, P. A. Lowe, *Proc. Natl. Acad. Sci. USA* **1983**, *80*, 3671–3675.

[151] N. S. Dunn-Coleman, P. Bloebaum, R. M. Berka, E. Bodie, N. Robinson, G. Armstrong, M. Ward, M. Przetak, G. L. Carter, R. LaCost, *Biotechnology. (N. Y).* **1991**, *9*, 976–981.

[152] V. V Starovoitova, T. I. Velichko, L. A. Baratova, I. Y. Filippova, G. I. Lavrenova, *Biochem.* **2006**, *71*, 320–324.

[153] D. Brady, J. Jordaan, *Biotechnol. Lett.* **2009**, *31*, 1639–1650.

[154] U. Hanefeld, L. Gardossi, E. Magner, *Chem. Soc. Rev.* **2009**, *38*, 453–468.

[155] O. Barbosa, R. Torres, C. Ortiz, A. Berenguer-Murcia, R. C. Rodrigues, R. Fernandez-Lafuente, *Biomacromolecules* **2013**, *14*, 2433–2462.

[156] E. Katchalski-Katzir, *Trends Biotechnol.* **1993**, *11*, 471–478.

[157] A. Liese, L. Hilterhaus, *Chem. Soc. Rev.* **2013**, *42*, 6236–6249.

[158] A. J. Straathof, S. Panke, A. Schmid, *Curr. Opin. Biotechnol.* **2002**, *13*, 548–556.

[159] R. C. Rodrigues, C. Ortiz, Á. Berenguer-Murcia, R. Torres, R. Fernández-Lafuente, *Chem. Soc. Rev.* **2013**, *42*, 6290–6307.

[160] I. Mingarro, C. Abad, L. Braco, *Proc. Natl. Acad. Sci. USA* **1995**, *92*,

3308–3312.

[161] R. Fernandez-Lafuente, V. Rodriguez, C. Mateo, G. Penzol, O. Hernandez-Justiz, G. Irazoqui, A. Villarino, K. Ovsejevi, F. Batista, J. M. Guisan, *J. Mol. Catal. B Enzym.* **1999**, *7*, 181–189.

[162] T. Montes, V. Grazú, F. López-Gallego, J. A. Hermoso, J. L. García, I. Manso, B. Galán, R. González, R. Fernández-Lafuente, J. M. Guisán, *Appl. Environ. Microbiol.* **2007**, *73*, 312–319.

[163] K. Hernandez, R. Fernandez-Lafuente, *Enzyme Microb. Technol.* **2011**, *48*, 107–122.

[164] O. L. Tavano, *J. Mol. Catal. B Enzym.* **2013**, *90*, 1–11.

[165] C. Mateo, J. M. Palomo, G. Fernandez-Lorente, J. M. Guisan, R. Fernandez-Lafuente, *Enzyme Microb. Technol.* **2007**, *40*, 1451–1463.

[166] C. Garcia-Galan, Á. Berenguer-Murcia, R. Fernandez-Lafuente, R. C. Rodrigues, *Adv. Synth. Catal.* **2011**, *353*, 2885–2904.

[167] R. Torres, C. Ortiz, B. C. C. Pessela, J. M. Palomo, C. Mateo, J. M. Guisán, R. Fernández-Lafuente, *Enzyme Microb. Technol.* **2006**, *39*, 167–171.

[168] N. R. Mohamad, N. H. C. Marzuki, N. A. Buang, F. Huyop, R. A. Wahab, *Biotechnol. Biotechnol. Equip.* **2015**, *2818*, 1–16.

[169] C. Mateo, O. Abian, R. Fernandez-Lafuente, J. M. Guisan, *Biotechnol. Bioeng.* **2000**, *68*, 98–105.

[170] T. Diaz, U. Stahl, F. Batista-Viera, J. Carlsson, *Biotechnol. Tech.* **1995**, *9*, 533–538.

[171] D. Beale, C. M. Kent, *Biochim. Biophys. Acta, Protein Struct.* **1977**, *494*, 209–221.

[172] K. A. Joshi, J. Tang, R. Haddon, J. Wang, W. Chen, A. Mulchandani,

*Electroanalysis* **2005**, *17*, 54–58.

[173] L. Huang, Z. M. Cheng, *Chem. Eng. J.* **2008**, *144*, 103–109.

[174] L. Chronopoulou, G. Kamel, C. Sparago, F. Bordi, S. Lupi, *Soft Matter* **2011**, *7*, 2653–2662.

[175] J. Guisan, R. Fernandez-Lafuente, V. Rodriguez, A. Bastida, G. Alvaro, in *Stab. Stab. Enzym.* (Eds.: W. Van der Tweel, A. Harder, R. Buitelar), Elsevier, Amsterdam, **1993**, pp. 55–62.

[176] C. Mateo, V. Grazú, B. C. C. Pessela, T. Montes, J. M. Palomo, R. Torres, F. López-Gallego, R. Fernández-Lafuente, J. M. Guisán, *Biochem. Soc. Trans.* **2007**, *35*, 1593–1601.

[177] P. V. Iyer, L. Ananthanarayan, *Process Biochem.* **2008**, *43*, 1019–1032.

[178] C. Mateo, O. Abian, R. Fernandez-Lafuente, J. M. Guisan, *Enzyme Microb. Technol.* **2000**, *26*, 509–515.

[179] L. Lei, Y. Bai, Y. Li, L. Yi, Y. Yang, C. Xia, *J. Magn. Magn. Mater.* **2009**, *321*, 252–258.

[180] C. Mateo, R. Torres, G. Fernández-Lorente, C. Ortiz, M. Fuentes, A. Hidalgo, F. López-Gallego, O. Abian, J. M. Palomo, L. Betancor, et al., *Biomacromolecules* **2003**, *4*, 772–777.

[181] E. Katchalski-Katzir, D. M. Kraemer, *J. Mol. Catal. B Enzym.* **2000**, *10*, 157–176.

[182] C. Mateo, O. Abian, G. Fernández-Lorente, J. Pedroche, R. Fernández-Lafuente, J. M. Guisan, A. Tam, M. Daminati, *Biotechnol. Prog.* **2002**, *18*, 629–634.

[183] J. M. Goddard, D. Erickson, *Anal. Bioanal. Chem.* **2009**, *394*, 469–479.

[184] D. R. Walt, V. I. Agayn, *TrAC Trends Anal. Chem.* **1994**, *13*, 425–430.

[185] I. Migneault, C. Dartiguenave, M. J. Bertrand, K. C. Waldron, *Biotechniques* **2004**, *37*, 790–802.

[186] O. Barbosa, C. Ortiz, Á. Berenguer-Murcia, R. Torres, R. C. Rodrigues, R. Fernandez-Lafuente, *RSC Adv.* **2014**, *4*, 1583–1600.

[187] Y. Wine, N. Cohen-Hadar, A. Freeman, F. Frolow, *Biotechnol. Bioeng.* **2007**, *98*, 711–718.

[188] L. Cao, F. van Rantwijk, R. A. Sheldon, *Org. Lett.* **2000**, *2*, 1361–1364.

[189] R. Schoevaart, M. W. Wolbers, M. Golubovic, M. Ottens, A. P. G. Kieboom, F. van Rantwijk, L. A. M. van der Wielen, R. A. Sheldon, *Biotechnol. Bioeng.* **2004**, *87*, 754–762.

[190] K. Tatsumoto, K. K. Oh, J. O. Baker, M. E. Himmel, *Appl. Biochem. Biotechnol.* **1989**, *20/21*, 293–308.

[191] T. Yamazaki, W. Tsugawa, K. Sode, *Biotechnol. Lett.* **1999**, *21*, 199–202.

[192] L. Betancor, F. López-Gallego, A. Hidalgo, N. Alonso-Morales, G. D.-O. C. Mateo, R. Fernández-Lafuente, J. M. Guisán, *Enzyme Microb. Technol.* **2006**, *39*, 877–882.

[193] J. Lee, J. Kim, J. Kim, H. Jia, M. I. Kim, J. H. Kwak, S. Jin, A. Dohnalkova, H. C. Park, H. N. Chang, et al., *Small* **2005**, *1*, 744–753.

[194] M. Il Kim, J. Kim, J. Lee, S. Shin, H. Bin Na, T. Hyeon, H. G. Park, H. N. Chang, *Microporous Mesoporous Mater.* **2008**, *111*, 18–23.

[195] F. López-Gallego, L. Betancor, C. Mateo, A. Hidalgo, N. Alonso-Morales, G. Dellamora-Ortiz, J. M. Guisán, R. Fernández-Lafuente, *J. Biotechnol.* **2005**, *119*, 70–75.

[196] A. H. Korn, S. H. Feairheller, E. M. Filachione, *J. Mol. Biol.* **1972**, *65*, 525–529.

[197] M. F. Butler, Y. F. Ng, P. D. A. Pudney, *J. Polym. Sci. Part A Polym.*

*Chem.* **2003**, *41*, 3941–3953.

[198] H. W. Sung, D. M. Huang, W. H. Chang, R. N. Huang, J. C. Hsu, *J. Biomed. Mater. Res.* **1999**, *46*, 520–530.

[199] D. P. Speer, M. Chvapil, C. D. Eskelson, J. Ulreich, *J. Biomed. Mater. Res.* **1980**, *14*, 753–764.

[200] W. Fuerst, A. Banerjee, *Ann. Thorac. Surg.* **2005**, *79*, 1522–1528.

[201] R. A. A. Muzzarelli, *Carbohydr. Polym.* **2009**, *77*, 1–9.

[202] S.-H. Chiou, T.-C. Hung, R. Giridhar, W.-T. Wu, *Prep. Biochem. Biotechnol.* **2007**, *37*, 265–275.

[203] I. A. Cavello, J. C. Contreras-Esquivel, S. F. Cavalitto, *Process Biochem.* **2014**, *49*, 1332–1336.

[204] A. M. Rangel-Rodriguez, S. Conxita, V. Susana, S. G. Flores-Gallardo, J. C. Contreras-Esquivel, L. Licea-Jimenez, *Appl. Biochem. Biotechnol.* **2014**, *174*, 2941–2950.

[205] S. Cosnier, *Biosens. Bioelectron.* **1999**, *14*, 443–456.

[206] L. Cao, *Curr. Opin. Chem. Biol.* **2005**, *9*, 217–226.

[207] K. Ichimura, S. Watanabe, *J. Polym. Sci. Polym. Chem. Ed.* **1980**, *18*, 891–902.

[208] M. T. Reetz, A. Zonta, J. Simpelkamp, *Biotechnol. Bioeng.* **1996**, *49*, 527–534.

[209] A. C. Pierre, *Biocatal. Biotransform.* **2004**, *22*, 145–170.

[210] L. Wilson, A. Illanes, B. C. C. Pessela, O. Abian, R. Fernández-Lafuente, J. M. Guisán, *Biotechnol. Bioeng.* **2004**, *86*, 558–562.

[211] J. Lalonde, A. Margolin, in *Enzym. Catal. Org. Chem.* (Eds.: K. Drauz, H. Waldmann), Wiley-VCH, Weinheim, **2002**, pp. 163–184.

[212] M. Köhler, W. Fritzsche, *Nanotechnology: An Introduction to Nanostructuring Techniques*, Wiley-VCH, Weinheim, **2007**.

[213] L.-J. Qi, W.-Q. Li, X.-J. Yang, Y.-C. Fang, M. Lu, *Chin. Phys. Lett.* **2005**, *22*, 431–434.

[214] K. Choy, *Prog. Mater. Sci.* **2003**, *48*, 57–170.

[215] S. W. Chang, R. Ayothi, D. Bratton, D. Yang, N. Felix, H. B. Cao, H. Deng, C. K. Ober, *J. Mater. Chem.* **2006**, *16*, 1470–1474.

[216] R. Yang, L. Zhang, Y. Wang, Z. Shi, D. Shi, H. Gao, E. Wang, G. Zhang, *Adv. Mater.* **2010**, *22*, 4014–4019.

[217] X. N. Xie, H. J. Chung, C. H. Sow, A. T. S. Wee, *Mater. Sci. Eng., R* **2006**, *54*, 1–48.

[218] P. W. K. Rothemund, *Nature* **2006**, *440*, 297–302.

[219] N. Mojarad, J. Gobrecht, Y. Ekinci, *Sci. Rep.* **2015**, *5*, 9235.

[220] M. Burkhardt, H. I. Smith, D. A. Antoniadis, T. P. Orlando, M. R. Melloch, K. W. Rhee, M. C. Peckerar, *J. Vac. Sci. Technol. B* **1994**, *12*, 3611–3613.

[221] A. F. G. Leontowich, A. P. Hitchcock, B. Watts, J. Raabe, *Microelectron. Eng.* **2013**, *108*, 5–7.

[222] A. N. Broers, *J. Electrochem. Soc.* **1981**, *128*, 166–170.

[223] S. Matsui, K. Mori, K. Saigo, T. Shiokawa, K. Toyoda, S. Namba, *J. Vac. Sci. Technol. B* **1986**, *4*, 845–849.

[224] K. Arshak, M. Mihov, *Adv. Mater.* **2005**, *7*, 193–197.

[225] T. Junno, S.-B. Carlsson, H. Xu, L. Montelius, L. Samuelson, *Appl. Phys. Lett.* **1998**, *72*, 548–550.

[226] B. Klehn, U. Kunze, *J. Appl. Phys.* **1999**, *85*, 3897–3903.

[227] G. Meyer, K.-H. Rieder, *Surf. Sci.* **1997**, *377–379*, 1087–1093.

[228] L. Bartels, G. Meyer, K.-H. Rieder, *Appl. Phys. Lett.* **1997**, *71*, 213–215.

[229] A. A. Tseng, L. Z., *Nanosci. Nanotechnol.* **2007**, *7*, 2582–2592.

[230] J. S. Logan, M. J. Hait, H. C. Jones, G. R. Firth, D. B. Thompson, *J. Vac. Sci. Technol. B* **1989**, *7*, 1392–1396.

[231] S. Maniv, C. Miner, W. D. Westwood, *J. Vac. Sci. Technol. B* **1981**, *18*, 195–198.

[232] M. Ritala, M. Leskelä, *Nanotechnology* **1999**, *10*, 19–24.

[233] C. Lin, Y. Liu, S. Rinker, H. Yan, *Chemphyschem* **2006**, *7*, 1641–1647.

[234] S. Douglas, H. Dietz, T. Liedl, B. Högberg, *Nature* **2009**, *459*, 414–418.

[235] I. Bald, A. Keller, *Molecules* **2014**, *19*, 13803–13823.

[236] E. S. Andersen, M. Dong, M. M. Nielsen, K. Jahn, R. Subramani, W. Mamdouh, M. M. Golas, B. Sander, H. Stark, C. L. P. Oliveira, et al., *Nature* **2009**, *459*, 73–76.

[237] R. M. Zadegan, M. D. E. Jepsen, K. E. Thomsen, A. H. Okholm, D. H. Schaffert, E. S. Andersen, V. Birkedal, J. Kjems, *ACS Nano* **2012**, *6*, 10050–10053.

[238] A. Gopinath, P. W. K. Rothemund, *ACS Nano* **2014**, *8*, 12030–12040.

[239] J. F. Graveland-Bikker, I. A. T. Schaap, C. F. Schmidt, C. G. De Kruif, *Nano Lett.* **2006**, *6*, 616–621.

[240] H. Morgan, D. J. Pritchard, J. M. Cooper, *Biosens. Bioelectron.* **1995**, *10*, 841–846.

[241] D. Fotiadis, S. Scheuring, S. A. Müller, A. Engel, D. J. Müller, *Micron* **2002**, *33*, 385–397.

[242] K. B. Lee, J. H. Lim, C. A. Mirkin, *J. Am. Chem. Soc.* **2003**, *125*, 5588–5589.

[243] S.-H. Lim, M. Yamaguchi, O. Nishimura, Y. Mie, T. Tamura, B.-W. Kim, M. Suzuki, *J. Nanosci. Nanotechnol.* **2009**, *9*, 7318–7323.

[244] S. K. Kufer, E. M. Puchner, H. Gumpp, T. Liedl, H. E. Gaub, *Science (80-. ).* **2008**, *319*, 594–596.

[245] F. Jiang, K. Khairy, K. Poole, J. Howard, D. J. Müller, *Microsc. Res. Tech.* **2004**, *64*, 435–440.

[246] S. Takeda, C. Nakamura, C. Miyamoto, N. Nakamura, M. Kageshima, H. Tokumoto, J. Miyake, *Nano Lett.* **2003**, *3*, 1471–1474.

[247] N. J. Berridge, in *Adv. Enzymol. Relat. Areas Mol. Biol.* (Ed.: F.F. Nord), John Wiley & Sons, Hoboken, **1954**, pp. 423–448.

[248] T. Brock, *Chemik* **2015**, *69*, 386–388.

[249] T. C. Jones, *Met. Finish.* **2010**, *108*, 176–179.

[250] O. I. Strube, A. Buengeler, W. Bremser, *Biomacromolecules* **2015**, *16*, 1608–1613.

[251] O. I. Strube, A. Buengeler, W. Bremser, *Macromol. Mater. Eng.* **2016**, *301*, 801–804.

[252] A. A. Ruediger, Master Thesis: Enzyme-Catalyzed Deposition of Casein Biocoatings, University of Paderborn, Department of Chemistry, **2013**.

[253] A. Buengeler, Bachelor Thesis: Enzyme Mediated Deposition of Eumelanin Nanoparticles via Site-Specific In-Situ Syntheses, University of Paderborn, Department of Chemistry, **2014**.

[254] L. Henke, N. Nagy, U. J. Krull, *Biosens. Bioelectron.* **2002**, *17*, 547–555.

[255] D. M. Mulvihill, P. F. Fox, *J. Dairy Sci.* **1977**, *44*, 533–540.

[256] K. Shindo, S. Arima, *Agr. Biol. Chem.* **1979**, *28*, A177–A180.

[257] C. G. De Kruif, *Langmuir* **1992**, *8*, 2932–2937.

[258] A. Bouchoux, B. Debbou, G. Gésan-Guiziou, M.-H. Famelart, J.-L. Doublier, B. Cabane, *J. Chem. Phys.* **2009**, *131*, 165106.

[259] O. I. Strube, A. A. Ruediger, W. Bremser, *J. Biotechnol.* **2015**, *201*, 69–74.

[260] A. A. Ruediger, E. Terborg, W. Bremser, O. I. Strube, *Prog. Org. Coat.* **2016**, *94*, 56–61.

[261] O. I. Strube, A. A. Ruediger, W. Bremser, *Int. J. Adhes. Adhes.* **2015**, *63*, 9–13.

[262] L. Bonnaillie, P. Tomasula, *Polymers (Basel).* **2015**, *7*, 91–114.

[263] T. H. McHugh, J. M. Krochta, *Food Technol. (Chicago, IL, U. S.)* **1994**, *48*, 97–103.

[264] J. H. Park, R. Olivares-Navarrete, R. E. Baier, A. E. Meyer, R. Tannenbaum, B. D. Boyan, Z. Schwartz, *Acta Biomater.* **2012**, *8*, 1966–1975.

[265] J. Rnjak-Kovacina, T. M. Desrochers, K. A. Burke, D. L. Kaplan, *Macromol. Biosci.* **2015**, *15*, 861–874.

[266] R. S. Benson, *Nucl. Instruments Methods Phys. Res. Sect. B Beam Interact. with Mater. Atoms* **2002**, *191*, 752–757.

[267] K. Pan, Q. Zhong, *Soft Matter* **2015**, *11*, 5898–5904.

[268] R. Dicharry, P. Ye, G. Saha, R. Parnas, A. D. Asandei, *Polym. Prepr. (Am. Chem. Soc., Div. Polym. Chem.)* **2006**, *47*, 87–88.

[269] P. Guerrero, A. Retegi, N. Gabilondo, K. De La Caba, *J. Food Eng.* **2010**, *100*, 145–151.

[270] P. J. Elms, J. D. Chodera, C. Bustamante, S. Marqusee, *Proc. Natl. Acad. Sci.* **2012**, *109*, 3796–3801.

[271] Y. Piquilloud, A. Reinharz, M. Roth, *Biochim. Biophys. Acta - Enzymol.* **1970**, *206*, 136–142.

[272] B. Keil, *Specificity of Proteolysis*, Springer, Berlin, **1992**.

[273] B. J. Kirby, E. F. Hasselbrink, *Electrophoresis* **2004**, *25*, 187–202.

[274] Y. Gu, D. Li, *J. Colloid Interface Sci.* **2000**, *226*, 328–339.

[275] K. J. Laidler, J. H. Meiser, *Physical Chemistry*, Benjamin/Cummings Pub. Co., Menlo Park, **1982**.

[276] D. G. Dalgleish, *J. Dairy Res.* **1979**, *46*, 653–661.

[277] A. C. M. Van Hooydonk, C. Olieman, H. G. Hagedoorn, *Neth. Milk Dairy J.* **1984**, *38*, 207–222.

[278] B. P. Lee, P. B. Messersmith, J. N. Israelachvili, J. H. Waite, *Annu. Rev. Mater. Res.* **2011**, *41*, 99–132.

[279] S. H. Imam, C. Bilbao-Sainz, B.-S. Chiou, G. M. Glenn, W. J. Orts, *J. Adhes. Sci. Technol.* **2013**, *27*, 1972–1997.

[280] C. Fant, H. Elwing, F. Höök, *Biomacromolecules* **2002**, *3*, 732–741.

[281] R. C. Ferguson, S. K. Mendon, J. W. Rawlins, S. F. Thames, *J. Renew. Mater.* **2014**, *3*, 166–172.

[282] Q. Lin, N. Chen, L. Bian, M. Fan, *Int. J. Adhes. Adhes.* **2012**, *34*, 11–16.

[283] S. D'Amico, U. Müller, E. Berghofer, *J. Appl. Polym. Sci.* **2013**, *129*, 2429–2434.

[284] E. S. Lower, *Pigment Resin Technol.* **1983**, *12*, 9–14.

[285] B. Kasemo, *J. Prosthet. Dent.* **1983**, *49*, 832–837.

[286] M. Takemoto, S. Fujibayashi, M. Neo, J. Suzuki, T. Kokubo, T. Nakamura, *Biomaterials* **2005**, *26*, 6014–6023.

[287] J. P. Li, P. Habibovic, M. van den Doel, C. E. Wilson, J. R. de Wijn, C. A. van Blitterswijk, K. de Groot, *Biomaterials* **2007**, *28*, 2810–2820.

[288] A. V. Pocius, *Adhesion and Adhesives Technology: An Introduction*, Carl Hanser Verlag, München, **2012**.

[289] Q. Xu, J. Ma, J. Zhou, Y. Wang, J. Zhang, *Chem. Eng. J.* **2013**, *228*, 281–289.

[290] A. Varzi, R. Raccichini, M. Marinaro, M. Wohlfahrt-Mehrens, S. Passerini, *J. Power Sources* **2016**, 10.1016/j.jpowsour.2016.03.072.

[291] A. A. Ruediger, W. Bremser, O. I. Strube, *Macromol. Mater. Eng.* **2016**, *301*, 1181–1190.

[292] A. A. Ruediger, W. Bremser, O. I. Strube, *J. Coatings Technol. Res.* **2016**, *13*, 597–611.

[293] B. Panjwani, S. K. Sinha, *J. Mech. Behav. Biomed. Mater.* **2012**, *15*, 103–111.

[294] E. T. Vandenberg, L. Bertilsson, B. Liedberg, K. Uvdal, R. Erlandsson, H. Elwing, I. Lundström, *J. Colloid Interface Sci.* **1991**, *147*, 103–118.

[295] D. Janssen, R. De Palma, S. Verlaak, P. Heremans, W. Dehaen, *Thin Solid Films* **2006**, *515*, 1433–1438.

[296] J. A. Howarter, J. P. Youngblood, *Langmuir* **2006**, *22*, 11142–11147.

[297] J. Diao, D. Ren, J. R. Engstrom, K. H. Lee, *Anal. Biochem.* **2005**, *343*, 322–328.

[298] K. Shindo, S. Arima, *J. Fac. Agric. Hokkaido Univ.* **1979**, *59*, 284–293.

[299] J. M. Harris, K. Yoshinaga, *J. Bioact. Compat. Polym.* **1989**, *4*, 281–295.

[300] Y. Wang, Y.-L. Hsieh, *J. Polym. Sci. Part A Polym. Chem.* **2004**, *42*, 4289–4299.

[301] A. Nicholas, M. Scott, N. Kennedy, M. Jones, *Biochim. Biophys. Acta* **2000**, *1463*, 167–178.

[302] N. A. Alcantar, E. S. Aydil, J. N. Israelachvili, *J. Biomed. Mater. Res.* **2000**, *51*, 343–351.

[303] O. Pop-Georgievski, Š. Popelka, M. Houska, D. Chvostová, V. Proks, F. Rypáček, *Biomacromolecules* **2011**, *12*, 3232–3242.

[304] C. Pale-Grosdemange, E. S. Simon, K. L. Prime, G. M. Whitesides, *J. Am. Chem. Soc.* **1991**, *113*, 12–20.

[305] H. W. Deckman, J. H. Dunsmuir, *Appl. Phys. Lett.* **1982**, *41*, 377–379.

[306] J. C. Hulteen, R. P. Van Duyne, *J. Vac. Sci. Technol. A Vacuum, Surfaces, Film.* **1995**, *13*, 1553–1558.

[307] X. Ye, L. Qi, *Sci. China Chem.* **2014**, *57*, 58–69.

[308] P. Born, S. Blum, A. Munoz, T. Kraus, *Langmuir* **2011**, *27*, 8621–8633.

[309] A. S. Dimitrov, K. Nagayama, *Langmuir* **1996**, *12*, 1303–1311.

[310] T. Riedl, M. Strake, W. Sievers, J. K. N. Lindner, *Mater. Res. Soc. Symp. Proc.* **2014**, *1663*, 6 pp.

[311] D. Gogel, M. Weinl, J. K. N. Lindner, B. Stritzker, *J. Optoelectron. Adv. Mater.* **2010**, *12*, 740–744.

[312] A. Mesarwi, A. Ignatiev, *Surf. Sci.* **1991**, *244*, 15–21.

[313] D. M. Thornburg, R. J. Madix, *Surf. Sci.* **1990**, *226*, 61–76.

[314] D. G. Brown, U. Weser, *Z. Naturforsch. B* **1979**, *34*, 989–994.